



National Library
of Canada

Acquisitions and
Bibliographic Services

395 Wellington Street
Ottawa ON K1A 0N4
Canada

Bibliothèque nationale
du Canada

Acquisitions et
services bibliographiques

395, rue Wellington
Ottawa ON K1A 0N4
Canada

Your file *Votre référence*

Our file *Notre référence*

The author has granted a non-exclusive licence allowing the National Library of Canada to reproduce, loan, distribute or sell copies of this thesis in microform, paper or electronic formats.

The author retains ownership of the copyright in this thesis. Neither the thesis nor substantial extracts from it may be printed or otherwise reproduced without the author's permission.

L'auteur a accordé une licence non exclusive permettant à la Bibliothèque nationale du Canada de reproduire, prêter, distribuer ou vendre des copies de cette thèse sous la forme de microfiche/film, de reproduction sur papier ou sur format électronique.

L'auteur conserve la propriété du droit d'auteur qui protège cette thèse. Ni la thèse ni des extraits substantiels de celle-ci ne doivent être imprimés ou autrement reproduits sans son autorisation.

0-612-68119-X

Canada

DEVELOPMENT OF A FLUIDIZED BIOREACTOR SYSTEM
USING IMMOBILIZED YEAST FOR
CONTINUOUS BEER PRODUCTION

by
Heather Pilkington

Department of Chemical and Biochemical Engineering
Graduate Program
in
Engineering Science

Submitted in partial fulfillment
of the requirements for the degree of
Doctor of Philosophy

Faculty of Graduate Studies
The University of Western Ontario
London, Ontario
February, 2000

© Heather Pilkington 2000

ABSTRACT

For centuries, breweries have produced their products using batch fermentations, which utilize freely suspended yeast in large fermenters. Wort, a complex natural medium consisting of carbohydrates, nitrogen compounds, vitamins, and ions is metabolized by yeast to produce beer. Rapid continuous fermentation, using immobilized yeast and the associated free cells, could be an effective approach to improving brewery productivity.

Fermentations were performed using brewer's wort and an industrial strain of *Saccharomyces cerevisiae* immobilized in kappa-carrageenan beads. Batch kinetics using immobilized and freely suspended yeast were studied. A continuous fermentation system, utilizing a gas-lift draft tube bioreactor, was designed and installed in a commercial pilot plant. Continuous fermentations were performed to evaluate yeast flavour metabolite production and the merits of the new pilot plant bioreactor system.

Over six months of continuous fermentation, freely suspended cells in the liquid phase retained viabilities greater than 90%, while immobilized cell viability decreased to less than 60%. Scanning electron micrographs revealed that cells located near the bead core had an irregular shape and fewer bud scars, suggesting impaired growth.

Data collected on secondary yeast metabolites produced during continuous beer fermentations, highlighted the importance of controlling oxygen in the fluidizing gas, and residence time, for flavour formation. The following flavour compounds were measured in the liquid phase: diacetyl, acetaldehyde, ethyl acetate, isobutanol, isoamyl acetate, isoamyl alcohol, ethyl hexanoate, and ethyl octanoate. It was found that concentrations of diacetyl and acetaldehyde remained at unacceptably high concentrations even when the oxygen in the fluidizing gas was minimal. However, diacetyl concentration was reduced by 46% when a commercial preparation of alpha-acetolactate decarboxylase was added to the wort supplying the continuous fermentation.

A secondary 48-hour batch-holding period, at 21°C, resulted in a flavour profile within the range of market beers, without the need for enzyme addition.

Continuous fermentation using a gas-lift bioreactor could potentially replace batch fermentation technology currently used in commercial breweries. In the past, flavour formation in continuous fermentations and process complexity were major

stumbling blocks to commercialization, but by integrating the operational advantages of a gas-lift bioreactor with the biochemical principles associated with flavour formation discussed in this work, success is more probable.

Keywords: yeast, beer, fermentation, flavour, immobilization.

EPIGRAPH

“There has been a noticeable trend in the roles of Biochemical Engineers as a result of the advances in the new biotechnology. This trend has been the movement away from biochemical equipment design and operations, toward the understanding at the cellular level of biochemical and biological systems. It is my belief that this trend is a healthy one since the integration of engineering concepts with biological principles is one of the major contributions from Biochemical Engineering to the new biotechnology.”

- Daniel I.C. Wang, MIT

Dedicated to
my husband, Glen Burston
and my mother, Diane Pilkington

ACKNOWLEDGEMENTS

The author acknowledges the enthusiastic support and guidance she received from her Chief Academic Supervisor Dr. Argyrios Margaritis. The author appreciates Dr. Margaritis' mentorship in biochemical engineering and his efforts to provide a beneficial and stimulating university-industry collaborative graduate experience with Labatt Brewing Company Limited in London, Ontario. Dr. Inge Russell, the author's Industrial Advisor from Labatt Brewing Company Limited, is thanked for providing ongoing support, advice, mentoring, and above all, inspiration throughout the course of this project. The support of Dr. Leaist as a member of her advisory committee at the University of Western Ontario is also appreciated.

The work presented in this thesis was undertaken in collaboration with the Labatt Technology Development Department in London, Ontario. In addition the assistance, counsel and encouragement of the following members of the Labatt staff is greatly appreciated: A. Abra, G. Arsenault, G. Austin, K. Bond, T. Dowhanick, T. Goring, A. Griffiths, I. Hancock, H. Heggart, L. Hicks, C. Hysen, J. Kerr, J. Killan, L. Leff, E. Leiska, D. Maradyn, M. McGarrity, R. McKee, C. McRoberts, N. Mensour, N. Nolan, J. Riddell, J. Sobczak, R. Stewart, D. Thompson, A. Tinginys, B. Vandermeer, C. Von der Heide, and G. Ylimaki. The author gives special thanks to her colleague Mr. N. Mensour, P.Eng., for their many lively discussions on continuous fermentation. In addition, the support from the upper management of Labatt Brewing Company Limited, including C. Murray and L. Macauley, is greatly appreciated.

The Analytical Chemistry Department and the Quality Control Chemistry Department from Labatt Brewing Company Limited are acknowledged for performing, calibrating, and validating the chemical analyses used in this work.

Mr. N. Mensour and Dr. M. McGarrity of the Labatt Technology Development Department are acknowledged for the joint work that was conducted to study the effects of oxygen during post-fermentation processing.

Thanks are also given to the following people: Ms. K. Ross for assistance with the thesis graphics, Dr. A. Smith from the University of Guelph for her assistance with the scanning electron microscopy used in this thesis, Dr. C. Briens of UWO for the valuable

discussions on mass transfer in immobilized cell systems and Dr. D. Bellhouse of STATLAB/UWO for the valuable discussions on experimental design and statistics.

The author wishes to thank NSERC for financial support through an Industrial Post Graduate Fellowship, the Faculty of Graduate Studies, UWO, for financial support through a Graduate Research Fellowship, and the Faculty of Graduate Studies, UWO, for financial support through a Special University Scholarship. The Department of Chemical and Biochemical Engineering, UWO is also acknowledged for financial support through the granting of Teaching Assistantships. This research has also been supported by an NSERC Individual Research Grant No. 4388 awarded to Dr. A. Margaritis on the study of immobilized yeast cells systems in fluidized bioreactors.

TABLE OF CONTENTS

	Page
CERTIFICATE OF EXAMINATION	ii
ABSTRACT	iii
EPIGRAPH	v
ACKNOWLEDGEMENTS	vi
TABLE OF CONTENTS	viii
LIST OF TABLES	xiii
LIST OF FIGURES	xv
LIST OF APPENDICES	xxiii
NOMENCLATURE	xxiv
GLOSSARY OF BREWING TERMINOLOGY	xxviii
CHAPTER 1. INTRODUCTION	1
CHAPTER 2. LITERATURE REVIEW	2
2.1 Nature's Oldest Biotechnology Process:	
Traditional Beer Fermentation	2
2.1.1 Raw Materials Used in Beer Fermentation	2
2.1.2 The Brewing Process	4
2.1.3 Primary Batch Fermentation	5
2.1.4 Aging, Filtration, and Final Processing	6
2.2 Metabolism of Wort Nutrients by Yeast for Beer Production	7
2.2.1 Uptake of Wort Nutrients by Yeast	7
2.2.2 Yeast Excretion Products	18
2.3 Continuous Fermentation Using Immobilized Yeast Cells	30
2.3.1 Practical Importance of Cell Immobilization	30
2.3.2 Properties of Immobilized Cell Systems	32
2.3.3 Methods for Measurement of Immobilized Cell	
Viability and Vitality	37

	Page
2.3.4 Methods for Determining Cell Distribution and Growth Patterns within Immobilized Cell Matrices	42
2.4 The Effects of Immobilization on Yeast Metabolism and Beer Flavour	46
 CHAPTER 3. THEORETICAL CONSIDERATIONS	 53
3.1 Batch Microbial Growth Kinetics of Freely Suspended Cells	53
3.2 Kinetics of Freely Suspended Cell Growth in Continuous Stirred Tank Bioreactors	56
3.3 Ethanol Production during Beer Fermentation	57
3.4 Gas-Liquid Mass Transfer in Freely Suspended Cell Systems	59
3.5 External and Internal Mass Transfer Characteristics of Immobilized Cells	61
3.5.1 External Mass Transfer in Immobilized Cell Systems	63
3.5.2 Internal Mass Transfer in Immobilized Cell Systems	68
 CHAPTER 4. MATERIALS AND METHODS	 75
4.1 Yeast Strain and Characteristics	75
4.2 Preparation of Yeast Inoculum	75
4.3 Wort Fermentation Medium	76
4.4 Immobilization Methodology	76
4.5 Cumulative Particle Size Distribution	78
4.6 Yeast Cell Enumeration and Viability	78
4.7 Microbiological Analyses	79
4.8 Scanning Electron Microscopy (SEM) of Yeast Immobilized in Kappa-Carrageenan Gel Beads	81
4.9 Bioreactor Sampling Protocol	81
4.10 Dissolved Oxygen Measurement	82
4.11 Chemical Analyses	85
4.11.1 Ethanol	85

	Page
4.11.2 Carbohydrate Summary	86
4.11.3 Specific Gravity	86
4.11.4 Total Diacetyl	87
4.11.5 Beer Volatiles	87
4.11.6 Free Amino Nitrogen (FAN)	88
CHAPTER 5. CONTINUOUS FERMENTATION USING A GAS-LIFT BIOREACTOR SYSTEM	90
5.1 Gas-lift Draft Tube Bioreactor Description	90
5.1.1 Bioreactor Body	90
5.1.2 Bioreactor Headplate	91
5.1.3 Sanitary Valves for Aseptic Sampling	96
5.2 Flow Diagram of Continuous Beer Fermentation System	97
5.2.1 Wort Collection and Storage	98
5.2.2 Continuous Fermentation using Gas-Lift Draft Tube Bioreactor System	100
5.2.3 Product Collection	100
5.2.4 Glycol Cooling Loop	101
5.3 Bioreactor Sterilization Protocol	101
5.4 Fermentation System Startup	102
CHAPTER 6. KAPPA-CARRAGEENAN GEL IMMOBILIZATION OF LAGER BREWING YEAST	109
6.1 Experimental Procedure	114
6.2 Results and Discussion	116
CHAPTER 7. FLAVOUR PRODUCTION IN A GAS-LIFT CONTINUOUS BEER FERMENTATION SYSTEM	141
7.1 Experimental Procedure	141

	Page
7.1.1 Effect of Relative Amounts of Air in the Bioreactor Fluidizing Gas on Yeast Metabolites during Primary Continuous Fermentation	141
7.1.2 Post Fermentation Batch Holding Period: Effects of Oxygen Exposure on Yeast Metabolites	142
7.1.3 Effect of Liquid Residence Time on Yeast Metabolites during Continuous Primary Beer Fermentation	144
7.1.4 Using a Commercial Preparation of Alpha-Acetolactate Decarboxylase to Reduce Diacetyl during Continuous Primary Beer Fermentation	144
7.2 Results and Discussion	148
7.2.1 Effect of Relative Amounts of Air in the Bioreactor Fluidizing Gas on Yeast Metabolites during Primary Continuous Fermentation	148
7.2.2 Post Fermentation Batch Holding Period: Effects of Oxygen Exposure on Yeast Metabolites	161
7.2.3 Effect of Liquid Residence Time on Yeast Metabolites during Continuous Primary Beer Fermentation	171
7.2.4 Using a Commercial Preparation of Alpha-Acetolactate Decarboxylase to Reduce Diacetyl during Continuous Primary Beer Fermentation	178
 CHAPTER 8. CONCLUSIONS	 184
 CHAPTER 9. RECOMMENDATIONS	 187
 BIBLIOGRAPHY	 189
 APPENDICES	 203

VITA

Page
252

LIST OF TABLES

Table	Page	
2.1	Classification of amino acids according to their speed of absorption from wort by ale yeast under brewery conditions	14
2.2	Ionic nutrients required by brewing yeast	18
2.3	Percent utilization of amino acids in wort at 80% attenuation in batch free cell and continuous immobilized cell packed bed fermentations	49
2.4	Analysis of flavour volatiles from beer produced using a continuous immobilized cell fermenter	51
2.5	Analysis of some key flavour compounds in two stage continuous fermentation system	51
3.1	Experimental methods to determine diffusion coefficients in immobilization matrices	72
3.2	Effective diffusivities of some substrates in immobilization matrices	73
4.1	Sample volume requirements for various chemical analyses	82
5.1	Detailed parts description for flow diagram shown in Figure 5.6	105
5.2	Temperature profile of water in wort storage vessel (T-1 or T-2)	107
6.1	Yield, $Y_{p/s}$, of product, P, ethanol from substrates, glucose (Glc), fructose (Frc), maltose (Mal) and maltotriose (DP3) for R1, R2, R3, and freely suspended cell control fermentation	130
6.2	Bioreactor productivity of ethanol for immobilized cell batch fermentations (R1, R2, and R3) compared with freely suspended cell batch fermentations	130
6.3	Viability (methylene blue) and concentration of freely suspended and immobilized lager yeast cells entrapped in kappa-carrageenan gel beads over fermentation time	134
7.1	Air volumetric flow rates supplied to the bioreactor through the sparger during continuous fermentation	141

Table	Page
7.2 Summary table of effect of air volumetric flow rate to the bioreactor through the sparger on liquid phase yeast and key yeast metabolite concentrations in the bioreactor at a residence time, R_t , of 1.18 days, averages at pseudo-steady state	149
7.3 (a) Summary table of effect of bioreactor residence time on liquid phase yeast and key yeast metabolite concentrations, averages at pseudo-steady state; (b) Summary table of the effect of bioreactor residence time on liquid phase yeast and key yeast metabolite flow rates at the bioreactor outlet, averages at pseudo-steady state	171
7.4 Mass balances on free amino nitrogen and total fermentable carbohydrate (as glucose) based on average data in Table 7.3, effect of bioreactor residence time	174
7.5 Summary of average pseudo-steady state effect of ALDC addition to wort fermentation medium on diacetyl concentration during continuous beer fermentation in a gas lift bioreactor	183

LIST OF FIGURES

Figure	Page
2.1 Schematic of a traditional batch brewing process	2
2.2 Embden-Meyerhof-Parnas (EMP, glycolysis, glycolytic) pathway	8
2.3 Krebs Cycle	10
2.4 Regenerating NAD ⁺ by fermenting yeast	11
2.5 The contribution of carbohydrate catabolism to intermediate compounds for biosynthetic reactions	13
2.6 Production of higher alcohols	21
2.7 Metabolic interrelationships leading to ester formation	23
2.8 Formation of diacetyl and 2,3-pentanedione as by-products of pathways leading to the formation of the amino acids valine and isoleucine	26
2.9 Reduction of diacetyl to acetoin and 2,3-butanediol	27
2.10. Interrelationship between yeast metabolism and production of beer flavour compounds	29
2.11 Basic methods of cell immobilization	33
3.1 (a) Growth and (b) non-growth associated product formation during microbial batch fermentation, where X is the concentration of cells, P is the concentration of product, and t is batch fermentation time	55
3.2 Schematic of a well-mixed continuous stirred tank reactor (CSTR) containing freely suspended cells, where F is the volumetric flow rate of medium entering the bioreactor, S_0 is the initial substrate concentration, X is the biomass concentration, P is the product concentration, and V_R is the bioreactor working volume	56
3.3 Transport of oxygen from the gas phase to an immobilized cell matrix; 1, gas phase; 2, liquid film; 3, bulk liquid phase; 4, liquid film; 5, solid matrix; 6, microcolony containing cells	61

Figure	Page	
3.4	Concentration profiles for overall mass transfer of substrate from the bulk liquid phase into a gel bead	66
4.1	The static mixer process for making kappa-carrageenan gel beads	77
5.1	Schematic of gas-lift draft tube bioreactor system for primary beer fermentation	92
5.2	Photograph of the gas-lift draft tube bioreactor vessel	93
5.3	Detailed scale drawing of 13 L (8 L working volume) gas-lift draft tube bioreactor vessel	94
5.4	Detailed drawing of bioreactor vessel headplate; 1-liquid withdrawal port for oxygen sensor; 2-thermowell for temperature sensor, linked to thermostatic controller; 3-temperature probe; 4-liquid return port for oxygen sensor; 5-inoculation port; 6-membrane sample port with stainless steel cap	95
5.5	Profile of liquid withdrawal port for oxygen sensor with filter unit submerged in bioreactor liquid phase	96
5.6	Detailed equipment and flow diagram for continuous primary beer fermentation using a gas-lift bioreactor system (see Table 5.1 for detailed equipment description)	104
5.7	Dissolved oxygen concentration in the wort versus hold time in wort storage vessel (T-1 or T-2) under different tank filling conditions	107
5.8	Cumulative particle size distribution of kappa-carrageenan gel beads	108
6.1	Gelation mechanism of carrageenan	110
6.2	Chemical structures of lambda-, iota-, and kappa-carrageenans	111
6.3	Schematic of the utilization of wort constituents by immobilized yeast during primary fermentation	113
6.4. a)	R1, maltose, maltotriose, glucose, fructose, and ethanol concentration versus fermentation time for repeated batch fermentations using lager yeast cells immobilized in kappa-carrageenan gel beads	117

Figure	Page
6.4. b) R2, maltose, maltotriose, glucose, fructose, and ethanol concentration versus fermentation time for repeated batch fermentations using lager yeast cells immobilized in kappa-carrageenan gel beads	118
6.4. c) R3, maltose, maltotriose, glucose, fructose, and ethanol concentration versus fermentation time for repeated batch fermentations using lager yeast cells immobilized in kappa-carrageenan gel beads	119
6.5 Maltose, maltotriose, glucose, fructose, and ethanol concentration versus fermentation time for freely suspended lager yeast control fermentations (no immobilized cells)	120
6.6. a) Maltose concentration versus fermentation time for repeated batch fermentations, R1, R2, and R3, using lager yeast cells immobilized in kappa-carrageenan gel beads	121
6.6. b) Ethanol concentration versus fermentation time for repeated batch fermentations, R1, R2, and R3 using lager yeast cells immobilized in kappa-carrageenan gel beads	122
6.7. a) Immobilized lager yeast cell concentration per total bioreactor volume versus fermentation time for R1, R2, and R3 fermentations. Error bars are equal to plus or minus the SEM (n = 2)	123
6.7. b) Concentration per total bioreactor volume of lager yeast cells released into the bulk liquid phase versus fermentation time for R1, R2, and R3 fermentations. Error bars are equal to plus or minus the SEM (n = 2)	124
6.7. c) Total (immobilized and liquid phase) lager yeast cell concentration per total bioreactor volume versus fermentation time for R1, R2, and R3 fermentations. Error bars are equal to plus or minus the SEM (n = 2)	125
6.8 Profile of immobilized, liquid phase, and total (immobilized and liquid phase) cell concentration versus fermentation time for R1, the first of three repeated batch fermentations using lager yeast cells immobilized in kappa-carrageenan gel beads	126

Figure	Page
6.9 Control fermentation freely suspended lager yeast cell concentration per total bioreactor volume versus fermentation time. No immobilized cells were present during this fermentation. Error bars represent plus or minus the SEM (n = 3)	127
6.10 Immobilized lager yeast concentration per mL of gel bead versus fermentation for R1, R2, and R3 fermentations. Error bars are equal to plus or minus the SEM (n = 2)	128
6.11 Immobilized lager yeast cell viability (methylene blue) versus fermentation time for R1, R2, and R3 fermentations	132
6.12 $\ln(X/X_0)$ versus batch fermentation time during the exponential growth phase of the averaged freely suspended yeast control fermentations, where X is the cell concentration at time, t, and X_0 is the cell concentration at time, t = 0	133
6.13 Kappa-carrageenan gel bead containing immobilized lager yeast at zero time fermentation	136
6.14 Pod of lager yeast entrapped in kappa-carrageenan gel bead after two days of batch fermentation, showing bud scars on individual yeast cells	137
6.15 Outer edge of kappa-carrageenan gel bead showing lager yeast cells after two months of continuous fermentation	137
6.16 Lager yeast cells at outer region of kappa-carrageenan gel bead after two months of continuous fermentation	138
6.17 Lager yeast cells at the center of a kappa-carrageenan bead after two months continuous fermentation	138
6.18 Entire kappa-carrageenan gel bead after six months continuous fermentation, many fractured beads had hollow centers	139
7.1 The action of alpha-acetolactate decarboxylase (ALDC)	145
7.2 Liquid phase yeast cell concentration versus relative continuous fermentation time	150

Figure	Page
7.3 Liquid phase yeast viability versus relative continuous fermentation time	151
7.4 Free amino nitrogen concentration remaining in wort versus relative continuous fermentation time	152
7.5 Liquid phase ethanol and total fermentable carbohydrate (as glucose) concentration versus relative continuous fermentation time	153
7.6 Liquid phase total diacetyl concentration versus relative continuous fermentation time	154
7.7 Liquid phase acetaldehyde concentration versus relative continuous fermentation time	155
7.8 Ethyl acetate concentration versus relative continuous fermentation time	156
7.9 Liquid phase isoamyl acetate, ethyl hexanoate and ethyl octanoate concentration versus relative continuous fermentation time	157
7.10 Liquid phase isoamyl alcohol and isobutanol concentration versus relative continuous fermentation time	158
7.11 Liquid phase 1-propanol concentration versus relative continuous fermentation time	159
7.12 Mean fermentable glucose concentration versus post fermentation hold time for aerobic and anaerobic treated samples after continuous primary fermentation in a gas lift bioreactor. Error bars are equal to plus or minus the standard error of the mean, n = 2	162
7.13 Mean ethanol concentration versus post fermentation hold time for aerobic and anaerobic treated samples after continuous primary fermentation in a gas lift bioreactor. Error bars are equal to plus or minus the standard error of the mean, n = 2	162
7.14 Mean acetaldehyde concentration versus post fermentation hold time for aerobic and anaerobic treated samples after continuous primary fermentation in a gas lift bioreactor. Error bars are equal to plus or minus the standard error of the mean, n = 2	163

Figure	Page
7.15 Mean total diacetyl concentration versus post fermentation hold time for aerobic and anaerobic treated samples after continuous primary fermentation in a gas lift bioreactor. Error bars are equal to plus or minus the standard error of the mean, n = 2	164
7.16 Mean ethyl acetate concentration versus post fermentation hold time for aerobic and anaerobic treated samples after continuous primary fermentation in a gas lift bioreactor. Error bars are equal to plus or minus the standard error of the mean, n = 2	165
7.17 Mean isoamyl acetate concentration versus post fermentation hold time for aerobic and anaerobic treated samples after continuous primary fermentation in a gas lift bioreactor. Error bars are equal to plus or minus the standard error of the mean, n = 2	165
7.18 Mean ethyl hexanoate concentration versus post fermentation hold time for aerobic and anaerobic treated samples after continuous primary fermentation in a gas lift bioreactor. Error bars are equal to plus or minus the standard error of the mean, n = 2	166
7.19 Mean isoamyl alcohol concentration versus post fermentation hold time for aerobic and anaerobic treated samples after continuous primary fermentation in a gas lift bioreactor. Error bars are equal to plus or minus the standard error of the mean, n = 2	167
7.20 Mean 1-propanol concentration versus post fermentation hold time for aerobic and anaerobic treated samples after continuous primary fermentation in a gas lift bioreactor. Error bars are equal to plus or minus the standard error of the mean, n = 2	167
7.21 Mean isobutanol concentration versus post fermentation hold time for aerobic and anaerobic treated samples after continuous primary fermentation in a gas lift bioreactor. Error bars are equal to plus or minus the standard error of the mean, n = 2	168

Figure	Page
7.22 Radar graph of normalized concentration data obtained after 48 hours of aerobic or anaerobic holding, following continuous primary fermentation in a gas lift bioreactor. The normalized data is based on the averages of duplicate samples and the commercial beer data was taken as the midpoint of the data listed in Appendix 4.	170
7.23 Liquid phase yeast cell concentration versus relative continuous fermentation time, effect of liquid residence time in bioreactor	172
7.24 Liquid phase ethanol and fermentable glucose concentration versus relative continuous fermentation time, effect of liquid residence time in bioreactor	173
7.25 Liquid phase free amino nitrogen and 1-propanol concentration versus relative continuous fermentation time, effect of liquid residence time in bioreactor	174
7.26 Liquid phase total diacetyl and acetaldehyde concentration versus relative continuous fermentation time, effect of liquid residence time in bioreactor	175
7.27 Liquid phase isobutanol and isoamyl alcohol concentration versus relative continuous fermentation time, effect of liquid residence time in bioreactor	176
7.28 Liquid phase ethyl acetate and isoamyl acetate concentration versus relative continuous fermentation time, effect of liquid residence time in bioreactor	177
7.29 Liquid phase total diacetyl concentration versus continuous fermentation time, effect of ALDC addition to the wort fermentation medium, Experiment 2	179
7.30 Liquid phase specific gravity and ethanol concentration versus continuous fermentation time, effect of ALDC addition to the wort fermentation medium, Experiment 2	179

Figure		Page
7.31	Liquid phase cell concentration versus continuous fermentation time, effect of ALDC addition to the wort fermentation medium, Experiment 2	180
7.32	Liquid phase total diacetyl concentration versus continuous fermentation time, effect of ALDC addition to the wort fermentation medium, Experiment 3	181
7.33	Liquid phase ethanol concentration and specific gravity versus continuous fermentation time, effect of ALDC addition to the wort fermentation medium, Experiment 3	182
7.34	Liquid phase cell concentration versus continuous fermentation time, effect of ALDC addition to the wort fermentation medium, Experiment 3	182

LIST OF APPENDICES

Appendix		Page
APPENDIX 1.	Tabulation of experimental results for Tables and Figures in main text	203
APPENDIX 2.	Concentration of some components in Brewer's wort	237
APPENDIX 3.	Bioreactor volumetric productivity calculations	239
APPENDIX 4.	Statistical analyses of data	241
APPENDIX 5.	Structural formulae of key yeast substrates and metabolic products	243
APPENDIX 6.	Typical concentrations and threshold values for flavour compounds in market beers	247
APPENDIX 7.	Copyright releases from previous publications	249

NOMENCLATURE

A_s	surface area of a sphere, m^2
C	molar concentration of solute (amount per total volume of immobilization matrix), mol/m^3
C_A^{sc}	concentration of solute A in liquid at liquid-solid interface, mol/m^3
C_A^I	concentration of solute A in the immobilization matrix, mol/m^3
C_A^{sl}	concentration of solute A in the immobilization matrix at liquid-solid interface, mol/m^3
$C_{A,l}$	concentration of solute A in the liquid at the gas-liquid interface, mol/m^3
$C_{A,L}^f, C_A^L$	concentration of solute A in bulk liquid phase, mol/m^3
$C_{A,L}^*$	solubility of solute A in the liquid phase, mg/L or mol/m^3
$C_{A,L,critical}$	concentration of solute A in the liquid phase when Q_{O_2} is max, mol/m^3
C_L	concentration of solute in the liquid void phase, mol/m^3
$C_{L,O}$	dissolved oxygen concentration, mg/L
C_S^f	equilibrium solute concentration in entire matrix volume, mol/m^3
D	diffusion coefficient in the immobilization matrix, m^2/s
D_a	diffusion coefficient in the aqueous phase, m^2/s
D_c	critical dilution rate, h^{-1}
D_e	effective diffusion coefficient in the immobilization matrix, m^2/s
D_L	diffusion coefficient in the bulk liquid phase, m^2/s
D_R	dilution rate, h^{-1}
d_p	particle diameter, m
F	volumetric flow rate, mL/min or m^3/s
H	Henry's Law constant, $atm \cdot L/mg$
I	current, A
J, J_A	molar flux, $mol/m^2 \cdot s$
k_G	local gas side mass transfer coefficient, $mol/(m^2 \cdot s \cdot atm)$
k_L	local liquid side mass transfer coefficient, m/s
k_{La}	liquid side volumetric mass transfer coefficient, s^{-1}
K_G	overall gas side mass transfer coefficient, $mol/(m^2 \cdot s \cdot atm)$

K_L	overall liquid side mass transfer coefficient, m/s
K_s	Monod Constant, mol/m ³ or kg/m ³
L	characteristic length, $L = V_p/S_x$, m
M_A	molecular weight of solvent A, g/mol
M_B	molecular weight of solvent B, g/mol
N_A	overall volumetric gas-liquid flux of solute A, mol/m ³ s
$N_{A,L}$	liquid side film volumetric flux of solute A, mol/m ³ s
\underline{N}_A	overall gas-liquid flux of solute A, mol/m ² s
$\underline{N}_{A,G}$	gas side film flux of solute A, mol/m ² s
$\underline{N}_{A,L}$	liquid side film flux of solute A, mol/m ² s
OUR	oxygen uptake rate, mol/m ³ h
P	product concentration, g/100 mL or kg/m ³
Pa	Pascals
$P_{A,G}$	partial pressure of solute A in the gas phase, atm
$P_{A,G}^*$	solubility of solute A in gas phase, atm
$P_{A,L}$	partial pressure of solute A in the gas phase at the gas-liquid interface, atm
P_0	product concentration at time, $t = 0$, g/100 mL or kg/m ³
Q	volumetric flow rate, m ³ /s
Q_{O_2}	specific rate of oxygen consumption, mol/(kg _{dwc} h)
r	radial coordinate in sphere, m
r_p	rate of formation of product, kg/m ³ h
r_s	rate of consumption of substrate, kg/m ³ h
r_x	rate of biomass production, kg _{dwc} /m ³ h
R	radius of spherical immobilization matrix, m
R_t	bioreactor liquid residence time, h or days
s	rate of surface renewal, s ⁻¹
S	substrate concentration, g/100 mL or kg/m ³
STP	standard temperature and pressure
S_0	substrate concentration at time, $t = 0$, g/100 mL or kg/m ³
S_x	external surface area, m ²
t	time, s, h or days

t_d	biomass doubling time, h
t_s	exposure time of a fluid element, s
T	temperature, K
V_A	solute molar volume at boiling point, m^3/mol
V_L	liquid volume, m^3
V_p	volume of particle, m^3
V_R	bioreactor working volume, V_R , L or m^3
V_{beer}	bioreactor volumetric productivity of beer, $m^3 \text{ beer}/(m^3 h)$
$V_{ethanol}$	bioreactor volumetric productivity of ethanol, $kg/(m^3 h)$
x	space coordinate, m
X	biomass concentration kg_{dwc}/m^3 or cells/mL
X_0	biomass concentration at time $t = 0$, kg_{dwc}/m^3 or cells/mL
$Y_{p,s}$	yield of product from substrate, g product/g substrate consumed
$Y_{p,X}$	yield of product from biomass, g product/g biomass
$Y_{X,S}$	yield of biomass from substrate, g biomass/g substrate consumed

Greek Symbols

α	kinetic model parameters of Leudeking and Piret
β	kinetic model parameters of Leudeking and Piret
ρ	density, kg/m^3
δ	diffusion path, film thickness, m
μ	specific growth rate, h^{-1}
μ_{max}	maximum specific growth rate, h^{-1}
μ_B	viscosity of solvent, Pa s
u_r	relative velocity, m/s
ω	specific death rate, h^{-1}

Dimensionless Numbers

Bi	Biot Number, $Bi = k_L L/D_c$
K_p	equilibrium solute partitioning coefficient, $K_p = C_{A^1} / C_{A,L}^e$
n	integer number (number of terms)
Re	Reynolds Number, $Re = u_r \rho d_p / \mu_B$
Sc	Schmidt Number, $Sc = \mu_B / \rho D_L$

Sh	Sherwood Number, $Sh = k_L d_p / D_L$
Φ	Thiele Modulus, $\Phi = L(\mu_{\max}/D_e K_s)^{1/2}$
η	Effectiveness Factor, $\eta = (\text{observed reaction rate} / \text{rate obtained with no mass-transfer resistance})$
ε	void fraction, $\varepsilon = 1 - \phi_p$
ϕ_p	polymer volume fraction
τ	tortuosity factor

GLOSSARY OF BREWING TERMINOLOGY

Adjunct: A term, which refers to any agricultural product, other than malted barley, which is used as a source of sugar in the brewing process.

Apparent Extract (AE): The measure of extract in the beer is expressed in degrees Plato (not used for beer which has been de-alcoholized). No allowance is made for the effect of alcohol on the specific gravity.

Cereal Cooker: The unmalted cereals must be cooked prior to their addition to the mash tun. This is to ensure liquefaction of the starch.

Chill Haze: Haze (protein – polyphenols), which forms when the beer is chilled during aging.

Dropping: Yeast is removed from the fermented wort, with centrifuges or by flocculation.

Flavour stability: The ability of a beer to maintain its original (fresh) flavour over a period of time.

Flocculate/Flocculation: The aggregation of yeast into small masses, which often leads to the rapid precipitation of yeast to the bottom of the fermenter.

Fusel Alcohols: Higher alcohols, i.e., butanol and 1-propanol.

Green Beer: Fermented wort prior to any conditioning (aging).

Hectoliter (hecto = 100): 100 L.

High Gravity Wort: Wort with an initial gravity of above 12°P.

Hops: A bittering substance added during wort boiling to flavour the beer.

Kettle: The vessel where the wort is boiled.

Lauter Tun: A vessel where the soluble components from the mash (mostly carbohydrates) are separated from the insoluble fraction (grain husks).

Malting: Malting involves germination of the barley until the starchy endosperm has undergone some degradation by the malt enzymes, α - and β -amylase.

Mashing: A process whereby the malt, usually some unmalted cereals and water are mixed and the enzymes formed during malting continue to hydrolyze the starch material.

Mash Tun: The vessel where the mashing process occurs.

Normal Gravity Wort: Wort with an initial gravity of 10-12°P, which results in a beer of 4-5% (v/v) ethanol content at the end of fermentation.

Pitching: The wort is inoculated (or pitched) with yeast.

Plato: Also degrees Plato (°P). Term used to describe wort and beer density. Refers to the numerical value of a percentage (w/v) sucrose solution in water at 20°C whose specific gravity is the same as the wort in question.

Specific Gravity: See Plato.

Spent Grains: The insoluble fraction of the grains, which can be dried and sold as cattle feed.

Spent Hops: The solid material removed by the hop strainer.

Sweet Wort: The liquor, which is collected after filtration of the mash.

Total Fermentable Carbohydrate (as glucose): Equal to $[glc] + [fruc] + 1.053[malt] + 1.106[DP3]$

Trub or Break: Heat sensitive proteins coagulated during wort boiling that form a precipitate known as trub or break.

Wort: Liquid extracted from a mash of malt or malt and adjunct.

CHAPTER 1. INTRODUCTION

The traditional beer fermentation process utilizes free yeast cells and is essentially a batch operation, typically seven to fourteen days in duration. As with many industrial processes throughout history, the beer industry could make significant gains in efficiency and productivity by advancing from batch to continuous processing. There has been significant research conducted in the area of immobilized yeast for continuous primary beer fermentation in the past decade (Masschelein and Vandebussche, 1999). Currently, there are industrial scale systems available for beer maturation, which utilize immobilized cells (Pajunen et al. 1987). However, there have been no reports of breweries using industrial scale immobilized yeast cell systems for continuous primary fermentation. There is a need for additional research on the effects of immobilization on yeast viability and vitality, on bioreactor system design, and on yeast flavour metabolite production in order to take continuous primary fermentation to the next level of development.

For this study, fermentations were carried out using brewer's wort and an industrial strain of *Saccharomyces cerevisiae* yeast immobilized in kappa-carrageenan beads. The following detailed objectives for this investigation were formulated:

- 1) Design and construct a continuous primary fermentation system, utilizing a gas-lift draft tube bioreactor, in a commercial brewery pilot plant;
- 2) Examination of the batch kinetics of free and immobilized *Saccharomyces cerevisiae* industrial yeast strain LCC3021;
- 3) Examination of immobilized and freely suspended yeast cell viability (methylene blue) and morphology (using scanning electron microscopy) over extended continuous fermentation time in a gas-lift bioreactor system;
- 4) Examination of yeast flavour metabolite production during continuous primary beer fermentation in a gas-lift bioreactor system using cells immobilized in kappa-carrageenan gel beads.

CHAPTER 2. LITERATURE REVIEW

In this chapter a brief outline of the brewing process is given to orient the reader and a discussion of yeast metabolism during batch fermentation is provided. The concept of continuous primary beer fermentation using immobilized yeast cells is then introduced, followed by a review of the current findings on the production of beer flavour and aroma compounds during continuous fermentation processes.

2.1 Nature’s Oldest Biotechnology Process: Traditional Beer Fermentation

Even in the huge mega-breweries of today, the process of making beer is still essentially a natural one and uses the raw materials water, malt, hops, and yeast. Many breweries will also incorporate adjuncts such as rice or corn and/or other processing aids. Figure 2.1, illustrates the basic steps in the beer production process.

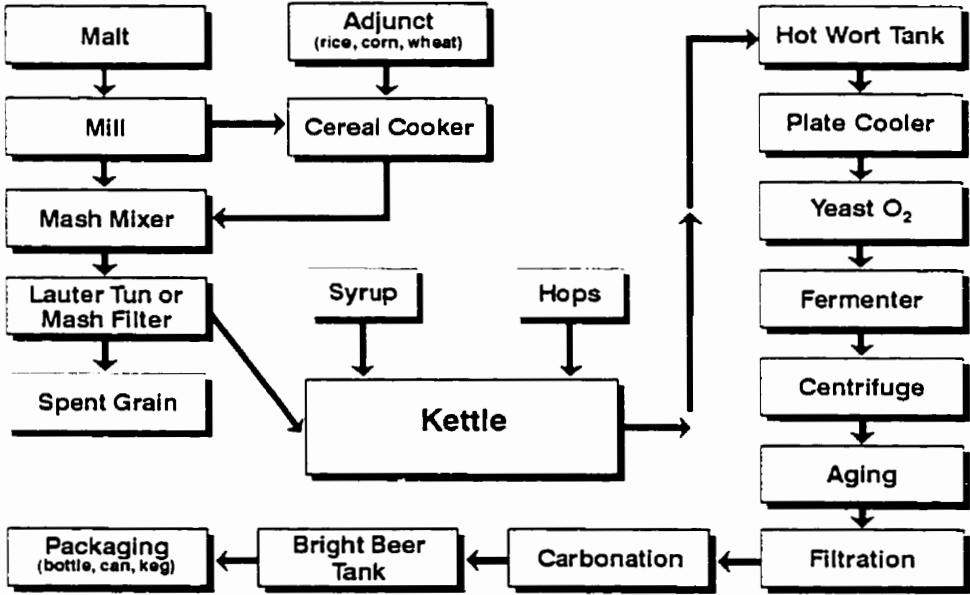


Figure 2.1. Schematic of a traditional batch brewing process.

2.1.1 Raw Materials Used in Beer Fermentation

a) Water

Typically, breweries use between 4 and 12 volumes of water to brew one volume of beer. Where water is an expensive commodity, or in short supply, more attention is

given to reducing water use. Larger breweries often use municipal water supplies, some use well-water. The water that is to be used for brewing must be potable and very pure so that it does not cause off-notes in the finished product. Water is usually treated within the brewery by filtration processes and there may be an inclusion of salts or occasionally organic acids.

b) Malt and Malt Substitutes (Adjuncts)

Under carefully controlled conditions of temperature and humidity, malt cereal, usually barley is allowed to germinate for a specific time period (after 4-6 days), followed by a drying process at controlled temperatures (71-92°C) to arrest growth of the embryo. Malting brings about changes in the barley kernel and this "modification" results in malt, which can then be efficiently extracted. The malting process produces an easily ground product which provides a plentiful source of enzymes to break down the food polymers (i.e. starches and proteins) of malt. When ground malt is extracted with warm water, the resultant extract is called "sweet wort".

The starch from malt is often supplemented by the addition of adjuncts. Examples of adjuncts include corn grits, corn flakes, rice and wheat. Syrups derived from corn, barley or wheat and produced using an acid or acid/enzyme treatment and concentration process, are frequently used, as is cane sugar in Australia and South America. One by-product from this stage of brewing is the spent grain, which consists of protein, cellulose and the residual sugars and starch, which were not extracted into the wort solution. Spent grain is used both wet and dry as livestock feed. "Hot kettle break" or trub is also produced in the brewhouse and this is the coagulated protein, which is separated from the wort after boiling in the brew kettle.

c) Hops

Hops are hardy climbing herbaceous perennial plants. Hops are used in the brewing industry as cones (kiln-dried), in the powdered form (as pellets), as liquids (solvent extracts), as liquid carbon dioxide extracts, or as hop oils (distilled essential oil of hops). Hops are usually added during the brewing stage as seen Figure 2.1 and provide the beer with both its characteristic bitter flavour and with additional flavour complexity.

2.1.2 The Brewing Process

The brewing process serves several important functions: a sweet liquid sugar solution called wort is produced by converting the starch in malt and adjuncts into sugar (extract); protein and other ingredients are present which support yeast growth and fermentation; malts husks are removed in the form of spent grains; and natural flavouring elements of hops and malt are extracted in the wort solution. The cereal cooker, malt mill, mash mixer, lauter tun, kettle, hot wort tank, and cooler are the major pieces of equipment involved in the traditional brewing process (Hardwick, 1995; Kunze, 1996).

a) Cereal Cooker

Adjuncts such as corn grits, corn flakes, rice, wheat, or raw barley are added to the cereal cooker along with warm water and a small amount of malt. As the mash is heated in the cooker the enzymes from malt become more active and break down the starch. The temperature in the cooker is raised to boiling to ensure that the starch absorbs water and to fluidize the slurry. The enzymes from the malt are very important at this point, the starch degrades and the solution becomes more fluid and can be more easily pumped to the mash mixer, where the conversion of starch to sugar is completed. If no malt were added, the adjunct and water mixture would become a thick, solid paste.

b) Malt Mill

In the malt mill, the kernels of malt are ground such that the husks allow the starch and enzymes to be released for conversion to sugars. If the malt is ground too finely the husks may not be able to form a proper filter bed in the lauter tun downstream. Skill and experience are required to perfect the grinding regime.

c) Mash Mixer

Mashing is the term used to describe the process occurring in the mash mixer. The purpose of this unit is to mix the malt, unmalted cereals (eg. corn grits) and water and then, with the addition of heat, produce a sweet sugar solution, which can later be fermented by yeast into a high quality beer. Enzymes found in the malt help to produce wort. The beta- glucanases attack the barley gums, proteases act on proteins in the outer husk and seed coat of the barley kernel, and alpha- and beta-amylases attack the starches and polysaccharides to cleave them into simple sugars that yeast cells can metabolize.

Temperature is varied with time in the mash mixer so that each enzyme has an adequate amount of time at its optimum activity to perform its given conversion.

d) Lauter Tun

The bottom of this vessel is covered by false slotted bottom. The purpose of lautering is to separate the liquid part of the mash from the insoluble fraction (spent grains). The husks or spent grains form a depth filter upon the false slotted bottom of the lauter tun and this filter clarifies the wort as it passes through. A rotating shaft above the grain bed supports a number of blades. These gently disturb the grain bed so that channeling will not occur. Wort is sent through the grain bed and recycled back to the lauter tun until the wort runs clear, at which point the wort is sent to the kettle.

d) Kettle

The clarified wort is sent to the kettle, where hops are added, and the wort is boiled. During kettle boiling malt enzymes are denatured, wort is sterilized by boiling and aromatic hop oils and bitter resins are extracted for bitterness and hop aroma qualities. "Kettle break" (proteins and tannins in wort which clump together) is formed and is removed to prevent haze formation during cold beer storage and the sugars present in the wort caramelize during the boiling process and the wort develops its characteristic amber shade. In the kettle, the pH is adjusted to the optimum level for fermentation and the wort is concentrated to the desired extract level (density) by evaporating unnecessary water in the form of steam.

2.1.3 Primary Batch Fermentation

In the traditional brewery, fermentation is a batch process. Oxygenated wort is placed in a fermenter with a defined amount of thick yeast slurry. During the primary fermentation stage, the yeast cells convert the sugar-rich wort to ethanol, carbon dioxide and flavour compounds. The yeast cells reproduce during primary fermentation, resulting in a many-fold increase in yeast biomass, which accounts for the waste yeast by-product, a portion of which is reused in the next batch. Waste yeast is often used in livestock feed to increase its nutritional value and there is a market for yeast in the food industry as vitamin supplements and texture enhancers.

After primary batch fermentation, centrifuges are commonly used to remove most of the yeast rapidly from the “green” beer. The biochemical pathways occurring in yeast during beer fermentation are described in greater detail in section 2.2.

2.1.4 Aging, Filtration, and Final Processing

After primary fermentation, the beer and the remaining low levels of yeast are sent to aging tanks. The beer is typically held at a low temperature with some yeast still present to allow a slow fermentation of the remaining sugars and the beer flavour to mature. During aging, certain protein and tannin substances precipitate eliminating some harsh and bitter flavours from the beer. These substances called “cold break” or “trub” have poor solubility in beer. If these proteins and tannins are not removed prior to packaging, they may settle out in the keg, bottle or can, making the beer hazy. After aging, the yeast and haze is removed from the vessels (Stewart, 1977).

Following aging, beer can be clarified by passing it through a filter that has been precoated with a filter aid such as diatomaceous earth powder. Diatomaceous earth is composed of silica and is mined from deposits of prehistoric diatomites. This type of filtering is referred to as “kieselguhr” in Germany and other European countries. Any yeast, “cold break”, or particulate matter remaining in the mature beer stream is removed during this filtration. The beer is then carbonated and sent to the packaging line where it is filled into bottles, kegs and cans for consumer distribution.

2.2 Metabolism of Wort Nutrients by Yeast for Beer Production

In this section, the current knowledge on yeast biochemistry of primary batch fermentation is detailed. Continuous beer fermentation processes are discussed later in separate sections.

2.2.1 Uptake of Wort Nutrients by Yeast

Brewer's wort is a complex and difficult to define mixture of components including sugars and carbohydrates, amino acids, peptides, proteins, vitamins, and ions which are discussed in the sections that follow.

2.2.1.1 Sugars and Carbohydrates

Brewer's wort contains the sugars sucrose, fructose, glucose, maltose and maltotriose as well as dextrin material. During batch fermentation, brewing yeast strains utilize sucrose, glucose, fructose, maltose and maltotriose in this approximate order, although some degree of overlap occurs. The majority of brewing strains leave the dextrans unfermented. Yeast cells are bounded by a cell wall and, within the wall, lies the yeast cell membrane. Most of the material dissolved in the wort liquid medium surrounding the yeast cells will diffuse freely through the cell wall to the cell membrane (Hough et al., 1982). The first step in the uptake of sugars by yeast is either the sugars passage intact across the cell membrane or its hydrolysis outside the cell membrane followed by entry into the cell by some or all of the hydrolysis products. Maltose and maltotriose are examples of sugars that pass intact across the cell membrane whereas sucrose is hydrolyzed by the extracellular enzyme invertase, and the hydrolysis products, glucose and fructose, are taken up into the cell. Maltose and maltotriose are the major sugars in brewer's wort and, once inside the cell, both sugars are hydrolyzed to glucose units by the alpha-glucosidase system (Lewis and Young, 1995). It is important to re-emphasize that the transport, hydrolysis and fermentation of maltose is particularly important in brewing, since maltose usually accounts for 50-60% of the fermentable sugar in wort.

Once the sugars are inside the cell, they are converted via the glycolytic pathway, also known as Embden-Meyerhof-Parnas (EMP) or glycolysis pathway, into pyruvate. Figure 2.2 shows the basic steps in the glycolytic pathway and where adenosine triphosphate (ATP) is broken down and created. This conversion to pyruvate generates a net total of 2 ATP molecules, which supply the yeast cell with energy (Hough et al., 1982). NAD^+ (nicotinamide adenine dinucleotide) is a cofactor for dehydrogenase enzymes controlling oxidative reactions in catabolism. Reduced NAD^+ (or NADH_2) is formed when electrons are transferred to NAD^+ as hydride ions $[\text{H}^-]$, seen in equation 2.1.

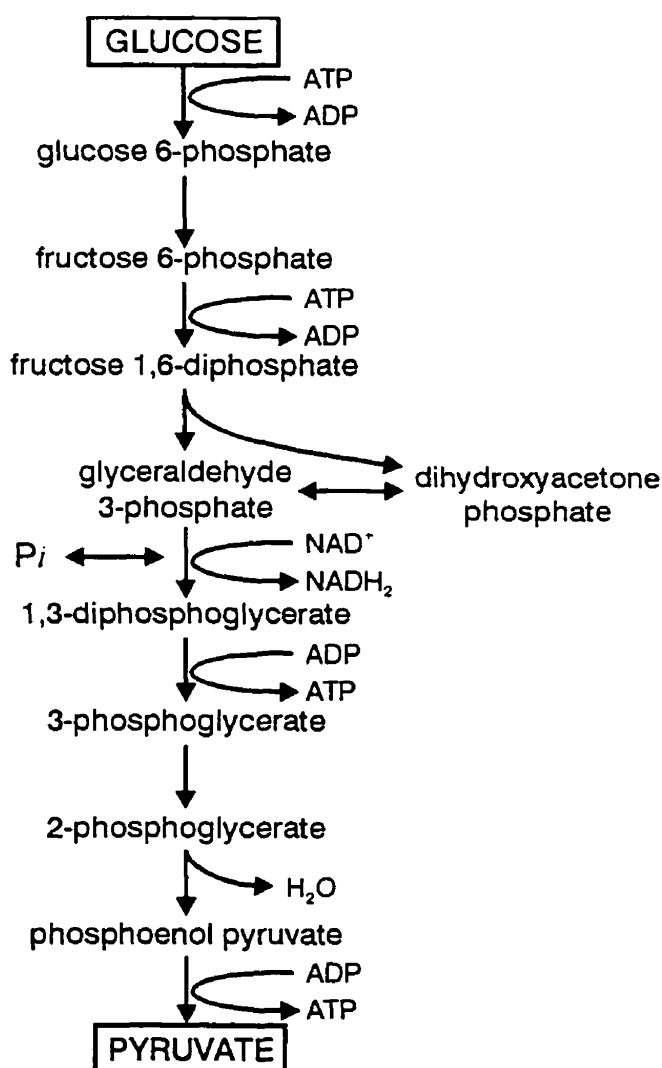
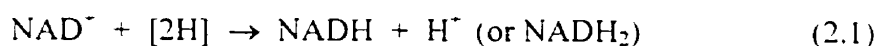
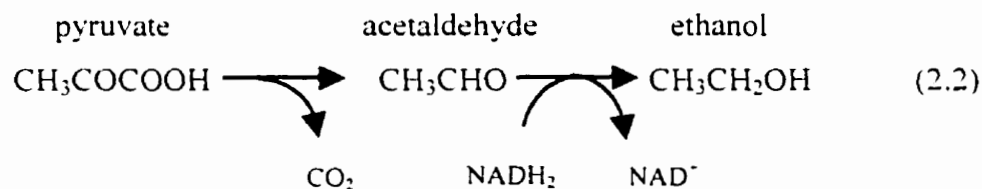


Figure 2.2. Embden-Meyerhof-Parnas (EMP, glycolysis, glycolytic) pathway (adapted from Hough et al., 1982).

When yeast are respiring in an aerobic environment, the Krebs cycle [also known as the tricarboxylic acid cycle (TCA)] and oxidative phosphorylation (also called the electron transfer chain) occurs. This massive electron transfer system produces large amounts of energy in the form of ATP. The synthesis of citrate, isocitrate and 2-oxoglutarate for nucleic acid and amino acid synthesis also occurs during the Krebs cycle and these organic acids will spill over into the fermented beer. The additional substrates that are generated from the Krebs cycle may be used to supply additional material for biosynthesis as seen in Figure 2.3. In respiring cells, molecular oxygen is used as the final hydrogen acceptor and glucose is completely oxidized. By the end of oxidative phosphorylation, one glucose molecule yields 2 ATP from the glycolytic pathway, 2 ATP from the Krebs cycle, and 24 ATP from oxidative phosphorylation. Thus, respiration of 1 glucose molecule yields 28 molecules of ATP overall. In respiring yeast, NAD^+ is regenerated using oxidative phosphorylation and the Krebs cycle (Aquila, 1997).

Under anaerobic conditions, the Krebs cycle may operate partially, but the extent of operation has yet to be determined. When yeast are in the fermentative state, NAD^+ is regenerated using a range of hydrogen acceptors as illustrated in Figure 2.4. Yeast are not tolerant of highly acidic environments for extended lengths of time. Pyruvic acid is converted to carbon dioxide and acetaldehyde and finally into ethanol, as in equation 2.2.



This serves two purposes, the cofactor NAD^+ molecules that were consumed during glycolysis are regenerated, and the yeast cell is detoxified by the conversion of pyruvic acid into carbon dioxide and ethanol. Other hydrogen acceptors used to restore the redox ratio of the cell include diacetyl, fumarate, oxaloacetate, aldehydes, and others (Lewis and Young, 1995).

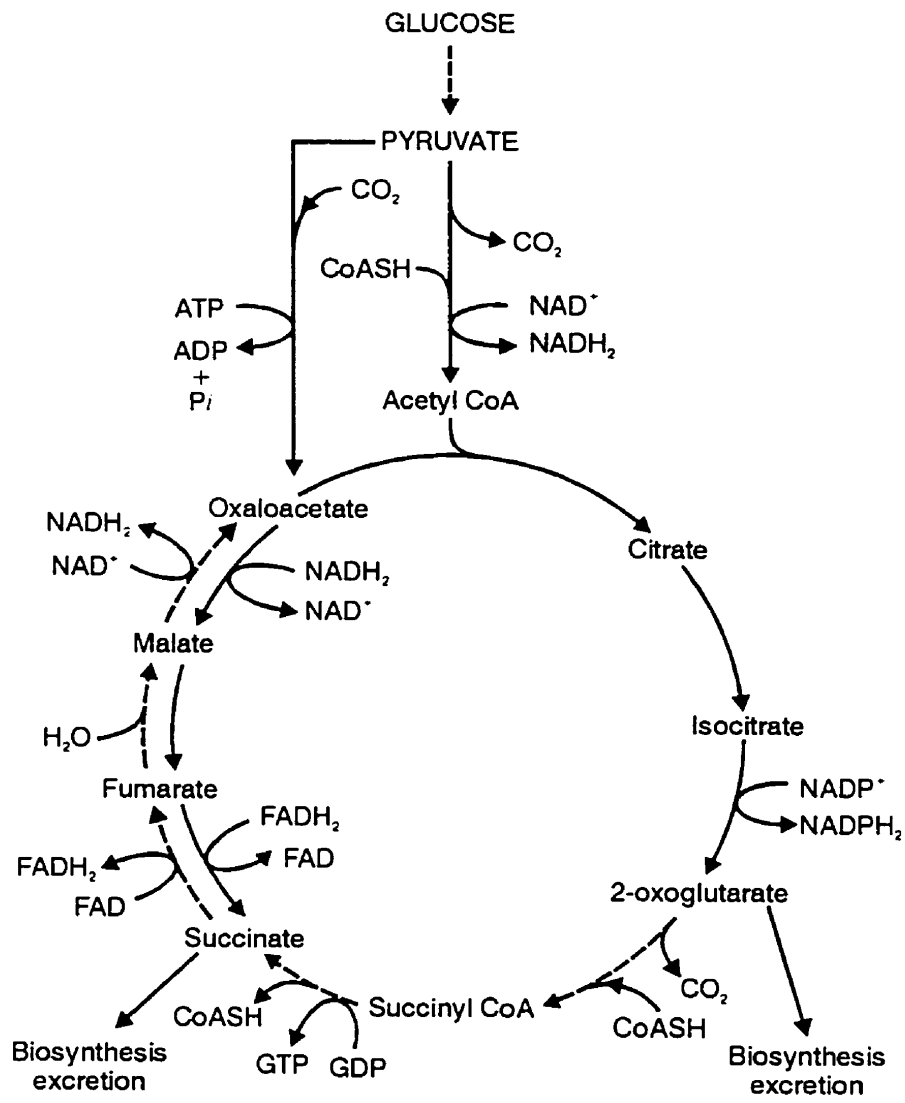


Figure 2.3. Krebs Cycle (adapted from Priest and Campbell, 1996).

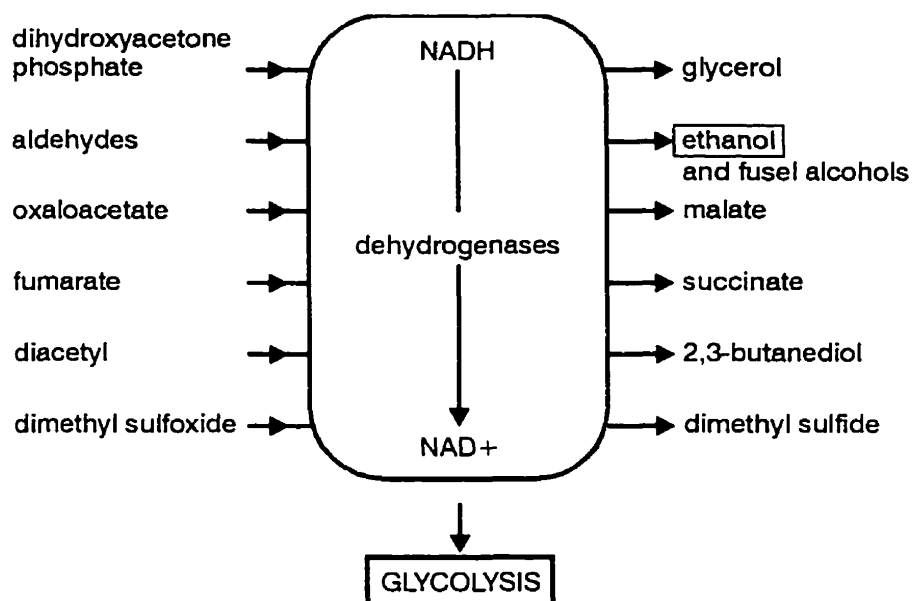


Figure 2.4. Regenerating NAD⁺ by fermenting yeast (adapted from Lewis and Young, 1995).

2.2.1.2 Control of Yeast Metabolism

Pasteur effect

If oxygen is introduced during fermentation, the yeast cell will revert to respiration. This means that pyruvate from glycolysis will move directly into the Krebs cycle and oxidative phosphorylation in the presence of glucose. In this case glucose is oxidized completely into carbon dioxide and water. A key observation of Pasteur was that the uptake of glucose is slower in respiring cells than in non-respiring (fermenting) cells. This is due to the fact that aerobic respiration produces more energy for the cell for each glucose molecule (or other carbon source) compared to fermentation, and therefore less substrate is needed to supply the yeast cell with a given amount of energy (Hough et al., 1982).

Crabtree effect (glucose repression, catabolite repression)

The Crabtree effect occurs when respiration is inhibited and fermentation occurs. Even if oxygen is present, if glucose levels are high, the fermentative pathway is used rather than the Krebs cycle. In *Saccharomyces cerevisiae*, a glucose sensitive yeast, respiration is repressed in the presence of a small [i.e. 0.4% (w/v)] concentration of glucose in the medium. This is regardless of the presence or absence of molecular

oxygen. During a typical brewery fermentation, wort contains about 1% glucose, so it can be assumed that the yeast cells are repressed. In the absence of repressive amounts of glucose and in the presence of molecular oxygen, glucose is completely oxidized to carbon dioxide and water through the glycolytic pathway and the Krebs cycle. Neither maltose nor maltotriose exhibits a repressive action on respiration.

This phenomenon may be explained somewhat by the model of Sols (Priest and Campbell, 1996). ATP has been shown to inhibit the enzyme 6-phosphofructokinase in the glycolytic pathway, whereas ADP and adenosine monophosphate (AMP) cause activation. Thus in high-energy situations (i.e. during respiration), the flux of glucose through the EMP pathway is lowered. Also, as ATP levels increase, the intracellular reserve of inorganic phosphate decreases and the operation of the glycolytic pathway also decreases, resulting in a lowered glucose flux.

Figure 2.5 shows how the glycolytic pathway and the Krebs cycle provide intermediates for biosynthetic reactions.

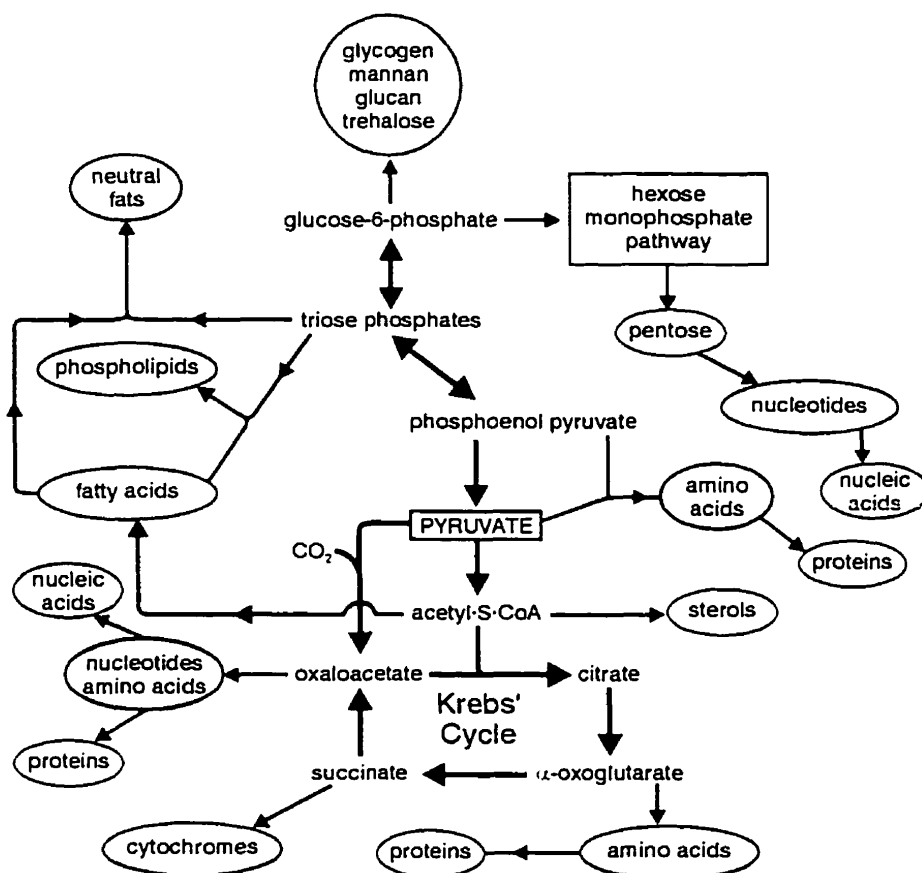


Figure 2.5. The contribution of carbohydrate catabolism to intermediate compounds for biosynthetic reactions (adapted from Hough et al., 1982).

2.2.1.3 Amino Acids, Peptides and Proteins

Active yeast growth involves the uptake of nitrogen, primarily as amino acids, for the synthesis of proteins and other nitrogenous compounds of the cell. Later in the fermentation as yeast multiplication stops, nitrogen uptake slows or ceases. In wort, the main nitrogen source for synthesis of proteins, nucleic acids and other nitrogenous cell components is the variety of amino acids formed from the proteolysis of barley proteins. Brewer's wort contains 19 amino acids and, as with wort sugars, the assimilation of amino acids is ordered. Four groups of amino acids have been identified on the basis of assimilation patterns (Table 2.1). Those in group A are utilized immediately following yeast pitching, whereas those in group B are assimilated more slowly. Utilization of

group C amino acids commences when group A types are fully assimilated. Proline, the most plentiful amino acid in wort and the sole group D amino acid, is utilized poorly or not at all (Jones and Pierce, 1964).

Table 2.1. Classification of amino acids according to their speed of absorption from wort by ale yeast under brewery conditions (adapted from Jones and Pierce, 1964).

A - Fast Absorption	B - Intermediate Absorption	C - Slow Absorption	D - Little or No Absorption
Glutamic acid	Valine	Glycine	Proline
Aspartic acid	Methionine	Phenylalanine	
Asparagine	Leucine	Tyrosine	
Glutamine	Isoleucine	Tryptophan	
Serine	Histidine	Alanine	
Threonine		Ammonia	
Lysine			
Arginine			

The metabolism of assimilated amino nitrogen is dependent on the phase of the fermentation and on the total quantity provided in the wort. The majority of amino nitrogen is ultimately utilized in protein synthesis and, as such, is vital for yeast growth. It is thought that amino acids are not usually incorporated directly into proteins but are involved in transamination reactions and a significant proportion of the amino acid skeletons of yeast protein are derived via the catabolism of wort sugars. This explains why the total amino content of wort is important in determining the extent of yeast growth, the amino acid spectrum being to some extent secondary.

The nitrogen obtained from the amino acids in wort is used to synthesize amino acids and ultimately proteins intracellularly. The yeast assimilates the wort amino acids and a transaminase system removes the amino group and the carbon skeleton is anabolised, creating an intracellular oxo-acid pool. The oxo-acid pool generated by the transaminases and anabolic reactions is a precursor of aldehydes and higher alcohols, which contribute to beer flavour. Thus the formation of higher alcohols (i.e. higher in number of carbon atoms than ethanol) is tied in with nitrogen metabolism.

Normally only the necessary amount of alpha-keto-acid (2-oxo-acid) is produced for the synthesis of required amounts of amino acids. The production is controlled by feedback inhibition of the required amino acid. However, as nitrogen shortage develops

later in the fermentation (e.g., by slow transfer of the remaining amino acids or by using wort with a high level of nitrogen free adjunct) feedback control deteriorates. Larger quantities of various keto- or oxo-acids are produced in an attempt to guarantee synthesis of missing amino acids. When the necessary nitrogen is not available, synthesis of missing amino acids is not possible and since accumulation of keto-acids is not tolerated by yeast, compounds are reduced to corresponding alcohols. Therefore higher alcohols of beer have structural similarity to amino acids. The reduction of a keto-acid to alcohol is the same as the mechanism of conversion as pyruvic acid to ethanol. Carbonyl by-products (for example, diacetyl) of the syntheses of certain of these keto-acids impart deleterious flavours to the beer if present in excess. A major aim of fermentation management is to ensure that these carbonyls are present at an appropriate concentration in the finished beer. This will be facilitated if the wort contains a suitable amino acid profile (Hough et al., 1982).

Thus the amino nitrogen composition of wort has a profound impact upon fermentation performance and on beer flavour. Where malt is used as the principal source of extract, the quantity and composition of amino acids are such that these problems are usually not encountered. However, care must be exercised when using adjuncts, many of which are relatively deficient in amino nitrogen.

2.2.1.4 Oxygen Requirements

Wort fermentation in beer production is largely anaerobic, but when the yeast is first pitched into wort, some oxygen must be made available to the yeast. Oxygen must be excluded, as far as it is possible, from all other parts of the process because it will have a negative effect on beer quality, particularly flavour stability (Takahashi and Kimura, 1996).

Oxygen has a marked influence on yeast activity and especially on yeast growth. Certain yeast enzymes only react with oxygen and other hydrogen acceptors cannot replace it. This applies to the oxygenases involved in the synthesis of unsaturated fatty acids and sterols, which are vital components of cell membranes. The traditional concept of beer fermentation was that growth occurred prior to the fermentation of most wort sugars and that non-growing, stationary phase cells carried out the fermentation. It is now

known that yeast growth, sugar utilization and ethanol production are coupled phenomena. For a brewery fermentation to proceed rapidly there must be sufficient amounts of yeast propagated. Inadequate growth of a brewer's yeast culture will result in poor attenuation, altered beer flavour, inconsistent fermentation times and recovered pitching yeasts which are unsuitable for subsequent fermentations (Hardwick, 1995).

Trace amounts of oxygen have profound stimulatory effects on yeast fermentation and particularly on yeast growth. Oxygen is necessary for normal yeast reproduction, although excessive wort aeration during batch fermentation causes undesirable flavour effects on the finished beer. Over-vigorous aeration of fermenting worts can lead to yeast "weakness", illustrated by increasingly sluggish fermentations characterized by longer lag phases, a slower specific rate of fermentation and/or residual sugar remaining in the final beer. Sterols and unsaturated fatty acids are both found in cell membranes and are critical for membrane function and integrity. Both of these lipid classes require molecular oxygen for their biosynthesis (Hough et al., 1982).

Lipids in beer quantitatively form an almost negligible component, but can influence both its organoleptic and physio-chemical properties. Malt is the main source of unsaturated fatty acids in wort. Wort concentrations of these acids are sub-optimal and can be growth-limiting. During fermentation, yeast can take up free fatty acids from wort, most of which are incorporated as structural lipids. Fatty acid composition is an extremely important variable in determining yeast membrane structure, morphology and function.

Ergosterol is the major sterol in brewing yeast strains and can account for over 90% of the total sterol. The biosynthetic pathway for sterol formation is complex. The ergosterol precursor sequences can be synthesized anaerobically, but the final reaction step requires molecular oxygen. The major function of sterols in yeast is to contribute to the structure and dynamic state of the membranes by modulating membrane fluidity under fluctuating environmental conditions (Lewis and Young, 1995).

Pitching yeasts are normally propagated under weakly aerated conditions or recovered from previous fermentations. In both cases, the cells are lipid-depleted and to promote normal growth and attenuation either pre-formed lipids must be added to the wort, or oxygen must be made available for lipid synthesis. In commercial brewing, only

the second alternative is feasible. Wort is cooled and aerated or oxygenated to 8-18 mg/L dissolved oxygen. Within a few hours of pitching, this oxygen is removed from the wort. During this time there is intensive synthesis of lipids (sterol and fatty acid) by the yeast (Hardwick, 1995).

There is a relationship between wort trub levels and wort dissolved oxygen at pitching. Trub contains high concentrations of unsaturated fatty acids, particularly linoleic acid. This linoleic acid is absorbed by yeast and has a negative effect on ester production (Lentini et al., 1994). In a similar manner, high concentrations of oxygen have a similar negative effect on ester production. The role of linoleic acid in ester biosynthesis is not fully understood but it has been suggested that it plays a role in modifying membrane structure and affects ester synthesizing enzymes, some of which are membrane bound.

2.2.1.5 Vitamin Requirements

Yeast vary widely in their need for vitamins for metabolism and, in a given strain, this need may also vary between active respiration and growth on the one hand, and alcoholic fermentation on the other. Almost all vitamins (except mesoinositol) required by yeast function as a part of a coenzyme, serving a catalytic function in yeast metabolism (Hough et al., 1982).

2.2.1.6 The Role of Ionic Species

Yeast requires a number of inorganic ions for optimum growth and fermentation. Appropriate concentrations of these elements allow for accelerated growth and increased biomass yield, enhanced ethanol production, or both with a higher final substrate to product yield. An imbalance in inorganic nutrition is reflected in complex, and often subtle, alterations of metabolic patterns and growth characteristics (for example, cellular morphology, tolerance to the environment and by-product formation) (Jones et al., 1981; Jones and Greenfield, 1984). The role played by these ionic species is both enzymatic and structural. Table 2.2 summarizes key roles of some ionic species utilized by yeast.

Table 2.2. Ionic nutrients required by brewing yeast (adapted from Jones et al. 1981; Jones and Greenfield, 1984).

Ion	Function in yeast cells
Mg ²⁺	Stimulation of synthesis of essential fatty acids Alleviation of inhibitory heavy metal effects Regulation of cellular ionic levels Activation of membrane ATPase Maintain membrane integrity and permeability
K ⁺	Central component in the regulation of divalent cation transport Essential for the uptake of H ₂ PO ₄ ⁻ Potent stimulator of glycolytic flux → significantly increases the levels of ATP, NAD(P)H, ADP and P _i
Zn ²⁺	Essential cofactor in a number of important metabolic enzymes, e.g. alcohol dehydrogenase Enhances riboflavin synthesis, activates acid and alkaline phosphatases Helps increase protein content of fermenting cells
Ca ²⁺	Not a requirement but may stimulate cell growth Protects membrane structure and helps maintain membrane permeability under adverse conditions Counteracts magnesium inhibition Plays an important role in flocculation
Mn ²⁺	Essential in trace amounts for yeast growth and metabolism Helps to regulate the effects of Zn ²⁺ Stimulates the synthesis of proteins and biosynthesis of thiamine
Cu ²⁺	Essential as an enzyme cofactor
Fe ²⁺	Small amounts required for the function of haeme-enzymes

2.2.2 Yeast Excretion Products

The following sections describe the key excretion products from yeast during the fermentation of wort to produce beer.

2.2.2.1 Ethanol

Although ethanol is one of the major excretion products made by yeast during wort fermentation, this primary alcohol has little impact on the flavour of the final beer with the exception of providing a warming effect. It also influences the extent to which other molecules contribute to flavour. The type and concentration of the many other yeast excretion products produced during wort fermentation primarily determine the flavour of the beer (Meilgaard, 1982). The formation of these excretion products depends on the overall metabolic balance of the yeast culture, and there are many factors that can alter this balance and consequently beer flavour. Yeast strain, fermentation temperature, adjunct type and level, fermenter design, wort pH, buffering capacity, wort gravity, etc., are all influencing factors.

Some volatiles are of great importance and contribute significantly to beer flavour, whereas others are important in building background flavour. The following groups of substances are found in beer: organic and fatty acids, alcohols, esters, carbonyls, sulphur compounds, amines, phenols and a number of miscellaneous compounds.

2.2.2.2 Organic and Fatty Acid Production

Some 110 acids, both organic and short-to medium-chain-length fatty acids are present in beer. In part these are derived from malt or other wort constituents, but a proportion arise during fermentation as a result of yeast metabolism. Organic acids contribute to the decrease in pH observed during fermentation and many are flavour-active. They arise from carbohydrate metabolism and include pyruvate, succinate, citrate, and acetate. It is presumed that most of these arise as a consequence of the incomplete tricarboxylic acid cycle, which occurs under anaerobic conditions. It has been observed that pyruvate is secreted into the wort during the active fermentation phase and that in later stages, when yeast growth has ceased, it is re-utilized and the accumulation of acetate occurs. This observation provides evidence for the overspill model of ethanol formation (Lewis and Young, 1995), previously discussed (Section 2.2.1.1). Thus, for pyruvate secretion to occur it would suggest that under conditions of high glycolytic flux the pathways devolving from pyruvate are rate-determining.

2.2.2.3 Production of Higher Alcohols

The flavour-active higher alcohols, also called fusel oils, that occur in beer and many spirits include n-propanol, isobutanol, 2-methyl-1-butanol and 3-methyl-1-butanol. However, more than 40 other alcohols have been identified. Regulation of the biosynthesis of higher alcohols is complex as seen in Figure 2.6, since they may be produced as by-products of amino acid catabolism or via pyruvate derived from carbohydrate metabolism.

The catabolic route, which is defined as a biochemical process in which organic compounds are metabolized (usually an energy-liberating process), involves a pathway in which the keto-acid produced from an amino acid transamination is decarboxylated to the corresponding aldehyde, then reduced to the alcohol via an NAD-linked dehydrogenase. In this way, for example, isobutanol may be produced from valine, 3-methyl-1-butanol from leucine and 2-methyl-1-butanol from isoleucine.

The anabolic route, which is defined as a biochemical process involving the synthesis of organic compounds and usually utilizes energy, uses the same pathways as those involved in the biosynthesis of amino acids. As in the catabolic route, the keto-acid intermediate is decarboxylated and the resultant aldehyde reduced to the alcohol.

The relative contribution made by the two pathways varies with individual higher alcohols. Since there is no corresponding amino acid, the anabolic route would seem to be the sole mechanism for the formation of n-propanol. In general, the catabolic route would seem to predominate during the early growth phase when exogenous amino nitrogen is plentiful. In the later stages when the wort becomes deficient in assimilable nitrogen, the anabolic route is probably the major source of higher alcohols.

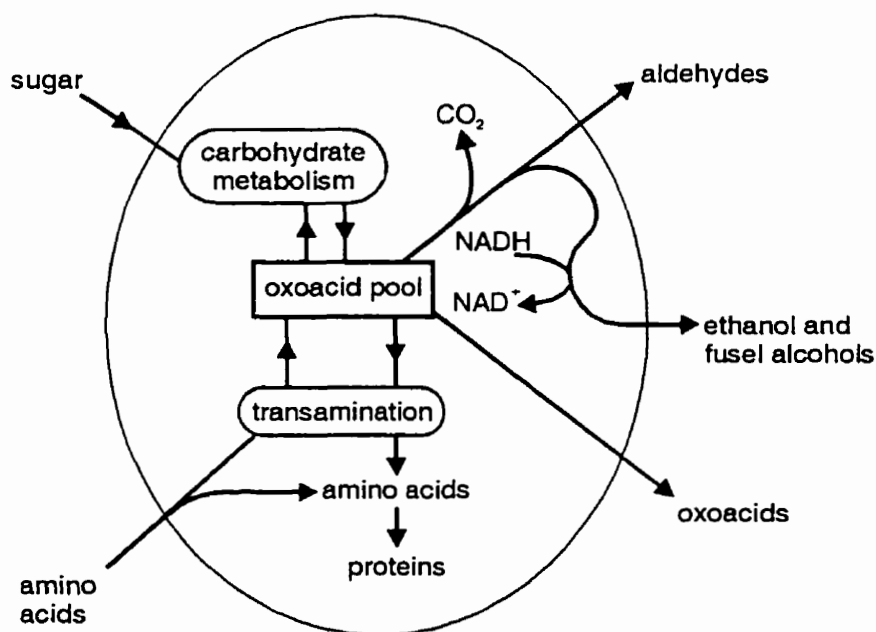


Figure 2.6. Production of higher alcohols (adapted from Lewis and Young, 1995).

The total concentration of higher alcohols produced during fermentation is linearly related to the extent of yeast growth. Thus, conditions that promote growth, such as increased provision of oxygen, will result in increased production of higher alcohols (Kunze, 1996). Similarly, supplementation of worts with additional amino nitrogen also results in stimulation of higher alcohol synthesis. In this case the nature of the amino acids present is reflected in the spectrum of higher alcohols produced. Application of pressure during fermentation, which may be accomplished by restricting the release of evolved carbon dioxide, results in reduced yeast growth and is accompanied by a similar reduction in the extent of higher alcohol formation.

2.2.2.4 Ester Production

Esters are important flavour components, which impart flowery and fruit-like flavours and aromas to beers. Their presence is desirable at appropriate concentrations but failure to properly control fermentation can result in unacceptable beer ester levels. Organoleptically important esters include ethyl acetate, isoamyl acetate, isobutyl acetate, ethyl caproate and 2-phenylethyl acetate (Meilgaard, 1982). In total, over 90 distinct esters have been detected in beer.

Many factors, in addition to the yeast strain employed, have been found to influence the amount of esters formed (Stewart et al., 1999) during a wort fermentation: wort composition (lipids amino acids, vitamins, inorganic nutrients, sugars, dissolved oxygen, trub, original specific gravity) and fermentation conditions (temperature, agitation, pH, pitching rate). Low levels of oxygen appear to enhance stimulate ester formation (Kunze, 1996).

Esters arise as a result of a reaction between an alcohol, which may be ethanol or of longer-chain-length, and a fatty acyl-CoA ester. The reaction is catalyzed by an alcohol acetyl transferase. The acyl- component of the activated fatty acid may be acetate, produced by the action of pyruvate dehydrogenase or it may be derived from the activation of wort fatty acids, from oxo-acids by oxidative decarboxylation, from the catabolism of fats, or from the biosynthesis of fatty acids (Hough et al., 1982).

The spectrum of esters produced is largely strain-specific. This may reflect the presence of a family of alcohol acetyl transferases with different substrate specificities. The relative activities of these enzymes will depend, to some extent on the availability of the respective substrates. The rate of formation and type of ethyl ester produced is influenced by the availability of the respective fatty acids. In the case of the synthesis of acetate esters, the availability of the corresponding higher alcohol is important.

An increase in the concentration of oxygen supplied at pitching is associated with a progressive decline in the ester content of the final beer. It is assumed that since increased oxygen availability promotes greater yeast growth, more of the acetyl-CoA pool is utilized in biosynthetic reactions, as seen in Figure 2.7, thereby restricting that available for ester synthesis (Hough et al., 1982). Norton and D'Amore (1994) have also stated that the concentration of esters decreases with an increase in oxygen availability because ester formation is catalysed by acetyl transferase. Acetyl transferase is inhibited by unsaturated fatty acids and ergosterol, which in turn will increase in the presence of oxygen.

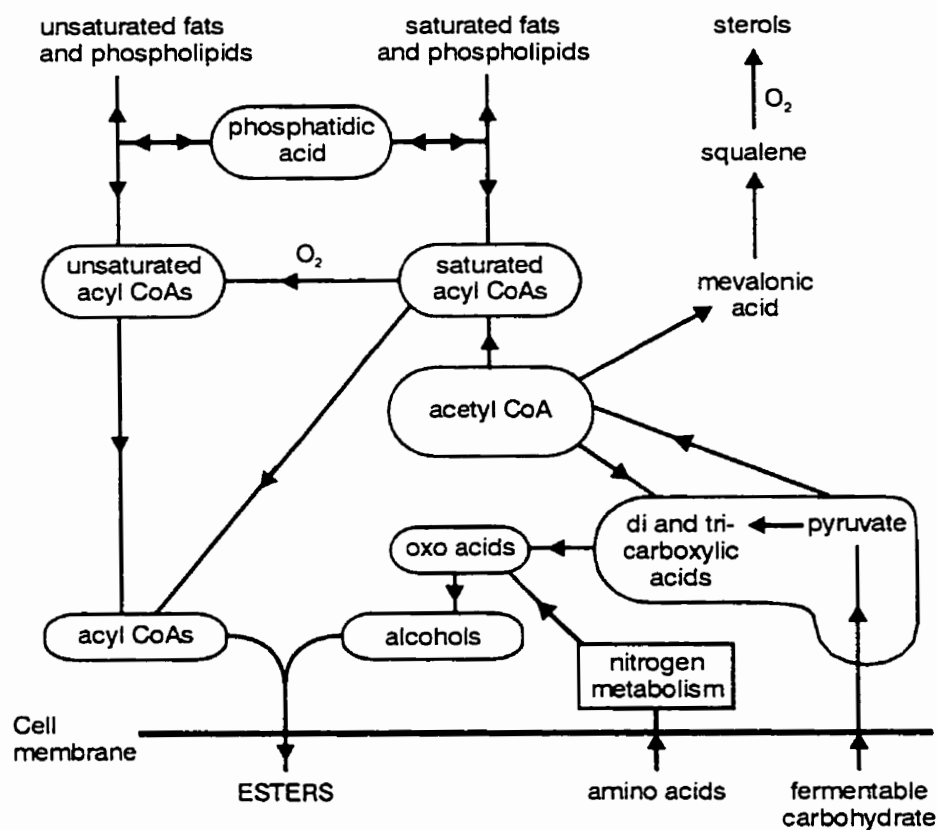
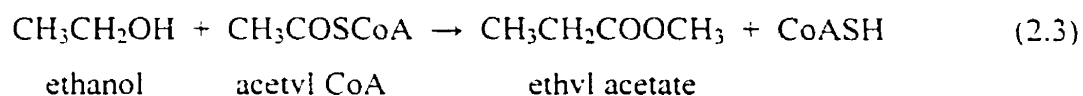


Figure 2.7. Metabolic interrelationships leading to ester formation (adapted from Hough et al., 1982).

Practical measures which can be taken to reduce overly high ester levels (particularly in high gravity worts) include using wort with a suitably low carbon to nitrogen ratio and an adequate supply of oxygen, both of which promote yeast growth and minimize ester synthesis. The application of pressure during fermentation also reduces both yeast growth and ester synthesis (Kunze, 1996). Likely reasons for this effect would appear to be that intracellular carbon dioxide accumulates causing a decrease in cellular pH control and a disruption of enzyme function. The ionic composition of wort may influence ester synthesis. Zinc, which as previously discussed is often added to wort to ensure adequate yeast growth, may also encourage the formation of the acetate esters of higher alcohols. The effect is probably a consequence of zinc stimulating the production of the higher alcohol from the corresponding oxo-acid, thereby increasing the supply of precursors for subsequent ester synthesis.

The major metabolic pathways that control ester synthesis in yeast are outlined in Figure 2.7. From this figure and from equation 2.3 below, it can be seen why ethyl acetate is the most common ester produced by yeast (Lewis and Young, 1995). This is due to the fact that the most common alcohol in yeast is ethanol, which is the alcoholic precursor of ethyl acetate. Esters of higher alcohols and ethyl esters of long-chain fatty acids are also common.



2.2.2.5 Carbonyls

Over 200 carbonyl compounds are reported to contribute to the flavour of beer. As a result of yeast metabolism during fermentation, various aldehydes and vicinal diketones, notably diacetyl are produced. Carbonyl compounds exert a significant influence on the flavour stability of beer. Excessive concentrations of carbonyl compounds are known to cause stale flavours in beer. The effects of aldehydes on flavour stability are reported as grassy notes (propanol, 2-methyl butanol, pentanol) and papery tastes (*trans*-2-nonenal, furfural) (Meilgaard, 1982).

Quantitatively, acetaldehyde is the most important aldehyde. It is produced via the decarboxylation of pyruvate and is an intermediate in the formation of ethanol. It may be present in beer at concentrations above its flavour threshold, at which it imparts a "grassy" or "green apple" character. Acetaldehyde accumulates during the period of active growth in batch fermentations. Levels usually decline in the stationary phase of growth late in fermentation. As with higher alcohols and esters, the extent of acetaldehyde accumulation is determined by the yeast strain and the fermentation conditions. Although the yeast strain is of primary importance, elevated wort oxygen concentration, pitching rate and temperature all favour acetaldehyde accumulation. In addition, the premature separation of yeast from fermented wort does not allow the re-utilization of excreted acetaldehyde associated with the latter stages of fermentation (Kunze, 1996).

Other important flavour-active carbonyls, whose presence in beer is established in the fermentation stage, are the vicinal diketones, diacetyl (2,3-butanedione) and 2,3-

pentanedione. Both compounds impart a "butterscotch" flavour and aroma to beer. Diacetyl is very important since its flavour threshold is ten-fold lower than that of 2,3-pentanedione (Meilgaard, 1982). The organoleptic properties of higher levels of vicinal diketones contribute to the overall palate and aroma of some ales but in most lagers they impart an undesirable character. A critical aspect of the management of lager fermentations and subsequent processing is to ensure that the mature beer contains concentrations of vicinal diketones lower than the flavour threshold.

Diacetyl and 2,3-pentanediones arise in beer as by-products of the pathways leading to the formation of valine and isoleucine (Figure 2.8). The alpha-acetohydroxy acids, which are intermediates in these biosyntheses, are in part excreted into the fermenting wort. Here they undergo spontaneous oxidative decarboxylation, giving rise to vicinal diketones. Further metabolism is dependent on yeast dehydrogenases. Diacetyl is reduced to acetoin and ultimately 2,3-butanediol, as in Figure 2.9 and 2,3-pentanedione to its corresponding diol (Hough et al., 1982). The flavour threshold concentrations of these diols are relatively high and, therefore, the final reductive stages of vicinal diketone metabolism are critical in order to obtain a beer with acceptable organoleptic properties.

The diacetyl concentration peak in batch fermentations occurs towards the end of the period of active growth. The reduction of diacetyl takes place in the latter stages of fermentation when active growth has ceased (Kunze, 1996). In terms of practical fermentation management the need to achieve a desired diacetyl specification is often the factor used to determine when the beer is to be moved to the conditioning phase and filtered or centrifuged (depending on the processing procedures). Thus, diacetyl metabolism is an important determinant of overall vessel residence time, which affects plant capacity.

The concentration of diacetyl present in the fermenting wort is a function of the rate formation of the diacetyl precursor, alpha-acetolactate, and the oxidative decarboxylation of the precursor to form diacetyl and the consequent reduction of diacetyl to acetoin. These reactions are influenced by the yeast strain, the wort composition, the type of fermenting vessel employed and the fermentation conditions. Fermentation conditions that favour yeast growth rate, and consequently an increased requirement for amino acid biosynthesis from pyruvate, would be expected to lead to

elevated levels of alpha-acetolactate. These conditions include high temperatures and pitching rates and an increased level of wort oxygen, but may be modulated by wort composition. Consequently, when the assimilable amino-nitrogen level is high, there will be a reduced requirement for amino acid synthesis and potentially a lower level of alpha-acetolactate. In addition, the presence of valine and isoleucine specifically inhibits the formation of alpha-acetohydroxy acids (Nakatani et al., 1984a; Nakatani et al., 1984b).

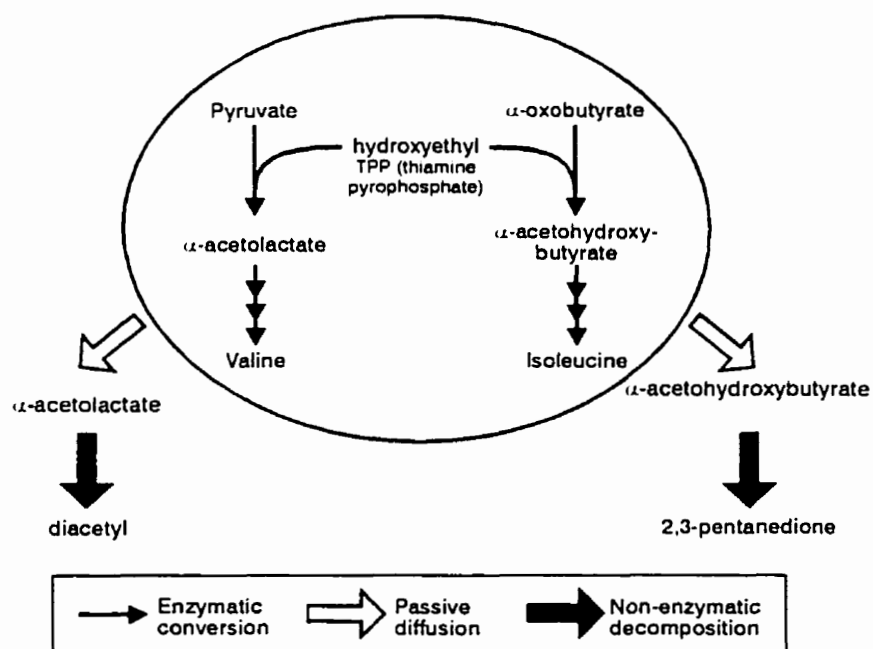


Figure 2.8. Formation of diacetyl and 2,3-pentanedione as by-products of pathways leading to the formation of the amino acids valine and isoleucine (adapted from Hough et al., 1982).

Higher levels of alpha-acetolactate in fermented wort do not always lead to high diacetyl concentrations in beer. The non-enzymatic oxidative decarboxylation of alpha-acetolactate is the rate-determining step in the diacetyl cycle. The presence of oxygen is not essential since metal ions such as Cu^{2+} , Fe^{3+} and Al^{3+} may serve as alternative electron donors. The rate of formation of diacetyl from alpha-acetolactate is influenced by pH. Within the range encountered in fermenting wort, a low pH promotes diacetyl formation but high wort pH's (>5.3) at pitching will promote yeast growth and elevated levels of alpha-acetolactate and potentially, therefore, diacetyl formation.

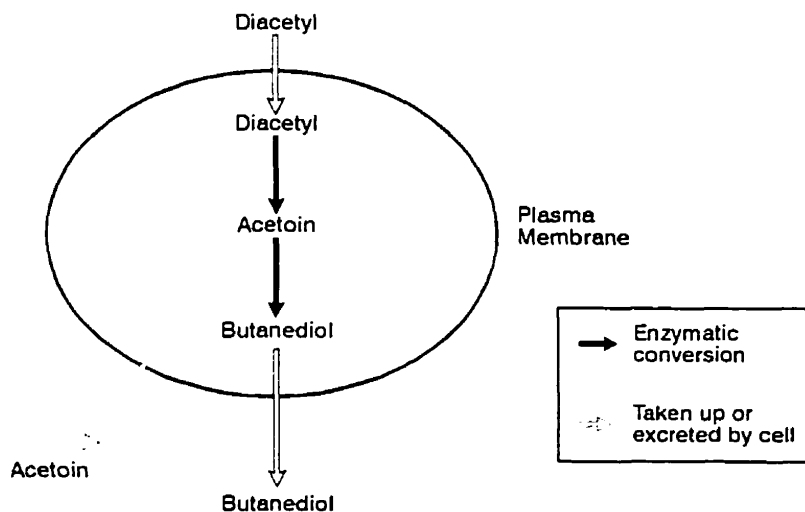


Figure 2.9. Reduction of diacetyl to acetoin and 2,3-butanediol (adapted from Russell and Stewart, 1992).

The reduction of vicinal diketones in the later stages of fermentation and during maturation requires the presence of adequate yeast in suspension in the fermented wort. Thus, where the yeast is particularly flocculent, premature separation may be accompanied by low rates of diacetyl reduction and potentially elevated levels in finished beer. Diacetyl removal is also affected by the physiological condition of the yeast. When the pitching yeast is in poor condition, such that the primary fermentation performance is suboptimal, the yeast present during the latter stages will be stressed and the period of diacetyl reduction prolonged (Kunze, 1996).

A number of strategies can be adopted to ensure that beer diacetyl specifications are achieved. Diacetyl removal can be attained post-fermentation in the conditioning stages of brewing, which is the basis for traditional lagering. This is a slow process, expensive in terms of time and conditioning capacity. Alternatively, one can ensure that minimum diacetyl concentrations are achieved before the beer is removed from the fermenter. It is necessary to select fermentation conditions such as pitching rate, wort dissolved oxygen and attemperation regimes, which provide an optimum profile. In practice, the aim is to promote the maximum alpha-acetolactate levels as early as possible, so that the resultant diacetyl may be rapidly reduced due to the presence of an

elevated suspended yeast count. Increasing the fermentation temperature approximately two-thirds through the fermentation cycle also stimulates this reductive phase.

There are a number of novel methods that are currently being developed to control beer diacetyl levels (Inoue, 1992). One involves the use of immobilized yeast technology (Pajunen et al., 1987). Research has also been conducted on the genetic modification of brewer's yeast strains in order to reduce their diacetyl formation potential. The third strategy involves the enzyme alpha-acetolactate decarboxylase which catalyses the direct formation of acetoin from alpha-acetolactate. Several bacterial species possess this enzyme activity but it is not present naturally in brewing yeast strains. The alpha-acetolactate decarboxylase gene has been isolated from *Acetobacter sp.* (the bacteria employed for vinegar manufacture) and inserted into brewing yeast. The fourth strategy involves the addition of the enzyme alpha-acetolactate decarboxylase, to the cold wort prior to fermentation. This enzyme transforms the acetolactate directly into acetoin, thus by-passing the diacetyl stage (Jepsen, 1993). Researchers have also examined the potential of immobilizing the enzyme alpha-acetolactate decarboxylase, thus allowing for its subsequent removal and reuse (Dulieu et al., 1996).

2.2.2.6 Sulphur Compounds

Sulphur compounds make a significant contribution to the flavour of beer. Although small amounts of sulphur compounds are acceptable or even desirable in beer, in excess they give rise to unpleasant off-flavours, and special measures such as purging with CO₂, or prolonged maturation times, are necessary to remove them. Many of the sulphur compounds present in beer are not directly associated with fermentation but are derived from the raw materials employed. However, the accumulation of hydrogen sulphide (rotten egg aroma) and sulphur dioxide (burnt match aroma) are dependent on yeast activity. Failure to manage fermentation properly can result in unacceptably high levels of these compounds occurring in the finished beer (Hough et al., 1982).

Dimethylsulphide (DMS) is one of the major flavour congeners found in continental European lager beers. This compound has the aroma characteristics of cooked corn (maize) or garlic. In beer it originates from two primary sources: the hydrolysis of malt S-methylmethionine (SMM) during mashing and from the reduction of

dimethylsulphoxide (DMSO) by yeast. Normally, the majority of the DMS is produced by yeast and 80% of that DMS comes from the DMSO in the wort. Malt variety has a direct influence on DMSO levels in wort (Hough et al., 1982).

To conclude section 2.2, Figure 2.10 summarizes the major metabolic interrelationships in yeast affecting the formation of beer flavour compounds.

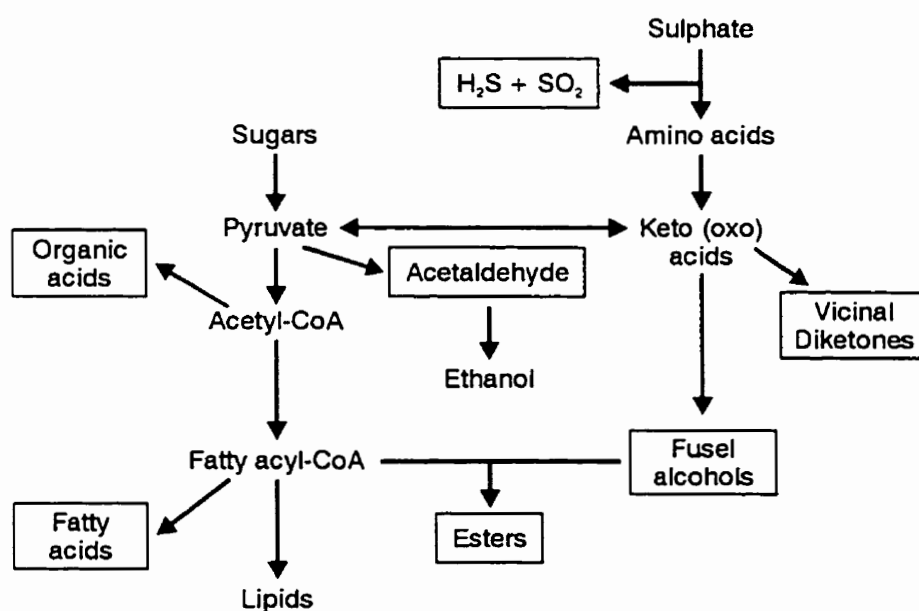


Figure 2.10. Interrelationship between yeast metabolism and production of beer flavour compounds (adapted from Hough et al., 1982).

¹2.3 Continuous Fermentation Using Immobilized Yeast Cells

In this section fundamental aspects of continuous fermentation using immobilized yeast cells for beer fermentation are reviewed.

2.3.1 Practical Importance of Cell Immobilization

Producing an alcoholic beverage such as beer using a continuous fermentation system offers several important advantages over the commonly used batch systems:

- a more uniform product;
- less process supervision;
- very high bioreactor volumetric productivity (product weight/unit time/unit bioreactor volume).

Immobilization may be used as a tool to confine intact cells to an inert carrier within a bioreactor. This "tool" will further increase the efficiency of a continuous fermentation system (Atkinson, 1986; Karel et al., 1985; Mensour et al., 1996) by providing:

- high cell densities per unit bioreactor volume which result in very high fermentation rates;
- the reuse of the same biocatalysts (yeast cells) for extended periods of time due to constant cell regeneration;
- easy separation of biocatalyst from the liquid phase where the desired products are present thus minimizing separation costs;
- improved tolerance or protection of cells from product inhibition;
- smaller bioreactor volumes which may lower capital costs.

Continuous fermentation using immobilized cells also allows for efficient plant utilization during peak sales periods. Continuous smaller-scale high rate fermentation systems can be stepped up to meet peak output when required. This is an improvement over the current technology, which utilizes large batch fermenters which are useful during peak production times, but are underutilized during off-times (Dunbar et al., 1988). It was also observed that immobilized cells are less susceptible than free cells to

¹ A version of section 2.4 has been published (Pilkington et al., 1998b).

the effects of certain inhibitory compounds, pH variations, and nutrient depletion (Cho et al., 1982; Margaritis and Wallace, 1982; Norton et al., 1995).

The process advantages offered by continuous fermentation will have a pronounced impact on the brewing industry. The traditional beer production process is operated in batch mode using free cells and it generally takes 5-7 days to complete primary fermentation. Initial studies show that a continuous immobilized cell system can reduce the time required for primary fermentation to as little as one day (Mensour et al., 1997). Coupled with a heat treatment process, maturation using immobilized cells has shortened the process from 5-21 days to 2 hours (Dillenhoffer and Ronn, 1996).

Many obstacles must be overcome to bring this continuous process to industrial fruition. Through multi-staged systems, some research groups have successfully produced a beer of acceptable quality using continuous fermentation. However, many of these systems are extremely complex and do not lend themselves to scale up or implementation in a location where sophisticated technical assistance is not available. Ideally, an industrial scale continuous beer fermentation system should be simple, robust, and not labour intensive to operate.

Other aspects of immobilized systems requiring more research before continuous fermentation becomes a viable industrial alternative to batch beer fermentation include:

- Process contamination may require that production be stopped, equipment sterilized and restarted. This could be a disadvantage if continuous fermentation startup time is significant;
- When the goal of the immobilized cell process is to produce an exact flavour match to an existing batch-produced beer, additional difficulty is added;
- New and unique challenges will be encountered when trying to produce a range of different products using immobilized cells. In order to avoid stopping and restarting a continuous immobilized cell process with new yeast, different products would have to be produced by using different worts or by further modifications downstream of primary fermentation;
- The addition of an immobilization matrix to the process could add complexity in terms of handling, shipping, costs, sanitation, and selection of the most suitable matrix for the bioreactor system being used;

- New scientific techniques continue to need further development for the study of the effects of immobilization on yeast cell metabolism and physiology.

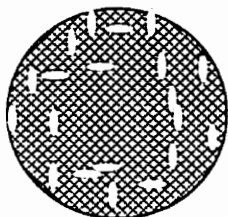
2.3.2 Properties of Immobilized Cell Systems

Whole-cell immobilization is defined as the localization of intact cells to a defined region of space with the preservation of catalytic activity (Karel et al., 1985). An immobilized cell system is described by Abbott (1978) to be any system in which microbial cells are confined within a bioreactor, thus permitting their reuse. Methods of immobilization include physical entrapment within a porous matrix, attachment or adsorption to a pre-formed carrier, self aggregation by flocculation or crosslinking agents, and cells contained behind a barrier. All of these methods have a similar purpose: to retain high cell concentrations within the bioreactor, leading to increased volumetric productivity of the system and lowered fermentation costs. Figure 2.11 illustrates basic immobilization techniques.

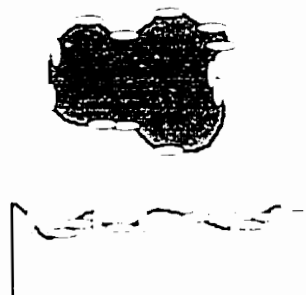
An immobilized cell system should have the following properties for large scale industrial application:

- the system should be simple, efficient, easy to operate and give good yields;
- the carrier material must be nontoxic, readily available and affordable;
- the carrier material should allow for high cell loading and physical strength;
- the cells should have a prolonged viability in the support.

(a) Cells entrapped or encased in a matrix



(b) Adsorption or attachment to a preformed carrier



(c) Self aggregation of cells



(d) Cells encapsulated or contained behind a barrier

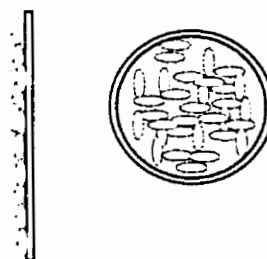


Figure 2.11. Basic methods of cell immobilization.

2.3.2.1 Physical Entrapment within a Porous Matrix

The entrapment of immobilized cells within a porous polymeric matrix such as calcium alginate (Bejar et al., 1992; Curin et al., 1987; Masschelein et al., 1985; Nakanishi et al., 1986; Nedovic et al., 1996; Pajunen et al., 1987; Ryder, 1985; Shindo et al., 1994; White and Portno, 1978) or kappa-carrageenan (Norton and D'Amore, 1994; Wang et al., 1982), along with some others (Gopal and Hammond, 1993; Okazaki et al., 1995), has been studied extensively. Polymeric beads are usually spherical with diameters ranging from 0.3 to 3.0 mm. Immobilizing yeast cells using entrapment is a relatively simple method and a high biomass concentration is facilitated. Margaritis et al. (1987) reported one of the first pilot scale gas-lift draft tube bioreactor systems, using immobilized yeast in calcium alginate beads to produce ethanol in repeated fed-batch operation.

Some researchers have moved away from entrapment matrices and are currently focusing on adsorption techniques for several reasons. At present, gel entrapment matrices are not produced economically on an industrial scale. Diffusion limitations due to the gel matrix and high biomass loadings can cause metabolite concentration gradients within the polymer beads. The concept of utilizing the different microenvironments within a gel entrapment matrix is being studied for wastewater treatment systems by dos Santos et al. (1996) who refer to the "magic bead concept" in which the nitrifying bacterium *Nitrosomonas europaea* and the denitrifier *Paracoccus denitrificans* are co-immobilized in double-layer gel beads. It was found that oxygen (de Beer et al., 1993; Hooijmans et al., 1990; Kurosawa and Tanaka, 1990; Wijffels et al., 1995), due to limitation of its uptake and diffusion, rarely penetrates greater than a few hundred micrometers into the gel bead when it is the limiting substrate. Thus, in a single-stage continuous air lift reactor, the aerobic nitrification step was carried out in the outer layer while the anaerobic denitrification took place in the bead core (dos Santos et al., 1996). This result may prove to be useful for achieving aerobic and anaerobic stages during beer fermentation.

Another limitation of gel entrapment includes the loss of gel mechanical integrity, by dissolution or by breakdown due to abrasion, compression, or internal gas accumulation (Gopal and Hammond, 1993). Researchers have treated alginate gel beads with stabilizing agents such as sodium meta-periodate and glutaraldehyde (Birnbaum et al., 1981) or Al^{3+} (Roca et al., 1995) to improve gel mechanical strength.

2.3.2.2 Attachment or Adsorption to a Preformed Carrier

Adsorption involves the reversible attachment of biomass to a solid support mainly by electrostatic, ionic and hydrogen bonding interactions. Because it is known that yeast cells have a net negative surface charge, a positively charged support will be most appropriate for immobilization (Bickerstaff, 1997). There are two main types of whole-cell adsorptive immobilization carriers: (a) carriers that allow adsorption only onto external surfaces, because pore sizes are too small to allow microorganisms to penetrate inside, and (b) carriers with large enough pores to allow adsorption onto internal surfaces (O'Reilly and Scott, 1995).

Biomass loading is generally lower in adsorbed cell systems than those obtainable in gel entrapment matrices, but mass transfer may be more rapid. Adsorptive matrices do not have the additional gel diffusion barrier between the cells and the bulk fermentation medium. Another advantage to using adsorption matrices is the regenerability of the support.

The strength of cell attachment to an adsorption carrier depends on both cell and matrix type. Since there is no barrier between cells and the surrounding medium, these immobilization matrices may have significant cell leakage. This is not appropriate for processes requiring a cell-free effluent. Environmental ionic strength, pH, temperature, along with physical stresses such as agitation and abrasion can induce cell desorption. Another limitation of adsorption cell carriers is the possibility of non-specific binding of charged materials within the fermentation medium (Bickerstaff, 1997).

2.3.2.3 Self Aggregation of Cells by Flocculation

The formation of cell aggregates by flocculation, shown in Figure 2.11 (c), is the most simple and least expensive immobilization method, but the least predictable. Stewart and Russell (1986) define flocculation as "the formation of an open agglomeration that relies upon molecules acting as bridges between separate particles." The natural flocculating ability of yeast cells may be exploited (Paiva et al., 1996) or crosslinkers may be added to bolster the process of aggregation for cells that do not do so naturally. The control of cell aggregation is important to maximize bioreactor efficiency. Factors which influence the natural flocculation characteristics of brewer's yeast strains include the genetic make-up of the strain, the cell wall structure and surface charge, the growth phase, incubation temperature, medium pH, cation composition of the medium, and other wort components (Stewart and Russell, 1986).

Weak flocculation activity will result in slow cell sedimentation rates, which could cause cells to be "washed out" of the bioreactor with the fermentation medium and result in a low cell concentration in the bioreactor with insufficient fermentation rates. On the other hand, larger flocs with a very high flocculation activity may result in low concentrations of active yeast cells due to the diffusion limitation of substrate to the cells inside the flocs (Kuriyama et al., 1993).

Dominion Breweries Limited in New Zealand (Coutts, 1956; Dunbar et al., 1988) has been successfully using a flocculent lager yeast strain for the continuous fermentation of beer for almost 40 years. This brewery uses a hold-up vessel followed by two stirred tank fermenters for the continuous primary fermentation. After primary fermentation, the flocculent yeast are separated from the green beer by gravity in a conical settler. Yeast is then recycled from the first stirred tank fermenter and the conical settler back into the hold-up vessel to achieve more precise control of the rate of fermentation. Labatt Brewing Company Limited in Canada was also active in earlier work on continuous primary fermentation of beer (Geiger and Compton, 1957).

Researchers at the VTT Biotechnology and Food Research Laboratory in Finland (Linko et al., 1996) compared the behavior of strongly and weakly flocculent yeast cells immobilized on two different carriers, Siran[®] (sintered glass) and Spezyme[®] (DEAE cellulose) for the primary fermentation of beer. They found that the strongly flocculent yeast cells accumulated on the immobilization carriers faster and consequently the desired wort attenuation was reached more quickly than with the weakly flocculent yeast strain. In addition, they noted that a genetically modified superflocculent yeast strain that flocculated too early for use in conventional batch fermentations, might prove to be very useful in continuous fermentations.

2.3.2.4 Cells Contained Behind a Barrier

In this type of immobilization, cells are confined to a desired area in the fermenter using a membrane. The cells may be suspended in the liquid phase or the cells may be attached to the surface and/or entrapped within the membrane matrix (Gekas, 1986). A barrier formed by the liquid-liquid interface between two immiscible fluids can also be used for immobilization (Karel et al., 1985). Cell retention behind a membrane barrier has not been widely used to immobilize yeast cells for the continuous production of beer, but there are several groups who have investigated the concept for continuous ethanol production (Inloes et al., 1983; Kyung and Gerhardt, 1984; Margaritis and Wilke, 1978a; Margaritis and Wilke, 1978b; Mulder and Smolders, 1986). Kyung and Gerhardt (1984) investigated continuous ethanol production using *Saccharomyces cerevisiae* immobilized in a membrane-contained fermenter. Microporous dialysis membranes provided a barrier

which retained the yeast cells in the fermenter and simultaneously allowed inhibitory fermentation products such as ethanol to be continuously removed in order to boost reactor productivity. The problem of membrane plugging must be overcome for this immobilization mode to become a practical industrial-scale method for continuous ethanol production in the future.

2.3.3 Methods for Measurement of Immobilized Cell Viability and Vitality

One of the greatest challenges facing fermentation researchers today is to find methods for measuring yeast viability and vitality that are accurate and practical for commercial use. Yeast viability is defined as the percentage of live cells in a sample, and yeast vitality is a measure of yeast activity or fermentation performance (Axcell and O'Connor-Cox, 1996; Lentini, 1993; Uttamlal and Walt, 1995). Lentini (1993) specifically describes yeast vitality as "a function of the total cell viability and the physiological state of the viable cell population". In order to efficiently and consistently produce quality beer using an immobilized cell system, one must understand the impact of such a system on yeast physiology and growth.

Many criteria are used to assess yeast cell viability and vitality. Consequently, the perceived viability of a yeast sample may vary depending on the criteria selected. It is often beneficial to monitor a combination of parameters to gain a more complete understanding of a yeast's physiological state. Some of the key methods for studying yeast vitality and viability are outlined in the following sections.

2.3.3.1 Use of Specific Dyes for Assessing Cell Viability and Vitality

Methylene blue is the dye most commonly used for yeast cell viability staining. Viable cells are able to reduce this stain to colourless, whereas non-viable cells are unable to reduce the stain rendering them a deep blue-purple shade (Lentini, 1993). Other brightfield stains which have been used to monitor yeast cell viability include methylene violet (Smart et al., 1999), aniline blue (Lee et al., 1981) and crystal violet (Evans and Cleary, 1985).

There are also many fluorescent stains designed to assess yeast cell viability and vitality. When fluorescent stains are used in conjunction with confocal microscopy

(Bancel and Hu, 1996; Lloyd et al., 1996; Parascandola and de Alteriis, 1996) or flow cytometry (Doran and Bailey, 1986a; Doran and Bailey, 1986b; Gift et al., 1996; Hutter, 1996; Lloyd et al., 1996) valuable information may be obtained on yeast cell growth and metabolic state. Kasten (1993) gives a comprehensive overview of stains available and fluorescence microscopy techniques.

2.3.3.2 Capacitance

The principle of this method is that the application of a radio frequency to a viable cell results in a charge buildup within the membrane, and a capacitance is generated (Lentini, 1993). Non-viable cells are unable to generate this capacitance. A linear correlation has been demonstrated between capacitance and viable yeast biomass (Austin et al., 1994).

Kronlöf and Virkajärvi (1996) recently showed that capacitance probes are suitable for monitoring viable yeast biomass in both freely suspended and immobilized cell systems. Yeast cells were immobilized on porous glass carriers (Siran[®]) and DEAE-cellulose (Spezyme[®]). They pointed out that although this method correlates well with methods such as staining for the detection of viable cells, it does not provide required additional information about the yeast cell's metabolic state. Therefore this method is often used in conjunction with other methods for measuring yeast vitality such as nicotinamide adenine dinucleotide (NADH) or adenosine triphosphate (ATP) assays.

2.3.3.3 The Power of Reproduction as a Viability Indicator

Standard plate count measures the ability of yeast cells to proliferate and form colonies on nutrient agar. It generally takes three days for visible colonies to form and viability is assessed by counting the number of colony forming units (CFU). Care must be taken when using this method on very flocculent yeast (Lentini, 1993).

Yeast viability by slide culture is also based on the ability of yeast cells to proliferate. A drop of yeast culture is placed on a film of nutrient agar and after approximately 18 hours of incubation the formation of microcolonies is observed under the microscope. Cells which have given rise to microcolonies are scored as viable whereas single cells that have not formed microcolonies are scored as non-viable

(Technical Committee and Editorial Committee of the ASBC, 1992). The technique is relatively less time-consuming than standard plate counts but still much slower than the staining techniques. An advantage of the slide culture method is that it is accurate at relatively lower yeast cell viabilities than the staining methods.

2.3.3.4 Viability and Vitality Methods based on Cell Metabolic State

a) Adenosine Triphosphate (ATP)

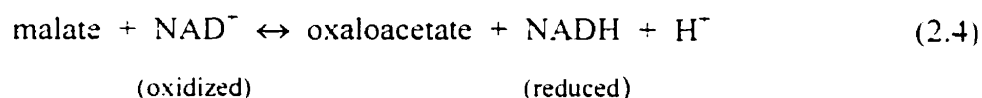
ATP (adenosine 5' triphosphate) is a good indicator of cell viability since it is present in all living cells and is degraded quickly when cells die. ATP allows for the detection of viable cells in a shorter amount of time (10-15 minutes) than with traditional plating techniques. Since the quantity of ATP per cell does not vary significantly for a given strain (but varies between strains), it can be inferred that the amount of ATP present in a biomass sample is proportional to the number of viable cells present. Another advantage of ATP as a viability indicator is the amount of ATP present in a cell does not vary greatly with growth rate. Therefore a correlation between ATP concentration and the amount of viable cell mass can be made (Gikas and Livingston, 1993).

Gikas and Livingston (1993) used ATP bioluminescence to characterize biomass viability in freely suspended and immobilized cell bioreactors. They concluded that the kinetic data obtained for freely suspended cells could not adequately describe immobilized biomass kinetics, because immobilized cells may be in significantly different metabolic states from freely suspended cells. They questioned whether differences in ATP levels between freely suspended and immobilized cells reflect differences in the biomass viable fraction or differences in metabolic state.

b) NADH Fluorosensor

NADH has successfully been used as a non-invasive, on-line method of monitoring freely suspended and immobilized yeast cell metabolism (Doran and Bailey, 1986a; Li, 1991). Viable cells contain nicotinamide adenine dinucleotide (NAD) coenzyme whereas non-viable cells normally lose their NAD (Chahal, 1992). The oxidized form, NAD^+ is used by dehydrogenases to accept electrons from their substrates. For example, in the enzymatic conversion of malate to oxaloacetate in the presence of oxygen, malate dehydrogenase (MDE) first binds to NAD^+ to form a complex of MDE-

NAD^+ . This complex then combines with malate to form a complex, MDE- NAD^+ -malate. From here, NADH, H^+ ion, and oxaloacetate are released, as seen in equation 2.4.



The reduced form, NADH, fluoresces while the oxidized form, NAD^+ , does not. NADH is strongly fluorescent with an emission maximum at 460 nm wavelength. The total NAD is the sum of NADH and NAD^+ . The reducing state is defined as the ratio of the reduced form to the total amount of NAD, given in equation 2.5.

$$\text{Reducing State} = [\text{NADH}] / ([\text{NAD}^+] + [\text{NADH}]) \quad (2.5)$$

Cell metabolic state determines the reducing state, which will remain constant unless there is a shift in metabolism. Thus, the influence of substrates such as oxygen on the reducing state may be predicted. When oxygen is in excess, the reducing state approaches zero because NADH is easily oxidized to form NAD^+ and H_2O , and when there is a lack of oxygen available to the cells, the reducing state approaches one. The concentration of NADH as well as the intensity of the fluorescent signal are influenced by the number of viable cells, the reducing state of the cells and environmental effects. Measuring NADH has an advantage over monitoring dissolved oxygen or pH because it measures, directly in real time, events occurring within the cell rather than changes in the cell's outside environment.

c) Specific Oxygen Uptake Rate (BRF Yeast Vitality Test)

Researchers at the Brewing Research Foundation International (BRFI) developed a method to determine the vitality of pitching yeast by measuring its specific oxygen uptake rate (Daoud and Searle, 1986). Various groups (Daoud and Searle, 1986; Kara et al., 1987; Martens et al., 1986) have shown a correlation between the oxygen uptake rate of yeast and fermentation performance, if yeast viability is less than 90%.

A reduced oxygen uptake rate parallels other yeast changes such as a reduction in yeast lipids, glycogen, acidification power test value, and yeast viability (Imai, 1996).

Generally, oxygen uptake rate correlates well with yeast fermentation performance, however, Wheatcroft et al. (1988) found that oxygen uptake rate did not correlate well with fermentation performance when the yeast had previously been acid-washed. Even though the acid-washed yeast showed decreased specific oxygen uptake rates, there was better fermentation performance than with non-acid-washed yeast.

The biocatalytic activity of the nitrogen-fixing bacterium, *Vibrio natriegens* (*Banckea natriegens*), immobilized on Celite[®], was studied by Gikas and Livingston (1996) using specific oxygen uptake rate [$\text{mg (O}_2\text{) g}^{-1}$ (dry biomass) h^{-1}]. Specific oxygen uptake rates for immobilized and free cells in a three phase air lift reactor were compared and it was found that the uptake rates were significantly lower for the immobilized bacterial cells, implying a lower metabolic activity in the immobilized cell system.

d) Acidification Power

The acidification power test developed by Opekarova and Sigler (1982) measures the drop in extracellular pH of a suspension of yeast cells after the addition of glucose. This method is useful for detecting large differences in yeast metabolic activity. The yeast acidification power test requires extensive yeast washing and multiple sample points which makes it impractical to use this test on immobilized cells *in situ*.

e) Intracellular pH (ICP) Method

The ICP method uses a pH-sensitive fluorescent reagent to measure the intracellular pH of individual cells. It was found that the intracellular pH of more active yeast cells does not decrease, even if the extracellular pH is low, whereas the intracellular pH of less active cells actually decreases under low extracellular pH conditions. This test may be able to detect more subtle changes in yeast cell vitality than the acidification power test (Imai, 1996).

f) Measurement of Yeast Vitality by Stress Response

As stated earlier, vitality may be considered a measure of yeast activity or fermentation performance. It has also been defined as the ability of cells to endure or overcome stress (Axcell and O'Connor-Cox, 1996). Therefore one could relate vitality to the response of yeast cells to stresses such as ethanol, heat shock, and high salt concentrations. Methylene blue, fluorescent dyes (Axcell and O'Connor-Cox, 1996), and

standard plate counts (Norton et al., 1995) may be used to assess the ability of cells to remain viable after being subjected to a given stress.

Norton et al. (1995) assessed the ethanol and heat tolerance of brewers' yeast entrapped in kappa-carrageenan gel. Free and immobilized *Saccharomyces cerevisiae* cells were exposed to ethanol concentrations of 0, 18%, and 19.4% (v/v) for a given length of time and viability was then measured using standard plate counts. Heat tolerance was measured by incubating yeast cells at 48°C for various lengths of time with periodic shaking. Cell viability following heat shock was also measured using standard plate counts. It was found that for immobilized cells there was a significant increase in yeast survival against ethanol as compared to free cells, but no distinct difference in heat resistance was noted. The study concluded that the carrageenan gel matrix provided protection to the entrapped yeast cells against ethanol. When entrapped cells were released from the carrageenan matrix, their ethanol tolerance returned to that of free cells.

g) Magnesium Release Test (MRT)

The Magnesium Release Test (Mochaba, 1997) is based on the observation that low molecular weight species such as magnesium, potassium, and phosphate ions are released by the yeast immediately following inoculation into glucose containing medium. Trials performed on *Saccharomyces cerevisiae* showed that cells which released greater quantities of magnesium immediately after inoculation into high gravity (16 °Plato) wort exhibited higher vitality and better fermentation performance than yeast which released lower amounts of magnesium. Subsequent fermentations performed using the more vital yeast were characterized by shorter lag phases, higher cell counts, higher end ethanol concentrations, and lower diacetyl levels.

2.3.4 Methods for Determining Cell Distribution and Growth Patterns within Immobilized Cell Matrices

2.3.4.1 Method of Successive Dissolution of Layers from Gel Beads

When calcium alginate is used to entrap yeast cells, calcium chelators such as phosphates and citrates may be used to dissolve "shells" of alginate and biomass from the beads (Cho et al., 1982; Gilson and Thomas, 1995; Roukas, 1994). By measuring the concentration and viability of cells inside each shell, information can be obtained about

the spatial distribution of viable cells within the entrapment matrix. Usually shells obtained using this method have a thickness greater than 50 μm . When biomass profiles are steep within the beads, greater resolution is required to obtain an accurate picture of yeast cell distribution. Released biomass from each shell is assessed for viability by using methylene blue staining, fluorescent dyes or by plating. Problems with this method include uniformity of dissolution of the matrix, finding a suitable nontoxic solution for dissolving the entrapment matrix, and overall accuracy limitations.

Recently, Parascandola and Alteriis (1996) studied the spatial growth patterns of *Saccharomyces cerevisiae* cells entrapped in starch-hardened gelatin discs. They used a multi-step digestion method to collect cells belonging to five different layers of the discs. Diluted trypsin was used to release the cells from the gelatin and yeast viability, from each of the layers, was then measured by staining the cells with the fluorescent stain Rhodamine 123 and examining them under a confocal microscope.

2.3.4.2 Physical Sectioning of Immobilized Cell Matrix

A biomass distribution can be obtained by slicing matrices containing yeast cells. To avoid matrix compression and to obtain an accurate distribution, the sample is often dried and embedded in a resin, or frozen. Shrinkage has been observed during this preparation (Wijffels, 1994). Beads can then be sliced using a microtome or razor blade and cell concentration within each section is obtained using image analysis and the appropriate viability or vitality stains. However, this invasive slicing method may cause alterations in cell distribution and other aberrations (Bancel and Hu, 1996).

2.3.4.3 NMR Imaging

Nuclear magnetic resonance imaging (NMRI) is a non-invasive technique to study spatially, the chemical and physical properties of small samples (Lewandowski et al., 1993). Lewandowski et al. (1993) used NMRI to better understand the dynamics of biofilm growth and external liquid film flow velocity distribution. These studies are of importance since the extent of biofilm growth is influenced by the local chemical environment and fluid flow conditions. Substrates must also be transferred through the biofilm-bulk medium interface to reach the cells. In addition, researchers were able to

gather information on velocity distribution using NMRI near microbially colonized surfaces with an imaging time of 8-16 minutes.

2.3.4.4 The Use of Confocal Microscopy for the Determination of Viable Cell Distribution within Porous Microcarriers

Confocal microscopy is a valuable tool for studying the viability of immobilized cells because of its unique ability to take optical sections of three dimensional objects in a non-invasive manner. This depth discrimination property allows only the region of the object that lies close to the focal plane to be imaged efficiently (Masters and Thaeer, 1994). Using confocal microscopy, one could potentially obtain three-dimensional images of yeast cell growth and viability distribution within porous microcarriers without actually disrupting the carrier matrix.

In an elegant study by Lim et al. (1992) the spatial distribution of mammalian cells grown on modified macroporous gelatin microcarriers was studied using confocal microscopy. Optical sectioning, employing confocal microscopy and ethidium bromide for cell staining, allowed the researchers to visualize the distribution of cells at different stages of growth within the macroporous microcarriers. They found that cells initially only attach to the external surface or within the external cavities of the macroporous microcarriers. Subsequently, there was a slow migration of cells toward the interior of the beads. Confocal microscopy revealed that penetration and growth of cells to within the outer half of the radius of the microcarriers accounted for 87% of surface utilization efficiency, whereas the central core, comprising the inner half radius of the spherical particles, contributed only 13% of the total available void fraction.

Bancel and Hu (1996) used confocal laser scanning microscopy to examine the distribution of viable hybridoma cells within macroporous microcarriers. Confocal microscopy was used to avoid the potential artifacts that may be generated using physical sectioning. A cationic fluorescent vital stain, dialkyl indocarbocyanine, was used for the hybridoma cells and a second stain, fluorescein isothiocyanate, with a different emission wavelength, was used to render the microcarriers uniformly fluorescent. The confocal microscope allowed the researchers to take serial optical sections of the immobilized cells and the carrier in a non-invasive manner with the maintenance of cell viability. Their

results showed that the initial spatial distribution of cells within the carrier affects the kinetics of cell growth and the maximum biomass loading possible. These factors will have a significant effect on immobilized cell bioreactor performance.

2.4 The Effects of Immobilization on Yeast Metabolism and Beer Flavour

One of the biggest challenges facing researchers investigating continuous beer fermentation lies in understanding the effects that this process change has on yeast metabolism and beer flavour. A brief review of recent research on beer flavour production using continuous immobilized cell fermentation processes is given below. The bioreactor configurations and designs used by the major research teams exploring immobilized yeast technology systems for beer fermentation, was reviewed recently by our group (Mensour et al., 1997).

Curin et. al. (1987) conducted repeated batch fermentations using alginate-entrapped yeast cells. A major focus of their study was to control operational parameters in order to lower diacetyl production. They found that immobilized yeast formed more vicinal diketones than free yeasts. By lowering the yeast pitching temperature, adjusting the volume ratio of carrier and wort, and keeping the initial concentration of oxygen in the wort below 2.0 mg/L, vicinal diketone levels could be lowered during immobilized cell fermentations.

Inoue (1987) reported that a reason for the increased vicinal diketone levels observed in immobilized cell fermentations is the suppression of yeast cell growth under immobilization conditions. The cells in the interior of the beads do not take up any oxygen and therefore do not grow. If an immobilized cell fermentation does not have enough cell growth, then there is inadequate free amino nitrogen consumption. The amino acids valine and isoleucine are the end products in the pathway, which produce vicinal diketones. These enzymes are effective feedback inhibitors of acetohydroxy acid synthetase, the enzyme which catalyses the production of the vicinal diketone precursor. Therefore, if an immobilized cell fermentation has inadequate free amino nitrogen (FAN) consumption, then there is no feedback inhibition of acetohydroxyacid production until valine and isoleucine begin to be consumed. Inoue states that oxygen deficiency causes this sluggish amino acid uptake rate. Masschelein et al., 1985, also drew similar conclusions regarding excessive diacetyl production when cell growth (reflected by inadequate removal of isoleucine and valine) is severely limited by immobilization or bioreactor configuration.

Shindo et al. (1994) compared the activity of acetohydroxyacid synthetase in cell-free extracts of free and immobilized yeast cells. They found that when the initial concentration of yeast immobilized in calcium alginate gel was increased, the production of diacetyl precursor was reduced by more than two thirds.

The process parameters affecting the removal of wort aldehydes in free and immobilized systems was examined by Debourg et al. (1994) for the production of low-alcohol beer. Wort carbonyls are major contributors to the worty off-flavours detected in low-alcohol beer. They found that immobilized cell fermentations, at high residence times and low temperatures were the best compromise between low alcohol content and sub-flavour-threshold aldehyde levels. Yeast cells were immobilized on either DEAE-cellulose particles or on sintered silicon carbide rods in a loop reactor configuration. Similar trends in aldehyde reduction were observed. The most significant factor controlling residual aldehyde levels in the beer was the fermenter residence time.

Batch studies were performed by Hinfray et al. (1994) on free and agar-entrapped *Saccharomyces cerevisiae* cells in order to examine the influence of oxygenation levels on glucose alcoholic fermentations. They indicated that past studies by Ryu et al. (1984) showed that small amounts of dissolved oxygen enhance the specific ethanol production rate of free *Saccharomyces cerevisiae* cells compared with anaerobic conditions. However, they observed that the beneficial effects of low oxygen on glucose fermentation were not found with immobilized cell cultures. The researchers speculated that this is due to mass transfer limitations. They also suggested that these same mass transfer limitations protect entrapped microorganisms from the inhibiting effects of high oxygenation levels during glucose fermentation.

Dominion Breweries in New Zealand (Dunbar et al., 1988) has been operating a commercial continuous fermentation system since 1956 using a highly flocculent yeast strain. Their system consists of a hold up vessel (HUV), 2 fermentation vessels (CF1 and CF2), a yeast separator (YS), and beer storage tanks. They have found that the flow rate at which they operated in their continuous system significantly affected the concentration of diacetyl and 2,3-pentanedione (vicinal diketones, VDKs) in each of the continuous fermentation vessels. When the residence time was high (flow rates low) peak VDK levels were reached in CF1 and then decreased in CF2 and further decreased in the yeast

separator. However, lower residence times (higher flow rates) caused higher peak VDK levels and there was no reduction found in the downstream components of the system. In the case with the higher flow rates/shorter residence times, greater beer productivities resulted. Therefore a higher flow rate/shorter residence time could be used if the beer was allowed some additional aging time until the final diacetyl level in the beer was about the same as that in the beer produced at the lower flow rate/longer residence time. The advantage of this was that the flow rate could be increased during periods of high demand, as long as there was adequate storage available for the increased maturation load. With regard to ester production, Dunbar et al. (1988) found the overall rate of ester production reached a maximum in the hold up vessel at the beginning of fermentation, when the yeast was most actively growing. Ester levels could be controlled by changing the top pressure in the CF fermentation vessels.

Masschelein et al. (1985) conducted fermentation studies using yeast cells immobilized in alginate gel. The effect of oxygen mass transfer to immobilized yeast cells was examined in terms of oxygen removal rates and fatty acid synthesis. It is known that the biosynthesis of a given mono-unsaturated fatty-acyl residue is produced from the corresponding saturated residue in a reaction involving NADPH and molecular oxygen. Therefore, if the cells at the center of a gel bead receive an inadequate amount of oxygen, one should see a shift in the fatty acid composition of those cells toward long chain saturated fatty acids reflecting this deficiency. Oxygen removal rates of free and immobilized cells were compared and it was found that oxygen removal by the immobilized yeast cells was noticeably less efficient than with the free cells. This supports the concept of oxygen transfer limitations in alginate gel immobilization matrices. As well, the fatty acid content of immobilized cells taken from the outer layer of the gel bead showed larger amounts of unsaturated fatty acids (72%) than the cells at the center of the bead (61%), which further indicated a restricted oxygen supply at the center of the bead.

In another study by Masschelein and Ramos-Jeunehomme (1985) the potential of alginate immobilized yeast in brewery fermentations was examined. They found that in free cell batch fermentations, amino acid uptake was more complete than that which occurred in a continuous immobilized cell packed bed bioreactor (Table 2.3).

Table 2.3. Percent utilization of amino acids in wort at 80% attenuation in batch free cell and continuous immobilized cell packed bed fermentations (adapted from Masschelein and Ramos-Jeunehomme, 1985).

Amino Acid	Percent Utilization at 80% Attenuation	
	Suspended Cells (Batch)	Immobilized Cells (Continuous)
Aspartic Acid	98.5	79
Glutamic Acid	97	0
Threonine	99.1	66.2
Serine	99.2	54
Asparagine	97	53.1
Lysine	87	19
Arginine	97	11
Methionine	98.1	85
Valine	92	19.2
Leucine	100	37.1
Isoleucine	99	28
Histidine	83.2	0
Glycine	91	0
Alanine	92	0
Phenylalanine	98.1	25.2
Tyrosine	98	13
Tryptophan	75.2	13

Yamauchi et al. (1994) with Kirin Breweries, developed an immobilized yeast multistage bioreactor system. The system consisted of a 2.0 L working volume continuous stirred tank reactor (CSTR) equipped with a marine impeller and an air sparger. The CSTR was supplied with 0.17 vvm of air. The process stream was then fed into a continuous centrifuge where yeast cells were removed so that the concentration of cells in the exit stream was 1.0×10^6 cells/mL. Following the centrifuge, was a packed bed reactor with a working volume of 1.9 L, containing 40% (v/v) of Kirin's porous spherical glass beads (Hyperemics[®]) held at 8°C. Following primary fermentation, the liquid was sent through a continuous heat exchanger and held at 70-80°C for 20-30 minutes. The final stage of the system was another packed bed reactor containing Hyperemics[®] beads at a temperature of 0°C. The average concentration of yeast cells was

5.0×10^6 cells/bead. Yamauchi et al. (1995) conducted studies using this system and found that higher alcohol production increased with increasing amino acid concentration in the wort, anaerobic conditions, increased temperature, increased agitation, increased growth, and increased ethanol concentration. Ester production is known to increase with reduced growth due to reduced oxygen supply, a larger acetyl CoA pool, and an increased higher alcohol supply. For this reason, Yamauchi et al. (1995) designed a two-stage bioreactor system where, in the first stage (CSTR), high levels of fusel alcohols were produced due to the high cell growth. In the second anaerobic stage, the packed bed reactor (PBR), they found that by keeping the yeast in a slight growth phase, extract consumption in the PBR was increased to the levels of a conventional batch fermentation.

Nakanishi et al. (1993), developed a continuous fermentation system which combines an aerobic stirred fermentation with an anaerobic immobilized cell fermentation stage. The aerobic stage allowed for increased yeast cell growth and consequent amino acid uptake, and the anaerobic packed bed immobilized cell reactor provided conditions which suppressed yeast growth, allowed for sugar consumption and reduced diacetyl. With these stages in series, Nakanishi et al. (1993) were able to shorten primary fermentation to one to two days, with no significant differences in flavour and taste from conventional beer.

The paper of White and Portno (1978) was one of the earliest to look at immobilized yeast cells for continuous beer fermentation. Calcium alginate was the immobilization matrix and a tower fermenter was used. They were able to operate the fermenter continuously for seven months with no deterioration in yeast fermentative ability. With regard to bacterial contamination, they found that their carrier did not have a tendency to entrap bacteria, and when the fermenter was provided with a wort which contained bacteria, they were able to wash out the bacteria using an injection of sterile wort. Table 2.4 shows the analysis of beer flavour volatiles made using the immobilized cell system after different time periods compared with corresponding levels in beer made by a conventional batch fermentation.

Table 2.4. Analysis of flavour volatiles from beer produced using a continuous immobilized cell fermenter (adapted from White and Portno, 1978).

Flavour Volatile	Level (mg/L) in effluent beer from tower after:							Level (mg/L) in beer from batch ferm.
	Week 1	Week 2	Month 1	Month 4	Month 5	Month 6	Month 7	
n-propanol	12	14	10	8	9	10	8	16
Iso-butanol	15	15	11	14	10	13	14	9
Iso-amyl alcohol	53	49	52	53	41	45	47	42
Ethyl acetate	12	12	12	17	12	10	5	8
Iso-amyl acetate	0.4	0.4	0.7	0.3	0.2	0.06	t	0.9
Ethyl caproate	0.02	t	0.07	0.03	t	0.01	0.01	0.06
Iso-butyl acetate	t	t	0.02	0.01	t	t	0.01	0.02
Ethyl n-butyrate	0.03	0.03	0.02	0.01	t	0.01	t	0.01
Acetaldehyde	4.5	6.1	1.5	9.2	13	13	13	2.9
Diacetyl	nm	nm	nm	0.26	0.14	0.3	0.4	nm

nm = not measured; t = trace (<0.01 mg/L)

Kronlöf and Virkajärvi (1996) have developed a two-stage continuous main fermentation process in which they attempted to mimic batch fermentation by having the growth phase located primarily in the first reactor and the non growth phase in the second reactor. Table 2.5 shows the concentrations of some key flavour compounds produced after the first and second reactors in their system. The numbers in the table represent the averages of five 42-day experiments. The corresponding percentage attenuation value is given at the top of each column.

Table 2.5. Analysis of some key flavour compounds in two stage continuous fermentation system (adapted from Kronlöf and Virkajärvi, 1996).

Flavour Compounds (mg/L)	After 1st Reactor		After 2nd Reactor	
	17% Porous glass	23% DEAE-Cellulose	62% Porous glass	63% DEAE-Cellulose
n-Propanol	7.7	10.6	19.2	18.3
2-Methyl propanol	3.6	7	10.6	14
2-Methyl butanol	4.9	7.4	15.6	16.8
3-Methyl butanol	9.5	19.1	29.1	37.1
Ethyl acetate	5	6.6	24.5	22.6
3-Methylbutyl acetate	0.2	0.3	1	0.8
Acetaldehyde	14.1	10.6	6.8	6.8
Total diacetyl	0.32	0.37	0.33	0.34

The above systematic literature review on freely suspended and immobilized yeast cells in batch and continuous beer fermentation processes showed that more work needs to be done on the biochemical and operational factors affecting the production of beer flavour compounds in immobilized yeast cell systems.

CHAPTER 3. FREE AND IMMOBILIZED CELL SYSTEMS: THEORETICAL CONSIDERATIONS

3.1 Batch Microbial Growth Kinetics of Freely Suspended Cells

Batch growth of a microorganism such as yeast consists of the following phases: lag phase, transition phase, exponential or logarithmic phase, a second transition phase, stationary phase, and death phase (Lewis and Young, 1995). The rate of microbial growth is given by equation 3.1.

$$dX / dt = \mu X \quad (3.1)$$

In equation 3.1, X is the cell concentration, μ is the specific growth rate of the cells and t is the fermentation time. During the exponential growth phase, the specific growth rate of the cells, μ , is constant and reaches its maximum, μ_{\max} as seen in equation 3.2.

$$dX / dt = \mu_{\max} X \quad (3.2)$$

The integration of equation 3.2 is given by equation 3.3, where, X_0 is the concentration of cells at time, $t = 0$.

$$\ln (X / X_0) = \mu_{\max} t \quad (3.3)$$

Thus the slope of a graph of $\ln (X / X_0)$ versus time, during the log phase of batch microbial growth, yields the maximum specific growth rate, μ_{\max} . The time to double the cell population during exponential growth, referred to as the "doubling time", t_d , is given by equation 3.4.

$$t_d = \ln(2) / \mu_{\max} \quad (3.4)$$

The Monod equation 3.5 relates the specific growth rate and the limiting substrate, which can be any limiting nutrient present in the liquid medium such as carbon source (e.g. glucose), assimilable nitrogen (e.g. amino acids, ammonium ions), dissolved oxygen and others. An important assumption in the Monod equation is that there is only one limiting substrate in the system. In the Monod equation S is the concentration of the limiting substrate, K_s is the saturation Monod constant, and, at $S = K_s$, $\mu = \frac{1}{2} \mu_{\max}$.

$$\mu = \mu_{\max} S / (K_s + S) \quad (3.5)$$

The μ_{\max} used in the Monod equation is achievable when S is significantly greater than K_s and the concentrations of all additional essential substrates remain unchanged (Bailey and Ollis, 1986).

Kinetic descriptions of product formation by cells parallel those used to describe cell growth. The simplest types of product formation kinetics arise when there is a direct stoichiometric relationship between product formation and substrate utilization or cell growth. The rate of formation of product, r_p , is given in equations 3.6 and 3.7 respectively, where r_s is the rate of substrate consumption, r_x is the rate of biomass growth, $Y_{p/S}$ is the yield of product from substrate consumed, and $Y_{p/X}$ is the yield of product from biomass produced.

$$r_p = -Y_{p/S} r_s \quad (3.6)$$

$$r_p = Y_{p/X} r_x \quad (3.7)$$

This type of product formation kinetics is often referred to as growth-associated product formation kinetics. Growth-associated product formation kinetics in a batch culture is illustrated in Figure 3.1 (a). Ethanol fermentation is an example of growth-associated product formation kinetics (Leudeking, 1967).

In many fermentations involving the formation of secondary metabolites, such as the flavour metabolites formed during beer fermentation, significant product formation occurs relatively late in a batch culture, sometimes during the stationary phase of growth. An example of this type of product formation kinetics from pharmaceutical fermentation is the production of penicillin. Sometimes this type of kinetics may be described by a simple non-growth-associated model, where the production rate is proportional to the cell concentration rather than growth rate, as illustrated in Figure 3.1 (b) (Bailey and Ollis, 1986). However, in many cases product formation kinetics for secondary metabolites are best described using the model of Leudeking and Piret (1959) which combines growth associated and non-growth associated contributions, as seen in equation 3.8.

$$r_p = \alpha r_x + \beta X \quad (3.8)$$

In Equation 3.8 α and β are kinetic model parameters. Leudeking-Piret kinetics is apt to be applicable when the product is the result of energy-yielding metabolism, as in several anaerobic fermentations. The first and second terms in equation 3.8 are associated with the energy used for growth and for maintenance, respectively. Gee and Ramirez (1994) developed a beer flavour model to describe batch fermentation dynamics for freely suspended yeast cells based upon fundamental knowledge of biochemical pathways.

Kinetic analyses of ester formation during batch beer production using freely suspended yeast cells have also been performed by García et al., 1994 and Nakatani et al., 1991.

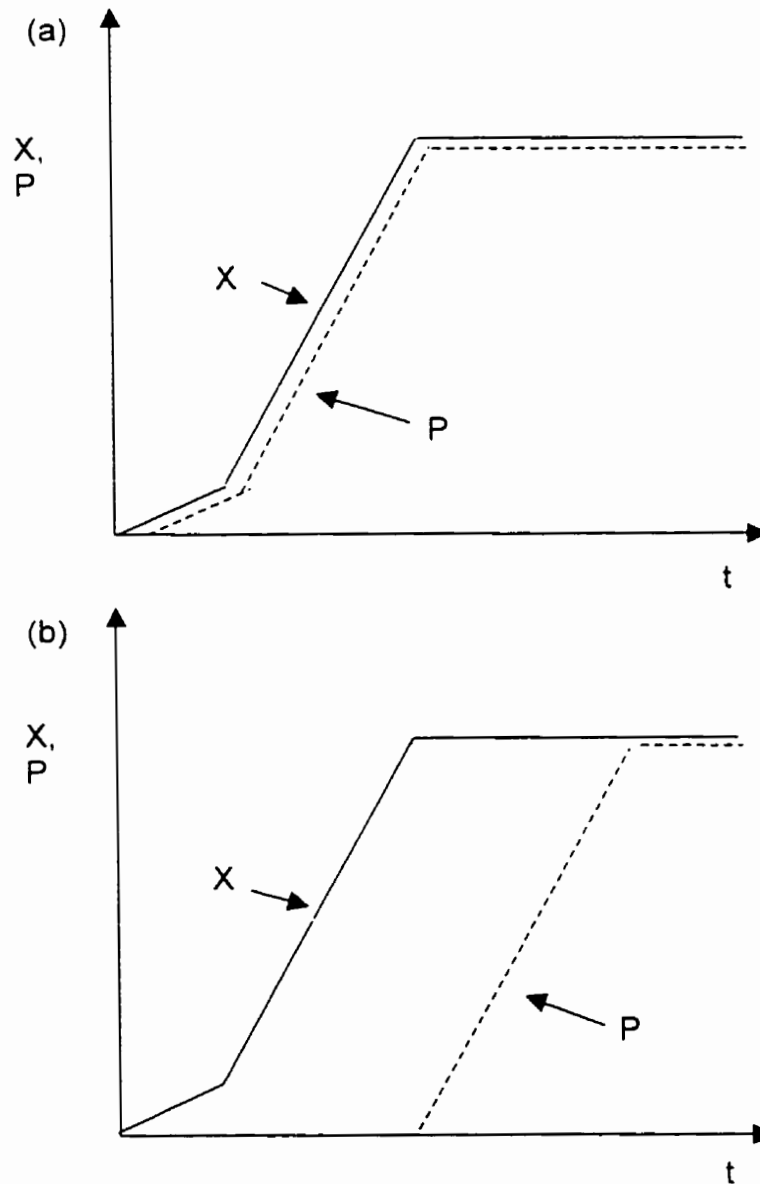


Figure 3.1. (a) Growth and (b) non-growth associated product formation during microbial batch fermentation, where X is the concentration of cells, P is the concentration of product, and t is batch fermentation time.

3.2 Kinetics of Freely Suspended Cell Growth in Continuous Stirred Tank Bioreactors

In a well-mixed continuous stirred tank bioreactor (CSTR) with a working volume, V_R , containing freely suspended cells, fresh liquid medium with a given inlet substrate concentration, S_0 , is continuously supplied to the bioreactor at a volumetric flow rate, F . Within the bioreactor, there is a concentration of freely suspended cells, X , substrate, S , and product, P . Assuming the system is well-mixed, the concentration of biomass, substrates and products will be the same in the outlet as within the bioreactor, as illustrated in Figure 3.2.

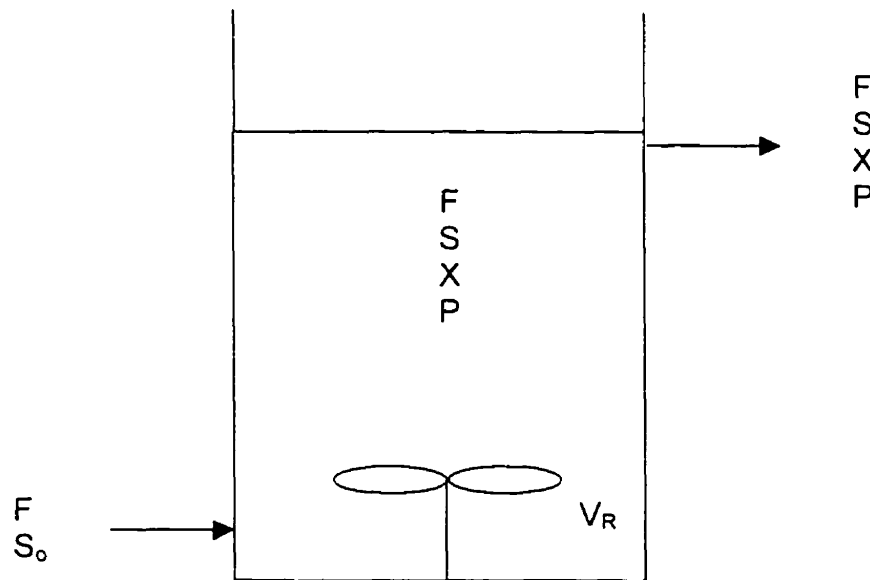


Figure 3.2. Schematic of a well-mixed continuous stirred tank reactor (CSTR) containing freely suspended cells, where F is the volumetric flow rate of medium entering the bioreactor, S_0 is the initial substrate concentration, X is the biomass concentration, P is the product concentration, and V_R is the bioreactor working volume.

By performing an unsteady state cell balance on the cells in Figure 3.2, equations 3.9 and 3.10 are obtained.

Rate of cell accumulation = rate of cells in – rate of cells out + rate of cells formed – rate of cells dying (3.9)

$$V_R (dX/dt) = FX_0 - FX + V_R\mu X - V_R\omega X \quad (3.10)$$

In equation 3.10, μ is the specific cell growth rate and ω is the specific cell death rate. When the liquid medium is sterilized then $X_0 = 0$ and $FX_0 = 0$. Assuming that the rate of cell death is negligible and by dividing equation 3.10 by the bioreactor working volume, V_R , equation 3.11 is obtained.

$$dX/dt = -XF/V_R + \mu X \quad (3.11)$$

The dilution rate, D_R , is a physical parameter controlled by both the working volume of the bioreactor and the volumetric flow rate of the fresh liquid medium and is given in equation 3.12. The specific growth rate of the cells, μ , is a biological parameter controlled by changing the nutrient composition (the limiting nutrient), pH, or temperature in the bioreactor.

$$D_R = F/V_R \quad (3.12)$$

Thus, equation 3.11 becomes equation 3.13.

$$dX/dt = -D_R X + \mu X \quad (3.13)$$

If the system is at steady state then the rate of accumulation dX/dt is equal to zero, and equation 3.14 is obtained.

$$\mu X = D_R X \quad \text{or} \quad \mu = D_R = F/V_R \quad (3.14)$$

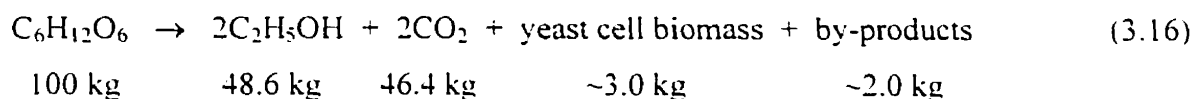
Therefore, if dilution rate increases, specific growth rate increases, until $D_R = \mu_{\max}$ and any with further increase in D_R (i.e. $D_R > \mu_{\max}$), the rate of cell removal is greater than the rate of cell generation in the bioreactor, and cell washout occurs. Critical dilution rate, D_c , is defined as the dilution rate at which the cell specific growth rate is at its maximum, μ_{\max} . Continuous stirred tank bioreactors, also called chemostat cultures, containing freely suspended yeast cells are operated under conditions where the $D_R < D_c$. The inverse of the dilution rate is referred to as the average liquid residence time, R_t within the bioreactor.

3.3 Ethanol Production during Beer Fermentation

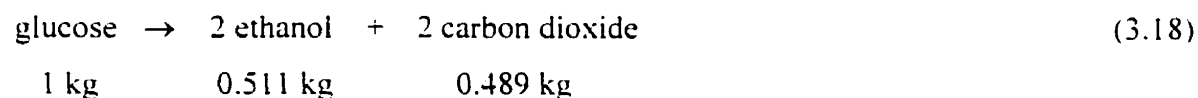
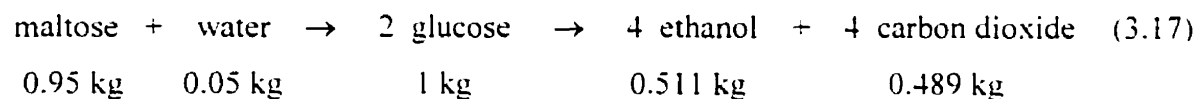
The formation of ethanol from glucose by yeast cell fermentation is expressed by the Gay-Lussac stoichiometric equation 3.15.



This means that on a kilogram basis 48.9% of the glucose is converted to carbon dioxide and 51.1% is converted to ethanol. Therefore the maximum theoretical yield of ethanol produced from glucose substrate consumed, $Y_{P/S}$, is 0.51. However, in practice it has been shown that during yeast cell fermentation, ethanol yields of only 90 - 95% of theoretical are achieved due to biomass production and other byproducts. A total approximate mass balance is shown in equation 3.16 (Hardwick, 1995).



From the Gay-Lussac equation it is assumed that glucose is the only carbon source of ethanol produced, however, there are other fermentable sugars, such as fructose, maltose and maltotriose which contribute to the production of ethanol. In wort, the reaction mechanism occurs through the intracellular hydrolysis of maltose and maltotriose to glucose, followed by fermentation of the total glucose pool. As indicated in equations 3.17 and 3.18, the disaccharide, maltose that is subsequently hydrolysed into its glucose monomer, increases the amount of fermentable sugars by about 5% due to the addition of water during hydrolysis (Hardwick, 1995). This means that only 0.95 kg of maltose is required to make the same amount of ethanol that would be produced from 1.0 kg of the monosaccharide glucose.



In equations 3.19 and 3.20, the yield of product, P, formed (ethanol) from glucose substrate, S, consumed (as glucose, fructose, maltose, maltotriose (DP3)), $Y_{P/S}$, is given on a mass basis. Thus total fermentable carbohydrate (as glucose) is defined on a kilogram basis as given in equation 3.21.

$$Y_{P/S} = (\Delta P / \Delta t) / (\Delta S / \Delta t) = (\Delta P / \Delta S) = (\text{product formed} / \text{substrate consumed}) \quad (3.19)$$

$$Y_{P/S} = \Delta [\text{ethanol}] / \Delta ([\text{glc}] + [\text{fruc}] + 1.053[\text{malt}] + 1.106[\text{DP3}]) \quad (3.20)$$

$$\text{Tot. ferm. carbohydrate (as glucose)} = [\text{glc}] + [\text{fruc}] + 1.053[\text{malt}] + 1.106[\text{DP3}] \quad (3.21)$$

The yield equations for biomass formed per substrate consumed, $Y_{X/S}$, and for product formed per unit biomass, $Y_{P/X}$, are derived in equations 3.22 through 3.24.

$$Y_{X/S} = (\Delta X / \Delta S) = (\text{biomass formed} / \text{substrate consumed}) \quad (3.22)$$

$$Y_{X/S} = \Delta [\text{kg dry wt. cells}] / \Delta ([\text{gluc}] + [\text{fruc}] + 1.053[\text{malt}] + 1.106[\text{DP3}]) \quad (3.23)$$

$$Y_{P/X} = (\Delta P / \Delta X) = (\Delta P / \Delta S) / (\Delta X / \Delta S) = Y_{P/S} / Y_{X/S} \quad (3.24)$$

Ethanol and beer bioreactor productivity calculations are given in equations 3.25 and 3.26.

$$V_{\text{ethanol}} = (\text{kg ethanol produced}) / (\text{m}^3 \text{ bioreactor volume} \cdot \text{h}) \quad (3.25)$$

$$V_{\text{beer}} = (\text{m}^3 \text{ of beer produced}) / (\text{m}^3 \text{ bioreactor volume} \cdot \text{h}) \quad (3.26)$$

3.4 Gas-Liquid Mass Transfer in Freely Suspended Cell Systems

In this section the basic mass transfer equations that describe the transport of oxygen molecules from the gas bubbles to the liquid phase within the bioreactor vessel are summarized.

Using the two-film theory of mass transfer, at steady state, the rate of oxygen transfer to a gas-liquid interface is equal to its transfer rate through the liquid-side film, as given in equations 3.27 to 3.29, where $\underline{N}_{A,G}$, $\underline{N}_{A,L}$ and \underline{N}_A are fluxes of A in the gas-side film, in the liquid film and overall respectively, and k_G and k_L are the local mass transfer coefficients for the gas and liquid phases (McCabe et al., 1993).

$$\underline{N}_{A,G} = k_G (P_{A,G} - P_{A,i}) \quad (3.27)$$

$$\underline{N}_{A,L} = k_L (C_{A,i} - C_{A,L}^f) \quad (3.28)$$

$$\underline{N}_{A,G} = \underline{N}_{A,L} = \underline{N}_A \text{ at steady state} \quad (3.29)$$

The parameters $P_{A,G}$ and $P_{A,i}$ are the partial pressures of A in the bulk gas phase and at the gas-liquid interface. The parameters $C_{A,i}$ and $C_{A,L}^f$ are the concentrations of A at the interface and in the bulk liquid phase.

Since it is difficult to measure $C_{A,i}$ and $P_{A,i}$, overall liquid and gas side driving forces may be used, which incorporate Henry's Law, where K_L and K_G are the overall liquid and gas side mass transfer coefficients. $C_{A,L}^*$ and $P_{A,G}^*$ are the solubilities of A at a given temperature in the liquid and gas phases respectively. The overall liquid and gas phase fluxes are given in equations 3.30 and 3.31.

$$\underline{N}_{A,L} = K_L (C_{A,L}^* - C_{A,L}^f) \quad (3.30)$$

$$\underline{N}_{A,G} = K_G (P_{A,G} - P_{A,G}^*) \quad (3.31)$$

The relationships of the overall liquid and gas phase mass transfer coefficients to the local mass transfer coefficients are given in equations 3.32 and 3.33.

$$1 / K_L = 1 / k_L + 1 / (H k_G) \quad (3.32)$$

$$1 / K_G = 1 / k_G + H / k_L \quad (3.33)$$

For sparingly soluble species such as oxygen, the liquid film resistance is controlling and thus basically all the resistance to mass transfer lies on the liquid-film side and equation 3.32 becomes equation 3.34. Thus K_L is approximately equal to k_L .

$$1 / K_L = 1 / k_L \quad (3.34)$$

In equation 3.35, the volumetric flux of A is given using $k_L a$ for a sparingly soluble gas such as oxygen, and the "a" term is the gas-liquid interfacial area per unit liquid volume of bioreactor (Bailey and Ollis, 1986). The volumetric mass transfer coefficient, $k_L a$, is a function of many factors within the bioreactor including the gas flow rate, agitation, temperature, medium composition, surface active agents, and type of sparger.

$$N_{A,L} = k_L a (C_{A,L}^* - C_{A,L}^f) \quad (3.35)$$

Therefore the maximum possible volumetric flux of oxygen at a given $k_L a$ occurs when the bulk liquid concentration of oxygen, $C_{A,L}^f$, is equal to zero, as given in equation 3.36.

$$N_{A,L} (\max) = k_L a (C_{A,L}^*) \quad (3.36)$$

In a bioreactor, containing X concentration of cells per unit volume, having a given Q_{O_2} , the rate of oxygen consumption and dissolved oxygen concentration, $C_{A,L}^f$, the rate of oxygen uptake, OUR, is seen in equation 3.37.

$$Q_{O_2} X = OUR \quad (3.37)$$

By performing an unsteady state mass balance in a bioreactor where microbes are growing, equation 3.38 is obtained.

$$dC_L/dt = k_L a (C_{A,L}^* - C_{A,L}^f) - Q_{O_2} X \quad (3.38)$$

At steady state equation 3.38 becomes equation 3.39.

$$k_L a (C_{A,L}^* - C_{A,L}^f) = Q_{O_2} X \quad (3.39)$$

If the bulk liquid phase oxygen concentration $C_{A,L}^f$ is greater than some critical concentration of oxygen, $C_{A,L}^{critical}$, then oxygen is no longer limiting and Q_{O_2} is constant and independent of $C_{A,L}^f$ and $Q_{O_2} = Q_{O_2}(\max)$.

3.5 External and Internal Mass Transfer Characteristics of Immobilized Cells

The study of the transfer of substrates and products to and from immobilized cells is important, especially when cells are entrapped throughout a gel matrix such as carrageenan. External mass transfer involves the transfer of nutrients from the bulk liquid medium to the carrier surface, while internal mass transfer describes the transfer of substrates and products within the carrier, and in and out of the cell. The concentration of metabolites, in the immediate vicinity of cells, may be altered in immobilized cell systems due to both internal and external mass transfer limitations. Such changes may force the cells to alter their metabolic states and thus, impact the efficiency and quality of a fermentation process. In this section the fundamental aspects of mass transfer for continuous beer fermentation are discussed. The transfer of one key fermentation substrate, oxygen, into an immobilized cell is shown in Figure 3.3.

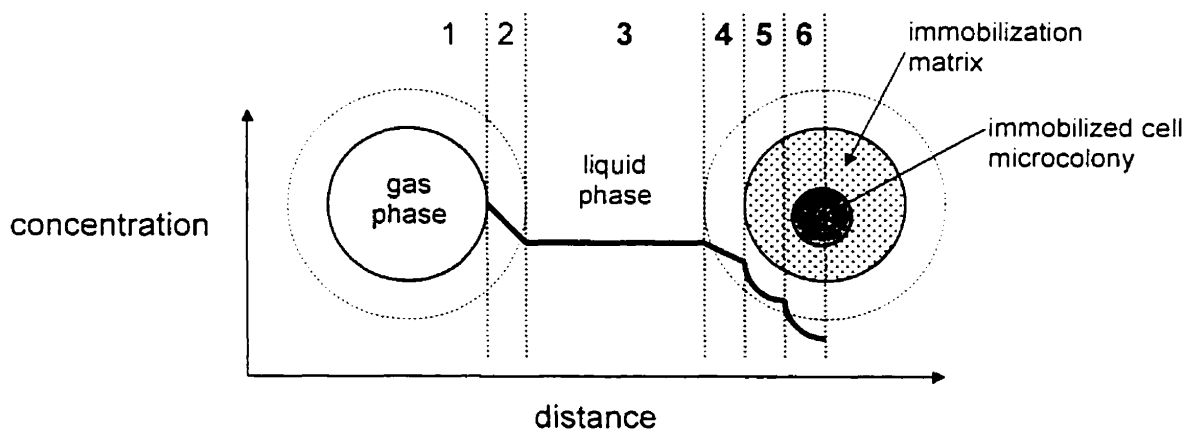


Figure 3.3. Transport of oxygen from the gas phase to an immobilized cell matrix: 1, gas phase; 2, liquid film; 3, **bulk liquid phase**; 4, liquid film; 5, solid matrix; 6, **microcolony containing cells** (adapted from Wijffels, 1994).

Alteration of physiological/metabolic properties of immobilized cells, or alteration of the local micro-environment in the immediate vicinity of immobilized cells, may cause changes in the kinetic behavior of cells upon immobilization. In the latter case, the local micro-environment may be described in terms of solute partitioning effects

¹A version of section 3.5 has been published (Pilkington et al., 1998a).

between the bulk liquid phase and the solid immobilization matrix, external film mass transfer resistance and internal mass transfer resistance (Merchant et al., 1987). The solute partitioning coefficient (K_p), the liquid film mass transfer coefficient (k_L), and the effective solute diffusivity within the immobilization matrix (D_e) respectively, quantify these phenomena. In order to determine overall effectiveness factors the above parameters need to be quantified.

“Effectiveness factor”, η , is used to represent the influence of mass transfer on the overall reaction process and is defined in equation 3.40 (Bailey and Ollis, 1986):

$$\eta = \frac{\text{(observed reaction rate)}}{\text{(rate which should be obtained with no mass transfer resistance)}} \quad (3.40)$$

Overall effectiveness factors allow one to determine whether a system is mass transfer limited or reaction rate limited. The Thiele Modulus, Φ , is used to characterize internal mass transfer resistance effects and is defined as the ratio of the reaction rate to the internal diffusion rate (see Nomenclature section for equation). This parameter represents the rate that substrate is consumed, relative to the rate at which it is supplied, by the diffusion process. A high value for the Thiele Modulus results in steep gradients of substrate concentration because of internal mass transfer limitations. These low substrate concentrations within the matrix lead to a reduced average rate of reaction relative to that which would be obtained if the concentration throughout the immobilization matrix was equal to the bulk liquid concentration. Eventually, active biomass is confined to only a thin outer layer at the surface of the matrix, because substrate is depleted in the interior of the bead (de Backer et al., 1996). Another parameter is the Biot Number, Bi , which is defined in equation 3.41 (Bailey and Ollis, 1986):

$$Bi = \frac{\text{characteristic film transport rate}}{\text{characteristic intraparticle diffusion rate}} \quad (3.41)$$

When $Bi \rightarrow \infty$ external mass transfer resistance may be neglected, and when $Bi \rightarrow 0$ the external resistance controls the nutrient supply to the immobilized cell particle (de Backer et al., 1996).

As seen in Figure 3.3, a substrate must travel through the bulk liquid medium, the external liquid film surrounding the immobilized cell particle, the liquid-solid interface, the liquid within the solid gel phase, the resistance caused by microcolony formation, and finally into the yeast cell where the reactions take place.

3.5.1 External Mass Transfer in Immobilized Cell Systems

External mass transfer refers to the transfer of nutrients from the bulk medium through the external liquid film surrounding the immobilized cell particle, and is characterized by the liquid film mass transfer coefficient, k_L . There are several mixing mechanisms involved in the mass transfer of components from the bulk liquid phase to the immobilized cell system. These include macro- and micro-mixing, axial dispersion, and convective fluid flow. Several theoretical models describing the mass transfer within the external liquid film at the liquid-solid interface are outlined below.

3.5.1.1 Theoretical Models for Mass Transfer at the Liquid-Solid Interface

a) Film Theory

This is the earliest and simplest theory, which describes mass transfer at a liquid-solid phase boundary. The model assumes that for a fluid flowing past a solid, the whole resistance to mass transfer is in the stagnant liquid film surrounding the solid particle (Hines and Maddox, 1985). The thickness of the film is greater than the laminar sublayer and this film provides the same resistance to mass transfer by molecular diffusion as that which exists for the true convective process. The mass transfer coefficient, k_L is related to the liquid film thickness, δ , and molecular diffusivity, D_L and is given by equation 3.43.

$$k_L = D_L / \delta \quad (3.42)$$

$$J_A = (D_L / \delta) (C_{A,L}^{\infty} - C_A^{sc}) = k_L (C_{A,L}^{\infty} - C_A^{sc}) \quad (3.43)$$

D_L is the molecular diffusivity and δ is the thickness of the stagnant film. The mass flux of component A diffusing through the liquid film of thickness, δ , is given by equation 3.43 where $C_{A,L}^{\infty}$ is the bulk substrate concentration, and C_A^{sc} is the external substrate concentration at the surface of the particle (Fig. 3.15). Equation 3.42 states that the mass transfer coefficient, k_L , is directly proportional to D_L . However, experimental results given by Geankoplis (1993) indicated that k_L is actually proportional to $D_L^{2/3}$.

b) Penetration Theory

Higbie in 1935 derived the penetration theory, for diffusion into a laminar falling liquid film, for short contact times. This theory assumes that the liquid surface is comprised of small fluid elements which contact the second phase for an average time, after which they penetrate into the bulk liquid (Hines and Maddox, 1985). Each element is then replaced by another element from the bulk liquid phase. For turbulent flow, the penetration theory renders a reasonable device for characterizing mass transfer. As shown in equation 3.44, the penetration theory predicts that the mass transfer coefficient k_L is proportional to the molecular diffusivity $(D_L)^{1/2}$:

$$k_L = [4 D_L / (\pi t_s)]^{1/2} \quad (3.44)$$

where t_s is the exposure time of the solute.

c) Surface Renewal Theory

Danckwerts in 1951 improved the penetration theory by replacing the constant exposure time with an average exposure time calculated from an assumed time distribution (Geankoplis, 1993). It was assumed that the chance of an element being replaced on the surface was independent of the time during which it had been exposed. In this case, the mass-transfer coefficient, k_L is proportional to $D_L^{1/2}$ as in equation 3.45.

$$k_L = (D_L s)^{1/2} \quad (3.45)$$

The mean surface renewal factor, s , in sec^{-1} , must be determined experimentally.

3.5.1.2 Mass Transfer Coefficient

The flux of a substrate, J_A , to the surface of an immobilized cell particle depends on the mass transfer coefficient, k_L , and on the bulk concentration of the substrate, $C_{A,L}^{\infty}$.

Therefore, the flux per unit area evaluated at the surface normal (i.e. perpendicular) to the surface of the immobilized cell particle is given in equation 3.46.

$$J_A = k_L (C_{A,L}^{\infty} - C_A^{sc}) \quad (3.46)$$

where $C_{A,L}^{\infty}$ is the bulk substrate concentration, and C_A^{sc} is the substrate concentration at the surface of the particle, as seen in Figure 3.4, and the driving force for mass transfer is $(C_{A,L}^{\infty} - C_A^{sc})$. The liquid film mass transfer coefficient, k_L , is correlated to external flow velocity and fluid properties by the empirical equations 3.47 to 3.50.

$$Sh = a + b Re^n Sc^m \quad (3.47)$$

The terms a, b, n and m are empirical constants (Willaert, 1996).

$$Sh = 1.01 Re^{1/3} Sc^{1/3} \quad \text{for } Re < 1 \quad (3.48)$$

$$Sh = 0.95 Re^{1/2} Sc^{1/3} \quad \text{for } 10 < Re < 10^4 \quad (3.49)$$

$$Sh = 2 + 0.73 Re^{1/2} Sc^{1/3} \quad (3.50)$$

Sh is the Sherwood Number and it is defined by equation 3.51.

$$Sh = k_L d_p / D_L \quad (3.51)$$

Re, the Reynolds number is defined in equation 3.53.

$$Re = v_r \rho d_p / \mu_B \quad (3.52)$$

Sc is the Schmidt number, defined in equation 3.53.

$$Sc = \mu_B / \rho D_L \quad (3.53)$$

D_L is the molecular diffusion coefficient of the diffusing component, μ_B is the fluid viscosity, d_p is the particle diameter, and v_r is the *relative* velocity between the fluid and the immobilized cell particle (Willaert et al., 1996).

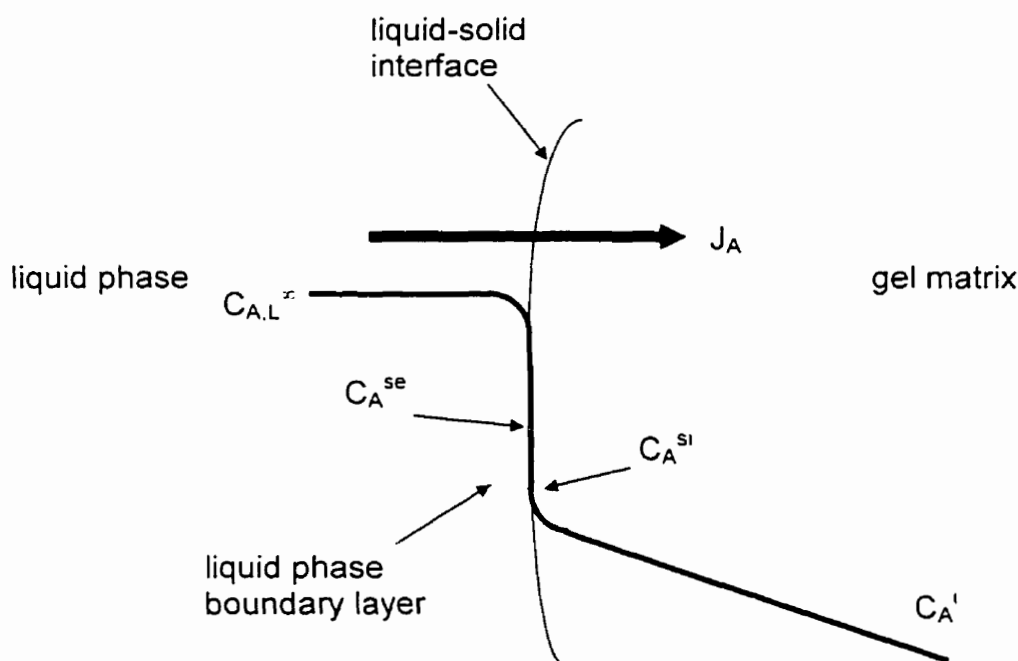


Figure 3.4. Concentration profiles for overall mass transfer of substrate from the bulk liquid phase into a gel bead.

Dissolved oxygen is often one of the key substrates diffusing into immobilized cell matrices. Oxygen must leave the air bubbles to dissolve into the liquid phase where it travels and then enters the immobilized cell matrix as a substrate (Figure 3.3). The main factors which affect solubility for sparingly soluble gases, such as oxygen, are the partial pressure in the gas phase, the presence of solutes in the liquid phase, and the temperature. Henry's Law (equation 3.54) correlates the gas solubility with its partial pressure in the gas phase:

$$C_{A,L}^* = P_{A,G} / H \quad (3.54)$$

where $C_{A,L}^*$ is the solubility of the gas in the liquid phase, $P_{A,G}$ is the partial pressure in the gas phase, and H is the Henry's Law constant. Temperature has a significant effect on gas solubility, because it affects Henry's Law constant H .

The presence of acids, salts, and sugars usually decreases the solubility of gases. A large number of experimental data for the Henry's Law constant exists in the literature (Perry, 1984). In order to find the solubility of oxygen in fermentation broth, one must know the temperature and total pressure. The oxygen partial pressure is then found and,

using Henry's Law, one can calculate oxygen solubility in pure water. This value is then corrected for the presence of salts, sugars, etc. (Schumpe et al., 1982). This value will still only be an approximation for a typical beverage fermentation because often the fermentation medium is a very complex liquid, with many components.

3.5.1.3 Equations for Predicting Solute Molecular Diffusivities in the Bulk Liquid Phase

There are several correlations available for predicting molecular diffusivities of specific solutes in the liquid phase. For dilute systems, the Wilke-Chang equation can be used as in equation 3.55. This equation is used for solutes that have smaller molar volumes, which are less than $0.500 \text{ m}^3 / \text{kg}\cdot\text{mol}$ (Geankoplis, 1993).

$$D_L = 1.173 \times 10^{-16} (\varphi M_B)^{1/2} [T / (\mu_B V_A^{0.6})] \quad (3.55)$$

where, M_B , is the molecular weight of solvent B, μ_B is the viscosity of B in Pa·s, V_A is the solute molar volume at the boiling point, T is the temperature in degrees Kelvin, and φ is the association parameter of the solvent (Geankoplis, 1993). The association parameter is 3.6 for water, 1.5 for ethanol, and 1.0 for other unassociated solvents. When values of V_A are greater than $0.500 \text{ m}^3/\text{kg mol}$, the Stokes-Einstein equation 3.56 is recommended.

$$D_L = 9.96 \times 10^{-16} T / \mu_B V_A^{1/3} \quad (3.56)$$

However, when predicting diffusivities for larger biological solutes (solute molecular weight above 1000), a more accurate approximation is the semi-empirical equation 3.57 suggested by Polson (1950), for dilute aqueous solutions.

$$D_L = 9.40 \times 10^{-15} T / \mu_B M_A^{1/3} \quad (3.57)$$

3.5.1.4 Partition Coefficient

Under equilibrium conditions between the solute concentrations in the solid immobilization matrix, C_A^i , and the bulk liquid phase, $C_{A,L}^\infty$, a partition coefficient, K_p , is defined by equation 3.58 (Merchant, 1986):

$$K_p = C_A^i / C_{A,L}^\infty \quad (3.58)$$

Reactor design factors such as reactor type, size and operating conditions will influence external mass transfer in immobilized cell systems by affecting the mass

transfer coefficient, k_L . Surface contact between the biocatalyst (e.g. immobilized yeast cell) and the growth medium (e.g. wort, wine must) could be maximized by optimizing liquid-solid mixing. Sufficient agitation is needed so that the thickness of the liquid film surrounding the solid immobilization matrix is minimized, which results in high values of k_L . At the same time, the shear on the immobilized cell particles must be adjusted so that there is no damage to the matrix or the cells, while still providing adequate bulk mixing (Oldshue and Herbert, 1992). This must be considered when choosing the type of mixing for immobilized cell bioreactors. If shear rates are too high, biomass may be lost from adsorption matrices, immobilized cell particles may break, and cell aggregates may be disrupted. It therefore becomes important to design a reactor which provides adequate mixing at a reasonable shear rate. Specific information on mixing in fluidized immobilized cell bioreactors is given by several authors including Chisti and Moo-Young (1993), Fan (1989), Heijnen et al. (1993), and Hwang and Fan (1986).

3.5.2 Internal Mass Transfer in Immobilized Cell Systems

Internal mass transfer pertains to the transfer of substrates and products within the carrier solid phase (Norton and D'Amore, 1994), and is of particular importance for entrapped cell systems. Fick's Law is used to define internal mass transport by molecular diffusion. If the pore sizes are very small and of the order of magnitude of the mean free path of a diffusing gas substrate, other types of diffusion such as Knudsen gas diffusion and transition gas diffusion (Geankoplis, 1993) must also be considered. It was also noted by Willaert et al. (1996) that when sufficient pressure difference is present across the system and porosity is high, transport of molecules may occur by convective flow through systems in which cells are immobilized using membranes or adsorption. For the purposes of this review it will be assumed that mass transfer occurs by diffusion only within the immobilized cell particle.

For a homogeneous phase system, the rate of transfer of a diffusing substance through a unit area is proportional to the concentration gradient measured normal to the section and is given by Fick's first law of diffusion in equation 3.59.

$$J = -D \frac{\partial C}{\partial x} \quad (3.59)$$

where J is the mass transfer rate of species A per unit area, C the concentration of diffusing species A in the entire immobilization matrix, x the distance and D is the diffusion coefficient of species A in the immobilization matrix, such as a polymeric gel.

Equation 3.60 defines the effective diffusion coefficient, D_e , for non-homogeneous immobilization matrices. Since this review deals mainly with immobilization of cells within gel beads, a spherical coordinate system may be used, with r representing the radial coordinate in a spherical immobilization matrix.

$$J = - D_e \partial C_L / \partial r \quad (3.60)$$

where J is the diffusional flux in the r direction, and C_L is the solute concentration in the liquid phase of the pores (Westrin and Axelsson, 1991). Hydrogels, such as calcium alginate and kappa-carrageenan, do not have well-defined permanent porous structures, and therefore the concept of liquid-filled pores is slightly misleading (Axelsson et al., 1994). However, the effective diffusion coefficient, D_e , is used in the expression for the Thiele Modulus and for the determination of the effectiveness factor of such immobilized cell carriers.

According to Westrin and Axelsson (1991), concentration in the total volume of the immobilization matrix is correlated with C_L using the void fraction (ϵ) which is accessible to the diffusing solute as in equation 3.61.

$$C = \epsilon C_L \quad (3.61)$$

Thus it follows that the relationship between the two diffusion coefficients is given as in equation 3.63.

$$D_e = \epsilon D \quad (3.62)$$

Because of exclusion and obstruction effects, the effective diffusion coefficient, D_e , through a porous support material is lower than the corresponding diffusion coefficient in the aqueous phase, D_a (Willaert et al., 1996). A fraction of the total volume ($1 - \epsilon$) is excluded from the diffusing solute, due to the presence of the support. A longer diffusional path length, denoted by the tortuosity factor (τ), results when the movement of solute is obstructed by the impermeable support matrix. One can quantify the effects of both of these factors on the effective diffusion coefficient using equation 3.63.

$$D_e = (\epsilon/\tau) D_a \quad (3.63)$$

It is often difficult to calculate ϵ and τ , so prediction using the polymer volume fractions are recommended (Muhr and Blanshard, 1982) using equation 3.64.

$$D = [(1 - \phi_p)^2 / (1 + \phi_p)^2] D_a \quad (3.64)$$

where ϕ_p is the polymer volume fraction. For low molecular weight solutes in cell-free supports, an approximate measure of ϵ is given by equation 3.65.

$$\epsilon = 1 - \phi_p \quad (3.65)$$

Westrin and Axelsson (1991), used equations 3.62 and 3.65 to rewrite equation 3.64 to derive an expression for D_c as a function of ϕ_p using equation 3.66

$$D_c = [(1 - \phi_p)^3 / (1 + \phi_p)^2] D_a \quad (3.66)$$

One limitation of the above equation is that although it does account for exclusion and obstruction effects of immobilization matrices, it does not account for other effects such as ionic interactions (Axelsson et al., 1994). In a review by Muhr and Blanshard (1982) it was noted that a polymer immobilization matrix may also affect solute diffusion by increasing hydrodynamic drag, altering the properties of the solvent and by polymer involvement. Muhr and Blanshard (1982) present a comprehensive evaluation of the effects of gel substance on the course of diffusion.

Researchers have found that the cell mass is mainly confined to a biolayer at the periphery of gel entrapment matrices, due to a lack of substrate at the center of the beads (Lewandowski et al., 1993). Internal mass transfer can be optimized by adjusting the immobilization matrix size, texture and porosity. Decreasing bead diameter is a good way of minimizing internal mass transfer limitations. However, a balance must be achieved so that the beads are large enough for easy separation from the bulk liquid phase and small enough to maximize mass transfer.

When qualitative studies on the dynamics of the growth of immobilized cells were first conducted, growth of biomass was described as expanding at similar rates throughout the beads following start-up. Because of diffusion limitations, over time the biomass eventually becomes confined mainly to areas near the gel surface. Using a conventional pseudo-homogeneous growth model to predict cell growth within gel entrapment matrices, led to an over-estimation of macroscopic substrate consumption rates. This occurred because this model did not account for diffusion limitations over larger micro-colonies (Salmon and Robertson, 1987, Wijffels et al., 1996). Wijffels et al.

(1996) theorize that one must regard biomass growth as expanding micro-colonies, rather than as a homogeneous increase of biomass in spherical "shells" within the gel beads, in order to incorporate diffusion limitation across micro-colonies in a dynamic growth model. When diffusion limitation over micro-colonies is incorporated into the dynamics of the immobilized cell system, the colony-expansion model predicts that inoculum size will affect substrate consumption rates. Numerous small micro-colonies form when high initial biomass concentrations are used, which only cause minor diffusion limitations. At low initial biomass concentrations, fewer but bigger colonies form causing significant diffusion limitations. Higher macroscopic substrate consumption rates resulted in the system containing beads with smaller microcolonies. These findings were confirmed experimentally in a continuous air lift loop bioreactor (Wijffels et al., 1996).

Table 3.1 shows a summary of experimental methods used to determine diffusion coefficients within gels (Willaert et al., 1996) and Table 3.2 lists some effective diffusivities found by various researchers.

Table 3.1. Experimental methods to determine diffusion coefficients in immobilization matrices (adapted from Willaert et al., 1996).

Concentration Gradient Methods: Steady State

True steady-state diaphragm cell

Pseudo-steady-state diaphragm cell

Concentration Gradient Methods: Transient

Time-lag diaphragm cell

Uptake/release from particles

Concentration profile in a semi-infinite slab

Finite couples method

Miscellaneous: capillary method, light interferometry,
electrode or mass spectrometric probe covering

Indirect methods: chromatographic breakthrough curves

Other Methods

Fourier transform pulsed-gradient spin-echo

Dynamic light scattering

Fluorescence recovery after photobleaching

Magnetic Resonance Imaging

Holographic relaxation spectroscopy

Table 3.2. Effective diffusivities of some substrates in immobilization matrices.

Type of Gel	Concentration of Gel (%w/v)	Type of Solute	Method of Measurement	Cell Type	Temp. (°C)	Effective Diffusivity De (X10 ⁶ cm ² /s)	Reference	
Ca-alginate	2	lactose	uptake/release from particles	no cells	30	4.3	Øyaas et al., 1995	
Ca-alginate	2	lactic acid	uptake/release from particles	no cells	30	6.9		
Ca-alginate	2	glucose	uptake/release from particles	no cells	30	6.4		
Ca-alginate	2	sucrose	uptake/release from particles	no cells	30	4.6		
Ca-alginate	2	succinic acid	uptake/release from particles	no cells	30	7.8		
Ca-alginate	2	glucose	uptake/release from particles	no cells	30	6.62		Merchant et al., 1987
Ca-alginate	2	glucose	diffusion cell	no cells	22-26	6.1*	Hannoun et al., 1986	
κ-carrageenan	4	glucose	uptake/release from particles	no cells	30	6.7	Etapé et al., 1992	
κ-carrageenan	4	ethanol	uptake/release from particles	no cells	30	10.1		
κ-carrageenan	3	glucose	uptake/release from particles	no cells	30	3.8-4.8	Venâncio et al., 1997	
κ-carrageenan	3.5	glucose	diffusion cell	no cells	25	3.8		
Ca-alginate	3	fructose	diffusion cell	no cells	30	6*		
Ca-alginate	3	glucose	diffusion cell	no cells	30	6.7*		
Ca-alginate	3	xylose	diffusion cell	no cells	30	9.01*		
Ca-alginate	3	lactose	diffusion cell	no cells	30	4.66*		
Ca-alginate	3	maltose	diffusion cell	no cells	30	4.6*		
Ca-alginate	3	sucrose	diffusion cell	no cells	30	4.67*		
Ca-alginate	3.5	oxygen	uptake/release from particles	<i>S. cerevisiae</i>	30	3.08-3.44		Kurosawa et al., 1989
Ca-alginate	2	glucose	diffusion cell	<i>S. cerevisiae</i>	22-26	5.1-6.0		Korgel et al., 1992
Ca-alginate	3.4-3.8	galactose	steady state	<i>S. cerevisiae</i>	30	6.2-3.4	Kurosawa et al., 1989	
κ-carrageenan	4	glucose	uptake/release from particles	<i>P. aeruginosa</i>	30	3.7-6.4		
Ca-alginate	0.5-1.5	xylose	uptake/release from particles	<i>S. cerevisiae</i>	30	1.5-6.3		
Ca-alginate	2	galactose	beads in well-stirred tank	<i>Z. mobilis</i>	30	3.5-5.7		

*reported by authors as diffusivities.

The overall effectiveness of immobilized cell reactors is affected by the rate of transfer of substrates and products to and from the immobilized cell system (external mass transfer) and by the rate of transport inside the immobilized cell system (internal mass transfer). In order to generate models for immobilized cell productivity and growth, one must determine if mass transfer is rate-limiting or if chemical reaction rates are limiting. If mass transfer resistances are limiting, one must also determine whether external or internal mass transfer resistances dominate.

More research is needed to develop highly accurate experimental methods for measuring the effective diffusivities of different solutes within immobilization matrices containing viable cells. Many of the methods listed in Table 3.2 assume that the matrix in which the diffusion takes place is homogeneous, throughout. Nava Saucedo et al. (1996) have shown that alginate gel matrices are actually heterogeneous with distinct internal zones. Furthermore, gelling conditions will also affect the degree of heterogeneity of a given gel matrix and consequently alter the diffusivity of a given solute in entrapment matrices. Correlations such as equation 3.66 (Muhler and Blanshard, 1982), which relate the molecular diffusivity of a given solute in the aqueous phase to the effective diffusivity within the matrix, account for exclusion and obstruction effects, but do not account for other effects such as ionic interactions, hydrodynamic drag, altered properties of the solvent and polymer involvement. A reliable and accurate non-invasive method to monitor immobilized cell viability and vitality under fermentation conditions, would allow researchers to directly examine the effects of mass transfer and the immobilization process on cell metabolic activity.

CHAPTER 4. MATERIALS AND METHODS

4.1 Yeast Strain and Characteristics

A lager brewing strain of *Saccharomyces cerevisiae*, Labatt Culture Collection (LCC) 3021, was used throughout this work. *Saccharomyces cerevisiae* is synonymous with *Saccharomyces uvarum* Beijerinck var. *carlsbergensis* Kudryavtsev, 1960 (Kurtzman, 1998). At 37°C LCC 3021 will not grow. This helps to distinguish LCC 3021 lager yeast from most ale yeast, which will grow at 37°C and higher temperatures. LCC 3021 is a bottom fermenting strain, as are most lager yeast, but there are exceptions. As well, this strain will ferment glucose, galactose, sucrose, maltose, raffinose, and melibiose, but not starches. The ability to ferment melibiose is one tool used by taxonomists to distinguish it from ale yeast.

As with most brewing strains, LCC 3021 is polyploid and reproduces by mitotic division. Under normal brewing conditions lager yeast does not reproduce by meiosis. This has the advantage of making the brewing strain genetically stable because crossover of genetic material is less likely (Kreger-van Rij, 1984).

4.2 Preparation of Yeast Inoculum

Yeast was taken from a vial cryogenically preserved in a -80°C freezer and streaked on Peptone Yeast-Extract Nutrient (PYN) agar (peptone, 3.5 g/L; yeast extract, 3.0 g/L; KH_2PO_4 , 2.0 g/L; $\text{MgSO}_4 \cdot 7\text{H}_2\text{O}$, 1.0 g/L; $(\text{NH}_4)_2\text{SO}_4$, 1.0 g/L; glucose, 20.0 g/L; agar, 20.0 g/L in dH_2O) growth medium to obtain well-separated colonies. A sterile loop consisting of several colonies was taken from the 3-4 day old plate of growing yeast, and these colonies were inoculated into a 10 mL volume of wort in a test tube. This was allowed to grow at 21°C overnight, thus the term "overnight culture", and then was added to a larger volume of wort, usually 200 mL, to increase yeast biomass. In consecutive days, this mixture was added to another larger volume of wort, and so on, until the desired amount of yeast biomass was propagated. Generally one expects to produce approximately 20 g of lager yeast per litre of wort. To prepare for yeast inoculation, the culture was centrifuged at 4°C and 1.0×10^4 rpm (radius = 0.06 m) for 10 min. After

centrifuging, the liquid was decanted and the appropriate wet weight of yeast was obtained from the pellet for pitching.

4.3 Wort Fermentation Medium

Labatt Breweries of Canada supplied brewery wort with a specific gravity of 17.5°P. The concentration of fermentable carbohydrates, specific gravity, and free amino nitrogen in the brewer's wort used for the fermentations throughout this work is given in Appendix A2.1. Additional detail on the wort composition is given by Dale et al., 1986, Hoekstra, 1975, Hough et al., 1982, Klopper, 1974, and Taylor, 1989.

Batch Fermentations: Wort was heated in an autoclave for 45 min at 100°C and then cooled, before inoculation with immobilized cell beads or freely suspended yeast.

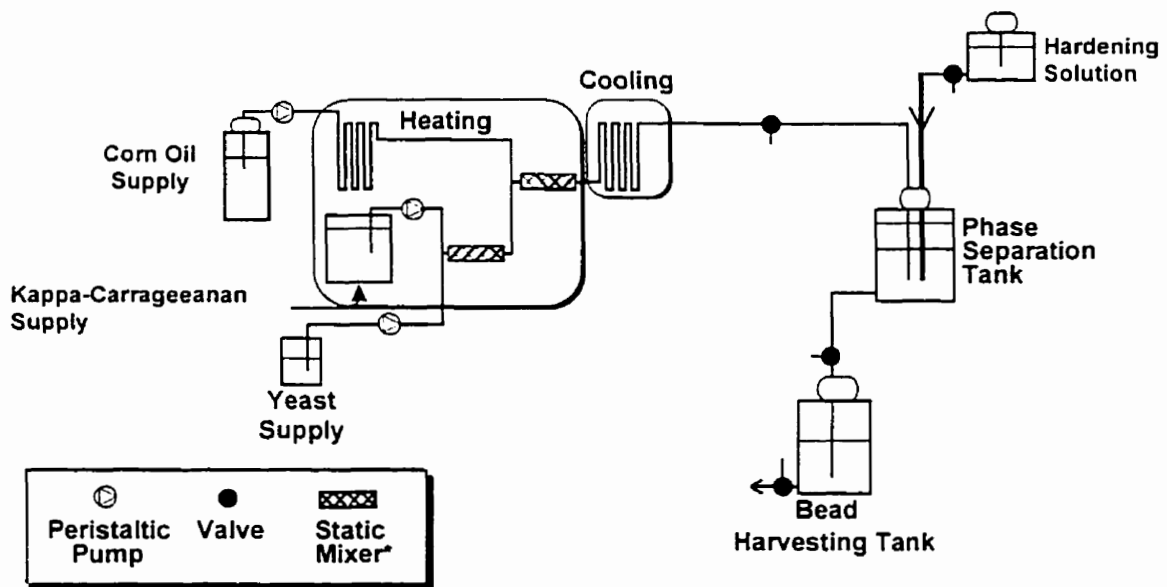
Continuous Fermentations: The wort used for the continuous fermentations was flash pasteurized (Fisher Plate Heat Exchanger, combi-flow Type Eurocal 5FH) prior to feeding into the gas lift bioreactor and this wort was monitored regularly for microbial contaminants, as described in section 4.6. If contamination was detected in the wort, it was immediately discarded and new wort was collected from the plant.

The flash pasteurizer was operated at a volumetric flow rate of 0.8 m³ / hr. The unit had a tubular holding section where the wort was held at an average temperature of 85°C with a minimum temperature of 80°C. The volume of the holding section was 1.13 x 10⁻² m³, giving a residence time in the holding section of 51 seconds. Following the heating step, the wort was rapidly cooled to a temperature of 2°C upon exiting the unit.

4.4 Immobilization Methodology

Kappa-carrageenan gel X-0909 was a generous gift from Copenhagen Pectin A/S. Kappa-carrageenan gel beads containing entrapped lager yeast cells were produced using the static mixer process, as described in detail by Neufeld et al. (1996), with initial cell loadings of 10⁷ – 10⁸ cells/mL of gel, which are specified for each experiment. As illustrated in Figure 4.1, the static mixer process is based on the formation of an emulsion between a non-aqueous continuous phase, vegetable oil (Mazola Corn Oil), and an

aqueous dispersed phase, kappa-carrageenan (3% w/v) in KCl (0.2% w/v) solution, inoculated with yeast, using in-line polyacetal static mixers (Cole-Parmer Instrument Co., USA). In the heating section of the schematic, where the yeast was rapidly mixed with the carrageenan solution and the emulsion was formed, the temperature was 37°C. Gelation of the kappa-carrageenan droplets within the emulsion was induced with rapid cooling in an ice bath and subsequent hardening in a potassium chloride bath (22 g/L). A 24-element static mixer of 6.4 mm in diameter was used to create the mixture of yeast and carrageenan. A second 42 element mixer of 12.7 mm in diameter was used to create the emulsion. The beads used for the experiments in this work were 0.5 mm < (bead diameter) < 2.0 mm.



*Static Mixer: fluid moves through the mixer (rather than the mixer through the fluid) allowing for mixing of fluids as they are pumped through the pipe line.

Figure 4.1. The static mixer process for making kappa-carrageenan gel beads.

4.5 Cumulative Particle Size Distribution of Kappa-Carrageenan Gel Beads Containing Immobilized Yeast Cells

Kappa-carrageenan gel beads were randomly sampled from a 30-L production run of gel beads in order to calculate a particle size distribution on a mass wet-weight basis. Each sample was approximately 500 g wet weight. Sieving was used to determine the bead particle size distribution. The beads were passed through a series of sieves with grid sizes of 2.0, 1.7, 1.4, 1.18, 1.0, and 0.5 mm. A 4.5 L volume of 22 g/L KCl solution was used facilitate the sieving of each bead sample. The kappa-carrageenan gel beads were assumed to be perfectly spherical so that the sieve diameter was taken as the particle diameter. It was also assumed that the particle density was uniform and independent of particle size.

4.6 Yeast Cell Enumeration and Viability

Freely Suspended Yeast Viability and Cell Concentration: The American Society of Brewing Chemists International methylene blue staining technique (Technical Committee and Editorial Committee of the ASBC, 1992) was used to measure yeast cell viability. The stain measures whether a yeast population is viable or non-viable based on the ability of viable cells to oxidize the dye to its colourless form. Non-viable cells lack the ability to oxidize the stain and therefore stain blue. Fink-Kuhles buffered methylene blue was prepared by mixing 500 mL of Solution A (0.1 g methylene blue / 500 mL dH₂O) with 500 mL of Solution B (498.65 mL of 13.6 g KH₂PO₄ / 500 mL d H₂O mixed with 1.25 mL of 2.5 g Na₂HPO₄·12H₂O / 100 mL d H₂O) to give a final buffered methylene blue solution with a pH of 4.6.

The diluted yeast solution was mixed with the methylene blue solution in a test tube, to a suspension of approximately 100 yeast cells in a microscopic field. A small drop the well-mixed suspension was placed on a microscope slide and covered with a cover slip. Following one to five minutes of contact with the stain, the cells stained blue and the cells remaining colourless were enumerated. The percentage of viable cells was

reported as a percentage of the total number of cells enumerated. Cell concentration was determined using a light microscope and a Hemacytometer (Hauser Scientific Company).

Immobilized Cell Viability and Cell Concentration: Gel beads were separated from the fermenting liquid by passing the mixture through a sterile sieve (500 μm pore mesh size) and rinsing with 10 mL of distilled water. Gel beads, 1 mL, containing entrapped yeast were added to a sterile 50 mL specimen container containing 19 mL of distilled water. The beads were then disrupted using a Polytron[®] (Brinkmann Instruments) apparatus, to release the cells from the gel. Cell viability and concentration were then measured as described for the freely suspended cells.

4.7 Microbiological Analyses

Liquid Phase Analyses: Samples were taken from continuous fermentations at least once a week for microbiological analyses. The wort that was used for continuous fermentations was also tested for contamination prior to transferring it into the bioreactor. To test for the presence of both aerobic and anaerobic bacteria, samples were plated on Universal Beer Agar (UBA, Difco Laboratories), with the addition of 10 mg/L of cycloheximide, and incubated at 28°C for 10 days. Plates that were tested for anaerobic bacterial contamination were placed in an anaerobic jar with an AnaeroGen[®] (Oxoid) packet, which takes up any oxygen remaining in the jar, creating an anaerobic environment. An anaerobic indicator (Oxoid), which turns pink in the presence of oxygen, was used to verify anaerobic conditions within the jar. Wild yeast contamination was tested by plating samples on yeast medium (YM agar, Difco Laboratories) plus CuSO_4 (0.4 g/L) incubated at 25°C for 7 days. Peptone Yeast-Extract Nutrient agar (PYN), described previously, was used to screen samples for non-lager yeast contaminants at 37°C for 7 days. The absence of yeast growth on PYN at 37°C indicated that no ale yeast or contaminants that grow at 37°C were present.

Gel Phase Analyses: An assay was developed in our laboratory to ensure that the immobilized cell beads to be used for fermentations were free of contaminating bacteria before being pitched into the bioreactor. The main concern was to avoid contamination

with beer spoilage organisms such as *Pediococcus sp.* and *Lactobacillus sp.* or wild yeast. A 3 mL volume of carrageenan gel beads was inoculated into 100 mL of several different selective liquid media described below and placed in 250 mL flasks at 25°C, and shaken at 100 rpm in an incubator shaker. NBB broth (Nachweis von Bierschädlichen Bakterien) (BBL cat # 98139, NBB Broth Base, 0.02 g/L cycloheximide) is a semi-selective medium which is used to test for beer spoilage bacteria, such as *Pediococcus sp.* and *Lactobacillus sp.* Copper sulphate broth (16 g/L YM broth, Difco; 0.4 g/L CuSO₄) is a semi-selective medium to test for wild yeast contaminants. Finally, Standard Methods (STA) + cycloheximide broth (16 g/L "Standard Methods" broth, Difco; 0.02 g/L cycloheximide) is used to test for bacteria found in water, wastewater, dairy products, and foods (Power and McCuen, 1988). The selective media were chosen to detect and identify potential beer spoilage organisms within three days. Contaminated samples were indicated by turbidity within the sample and a presumptive identification of the contaminants was made.

Respiratory Deficient (RD) Yeast Cell Detection Methodology: Triphenyltetrazolium Chloride (TTC) Overlay Technique: This method was used to distinguish respiratory deficient yeast from the rest of the population, and is based on the principle that TTC is a colourless salt that forms a red precipitate upon reduction. When TTC is overlaid onto yeast colonies growing on Yeast-Peptone-Dextrose (YPD) agar (yeast extract, 10 g/L; Peptone, 20 g/L; Dextrose, 20 g/L; Agar, 20 g/L in dH₂O), respiratory sufficient yeast will reduce the TTC, and these colonies will become dark pink to red. However, respiratory deficient yeast do not reduce the dye and retain their original colour.

Cultures were serially diluted to a suitable concentration of microorganisms, ~100 cells/ 0.2 mL, for plating. The YPD plates were then incubated for approximately 3 days at 21°C until yeast colonies were visible in an aerobic environment. Each plate was then overlaid with 20 mL of 50°C TTC overlay agar. After cooling the individual solutions to 50°C, TTC overlay agar was made by mixing 1:1 Solution A (12.6 g/L NaH₂PO₄; 11.6 g/L Na₂HPO₄; 30.0 g/L agar in dH₂O, autoclaved at 121°C, 15 min) with Solution B (2.0 g/L 2,3,5-triphenyltetrazolium chloride in dH₂O, autoclaved at 121°C, 15 min). Plates

were read after 3 hours of incubation at ambient temperature. Percent RD was reported as a percent of unstained colonies of the total number observed.

4.8 Scanning Electron Microscopy (SEM) of Yeast Immobilized in Kappa-Carrageenan Gel Beads

Kappa-carrageenan gel beads containing immobilized yeast were removed from the bioreactor through the sample port and placed in a 10 mL screw-cap glass vial, with the beads submerged in a small volume of fermentation broth. The vial was immediately covered in ice and transported in an insulated container to the SEM facility. Kappa-carrageenan gel beads containing immobilized yeast were fixed in 2% (v/v) glutaraldehyde prepared in Sorensen's phosphate buffer, 0.07 M, pH 6.8 (Hayat, 1972). This was followed by post-fixing in 1% (w/v) osmium tetroxide, prepared in the same buffer, and dehydration through a graded series of alcohol solutions 50, 70, 80, 90, 95, 100% (v/v), at 15 min for each, and then 3 changes at 100%. Before critical point drying (Ladd Research Industries, Burlington, VT) through carbon dioxide, some beads were frozen in liquid nitrogen, fractured and collected into 100% alcohol. Freeze fracturing allows the internal face of the beads to be exposed with minimum distortion. Following critical point drying, the samples were sputter-coated (Polaron SC500 sputter coater, Fison Instruments, England) with 30 nm of gold/palladium and then scanned with a Hitachi S-4500 field emission scanning electron microscope (Nissei Sangyo, Tokyo, Japan).

4.9 Bioreactor Sampling Protocol

The bioreactor sample port (Scandi-Brew Type T Membrane Sample Valve) reservoir was filled with 70% (v/v) ethanol solution to maintain aseptic conditions around the opening between samplings. In order to take a sample, the plug was removed from the base of the ethanol reservoir, drained, and rinsed thoroughly with ethanol, prior to opening the port. Samples were collected into a crimp vial or a screw-cap jar and volumes varied from 5-60 mL, depending on the analysis required. In order to test for microbiological contamination, 10 mL of the fermentation liquid was vacuum-pumped

though a sterile membrane filter unit. The membrane, 0.45 μm pore size, was placed on the appropriate selective medium, as described in Section 4.6.

For chemical analyses, 60 mL of sample was withdrawn through the septum from the 100 mL crimp-sealed vial and syringe-filtered through a Schleicher and Schull, FP-050, double-layer syringe filter system, 5 μm and 0.45 μm pore sizes. The required volume of sample was then dispensed into a 20 mL head space vial and crimped with a Teflon septum and aluminum cap. The required sample volumes are listed in Table 4.1.

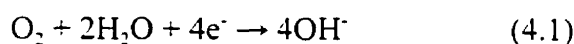
Table 4.1. Sample volume requirements for various chemical analyses.

Sample	Volume (mL)
ethanol	5
short-chain diols	10
beer volatiles	12
vicinal diketones	5
carbohydrates/specific gravity/ free amino nitrogen/protein	12

4.10 Dissolved Oxygen Measurement

The Dr. Thiedig Digox 5 dissolved oxygen analyzer measures dissolved oxygen in the range of 0.001 - 19.99 mg/L in wort, fermenting wort and beer (Anon, 1998). Vilachá and Uhlig, (1985) tested many instruments for dissolved oxygen measurement in beer and found the Digox analyser to give trust-worthy, precise values.

The electrochemical measurement method used by the Digox 5 is based on an amperometric three-electrode arrangement with a potentiometer. The measuring cell consists of a measuring electrode (cathode) and counter electrode (anode). These electrodes are exposed to the liquid in which the oxygen concentration is to be measured. A reaction at the measurement electrode occurs after fixing a defined measurement potential. At the large, silver, measurement electrode, molecules of oxygen are reduced to hydroxyl ions. Two water molecules react in equation 4.1, with one molecule of oxygen, while absorbing four electrons, giving four hydroxyl ions.



The stainless steel anode absorbs the four electrons released at the cathode in order to ensure the flow of current. In equation 4.2, the measurement current, I , is directly proportional to the oxygen concentration, $C_{L,O}$:

$$I = K \times C_{L,O} \quad (4.2)$$

where the constant, K , is influenced by the Faraday constant, the number of electrons converted per molecule, the cathode surface area, and the width of the boundary layer at the surface of the measurement electrode.

A constant, characteristic, measurement potential is critical for the selectivity (for oxygen) and precision of the measurement. The measuring voltage is stabilized by the reference electrode, which is not burdened by current. This, together with the potentiostat, which provides electronic feedback, provides a constant measurement potential. The surface of the measurement electrode is electrolytically connected to the reference electrode via a diaphragm.

The error, based on the measuring range of the final dissolved oxygen concentration, was $\pm 3\%$ (Anon, 1998). The dissolved oxygen analyzer was calibrated using the Thiedig Active Calibration, in which the Digox 5 produced a defined oxygen quantity based on Faraday's Law (0.500 mg/L) and then cross-checked this with the measured values in the matrix. This allowed the instrument to be calibrated under the pressure, temperature and flow conditions corresponding to those of the measurement, within one min. Because the exchange of molecules in the sensor is a diffusion process, it is influenced by temperature, resulting in faster reaction rates and increases in the measured current. Therefore, the Digox 5 is also equipped with a sensor, which measures the temperature and automatically compensates for fluctuations.

The Digox 5 has some advantages over membrane-based oxygen sensors. Because the Digox uses no electrolyte, the sensitivity loss is relatively slow and only minor deposits on the measurement electrode occur. Also, the sensitivity can be determined at any time, by performing an active calibration. It is a simple procedure to clean the electrode and recalibrate the instrument. In most membrane-sensors, silver chloride is deposited on the cathode, and the electrolyte solutions changes, resulting in progressively lower readings. For this reason membranes and electrolytes are recommended to be

changed every few weeks and then recalibrated, a lengthy and cumbersome task. Calibration of the membrane-based sensors is usually conducted in the lab at oxygen saturation levels, which could cause appreciable errors, especially in the wort and beer matrix at very low oxygen levels. Temperature will have a three-fold influence on membrane-based oxygen sensors: membrane permeability will change, the partial pressure of oxygen will change, and the solubility of oxygen in the electrolyte will change. Temperature compensation for these three factors in membrane-based sensors is difficult.

Dissolved Oxygen Measurement in the Wort During Storage: Flexible Tygon[®] food grade tubing (¼ inch i.d.) was aseptically connected to a sample port located near the top of the conical bases of the wort storage tanks, T-1 and T-2 (see section 4.2.1). A variable speed peristaltic pump provided volumetric flow rate of 11 L/hr through the dissolved oxygen analyzer block. ((Masterflex[®] L/S[™] Digital Standard Drive, Cole-Parmer cat. #P-07523-50)). Wort dissolved oxygen measurements were then recorded after 4-5 minutes.

Dissolved Oxygen Measurement in the Bioreactor: Prior to performing the dissolved oxygen measurements on the bioreactor, the Digox 5 analyser block was sanitized. The inlet of the sensor was connected to sterile, Tygon[®] Food Grade tubing (¼ inch i.d.). A 70% (v/v) ethanol solution was pumped through the analyzer at a volumetric flow rate of approximately 10 L/hr for 15 min. The dissolved oxygen analyzer was connected to a laboratory water tap and hot water (70°C) was passed through the sensor for a minimum of 2 hours. This methodology was used rather than steam sterilization because the analyzer block materials cannot tolerate temperatures of above 70°C. Following the two-hour sanitation period, the tubing at the inlet and outlet of the unit was clamped to maintain sterility within the analyzer. In a laminar flow hood, the freshly sterilized tubing was connected to the inlet and outlet of the analyzer. The free ends of the tubing were then aseptically clamped to the ¼" I.D. stainless steel ports on the bioreactor head plate and measurements were taken. When the ports on the bioreactor were not in use, they were sealed using a short length of sterilized Tygon[®] food grade tubing.

Dissolved oxygen was measured on-line in the gas lift bioreactor by withdrawing liquid from the fermentation through a port situated on the bioreactor head plate. The fermentation liquid exited the bioreactor through a stainless steel filter (see section 4.1.2) connected to a ¼ inch stainless steel pipe which penetrated the bioreactor head plate. The liquid then flowed through flexible Tygon[®] food grade tubing (¼ inch i.d.), which was connected to a variable speed peristaltic pump (Masterflex[®] L/S[™] Digital Standard Drive, Cole-Parmer cat. #P-07523-50), providing a volumetric flow rate of 11 L/hr through the dissolved oxygen analyzer block. The fermentation liquid was then recycled through a second quarter-inch stainless steel port, which penetrated the bioreactor head plate. Tygon[®] food grade tubing (Cole-Parmer, 1999) was used to connect the sensor to the bioreactor because of its supplier-specified low oxygen permeability of $30 \text{ cm}^3\text{mm}/(\text{s}\cdot\text{cm}^2\cdot\text{cmHg}) \times 10^{-10}$. The measurement was taken after 4-5 minutes of circulation.

4.11 Chemical Analyses

Calibrations were performed using the appropriate standard reagents. All reagents used for the analyses were >99% pure. Where necessary, subsequent purification via distillation was performed.

4.11.1 Ethanol

Ethanol concentration was determined using the internal standard gas chromatograph (GC) method of the Technical Committee and Editorial Committee of the American Society of Brewing Chemists (1992). Degassed samples were treated directly with isopropanol internal standard, 5% (v/v) and injected into a Perkin Elmer 8500 Gas Chromatograph equipped with a flame ionization detector (FID) and a Dynatech autosampler. A Chromosorb 102, 80-100 mesh column was used with helium as the carrier gas. Chromatographic conditions: flow rate of 20 mL/min, injector temperature of 175°C, detector temperature of 250°C, and column temperature of 185°C.

4.11.2 Carbohydrate Summary

Glucose, fructose, maltose, DP3 (maltotriose), DP4 (maltotetraose), poly-1 (polysaccharide peak 1) and glycerol concentrations in fermentation samples were quantified using a Spectra-Physics (SP8100XR) high performance liquid chromatograph (HPLC) equipped with a cation exchange column (Bio-Rad Aminex, HPX-87K) and a refractive index detector (Spectra-Physics, SP6040XR). The mobile phase was potassium phosphate, dibasic, 0.01 M, and the system was equipped with a Spectra-Physics (SP8110) auto sampler. The instrument was operated with a backpressure of 800 psi. The flow rate of sample and eluent through the column was 0.6 mL/min, with a column temperature of 85°C and a detector temperature of 40°C. The injection volume was 10 μ L.

4.11.3 Specific Gravity

The specific gravity of the wort and fermentation medium is described in this study in terms of Real Extract (degree Plato, °P), which is the accepted unit used in the brewing industry.

Fermentation samples were filtered as described in section 4.8 and vortexed prior to analysis with a digitalized density meter (Anton Paar DMA-58 Densitometer) to measure wort specific gravity (degree Plato). The fermentation samples were inserted into a glass u-tube, which oscillated electronically to determine the specific gravity, thus giving degree Plato indirectly.

Degree Plato refers to the numerical value of a percentage (w/v) sucrose solution in water at 20°C whose specific gravity is the same as the wort in question. Because the degree Plato scale and resulting tables relating solution specific gravity to solute concentrations are based on aqueous solution of sucrose, it is only an approximation of the amount of extract. Extract is a term referring to the total available soluble mass in a brewing material "as is", and /or potentially through processing (Hardwick, 1995) such as carbohydrates, proteins, tannins. Extract is still currently expressed in the brewing industry as specific gravity in degree Plato because of the lack of a more appropriate reference better related to the variability in compositions of worts of different origins.

4.11.4 Total Diacetyl

Total diacetyl (2,3-butanedione) in beer and fermentation samples was measured using a headspace analyte sampling technique, followed by capillary GC separation (Hewlett-Packard 5890) and electron capture detection (ECD) based on the method of the Technical Committee and Editorial Committee of the American Society of Brewing Chemists (1992). The method refers to "total diacetyl" because the method measures the amount of diacetyl and its precursor, alpha-acetolactate. The carrier gas was 5% methane in argon at 1.0 mL/min and a J & W DB-Wax column was used. The split ratio was 2:1 and the auxiliary gas was helium at 60 mL/min. Injector temperature was 105°C and detector temperature was 120°C.

The system was equipped with a Hewlett Packard 7694E headspace autosampler and 2,3-hexanedione was used as an internal standard. The sample cycle time was 40 min, with a vial equilibration time of 30 min at 65°C, a pressurization time of 2 min at 4.8 psig, a loop fill time of 0.2 min, a loop equilibration time of 0.1 min, and an injection time of 0.27 min. Carrier pressure was 18.8 psig, transfer line temperature was 95°C and loop temp was 65°C.

4.11.5 Beer Volatiles

Beer volatiles including acetaldehyde, ethyl acetate, isobutanol, 1-propanol, isoamyl acetate, isoamyl alcohol, ethyl hexanoate, and ethyl octanoate were measured using an internal standard (n-butanol) GC (Hewlett Packard 5890) headspace method and a flame ionization detector (FID). The carrier gas was helium at 6.0 mL/min and the GC was equipped with an Hewlett Packard 7694 headspace autosampler.

GC injector temperature was 200°C and detector temperature was 220°C. Oven temperature profile: 40°C (5 min), 40 - 200°C (10°C/min), 200 - 220°C (50°C/min), 220°C (5 min). The FID gases included the carrier at 6.0 mL/min, helium makeup at 30 mL/min and 28 psig, H₂ at 50 mL/min and 25 psig, and air at 300 mL/min and 35 psig.

The septum was purged at a flow rate of 0.8 mL /min. The head pressure was 4.0 psig. When the autosampler was connected via a needle in the injection port, the vial

pressure was 15.9 psig, the carrier pressure was 7.1 psig, the column head pressure was 4 psig, the split flow was 18 mL/min and the column flow was 6 mL/min. Zone temperatures: vial at 70°C, loop at 80°C, transfer line at 150°C.

The GC cycle time was 40 min, with a vial equilibration time of 35 min, a pressurization time of 0.25 min, a loop fill time of 0.1 min, a loop equilibration time of 0.1 min, an injection time of 3 min and a sample loop volume of 1 mL.

4.11.6 Free Amino Nitrogen (FAN)

The Free Amino Nitrogen International Method of the Technical Committee and Editorial Committee of the American Society of Brewing Chemists (1992) was used to determine the concentration of free amino nitrogen in a fermentation sample, using a Perkin Elmer LS50B spectrophotometer. This spectrophotometric method displays a colour reaction between ninhydrin and the nitrogen present in the sample. The amount of absorbance is directly related to the amount of free amino nitrogen present.

a) Colour Reagent: 19.83 g disodium hydrogen phosphate (Na_2HPO_4)
30.00 potassium dihydrogen phosphate (KH_2PO_4)
2.78 g ninhydrin monohydrate
1.50 g fructose

b) Dilution Reagent: 2.00 g potassium iodate (KIO_3)
596 mL distilled, deionized water
404 mL 95% (v/v) ethanol

Stored in refrigerator and used at room temp.

c) Glycine Stock Solution: 0.1072 g/100 mL distilled deionized water

d) Glycine Standard Solution: stock solution was diluted 1:100 (v/v) with distilled, deionized water. This standard contains 2 mg/L FAN.

The samples were diluted to a ratio of 100:1 with distilled water and 2 mL of the diluted sample were introduced into each of 3 test tubes. The blank was prepared by introducing 2 mL of distilled deionized water into each of 3 test tubes. Three test tubes containing 2 mL each of the glycine standard solution were also prepared.

For all samples, 1 mL of colour reagent was added and then they were placed in a 100°C water bath for exactly 16 min. The test tubes were then cooled in a 20°C water bath for 20 min. Five mL of the dilution reagent was then added to each test tube and mixed thoroughly. The samples were then allowed to stand for 10-15 min. The absorbance at 570 nm was then measured using a spectrophotometer and the amount of FAN in a sample was calculated using equation 4.3.

$$\text{FAN (mg/L)} = (A_p - A_B - A_F) 2d / A_S \quad (4.3)$$

Where FAN is the amount of free amino nitrogen in the sample in mg/L, A_p is the average of the absorbances of the test solutions, A_B is the average of the absorbances for the blanks, A_F is the average of the absorbances for the correction for dark worts and beers, 2 is the amount of FAN in the glycine standard solution, d is the dilution factor of the sample, and A_S is the average of the absorbances for the glycine standard solution.

CHAPTER 5. CONTINUOUS FERMENTATION USING A GAS-LIFT BIOREACTOR SYSTEM

A gas-lift draft tube bioreactor system was chosen for continuous beer fermentation because of its published excellent mass transfer (liquid-solid) and mixing characteristics. Liquid-solid mass transfer is especially important since it involves the transfer of nutrients from the liquid phase to the solid immobilized cell biocatalyst, providing substrates for the encapsulated yeast. These bioreactors also provide good aeration, low power consumption, and are simple to construct. This has made gas-lift bioreactor systems very attractive for large scale operations, such as those used commercially for wastewater treatment (Driessen et al., 1997; Heijnen, 1993).

5.1 Gas-lift Draft Tube Bioreactor Description

This section gives a detailed description of the gas-lift bioreactor used in this work.

5.1.1 Bioreactor Body

The 13 L (8 L working volume) gas-lift draft tube bioreactor designed for this work was a three phase fluidized bed (liquid/solid/gas) where the immobilized cells were kept in suspension by carbon dioxide gas driven internal liquid circulation (Heijnen, 1996) as shown in Figure 5.1. A photograph of the bioreactor vessel is given in Figure 5.2 and a detailed drawing with detailed dimensions is given in Figure 5.3. Carbon dioxide and air flow into the bottom cone of the bioreactor through a sintered stainless steel sparger (CO₂ purger nozzle, Part #9222, Hagedorn & Gannon, USA), 0.11 m length, 0.013 m outer diameter. Carbon dioxide was used as the fluidizing gas and air was used to supply oxygen to the yeast cells.

A draft tube, concentrically located inside the columnar bioreactor, functioned as the riser in this fluidized bed system while the outside annulus served as the downcomer. The internal draft tube was suspended from a cylindrical particle separator, seated on three stainless steel tabs in the expanded head region of the bioreactor. Keeping the draft

tube and particle separator fittings inside the bioreactor, minimized the risk of microbial contamination from the outside environment.

Originally, the bioreactor had a mesh screen to separate the immobilized cells from the liquid at the outlet. However, the screen was prone to plugging, so a stainless steel cylinder was used to separate the immobilized cell beads from the liquid phase as they moved over the top of the draft tube and flowed down the annulus. The particles would hit the cylinder and fall back down into the bulk liquid phase rather than leaving the bioreactor as overflow. Thus there was a small region near the bioreactor outlet that was free of immobilized cell particles. The bioreactor expanded head region also increased the surface area for gas bubble disengagement.

5.1.2 Bioreactor Headplate

In Figure 5.4 a schematic of the bioreactor headplate is given. Headplate ports were kept to a minimum to reduce the risk of contamination. The ports were either welded directly onto the headplate or compression fittings (Swagelok[®]) were used. The headplate incorporated an inoculation port, a thermowell, a thermometer, a septum for gas sampling, and liquid withdrawal and return ports for dissolved oxygen measurement. A temperature sensor was inserted into the thermowell, which fed back to the temperature controller system. The temperature controller gave feedback to a solenoid valve, which opened and closed the glycol supply to the bioreactor thermal jacket. Temperature was monitored using a thermometer (Cole-Parmer Waterproof Thermocouple thermometer, #90610-20) and a type T probe, which was welded into the bioreactor head plate. Dissolved oxygen was measured using a dissolved oxygen analyzer (Dr. Theidig, Digox 5), which required a flow of 9-11 L/hr of liquid broth through the analyzer block for accurate oxygen readings. Liquid was withdrawn from the bioreactor for oxygen measurement through a ¼ i.d. pipe that went through the headplate into the fermentation liquid. As shown in Figure 5.5, the tip of pipe was fitted with a filter to remove larger particulates from the liquid, as it was pumped through the dissolved oxygen analyzer. The liquid was then returned back to the bioreactor through another ¼" port in the headplate.

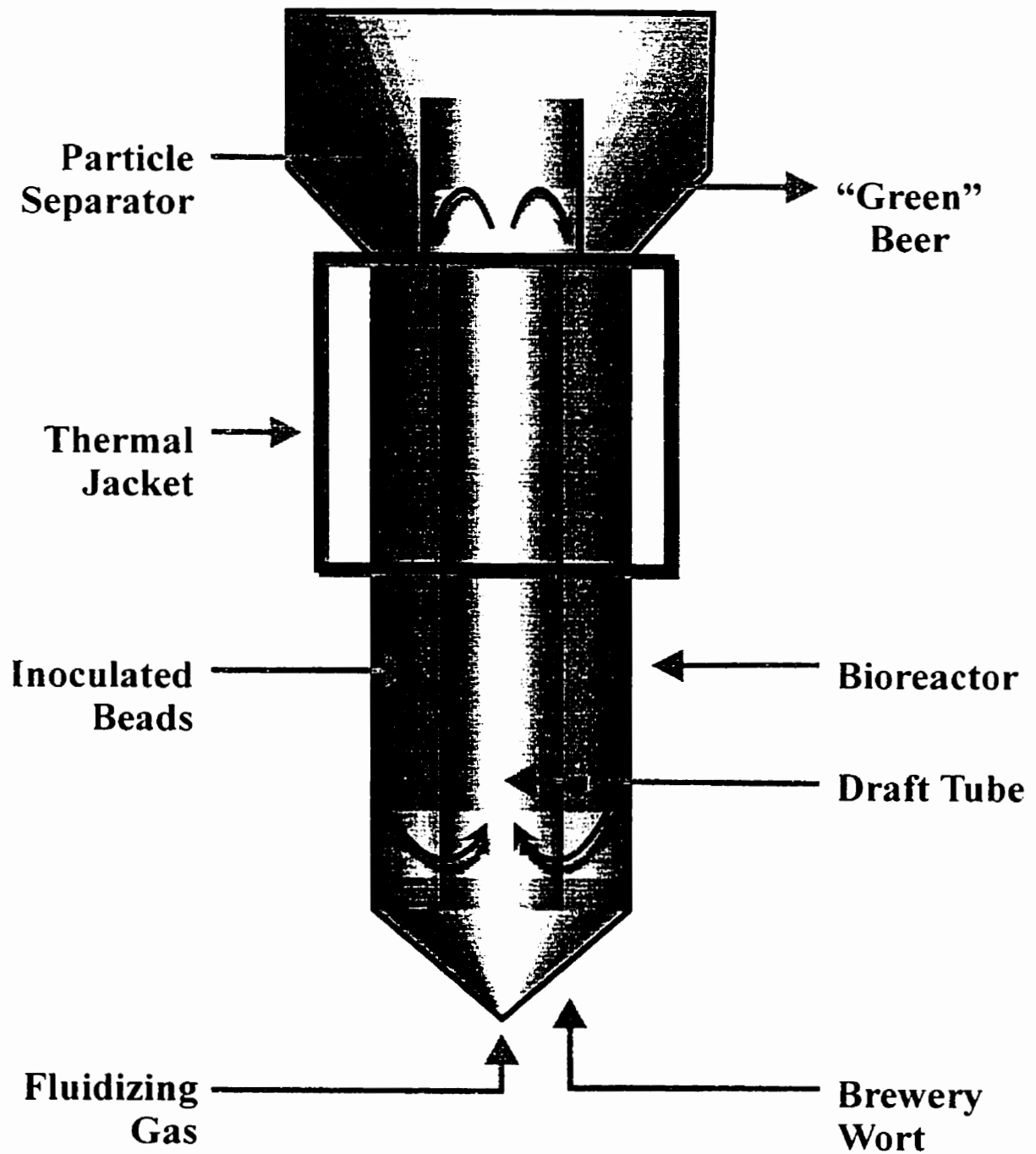


Figure 5.1. Schematic of gas-lift draft tube bioreactor system for primary beer fermentation.

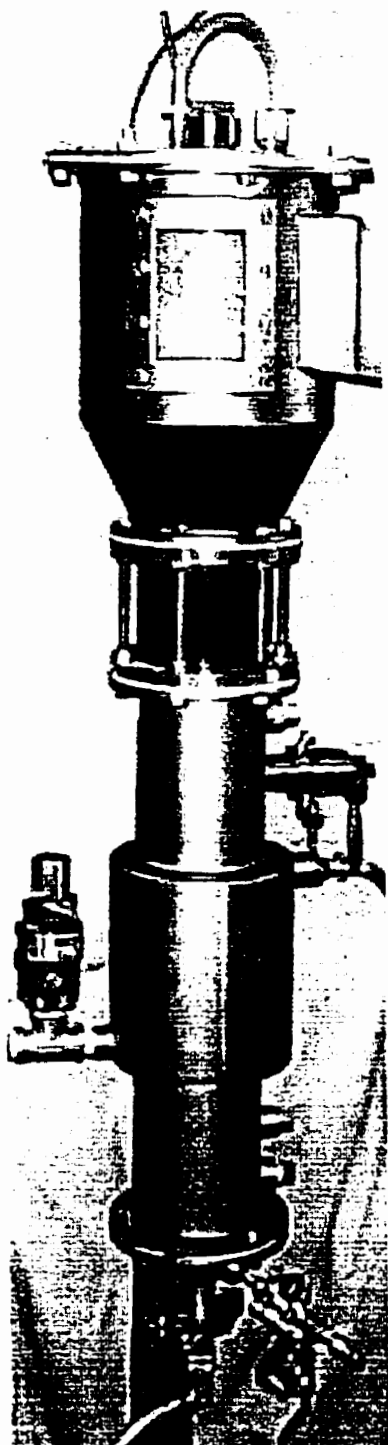


Figure 5.2. Photograph of the gas-lift draft tube bioreactor vessel.

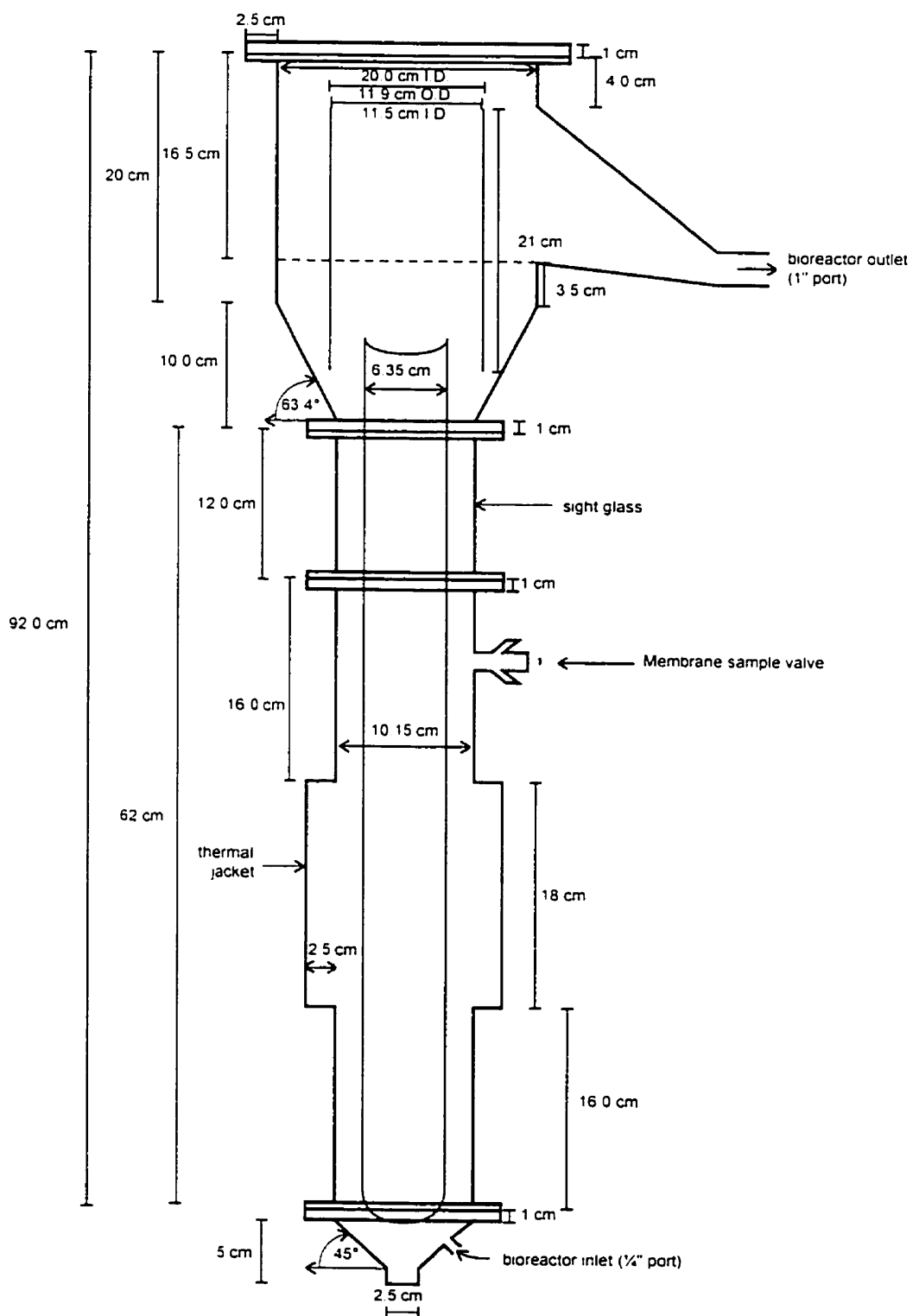


Figure 5.3. Detailed scale drawing of 13 L (8 L working volume) gas-lift draft tube bioreactor vessel.

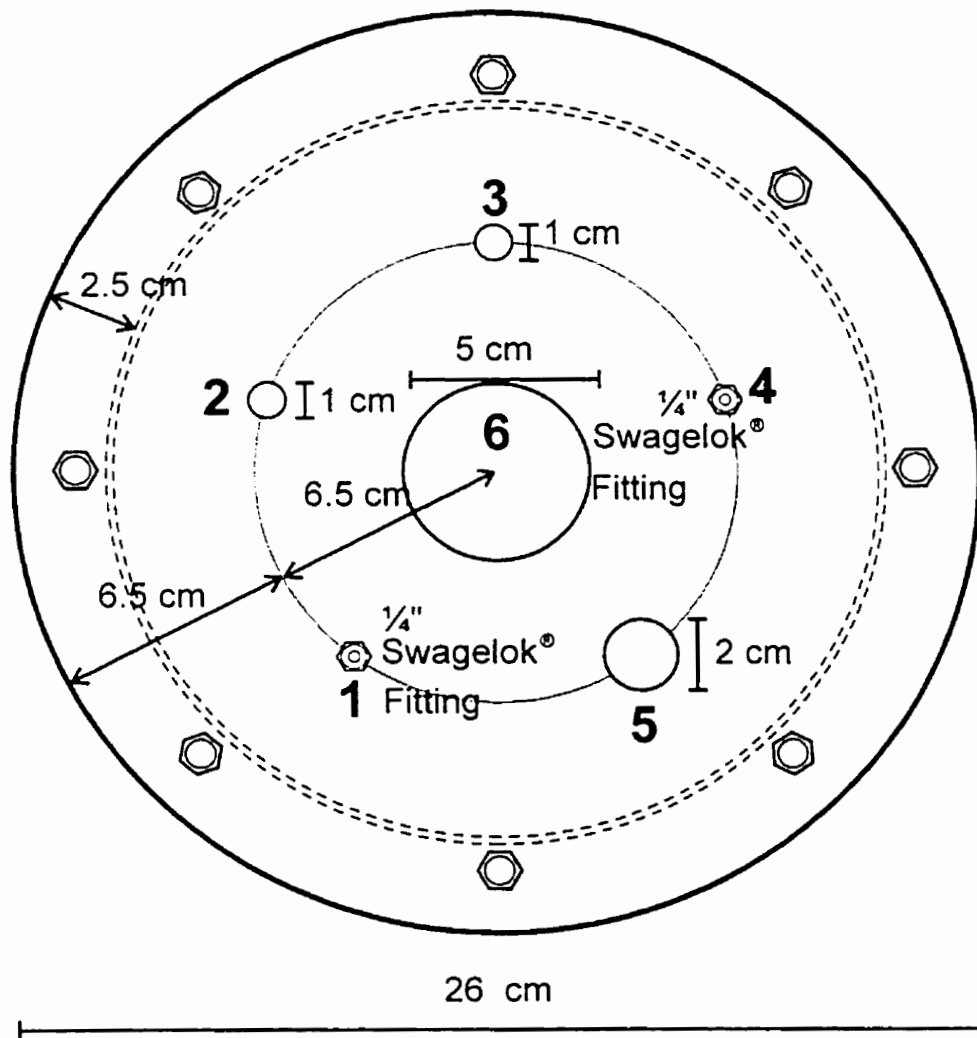


Figure 5.4. Detailed drawing of bioreactor vessel headplate: **1**-liquid withdrawal port for oxygen sensor; **2**-thermowell for temperature sensor, linked to thermostatic controller; **3**-temperature probe; **4**-liquid return port for oxygen sensor; **5**-inoculation port; **6**-membrane sample port with stainless steel cap.

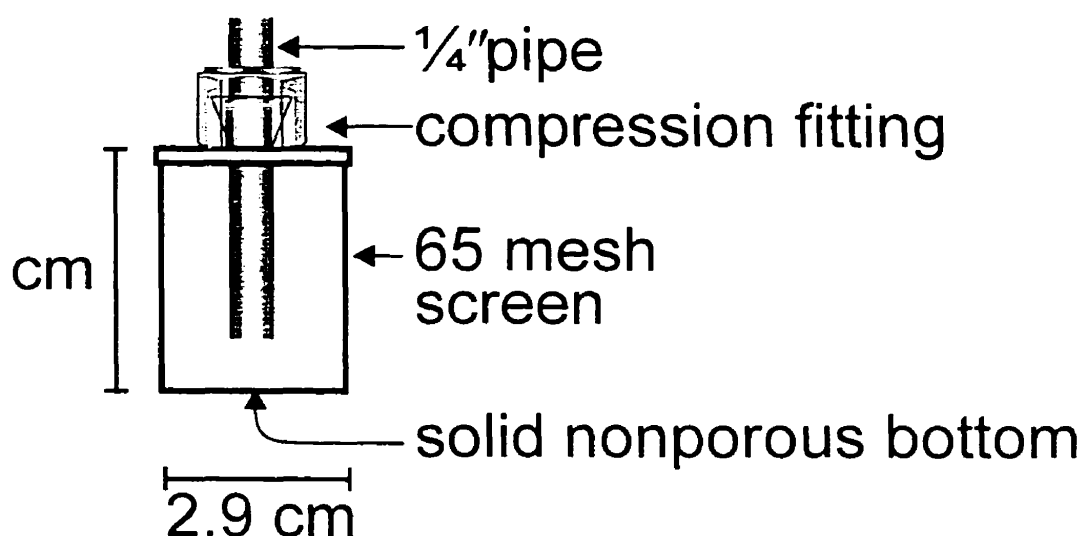


Figure 5.5. Profile of liquid withdrawal port for oxygen sensor with filter unit submerged in bioreactor liquid phase.

5.1.3 Sanitary Valves for Aseptic Sampling

The bioreactor was equipped with a membrane sample valve (Scandi-Brew[®]) welded into the bioreactor wall. The valve was designed for sampling under aseptic conditions. The membrane sealed directly against the fermentation liquid, allowing the valve to be fully sterilizable with steam and alcohol through two outlets (Figure 5.3). A small external reservoir of ethanol surrounded the membrane to maintain sterility between sampling. This valve was used for all bioreactor sampling and it was assumed that the composition of the liquid at the point of sampling was not significantly different than the composition of the liquid exiting the bioreactor outlet. As mentioned in the Materials and Methods chapter of this work, the bioreactor was sampled from a valve located on the outer wall of the bioreactor. In order to validate the assumption that the composition of the liquid exiting the bioreactor outlet was the same as the liquid sampled from the body of the bioreactor, mixing time studies were performed.

A pulse tracer method was used to determine mixing time in the gas-lift bioreactor (Chistie, 1989). A 1 mL volume of 10 N HCl was rapidly injected into the bioreactor annulus and the change in pH was logged over time, with time, $t = 0$ seconds at the time of the injection. The pH was returned to its original value by injecting 10 N NaOH. The pH electrode (Cole-Parmer, cat. #P-05990-90) was 277 mm in length and 3.5 mm in diameter. An Ingold Model 2300 Process pH Transmitter was used to monitor pH. A two-point pH calibration was performed with certified standard buffers, Beckman pH 7.0 green buffer, Part #566002 and Beckman pH 4.0 red buffer, Part #566000. The data was logged at a frequency of 3750 Hz for 300 seconds using a software program designed by Cheryl Hudson and John Beltrano in 1994, and modified by Norm Mensour in 1999 (University of Western Ontario, London, Ontario).

The pH data was then smoothed using the Savitsky-Golay algorithm in TableCurve 2D (Jandel Scientific Software, Labtronics, Guelph, Ontario). The Savitzky-Golay algorithm is a time-domain method of smoothing based on least squares quartic polynomial fitting across a moving window within the pH data (Anon, 1996). The smoothed data was then normalized and a plot of ΔpH versus time was generated. The mixing time was taken to the nearest minute, when the pH had reached ~95% of equilibrium value. The mixing time was measured using three different volumetric flow rates of carbon dioxide: 283 cm³/min, 472 cm³/min (volumetric flow rate used throughout this work), and 661 cm³/min. In all three cases the pH in the bioreactor had equilibrated (~95% cutoff) in less than 2 minutes, as seen in Appendix 1. The mixing time was deemed to be sufficiently short to validate our original assumption that the bioreactor was well-mixed. This allowed us to assume that the composition of the liquid sampled from the bioreactor wall was not significantly different from that which flowed from the outlet, with an average liquid residence time of 24 hours in the bioreactor. From the appended figures, a definite liquid recirculation superimposed on mixing by dispersion was seen, which is typical of gas-lift bioreactors (Chisti, 1989).

5.2 Flow Diagram of Continuous Beer Fermentation System

A flow diagram for the continuous beer fermentation system, which was housed in the Microbrewery Pilot Plant of Labatt Brewing Company Limited in London, Ontario,

is given in Figure 5.6 with a detailed parts description in Table 5.1. In summary, brewer's wort was collected from the London Labatt Plant, sterilized using a flash pasteurizer (Fisher Plate Heat Exchanger, combi-flow Type Eurocal 5FH), and stored in large holding tanks (T-1 and T-2). During continuous fermentation the wort was transferred at a controlled flow rate to the gas-lift bioreactor (BR-1) containing immobilized yeast cells. Fermented liquid left the bioreactor as overflow and was collected into a receiving vessel (T-3). In the following sections, the operation of the continuous beer fermentation system given in Figure 5.6 is detailed.

5.2.1 Wort Collection and Storage

Unoxygenated wort for continuous fermentation was collected from the Labatt London plant via piping into a 1600 L cylindroconical storage tank, pre-purged with carbon dioxide to minimize oxygen pickup by the wort. All tanks of this scale, including wort holding tanks, T-1 and T-2, were cleaned and sanitized as per Labatt Best Practices prior to their use. The wort was then flash pasteurized and transferred at 2°C into the available wort holding tank, T-1 or T-2 (also pre-purged with carbon dioxide). Wort was held in these tanks at 2°C for up to 2 weeks, supplying liquid to the continuously fermenting bioreactor, BR-1. At the end of the two-week period, the bioreactor feed was changed over so that wort was supplied from the second wort tank, which contained fresh wort. Two identical wort storage tanks, T-1 and T-2, were employed to minimize downtime during the changeover to fresh wort. In all cases, wort was tested for contamination a minimum of two days prior to being introduced into the bioreactor (BR-1). If the wort was contaminated, it was discarded and fresh wort was immediately collected and pasteurized.

Minimizing Wort Dissolved Oxygen Concentration During Storage: The goal was to store the wort with minimal oxygen, at a constant level, and at a low temperature, without freezing the wort. This was required to prevent undesirable staling reactions in the wort from chemical reactions with oxygen (Narziß et al., 1993), to provide a consistent supply of wort to the bioreactor, and to minimize the risk of wort contamination with microbes during storage. The large 1,600 L (net) cylindroconical vessels (T-1 and T-2) used to store the wort for the continuous fermentations, were originally designed as batch

fermenters, not wort storage tanks. Because of this, the cooling for these vessels was not adequate to maintain wort at 2°C. After three days of holding the wort, temperature varied as much as 15°C from one region of the tank to another (Table 5.2).

These warm regions in the tanks increased the risk of microbial growth. Thus, some agitation was needed in these tanks to ensure a uniform low temperature throughout.

For these reasons, a pipe sparger was installed into the base cone of each wort storage tank (T-1 and T-2). Experiments were performed to determine the best protocol for filling the tank with wort and maintaining constant low levels of dissolved oxygen. In the first experiment, the storage tank was filled with wort that had been collected without oxygenation and flash-pasteurized. Once the storage tank was filled with 1,600 L wort, 0.113 m³/hr of carbon dioxide was sparged into the base of the tank. During the second experiment, the wort was again collected without oxygenation and flash-pasteurized. This time, the storage tank was purged with carbon dioxide (0.85 m³/hr) for 3 hours prior to filling and a small amount of carbon dioxide (0.113 m³/hr) was continuously sparged into the storage vessel as the wort was being transferred into the tank. This low flow of carbon dioxide was continuously bubbled through the wort stored in the tank while it supplied wort to the continuous fermentation. For both experiments, wort dissolved oxygen concentration was monitored on a regular basis during a week of storage.

In Figure 5.7, dissolved oxygen concentration versus wort storage time is given. When the holding tank was not pre-purged with carbon dioxide, the air in the headspace of the tank allowed some pickup of oxygen by the wort. Thus, without prepurging the tank it took a significantly longer period of time for the dissolved oxygen concentration in the wort to reach a minimal and constant level. When the tank was pre-purged, the wort dissolved oxygen concentration remained at a constant low level throughout the storage period. Thus, pre-purging the wort storage tanks (T-1 and T-2), and continuing to provide a small flow of carbon dioxide through the wort during storage in order to keep a slight positive pressure on the tanks, was adopted as part of the wort storage procedure for all continuous fermentations.

The temperature profile in the storage vessels was also compared with and without 0.113 m³/hr of carbon dioxide sparging. This was performed on water rather than on wort using a Type T temperature probe connected to a thermometer (Cole-Parmer

Waterproof Thermocouple Thermometer, cat. #90610-20). City water (1.600 L) was collected into a wort storage tank and equilibrated for three days and the temperature of the water was recorded in different regions of the storage tank. The water in the tank was then sparged for 24 hours with 0.113 m³/hr carbon dioxide and the temperature was again recorded. Ambient temperature was recorded in each case and the temperature set point within the storage tank was 2.0°C.

As seen in Table 5.2, with carbon dioxide sparging, the temperature in the storage tanks was more uniform, with temperature ranging between 0.1 and 4.1°C in the regions measured, and the contents of the tanks did not freeze. This lower temperature helped to prevent unwanted growth of microbes in the wort during storage.

Gas was released from the wort storage tanks through a sterile gas filter situated at the top of the tank. Wort was then transferred using a variable speed peristaltic pump (P-1) (Masterflex[®] L/S™ Digital Standard Drive, Cole-Parmer cat. #P-07523-50) to the 8 L bioreactor (BR-1) inlet using Norprene[®] Food Grade L/S 16 flexible tubing.

5.2.2 Continuous Fermentation using Gas-Lift Draft Tube Bioreactor System

Wort was introduced near the bottom cone of the bioreactor, BR-1, through a ¼" port. A mixture of filter-sterilized (Millipore, Millex[®]-FG₅₀, 0.2 µm Filter Unit), air and carbon dioxide (99.99% purity) flowed into the bioreactor through the sintered stainless steel sparger. A rotameter (R-3) was used to control the carbon dioxide flow rate at STP, and a precalibrated mass flow controller (M-1) was used to control the flow rate of air at STP. Fermented liquid left the bioreactor as overflow and flowed through 1" I.D. reinforced PVC tubing into a 30 L stainless steel collection vessel (T-3) which was cooled with an external glycol coil and kept at a temperature of 4°C.

5.2.3 Product Collection

The product collection vessel (T-3) had a large inlet port (1" I.D.) which was designed so that the fermented liquid would flow down the collection vessel wall to minimize foaming. This vessel also had a sterile gas filter, (Millipore, Millex[®]-FG₅₀, 0.2 µm Filter Unit), for gas release from the bioreactor (BR-1) and the collection vessel (T-

3). The collection vessel was periodically emptied using a ¼" valve (V-12) situated 2" above the base of the tank.

5.2.4 Glycol Cooling Loop

Glycol was transferred from the London Brewery to the Microbrewery Pilot Plant at a temperature of -23°C and pressure of 45 psig, and circulated through cooling jackets for the wort holding tanks (T-1 and T-2), the gas-lift bioreactor (BR-1), and the product collection vessel (T-3). The two wort holding tanks and the bioreactor were equipped with liquid phase temperature probes which provided feedback to temperature controllers, which in turn controlled the flow of cold glycol to the vessel jackets. The wort holding tanks stored the wort at 2°C , while the temperature within the bioreactor was controlled at temperatures of 12°C to 22°C , depending upon the specific experiment. The product collection vessel did not have automatic temperature control, but rather, the flow of glycol was manually controlled to keep the vessel at approximately 4°C . It was not necessary to precisely control the temperature of the product collection vessel (T-3) because the liquid in this vessel was simply discarded and not analyzed or processed further.

Glycol was also used to jacket and cool the wort transfer lines from the wort tanks (T-1 and T-2) to the bioreactor (BR-1). Once the glycol had circulated through a given jacket, it was returned to a main line within the Pilot Plant Microbrewery and then was returned to the London Plant, generally at a temperature of -15°C and pressure of 40 psig.

5.3 Bioreactor Sterilization Protocol

The bioreactor (BR-1) was filled with a 2% (v/v) solution of Diversol[®] CX/A (DiverseyLever, Canada), a sanitizing detergent, and soaked overnight with gas sparging. The reactor was then drained and rinsed with cold water. This cycle of cleaning solution and water rinsing was repeated two times. In order to prepare the bioreactor for steam sterilization, the wort and gas lines were disconnected. The steam line was connected to the bioreactor inlet and the following valves were opened: the bioreactor inlet and purge valves (V-7, V-6), the gas inlet (V-17), product outlet valves (V-9, V-11), the membrane sampling valves (V-8, V-10), and collection vessel drain port (V12). The plant steam valve was then slowly opened and the bioreactor valves were adjusted so that a trickle of

steam was observed at the exit of each external opening. After 60 minutes of steam exposure, all the external valves on the bioreactor were closed (V-17, V-8, V-10, V-12) except the wort bypass valve (V-6). When the steam valve was closed, the wort bypass valve was closed and a sterile filter was connected to the collection vessel to prevent contamination by non-sterile air entering the system as it cooled. The bioreactor gas line was also reconnected at V-17 as the plant steam line was closed in order to maintain a positive pressure while the system cooled.

5.4 Fermentation System Startup

Brewer's wort was collected from the plant into a 20 L stainless steel pressure vessel and heated in an autoclave for 45 minutes at 100°C. Immobilized cells were aseptically transferred into the cooled wort (40% v/v). The sealed vessel was transported to the Microbrewery Pilot Plant where the bioreactor system was housed. The 20 L vessel was connected to a quick connect fitting (Cornelius Anoka, MN, USA), which was clamped to reinforced 3/8" PVC tubing (Cole-Parmer, USA). The other end of the PVC tubing was clamped to the membrane sampling valve (V-8) in the bioreactor wall. Filter-sterilized carbon dioxide was applied as 10 psig to the 20 L vessel and the membrane sample port was opened so that the immobilized cell mixture was transferred from the vessel into the bioreactor, without exposing the inoculum to the outside air environment. The internal components of the "quick connect" fittings of the 20 L vessel were removed to prevent plugging with immobilized cells upon transfer into the bioreactor. The cumulative particle size distribution (undersize) for the kappa-carrageenan gel beads is shown in Figure 5.8. The arithmetic mean particle diameter, D_{pam} , was calculated to be 1.252 mm and the Sauter mean particle diameter, D_{psm} , was 1.17 mm. The median particle diameter was 1.255 mm. The experimental data and mean particle diameter calculations are given in Appendix 1.

Following inoculation with immobilized cells, the bioreactor was operated in batch mode until the sugar and diacetyl concentrations reached targets of less than 3°Plato in terms of specific gravity and less than 100 µg/L diacetyl. The system was then prepared for continuous operation. In order to rinse with hot water and steam-sterilize the wort transfer line, valves V-2 (or V-4 for T-2), V-5, and V-6 were opened, while V-1 (or

V-3 for T-2) and V-7 were closed, isolating the wort line. The wort transfer line was rinsed with hot water at approximately 80°C, which was supplied through V-2 (or V-4 for T-2). Following the hot water rinse cycle, the plant steam line was connected at the same location and the wort transfer line was steam sterilized for a minimum of 30 minutes. At the same time that the steam line was shut off, the bypass valve (V-6) was also closed. Once the system had cooled, V-2 (or V-4 for T-2) was closed and the steam line was disconnected. The wort tank valve, V-1 (or V-3 for T-2), and the bypass valve (V-6) were opened and the wort transfer pump (P-1) was started. The wort was sent to the sewer drain via the bypass valve (V-6) until the condensate in the line was replaced with fresh cold wort. At that point the bypass valve was closed and the bioreactor inlet valve (V-6) on the reactor was opened, commencing the continuous fermentation process.

Every two weeks the tank, which supplied wort was alternated between storage tanks (T-1 and T-2). After two weeks of supplying wort from T-1, the continuous feed pump, P-1 was stopped and the valve (V-5) at the inlet of the bioreactor was closed. The wort transfer line was then connected to the second storage tank (T-2) and the line was flushed and sterilized as described in the previous paragraph. Continuous fermentation then resumed after only a short down time of less than one hour.

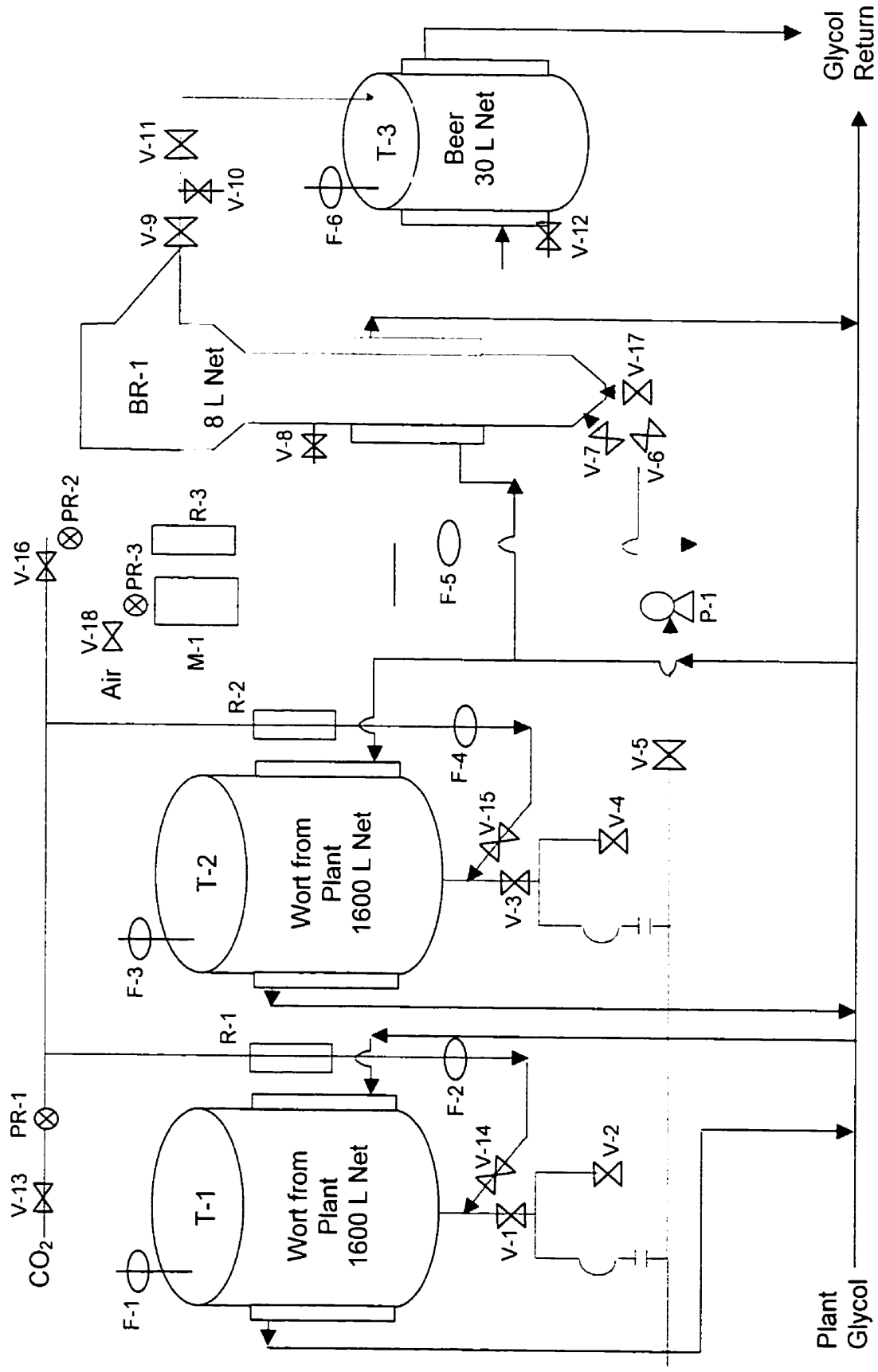


Figure 5.6. Detailed equipment and flow diagram for continuous primary beer fermentation using a gas-lift bioreactor system (see Table 5.1 for detailed equipment description).

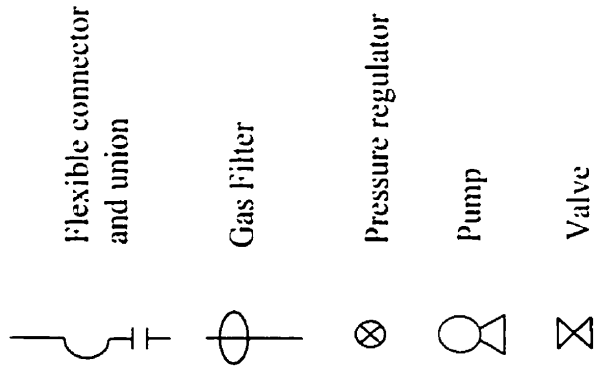
Table 5.1. Detailed parts description for flow diagram shown in Figure 5.6; PTFE, polytetrafluoroethylene; SS, stainless steel.

Item	Description	Size	Mat'l Const.
BR-1	Bioreactor	8 L net	316 SS
T-1	Storage tank for wort	1600 L net	316 SS
T-2	Storage tank for wort	1600 L net	316 SS
T-3	Storage tank for beer	30 L net	316 SS
P-1	Pump (peristaltic, variable speed) for wort transfer from T-1 to BR-1	<0.08 L/min	SS rollers on Norprene [®] Food flexible tubing
F-1	Filter for gas at outlet of T-1	<4 bar	polyprop., 0.2 micrometer PTFE membrane
F-2	Filter for gas at inlet of T-1	<2 bar	polyprop., 0.2 micrometer PTFE membrane
F-3	Filter for gas at outlet of T-2	<4 bar	polyprop., 0.2 micrometer PTFE membrane
F-4	Filter for gas at inlet of T-2	<2 bar	polyprop., 0.2 micrometer PTFE membrane
F-5	Filter for gas at inlet of BR-1	<2 bar	polyprop., 0.2 micrometer PTFE membrane
F-6	Filter for gas at outlet of T-3	<2 bar	polyprop., 0.2 micrometer PTFE membrane
M-1	Mass flow controller for air to BR-1	<500 sccm	316 SS, nylon, Viton [®] "O"-rings
R-1	Rotameter for carbon dioxide to T-1	<10 scfh	316 SS, acrylic block
R-2	Rotameter for carbon dioxide to T-2	<10 scfh	316 SS, acrylic block
R-3	Rotameter for carbon dioxide to BR-1	<2.5 scfh	316 SS, acrylic block
PR-1	Pressure regulator for carbon dioxide to T-1 & T-2	<100 psi	316 SS
PR-2	Pressure regulator for carbon dioxide to BR-1	<100 psi	316 SS
PR-3	Pressure regulator for air to BR-1	<100 psi	316 SS
V-1	Valve (butterfly) for wort in T-1	1"	316 SS, Viton [®] seat
V-2	Valve (butterfly) for wort in CIP loop in T-1	1"	316 SS, Viton [®] seat
V-3	Valve (butterfly) for wort in T-2	1"	316 SS, Viton [®] seat
V-4	Valve (butterfly) for wort in CIP loop in T-2	1"	316 SS, Viton [®] seat
V-5	Valve (ball) for wort at header	1/4"	316 SS, silicone seat
V-6	Valve (ball) for bypass at BR-1 wort inlet	1/4"	316 SS, silicone seat

Table 5.1 (cont'd). Detailed parts description for flow diagram shown in Figure 5.6.

V-7	Valve (ball) for BR-1 wort inlet	1/4"	316 SS, silicone seat
V-8	Valve (membrane sample) on wall of BR-1	12 mm	316 SS, silicone seat
V-9	Valve (butterfly) at BR-1 beer outlet	1"	316 SS, viton seat
V-10	Valve (membrane sample) for BR-1 wort outlet	12 mm	316 SS, silicone seat
V-11	Valve (butterfly), secondary, at BR-1 beer outlet	1"	316 SS, viton seat
V-12	Valve (ball) for emptying liquid from T-3	1/4"	316 SS, silicone seat
V-13	Valve (ball) for carbon dioxide line to T-1 & T-2	1/4"	316 SS, silicone seat
V-14	Valve (butterfly) for T-1 carbon dioxide inlet	1/2"	316 SS, silicone seat
V-15	Valve (butterfly) for T-2 carbon dioxide inlet	1/2"	316 SS, silicone seat
V-16	Valve (ball) for carbon dioxide line to BR-1	1/4"	316 SS, silicone seat
V-17	Valve (quick release) for BR-1 gas inlet	1/4"	316 SS, silicone seat
V-18	Valve (ball) for air line to BR-1	1/4"	316 SS, silicone seat

Symbols used in Figure 5.6:



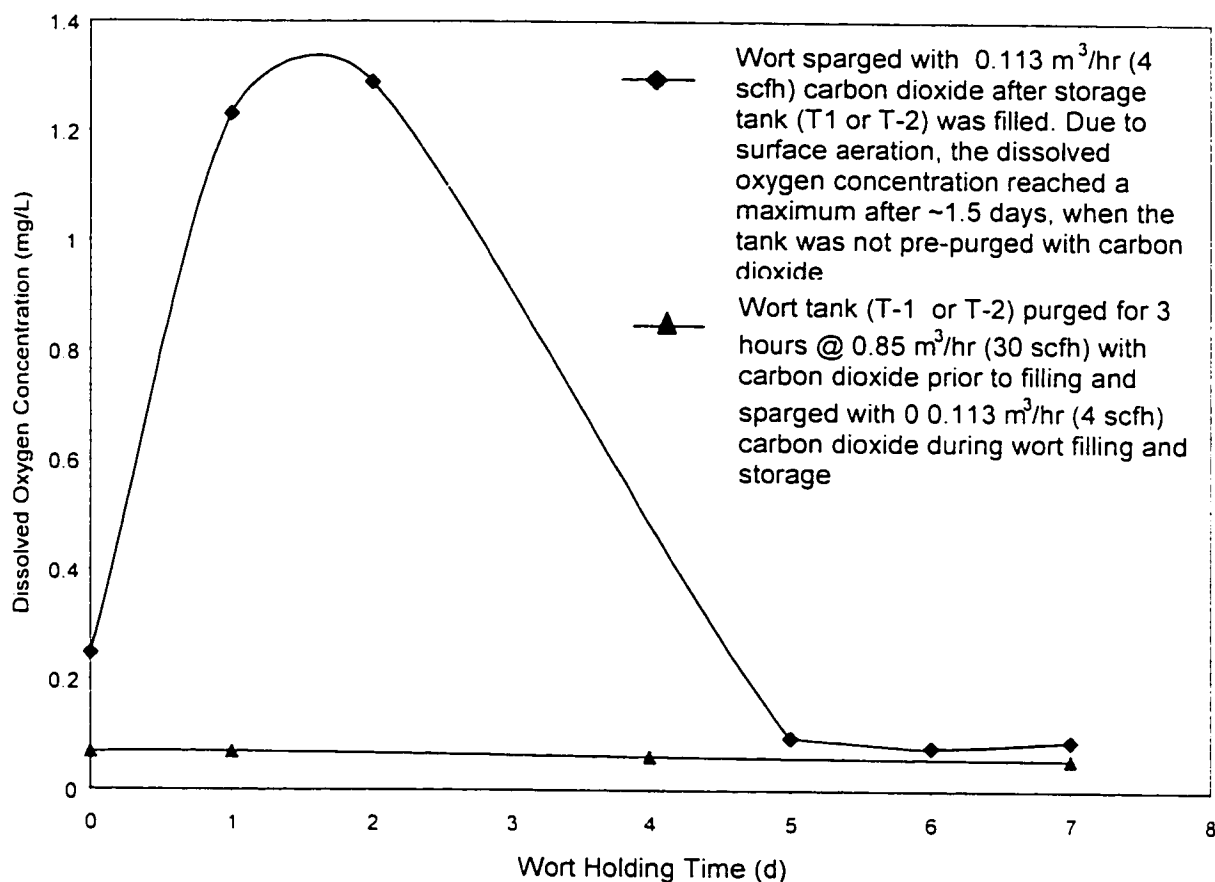


Figure 5.7. Dissolved oxygen concentration in the wort versus hold time in wort storage vessel (T-1 or T-2) under different tank filling conditions.

Table 5.2. Temperature profile of water in wort storage vessel (T-1 or T-2) after equilibrating for three days with no carbon dioxide sparging, and after 24 hours of carbon dioxide sparging at 0.113 m³/h.

Location of Measurement within Cylindroconical Vessel	Temperature (°C)	
	No CO ₂ Sparging	With CO ₂ Sparging
10 cm below liquid surface and 10 cm from the vessel wall	20.6	0.4
10 cm below liquid surface and at the center of the vessel	20.1	0.1
bottom of cylindrical section and 10 cm from vessel wall	3.8	3.7
bottom of cylindrical section and at the center of the vessel	3.7	4.1
Pilot Plant ambient	21.4	19.8

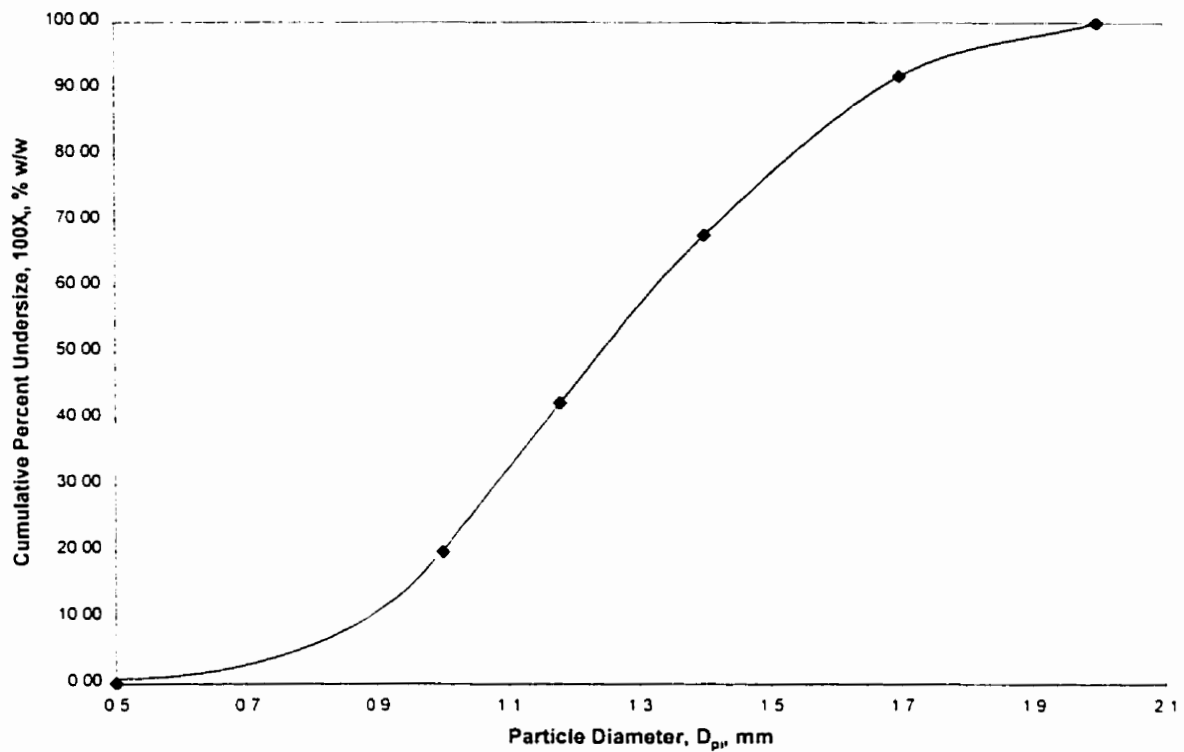


Figure 5.8. Cumulative particle size distribution of kappa-carrageenan gel beads containing immobilized yeast cells ($n = 5$)

¹CHAPTER 6. KAPPA-CARRAGEENAN GEL IMMOBILIZATION OF LAGER BREWING YEAST

Scientists have studied a variety of matrices for the physical entrapment of whole cells including calcium alginate (Bejar et al., 1992; Curin et al., 1987; Masschelein and Ramos-Jeunehomme, 1985; Nedovic et al., 1996; Shindo et al., 1994; White and Portno, 1978), agarose (Hooijmans et al., 1990; Lundberg and Kuchel, 1997), and carrageenan gels (Norton et al., 1995; Wang et al., 1982). Carrageenan is a food grade material and it has been favoured for cell encapsulation due to its superior mechanical strength compared to other gels (Büyükgüngör, 1992).

In the first part of this chapter, the yeast cell colonization within kappa-carrageenan gel beads was monitored over three cycles of repeated batch fermentation. The viability of the immobilized cells and the cells released into the liquid phase was examined. Fermentation parameters including ethanol, maltose, maltotriose, fructose, and glucose were followed throughout the repeated batch fermentations and then compared with control fermentations using only freely suspended yeast cells under the same nutrient conditions.

There has been little published information to date on the physical effects on cells after long term immobilization (Virkajärvi and Kronlöf, 1998) and continuous exposure to external stresses and fermentation products. The second part of this chapter examines the viability, cell population distribution and physical appearance of yeast cells immobilized within carrageenan gel beads over an extended period of continuous fermentation in a gas-lift bioreactor. Also examined over extended periods of time were the relative percentage of respiratory deficient yeast in the immobilized and freely suspended cell population of the bioreactor.

Carrageenan is made up of repeating 3-6-anhydrogalactose units and assorted carrageenans differ by the number and position of the sulfate ester groups on repeating galactose units. A schematic of the carrageenan gelation mechanism may be seen in Figure 6.1. When carrageenan is in the sol state, its polysaccharide chains are in a random coil configuration. When enough helices have formed to provide cross-links for a

¹ A version of section 6.0 has been published (Pilkington et al., 1999).

continuous network. gelation occurs. As more helices are formed, or, as the helices form aggregates, the gel becomes stronger and more rigid (Rees, 1972).

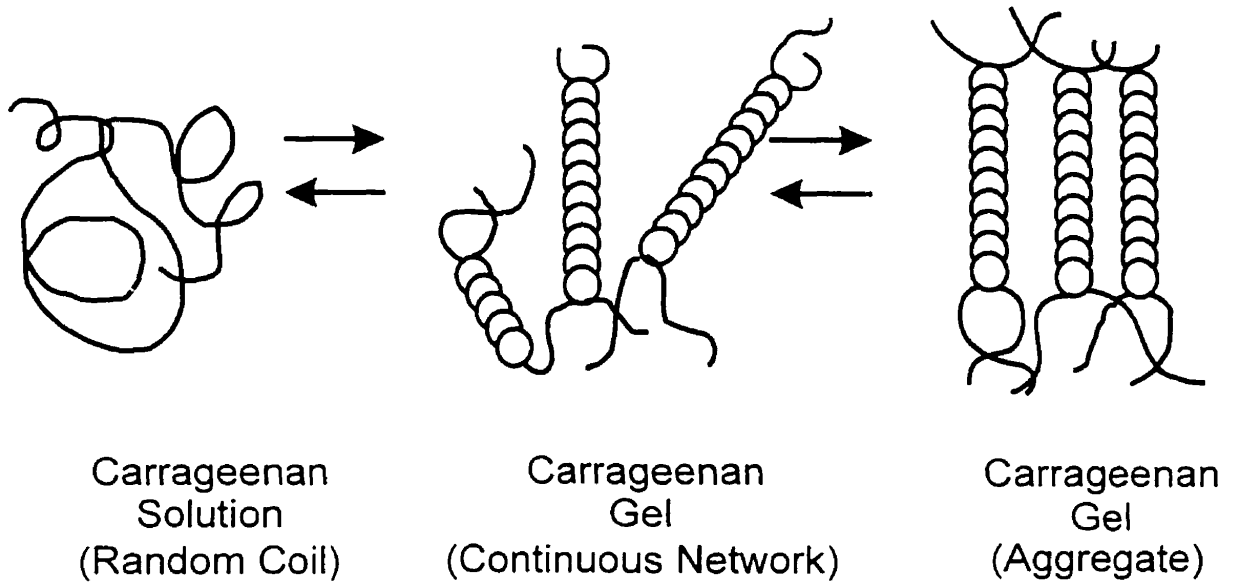


Figure 6.1. Gelation mechanism of carrageenan (adapted from Rees, 1972).

The three common types of carrageenan are lambda, iota, and kappa. As illustrated in Figure 6.2, they differ in sulfate ester content and the amount of sulfate ester will affect the solubility of the polysaccharide chain. Lambda-carrageenan is highly sulfated and lacks the ability to form a gel (Marrs, 1998). Iota-carrageenan forms a highly elastic, weak gel in the presence of calcium ions, and does not show significant syneresis. Syneresis occurs when the tendency of the gel to further form helices or aggregates is so strong that the network contracts causing “weeping” of liquid (Rees, 1972). Kappa-carrageenan is moderately sulfated and thus forms a stronger and more rigid gel in the presence of potassium ions, and will undergo some syneresis. The increased gel strength afforded by kappa-carrageenan makes it desirable for immobilizing whole yeast cells.

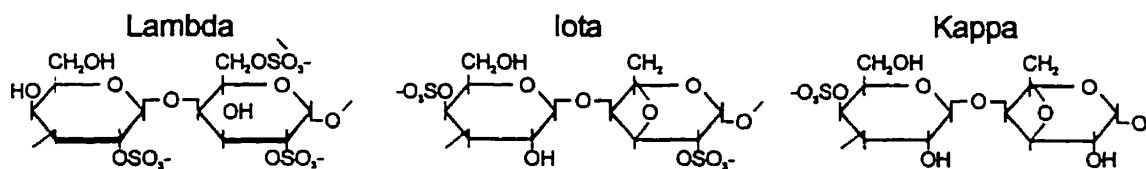


Figure 6.2. Chemical structures of lambda-, iota-, and kappa-carrageenans.

An important characteristic of carrageenan is its reversible thermogelation properties. As carrageenan solution is cooled, viscosity increases and gelation occurs. As the solution is heated, viscosity decreases and the carrageenan reverts back to the sol state. By controlling the composition of the gelling cation solution, the temperature at which carrageenan is transformed from a sol into a gel may be altered. Kappa-carrageenan gelling temperature increases with increasing potassium chloride concentration in solution. This phenomenon was used to engineer a process for cell immobilization, since severe temperature fluctuations can be avoided (Neufeld et al., 1996). The gelling temperature of the carrageenan can be controlled such that it is high enough to be a gel under fermentation conditions, yet low enough that the yeast cells may be mixed with the carrageenan in its sol state without detrimental effects on viability prior to bead gelification.

There are a number of factors, nevertheless, which indicate the need for further study on the effects of immobilization within gel matrices on yeast cell metabolism and physiology. Immobilized cells are not subjected to the same micro-environment as the free cells in the liquid phase because there are additional barriers from the gel matrix and other entrapped yeast cells which must be surmounted, before substrates can be transported to their surfaces (Figure 6.3). There have been many studies on mass transfer rates within gel matrices (Estapé et al., 1992; Hannoun and Stephanopoulos, 1986; Korgel et al., 1992; Kurosawa et al., 1989; Merchant et al., 1987; Øyaas et al., 1995; Venâncio and Tiexiera, 1997) to gain a better understanding of the potential negative effects that nutrient limitation to immobilized cells may have on fermentation performance. The effective diffusivities of small molecules within carrageenan gel are comparable with the diffusivities of the same molecules in water alone, and the gel allows molecular diffusion of small molecules, such as glucose and ethanol. However, in

a typical immobilized cell fermentation, nutrients are rapidly transported to the immobilized cell beads mainly by convective transport in addition to molecular diffusion (Hannoun and Stephanopoulos, 1986). Once the nutrients enter the beads, transport is relatively slow because molecular diffusion dominates. This means the yeast cells at the periphery of the gel beads may have a distinct nutritional advantage over those in the center of the beads.

The age of the immobilized yeast must also be considered. Entrapped cells age as a continuous fermentation proceeds over the course of months and they ferment under a defined set of pseudo-steady-state conditions. However, during batch fermentation, yeast cells are exposed to an environment that changes with time and the cells are only reused for a limited number of fermentations before disposal. More research is needed to study the long-standing effects of continuous fermentation on yeast cell vitality, relating to fermentation performance.

In Part A of this chapter, the kinetics of yeast colonization in kappa-carrageenan gel beads were examined during three cycles of repeated batch fermentation. Viability and cell concentrations of immobilized and freely suspended yeast were monitored, along with ethanol, degree Plato, and sugar concentration.

In Part B, the effects of fermentation time on cell position and distribution within the gel bead and yeast cell morphology were examined. Scanning electron microscopy (SEM) was used to examine kappa-carrageenan-immobilized yeast cells in different regions of the gel bead at four different times: 1) immediately after bead production; 2) after two days of batch fermentation; 3) after two months of continuous fermentation in a pilot scale gas lift bioreactor; 4) after six months of continuous fermentation in a pilot scale gas lift bioreactor. Yeast viability and concentration in both immobilized and liquid phase cells were also measured. Also examined was the relative percentage of respiratory deficient yeast (immobilized and free cells in the liquid phase) after five months of continuous fermentation in the gas lift bioreactor and this was compared with the percentages found in traditional batch beer fermentations. A production lager yeast strain was used throughout the study.

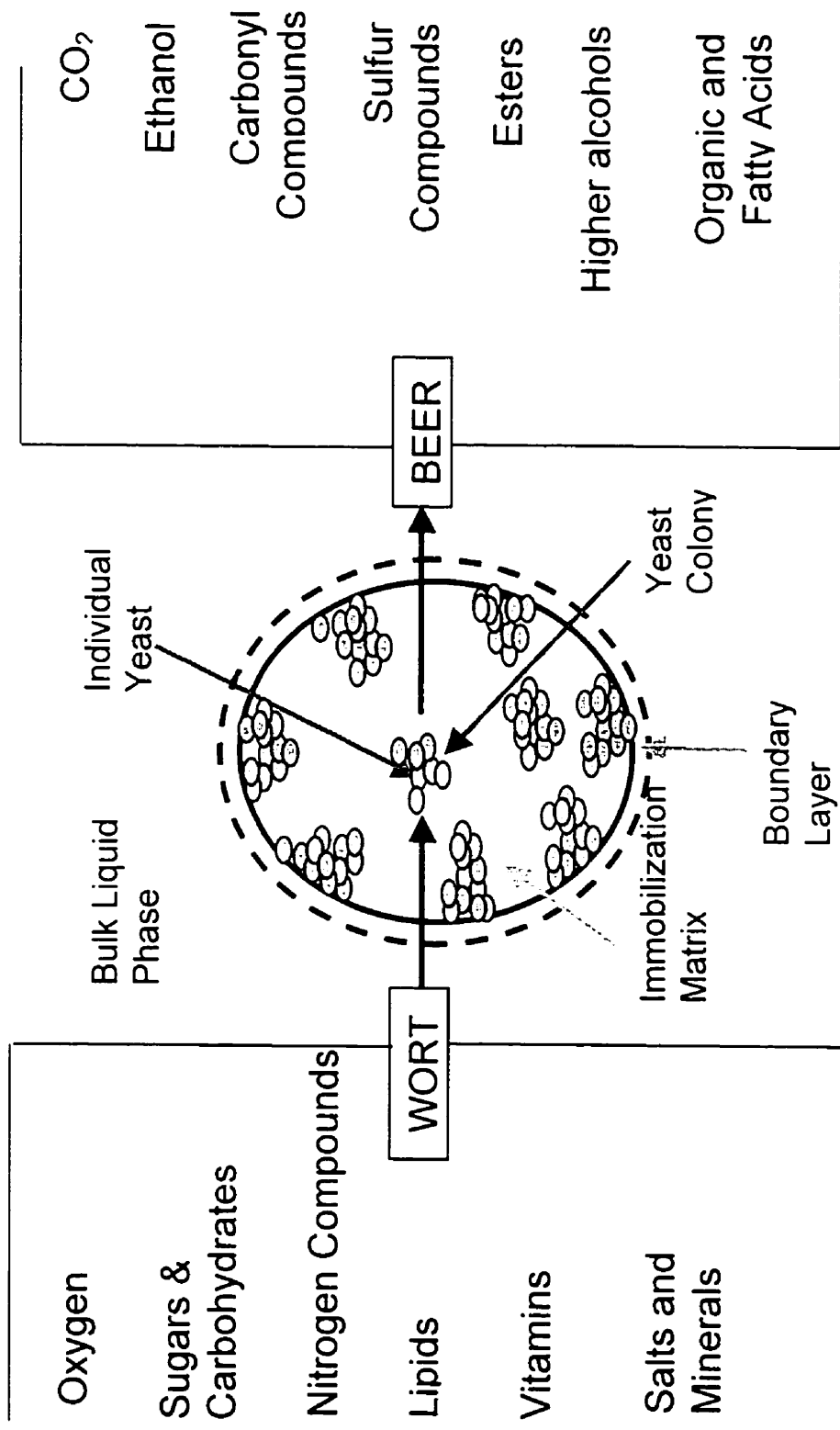


Figure 6.3. Schematic of the utilization of wort constituents by immobilized yeast during primary fermentation.

6.1 Experimental Procedure

Kappa-Carrageenan Gel Bead Production: kappa-carrageenan gel X-0909 was a generous gift from Copenhagen Pectin A/S. Kappa-carrageenan gel beads containing entrapped lager yeast cells were produced using the static mixer process with an initial cell loading of 2.6×10^7 cells/mL of gel (Patent Application 2133789 (Neufeld et al., 1996) and a bead diameter of 0.5 to 2.0 mm.

Fermentation Medium: Labatt Breweries of Canada supplied brewery wort with a specific gravity of 17.5°P as described in detail in the Materials and Methods section.

Part A: Repeated Batch Kinetics of Yeast Immobilized in Kappa-Carrageenan Gel Beads

Fermentations were conducted in 2 L Erlenmeyer flasks at 21°C, with shaking at 150 rpm. Carrier loading was 40% (v/v) of immobilized cell beads and the total fermentation volume was 1 L. Each fermentation was seven days in duration. In R1 fresh immobilized cell beads were pitched into wort and at the end of the fermentation these beads were separated from the fermented liquid by passing the mixture through a sterile stainless steel sieve (500 μ m mesh size). The beads were then repitched at the same proportion into fresh, sterile wort for a second (R2) and then third (R3) batch fermentation. Sampling was performed twice a day for the first three days, and then once per day for the fourth and fifth days of each fermentation. Fermentations were carried out in duplicate or triplicate. All fermentations were conducted with freely suspended cell control fermentations, which were conducted under the same conditions except that only free cells were pitched into the fermentations at a rate of 4 g/L. Samples were analyzed for free and immobilized cell viability and cell concentration, and liquid phase carbohydrate and ethanol concentrations

Yield factors, $Y_{P/S}$, of product ethanol, from substrate total fermentable glucose, were calculated using equation 3.20 for the three immobilized cell fermentation cycles and the free cell control. For all fermentations the yield factors were calculated from the start of fermentation to the time that maltose consumption was complete.

Ethanol productivity, V_{ethanol} , the amount of ethanol produced per total bioreactor working volume per unit fermentation time was calculated using equation 3.25 for R1, R2 and R3, and the free cell control from the start of fermentation to the time that maltose

consumption was complete. In the case of the yield factors and ethanol productivity, the contributions of the immobilized and freely suspended yeast cells were not distinguished from one another.

The local maximum specific growth rate, μ_{\max} , and cell doubling time was calculated for the averaged free cell control using equations 3.3 and 3.4.

Part B: Viability and Morphological Characteristics of Immobilized Yeast over Extended Fermentation Time

Batch Fermentation Conditions: Batch fermentations were conducted in 2 L Erlenmeyer flasks at 21°C, with shaking at 150 rpm. Carrier loading was 40% (v/v) with a total fermentation volume of 1 L.

Continuous Fermentation Conditions: Pilot scale gas lift draft tube bioreactors were used for continuous fermentations. All data collected were from an 8 L working volume bioreactor, except the 2 month scanning electron micrographs, which were collected from a 50 L bioreactor using the same fermentation medium and immobilization method. Immobilized cell beads at 40% (v/v) were fluidized within the bioreactors using a mixture of air and carbon dioxide. The bioreactors were operated under varying conditions with fermentation temperatures controlled at 12, 17 and 22°C and residence times held between 0.9 and 1.8 days. The gas lift reactor reached a maximum ethanol concentration of 73 kg/m³ during the six-month experiment, with an average concentration of 58 kg/m³.

Microbiological Analyses: Samples were taken from the liquid phase of the gas lift bioreactor at least once a week to test for contaminants including wild yeast, non-lager yeast, and aerobic and anaerobic beer spoilage bacteria. After five months, the liquid phase yeast cells were assayed in duplicate for respiratory deficient mutation.

Scanning Electron Microscopy (SEM): Kappa-carrageenan gel beads (1.0 – 1.5 mm diameter) containing immobilized lager yeast cells were sampled for SEM examination at four different times: 1) after immobilized cell bead production and before inoculation of beads into the fermentation medium; 2) after 2 days in batch fermentation; 3) after 2 months of continuous fermentation in a pilot scale gas lift draft tube bioreactor; 4) after 6 months of continuous fermentation in a pilot scale gas lift draft tube bioreactor. The

methodology for used for SEMs and the related sample preparation are described in section 4.7.

Using the methods described in section 4.6, yeast cell concentration and viability (immobilized and freely suspended) were assessed at the same times as the SEMs.

6.2 Results and Discussion

Part A: Repeated Batch Kinetics of Yeast Immobilized in Kappa-Carrageenan Gel Beads

Fermentation time was greatly reduced each time the immobilized cells were repitched into fresh wort, as seen in Figures 6.4 (a), (b), and (c) illustrating maltose, maltotriose, glucose, fructose and ethanol vs. fermentation time for the three repeated batch fermentation cycles. From these figures it can be seen that the time for complete sugar consumption was 64 hours for R1, 44 hours for R2, and 26 hours for R3. The freely suspended cell control fermentation which contained no immobilized cell beads, shown in Figure 6.5, took 82 hours for complete sugar consumption. One can also see from the graphs in Figure 6.4 that final ethanol concentrations were highest in the third of the three repeated batch immobilized cell fermentations. Because kappa-carrageenan is a hydrogel, some ethanol is carried over in beads when they were repitched into fresh wort. Consequently at time zero for R2 and R3, some ethanol was present in the fermentation liquid and the initial concentration of glucose, maltose, maltotriose, and fructose was lower in the immobilized cell fermentations (Figure 6.4) compared with the free cell control fermentation, as seen in Figure 6.5. Thus, yield factors were calculated for the fermentations so that the yield, g ethanol production per g sugar consumed, can be examined on a comparable basis.

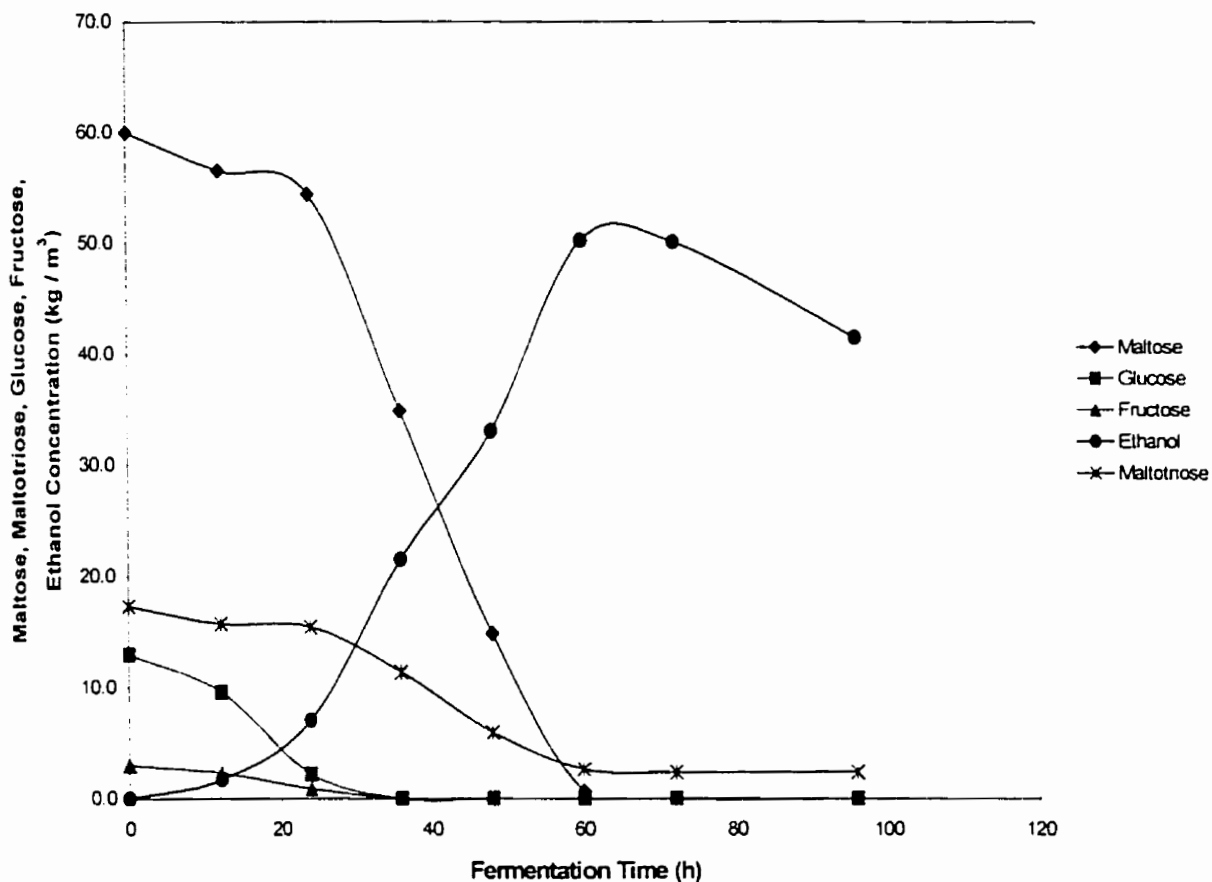


Figure 6.4. a) R1, maltose, maltotriose, glucose, fructose, and ethanol concentration versus fermentation time for repeated batch fermentations using lager yeast cells immobilized in kappa-carrageenan gel beads.

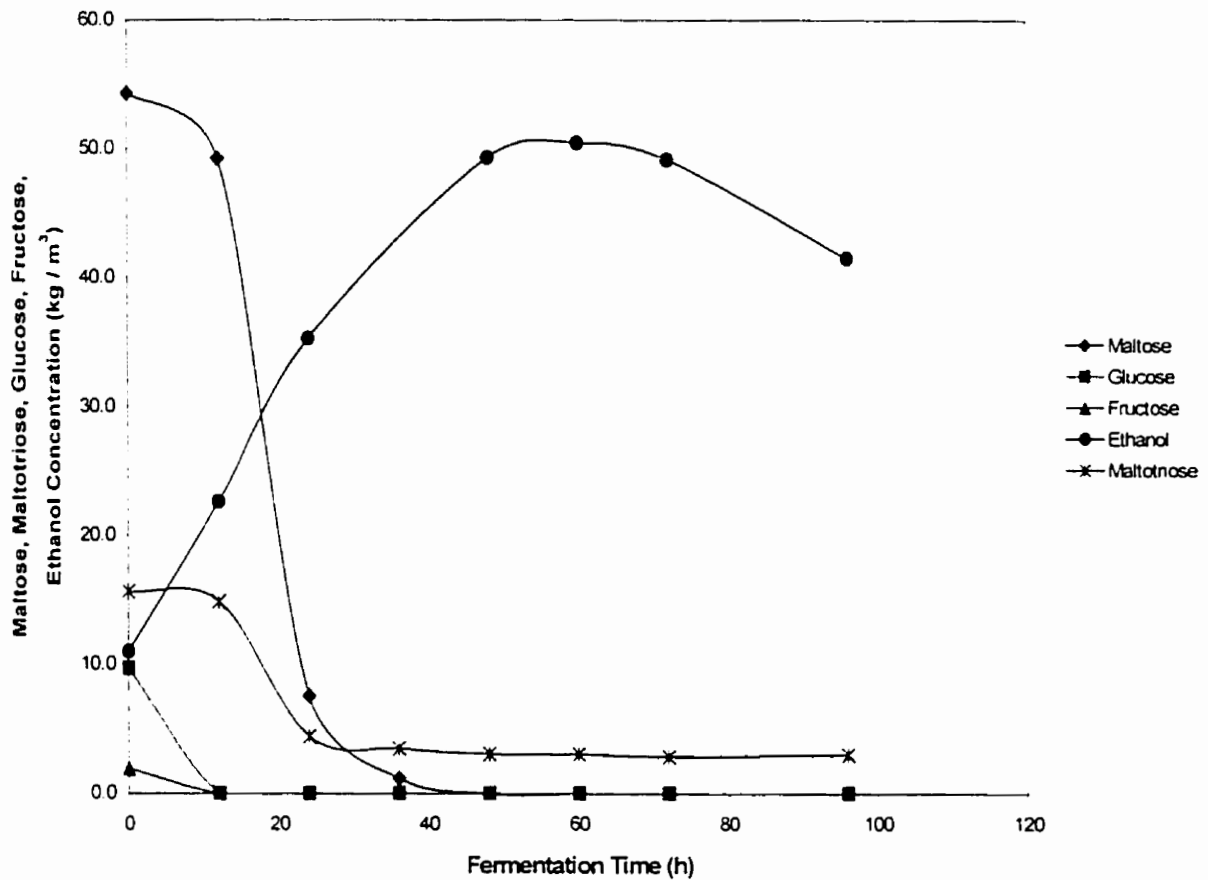


Figure 6.4. b) R2. maltose, maltotriose, glucose, fructose, and ethanol concentration versus fermentation time for repeated batch fermentations using lager yeast cells immobilized in kappa-carrageenan gel beads.

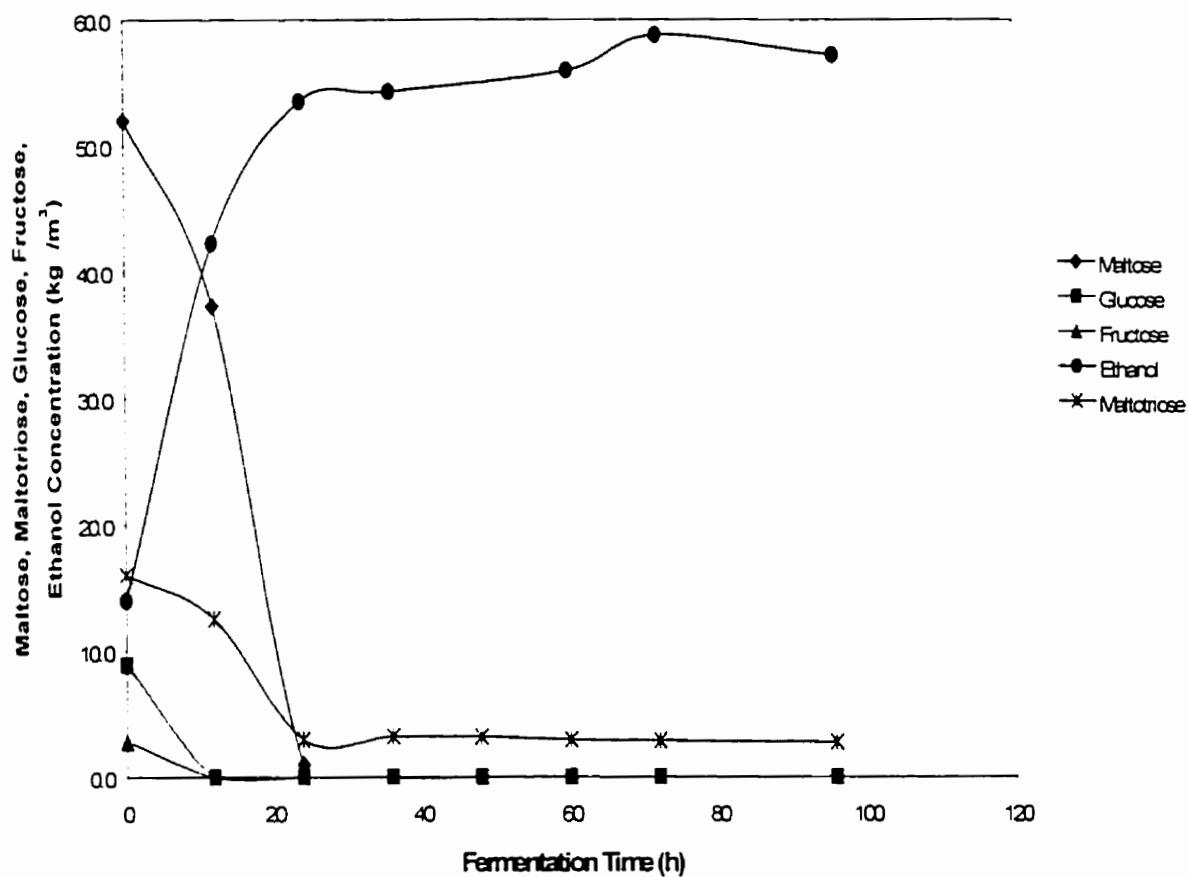


Figure 6.4. c) R3. maltose, maltotriose, glucose, fructose, and ethanol concentration versus fermentation time for repeated batch fermentations using lager yeast cells immobilized in kappa-carrageenan gel beads.

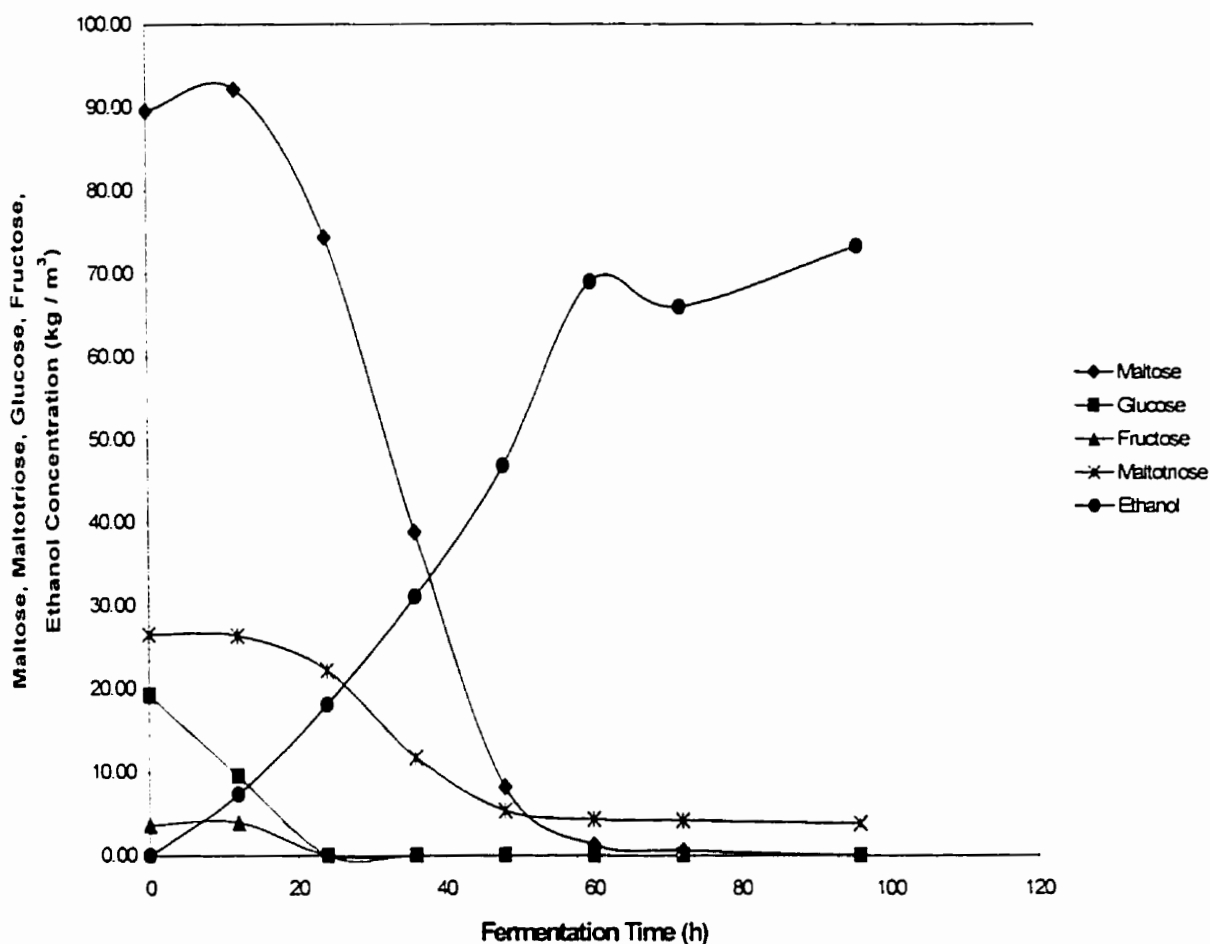


Figure 6.5. Maltose, maltotriose, glucose, fructose, and ethanol concentration versus fermentation time for freely suspended lager yeast control fermentations (no immobilized cells).

Figures 6.6 (a) and (b) compare maltose and ethanol concentrations respectively versus fermentation time of R1, R2, and R3. During repeated R1, maltose was taken up by the yeast cells almost immediately after pitching into fresh wort. Ethanol concentrations reached their peak earlier in repeated R1 and also reached higher concentrations than the first two batch fermentations. As shown in Figure 6.6 (b), the initial lag in ethanol production in R1 was drastically reduced when these immobilized cells were repitched in R2 and further reduced after repitching for R3.

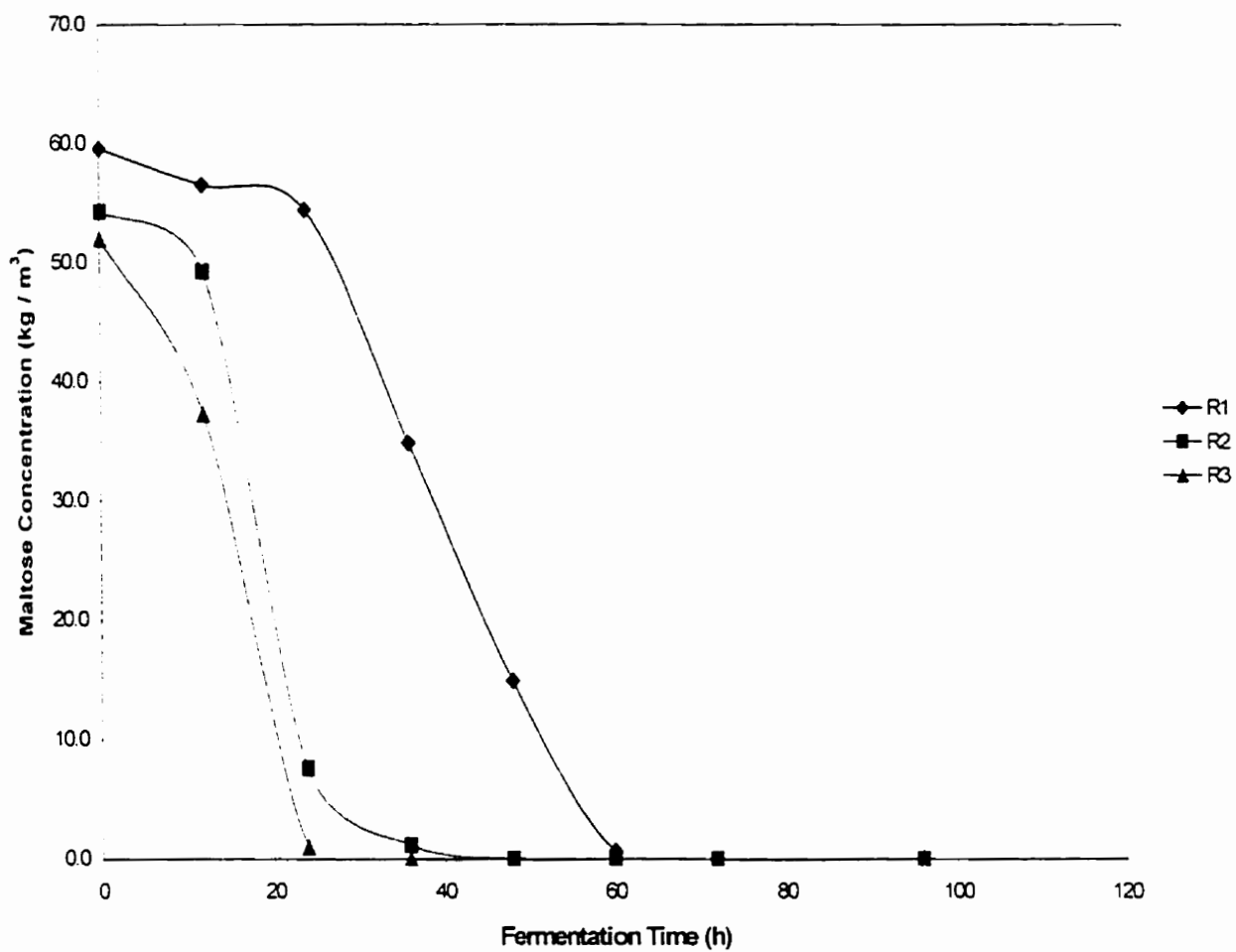


Figure 6.6. a) Maltose concentration versus fermentation time for repeated batch fermentations, R1, R2, and R3, using lager yeast cells immobilized in kappa-carrageenan gel beads.

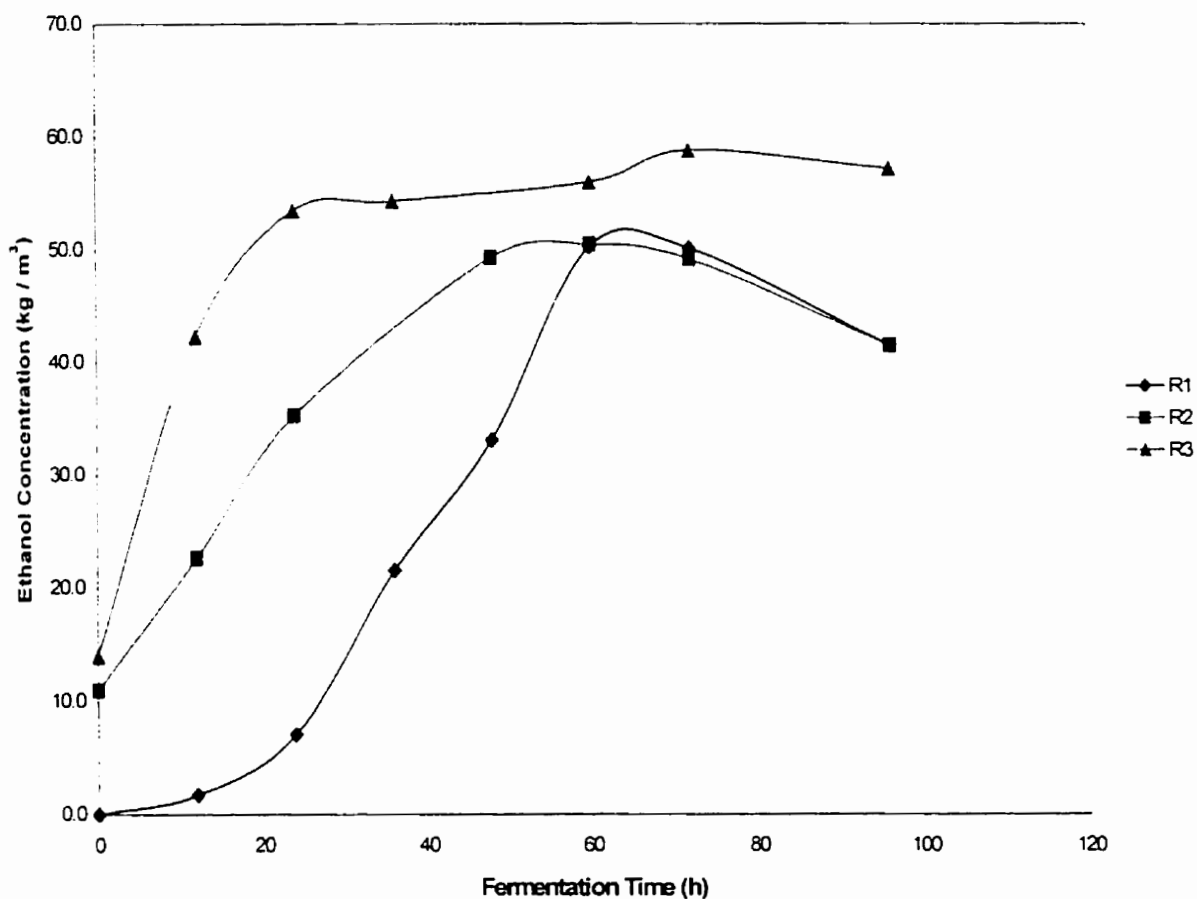


Figure 6.6. b) Ethanol concentration versus fermentation time for repeated batch fermentations. R1, R2, and R3 using lager yeast cells immobilized in kappa-carrageenan gel beads.

Figure 6.7 (a) shows immobilized cell concentration per total bioreactor volume vs. fermentation time for R1, R2 and R3. The free cells released from the immobilized cell matrix into the bulk liquid phase in these fermentations vs. time are shown in Figure 6.7 (b). In Figure 6.7 (c) the total of immobilized and free yeast cells per total reactor volume are shown for the three batches. Figure 6.7 (a) shows that the concentration of immobilized cells within the kappa-carrageenan gel continued to increase following their initial inoculation into wort for R1. When the beads were repitched into fresh wort for repeated R2, growth continued to occur within the gel beads. The third time that the encapsulated cells were repitched into fresh wort, the rate of increase in immobilized cell concentration had slowed. The concentration profile of free cells released from the

kappa-carrageenan gel matrix into the bulk liquid phase, immobilized cells, and total cells in the fermentation for R1 is shown in Figure 6.8.

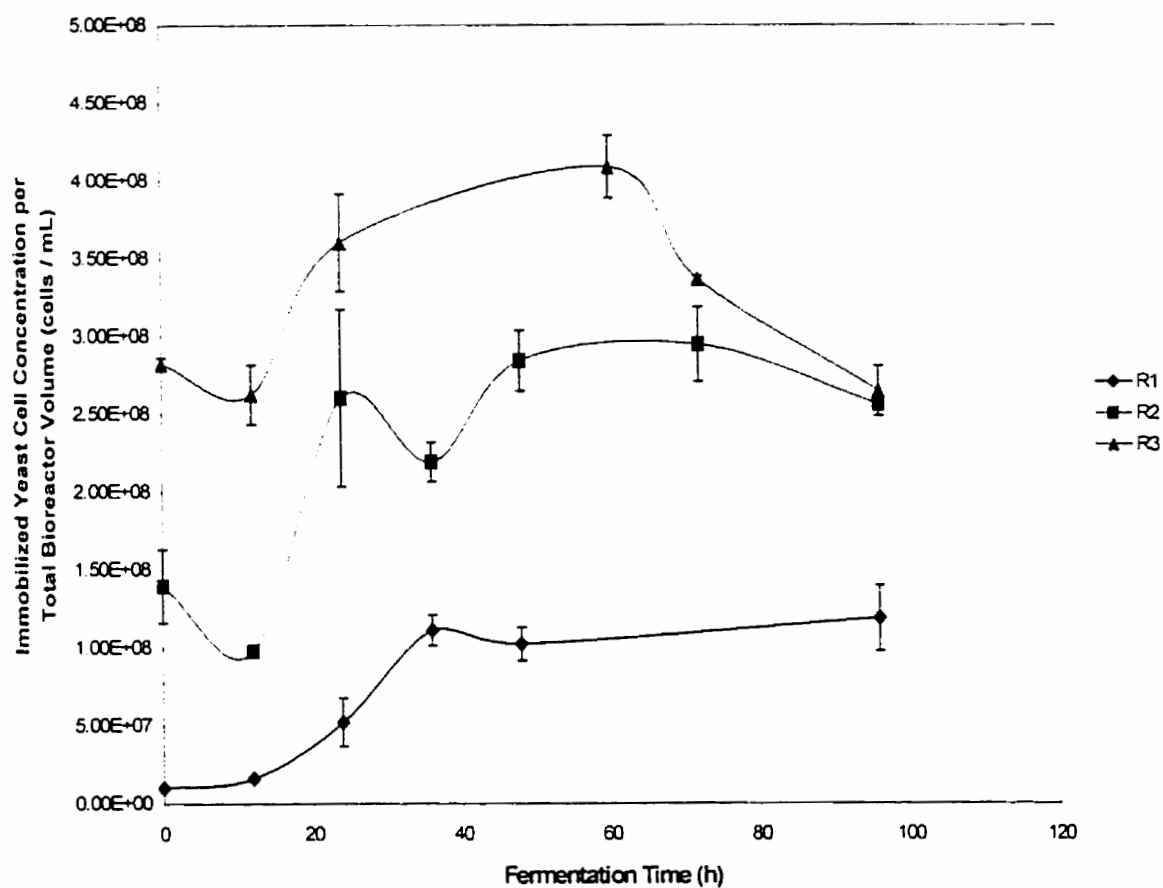


Figure 6.7. a) Immobilized lager yeast cell average concentration per total bioreactor volume versus fermentation time for R1, R2, and R3 fermentations. Error bars represent the upper and lower limits of the experimental data (n = 2).

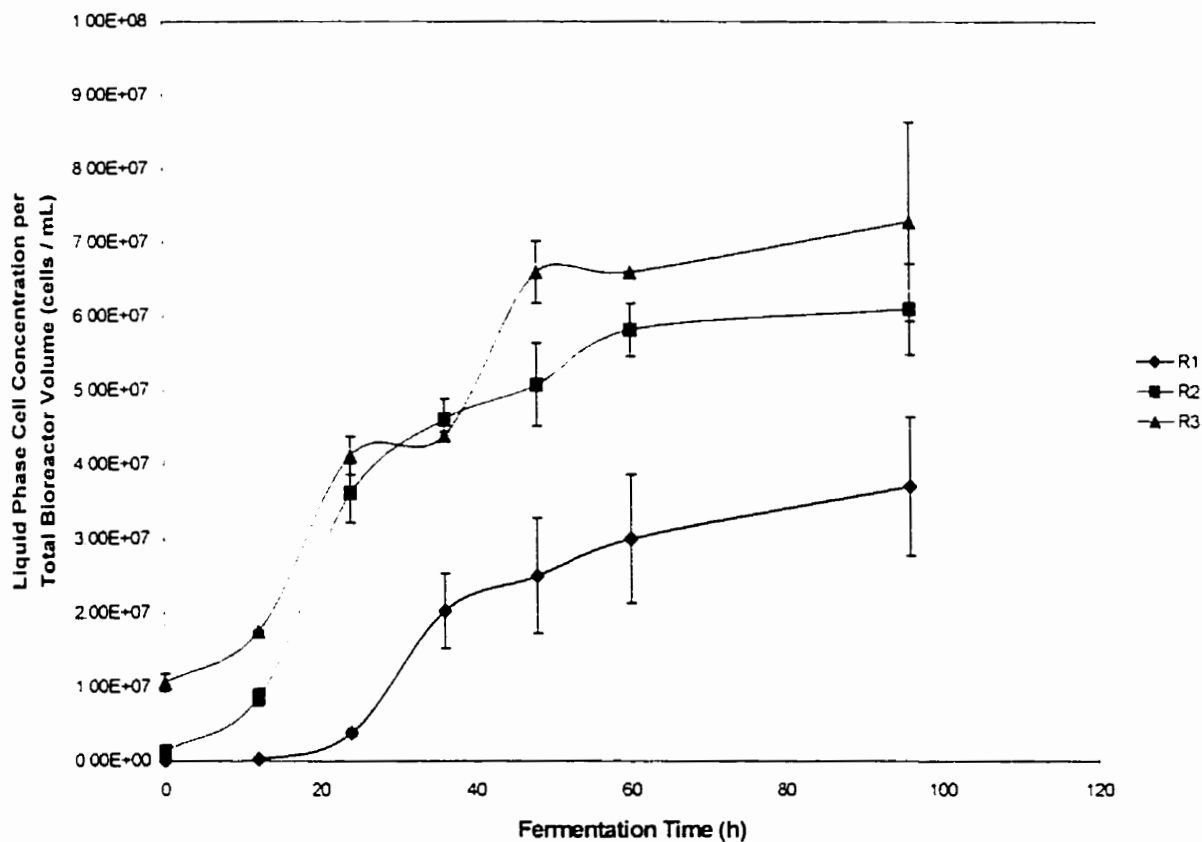


Figure 6.7. b) Concentration per total bioreactor volume of lager yeast cells released into bulk liquid phase versus fermentation time for R1, R2, and R3 fermentations. Error bars represent the upper and lower limits of the experimental data (n = 2).

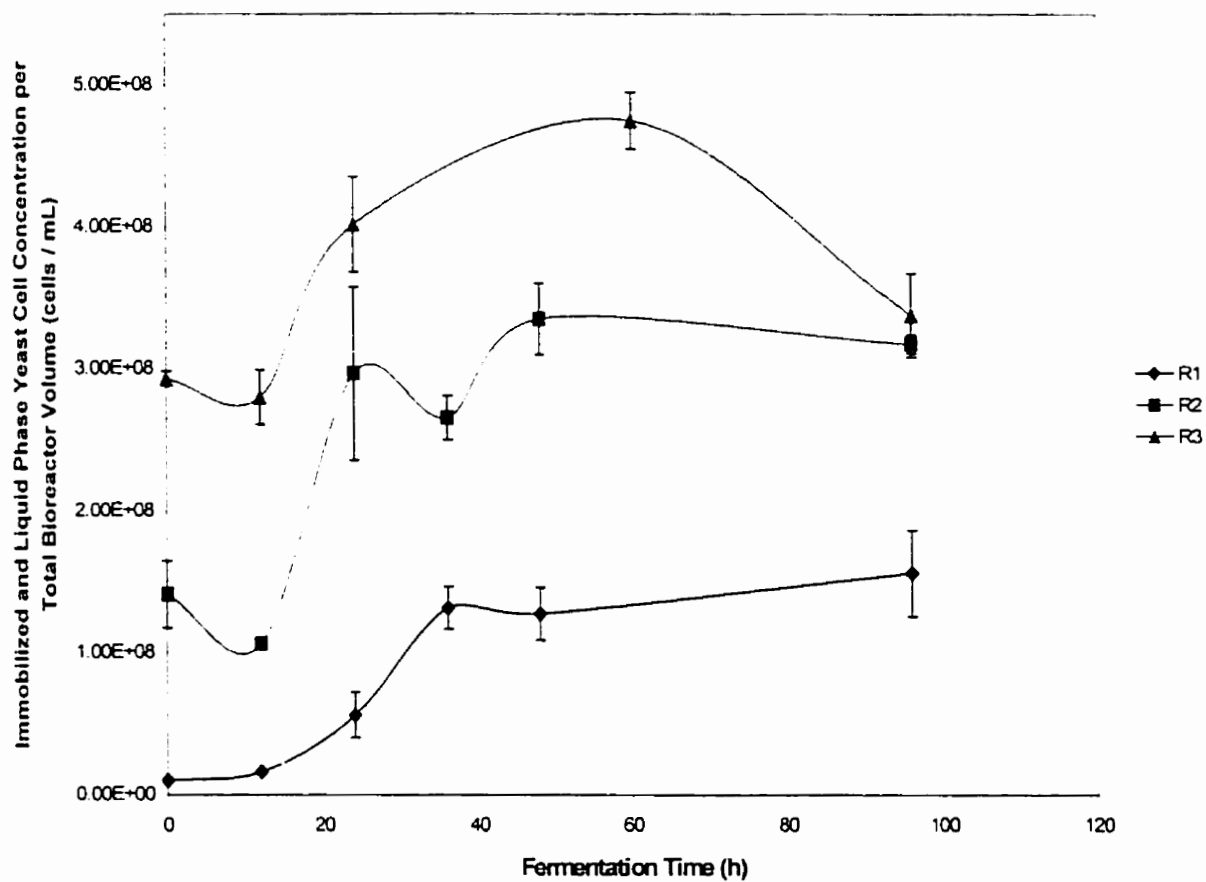


Figure 6.7. c) Total (immobilized and liquid phase) lager yeast cell concentration per total bioreactor volume versus fermentation time for R1, R2, and R3 fermentations. Error bars represent the upper and lower limits of the experimental data (n = 2).

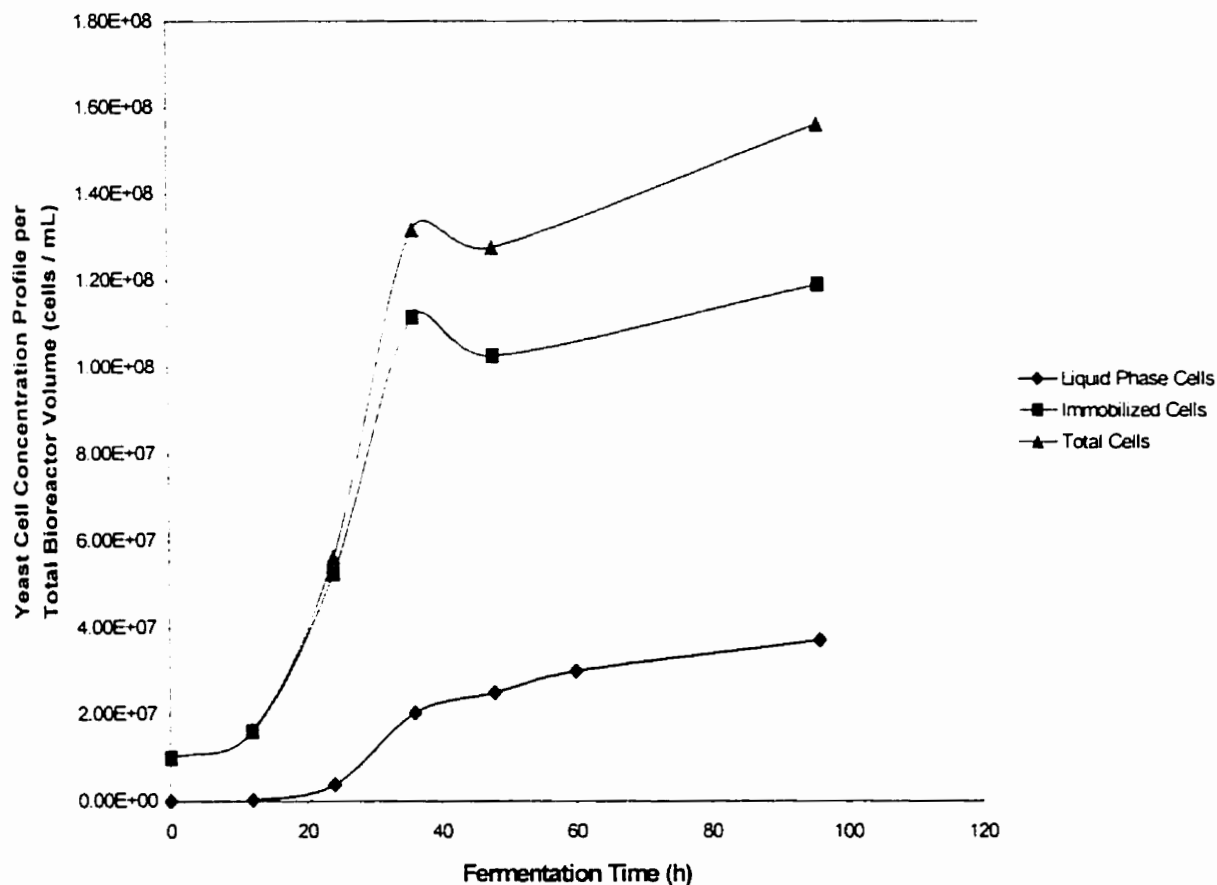


Figure 6.8. Profile of immobilized, liquid phase, and total (immobilized and liquid phase) cell concentration versus fermentation time for R1, the first of three repeated batch fermentations using lager yeast cells immobilized in kappa-carrageenan gel beads.

In R1, the immobilized cell concentration within the kappa-carrageenan gel bead was increasing at a similar rate to the control fermentation, which contained only liquid phase cells. This was confirmed by comparing the average growth curve of the free cell control fermentations in Figure 6.9 to the similar growth curve of cells immobilized in carrageenan in R1 in Figure 6.10. During R1, the gel beads were not yet fully colonized and the gel matrix did not appear to have an inhibitory effect on yeast cell growth within the beads. By R2, the matrix appeared to be restricting the growth of the cells within the gel bead, as indicated by a smaller increase of cell number during this fermentation cycle. This could be due to the nature of the gel or the crowding of the yeast cells within the beads, or to a lack of nutrient supply to the cells.

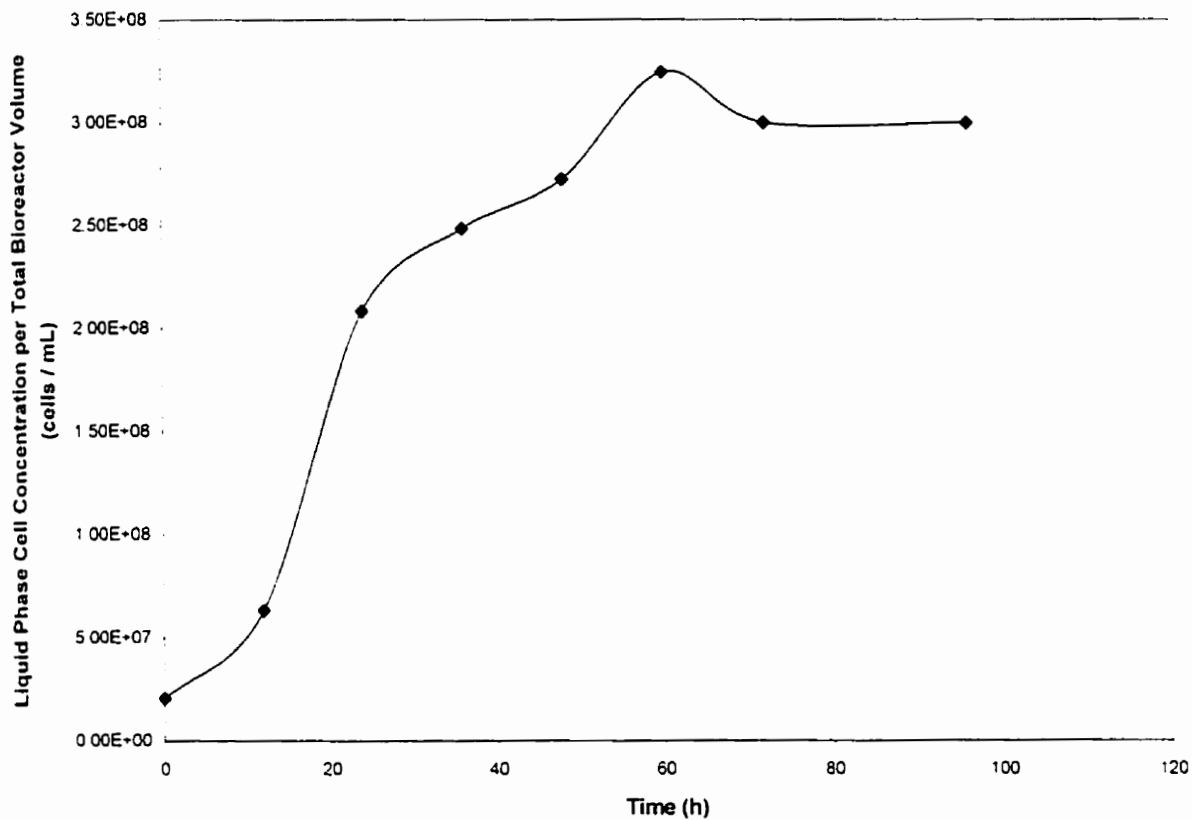


Figure 6.9. Control fermentation freely suspended lager yeast cell average concentration ($n = 3$) per total bioreactor volume versus fermentation time. No immobilized cells were present during these fermentations.

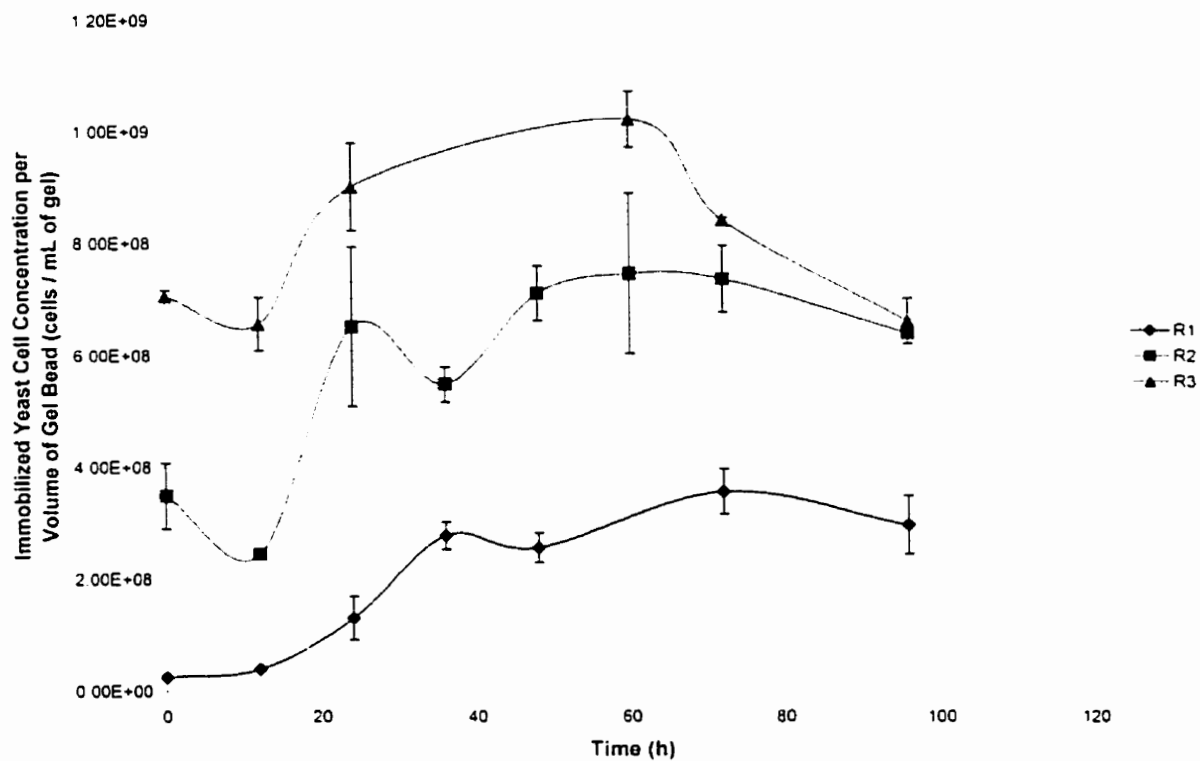


Figure 6.10. Immobilized lager yeast concentration per mL of gel beads versus fermentation time for R1, R2, and R3 fermentations. Error bars represent the upper and lower limits of the experimental data ($n = 2$).

In Table 6.1, the yields of ethanol from substrate fermentable sugars, $Y_{P/S}$, are shown for the three batch generations and the control. In Table 6.2, the bioreactor volumetric productivities of ethanol are also given, calculated using the data given in Table 6.1. The yields of ethanol from sugars for the fermentations were not significantly different from each other or from the control. Yields were all above 90% of the theoretical yield of 0.51 predicted from the Guy-Lussac equation. As mentioned earlier, biomass production and other by-products formed by the yeast cells prevent efficiencies from reaching higher than 95% of theoretical (Hardwick, 1995). The volumetric bioreactor productivity of ethanol in the three repeated batch fermentations varied significantly from batch to repeated batch. Ethanol productivity increased with each cycle of repeated batch fermentation and, by R3, the immobilized cells were more productive than the control fermentation. The total amount of ethanol produced in R2 was not significantly greater than that produced during R1, but the fermentation time was less than half of R1 and of the control fermentation. There are many factors that could contribute to this increased fermentation rate of immobilized cells with each batch repetition, such as yeast cell adaptation to the fermentation conditions and the progressively increasing cell concentration. The total number of cells per bioreactor volume only becomes significantly greater than that of the control by R3. In Figure 6.7 (b), the graph of freely suspended cell (released from the gel matrix) concentration in the bulk liquid vs. fermentation time demonstrated that the number of cells released from the gel beads increased with each batch generation. Once the beads became more fully loaded with yeast cells, they appeared to release more cells into the bulk liquid phase. Hüsken et al. (1996) conducted studies that examined bacterial cell colony expansion and eruption/release from kappa-carrageenan gel slabs. Vives et al. (1993) have reported that the maximum concentration of yeast cells they have achieved in kappa-carrageenan gel beads was 10^9 cells per gram of gel, which is the concentration that was reached within the gel particles by R2. Similar maximum cell concentrations were found during the continuous fermentations in Part B. However, maximum cell loadings in the gel matrix will depend upon the initial cell loading, the composition of the gel and other factors.

Table 6.1. Yield, $Y_{P/S}$, of product, P, ethanol from substrates, glucose (Glc), fructose (Frc), maltose (Mal) and maltotriose (DP3) for R1, R2, R3, and freely suspended cell control fermentation.

Batch	t_f	t_0	Glc _f	Frc _f	Mal _f	DP3 _f	P_f	Glc ₀	Frc ₀	Mal ₀	DP3 ₀	P_0	$Y_{P/S}$
Fermentation	(h)		(kg / m ³)										
R1	64.0	0.0	0.0	0.0	0.0	2.4	50.1	13.0	3.0	60.0	17.4	0.0	0.5
R2	44.0	0.0	0.0	0.0	0.0	3.1	49.0	9.7	2.0	54.3	15.7	11.0	0.5
R3	26.0	0.0	0.0	0.0	0.0	3.2	54.0	8.9	2.8	52.0	16.0	14.0	0.5
Free Cell Ctrl	82.0	0.0	0.0	0.0	0.0	4.2	66.0	19.5	3.6	91.2	27.3	0.0	0.5

*The symbol t_f is the time in hours to complete maltose uptake and the subscript f refers to the concentration of the given analyte at time, $t = t_f$.

Table 6.2. Bioreactor productivity of ethanol [$V_{\text{ethanol}} = (\text{kg ethanol produced}) / (\text{m}^3 \text{ bioreactor volume} \cdot \text{h})$] for immobilized cell batch fermentations (R1, R2, and R3) compared with freely suspended cell batch fermentations.

Fermentation	V_{Ethanol} (kg / m ³ hr)*
R1	0.470
R2	0.668
R3	1.246
Free Cell Control	0.805

* calculated when maltose uptake complete.

Another factor affecting the increased bioreactor volumetric productivity observed with each repeated batch fermentation, involves yeast cell adaptation. By the end of the first fermentation, yeast cells had adapted their metabolic machinery to the given fermentation conditions. This may result in a decrease in the lag phase at the beginning of subsequent batch fermentations, increasing the rate of fermentation. During this study all control fermentations were carried out with freshly prepared lager yeast. It would be interesting to repitch the freely suspended control yeast alongside the repitched immobilized cells to further examine this effect relative to the cell concentration effects.

Figure 6.11 indicates that immobilized cell viability, using the methylene blue method as an indicator, was low (< 50%) when the immobilized cells were initially pitched into wort in R1, but the viability of immobilized cells was above 90% after 48 hours of fermentation. The yeast cells rapidly colonized the beads, and viability remained high throughout R3. However by repeated R3, viability tapered off slightly toward the end of the fermentation. However, throughout all three repeated batch fermentations, the free cells that were released into the bulk liquid medium had higher viability than their immobilized counterparts. The immobilization matrix may have a negative effect on yeast cell viability (mass transfer limitations and/or spatial limitations), or viable yeast cells may be preferentially released from the immobilization matrix into the bulk liquid medium over non-viable cells.

Using the averaged data from three separate freely suspended yeast control fermentations contained in Appendix 1, a plot of $\ln(X/X_0)$ versus fermentation time, is given in Figure 6.12. The slope is equal to the local maximum specific growth rate of the cells at 21°C in brewer's wort, with shaking at 150 rpm. The local maximum specific growth rate of the yeast was found to be 0.096 hr^{-1} and the cell doubling time was 7.22 hours. The μ_{max} found in this work was defined as a local μ_{max} because, as mentioned in the Theory section, the true μ_{max} used in the Monod equation is achievable only when S is significantly greater than the Monod constant, K_s . More work is required to evaluate the Monod constant, K_s , of the limiting substrate in these fermentations, in order to confirm that the calculated local μ_{max} was a true maximum, as defined by the Monod equation.

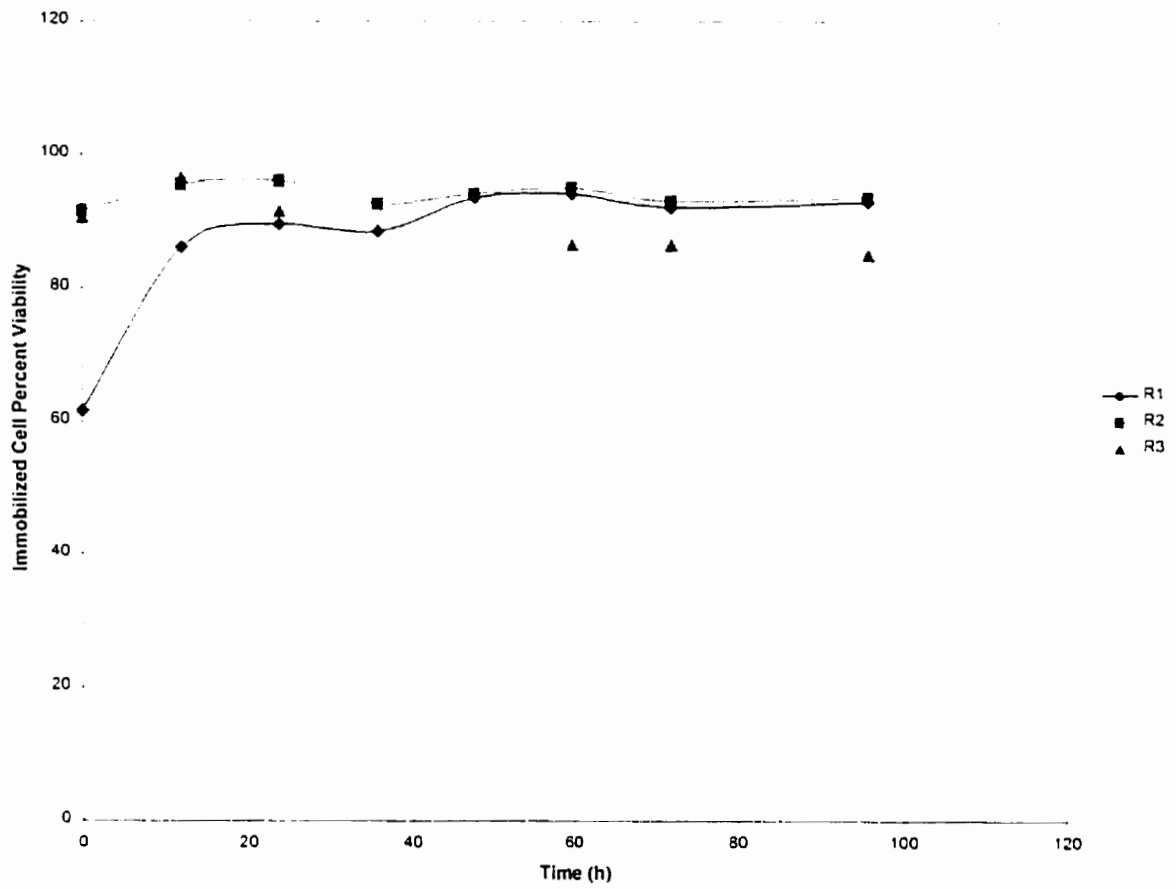


Figure 6.11. Immobilized lager yeast cell viability (methylene blue) versus fermentation time for R1, R2, and R3 fermentations.

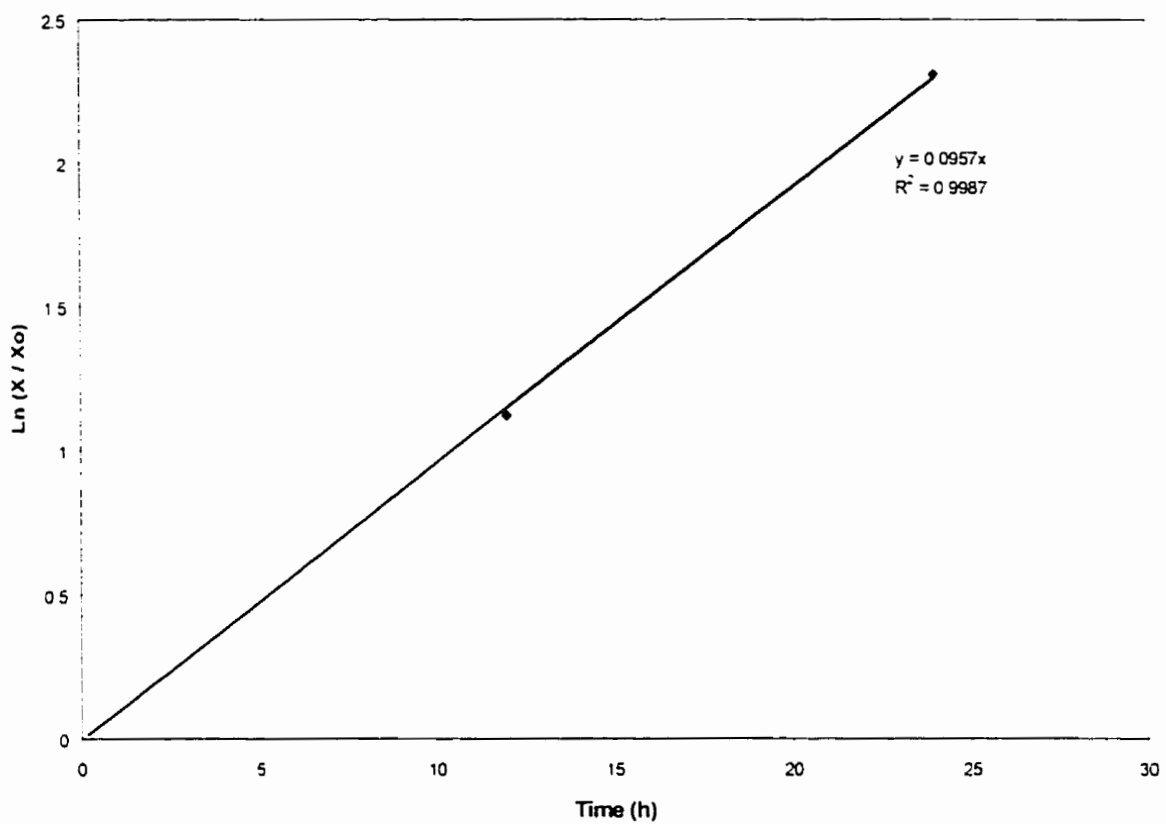


Figure 6.12. $\text{Ln}(X/X_0)$ versus batch fermentation time during the exponential growth phase of the averaged freely suspended yeast control fermentations, where X is the cell concentration at time, t , and X_0 is the cell concentration at time, $t = 0$ ($n = 3$).

Part B: Viability and Morphological Characteristics of Immobilized Yeast Over Extended Fermentation Time

Before the gel beads were exposed to fermentation medium, and following immobilized cell bead production using the static mixer process, the cell concentration was 2.6×10^7 cells/mL of gel bead (Table 6.3, where values are the averages of two samples). SEM imaging shows the cells to be individually and uniformly distributed throughout the gel bead (Figure 6.13).

Table 6.3. Viability (methylene blue) and concentration of freely suspended and immobilized lager yeast cells entrapped in kappa-carrageenan gel beads over fermentation time.

Time	Fermentation Mode	Freely Suspended Yeast In Liquid Phase		Immobilized Yeast in Gel Phase	
		Viability (%)	Cell Conc. (cells/mL in liquid)	Viability (%)	Cell Conc. (cells/mL of gel)
0	n/a	n/a	n/a	n/a	2.6E+07
2 days	Batch	98	5.5E+07	92	2.35E+08
2 months	Continuous	93	2.35E+08	76	8.60E+08
6 months	Continuous	92	2.11E+08	<50*	1.40E+09*

*Based on single sample.

Viability was >90% following 2 days of batch fermentation, and cell concentration within the gel bead had increased ten-fold (Table 6.3). Cells (>90% viable) had also begun to be released from the gel into the bulk liquid phase of the fermentation, yielding a concentration of 10^7 cells/mL of liquid. Small yeast colonies formed inside the gel beads, with many bud scars present on individual cells as seen in Figure 6.14.

Immobilized yeast cell viability decreased after 2 months of continuous fermentation in a gas lift bioreactor (Table 6.3), but the cells in the bulk liquid phase remained highly viable (>90%), and this finding was supported during several different continuous fermentations in pilot scale gas lift bioreactors. The SEM in Figure 6.15 showed that at two months large colonies of yeast had formed toward the periphery of the bead, confirming the results of other researchers (Bancel and Hu, 1996; Gòdia et al., 1987; Wada et al., 1979; Wang et al., 1982). A comparison of the morphology of yeast positioned toward the outer edge of an immobilized cell bead to the yeast positioned at the center of a gel bead was made in several samples using SEM imaging. The cells

located toward the periphery of the beads were ovoid and smooth with many bud scars (Figure 6.16), indicative of yeast multiplication (Smart, 1995). The cells that were imaged at the center of the bead (Figure 6.17) appeared malformed and displayed little evidence of bud scar formation. The lack of bud scars may be an indication of possible limitation of nutrients, such as oxygen, at the center of the beads. The surface irregularity observed on the surface of the yeast in Figure 6.17, may also be an indicator of cell aging (Barker and Smart, 1996; Smart, 1999).

The viability of the yeast immobilized within the carrageenan gel had dropped to below 50% after six months of continuous fermentation in the gas lift bioreactor. (Table 6.3). It should be noted that while only a single data point for immobilized cell concentration and viability was collected at six months, data at the five-month mark was similar, with an immobilized cell concentration of 1.14×10^9 cells/mL of gel and viability of <50%. While a gradual decline in immobilized cell viability was seen over time, the viability of the cells in the bulk liquid phase remained reliably high. In addition, even though immobilized cell viabilities were low in the beads as a whole, the bioreactor produced a fully fermented beer during its sixth month of continuous operation. Possible reasons for this finding include the significant contribution of the highly viable freely suspended yeast cells to the fermentation. As well, there is the potential contribution of viable immobilized cells located at the periphery of the gel bead where there are fewer barriers to mass transfer, as compared to the cells located at the center of the bead. It is unclear whether the immobilized cells had the ability to redistribute themselves within the gel matrix, or if these cells remained stationary where they were first located. A concentration of 10^9 cells/mL of gel bead was the maximum reached within these beads over the six-month period of continuous fermentation.

In Figure 6.18 an entire bead was imaged using SEM. This bead had a hollow center and, of the many beads examined, approximately half exhibited this structure. The hollow cavity could be a result of the carrageenan gel structure degradation and promoted further by the SEM preparation. This hollow cavity was not observed in fresh bead preparations. Previous work by others (Bancel et al., 1996) has shown that growing cells induced weakening of the gel network. Audet et al. (1988) reported that the addition of

locust bean gum to kappa-carrageenan modified the mechanical strength of gel beads for the immobilization of bacteria.

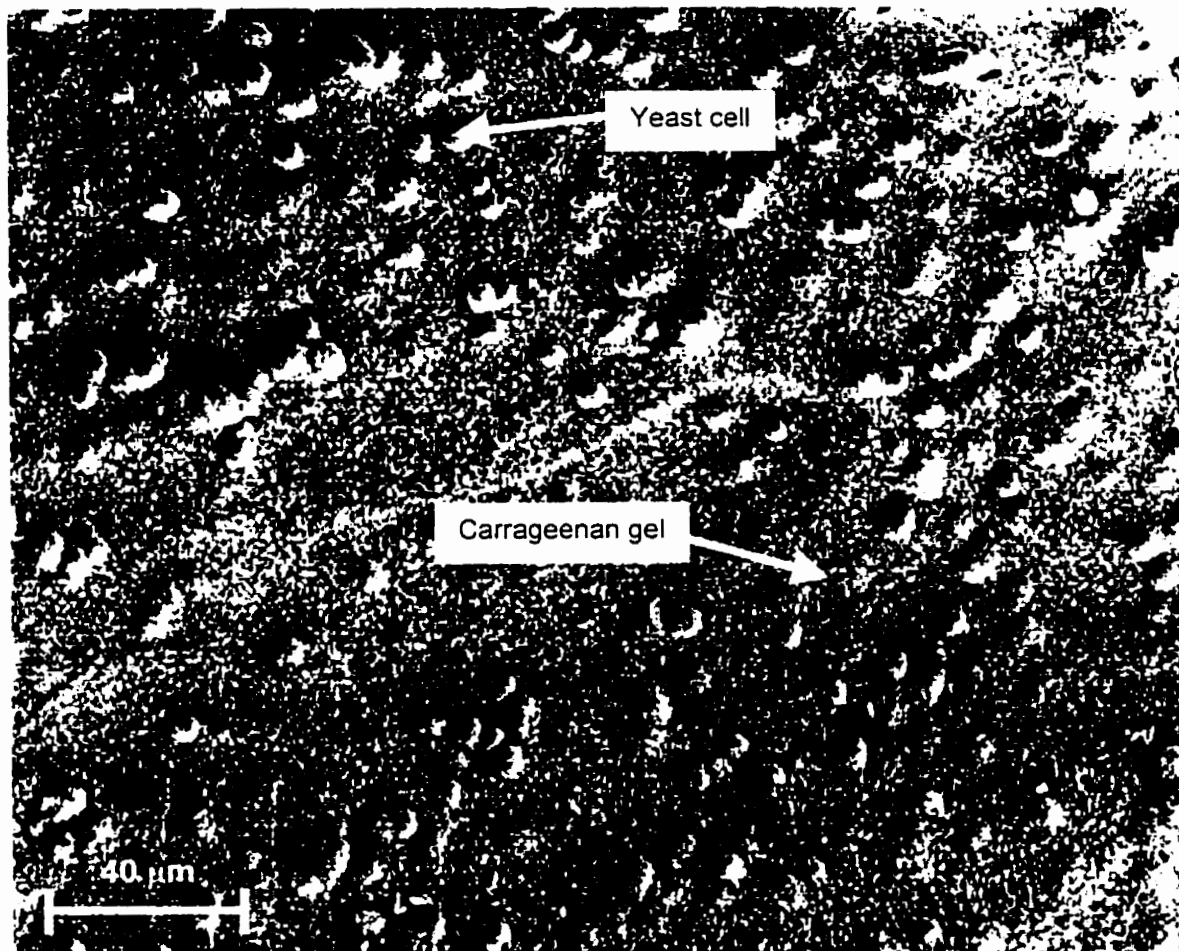


Figure 6.13. Kappa-carrageenan gel bead containing immobilized lager yeast at zero time fermentation.

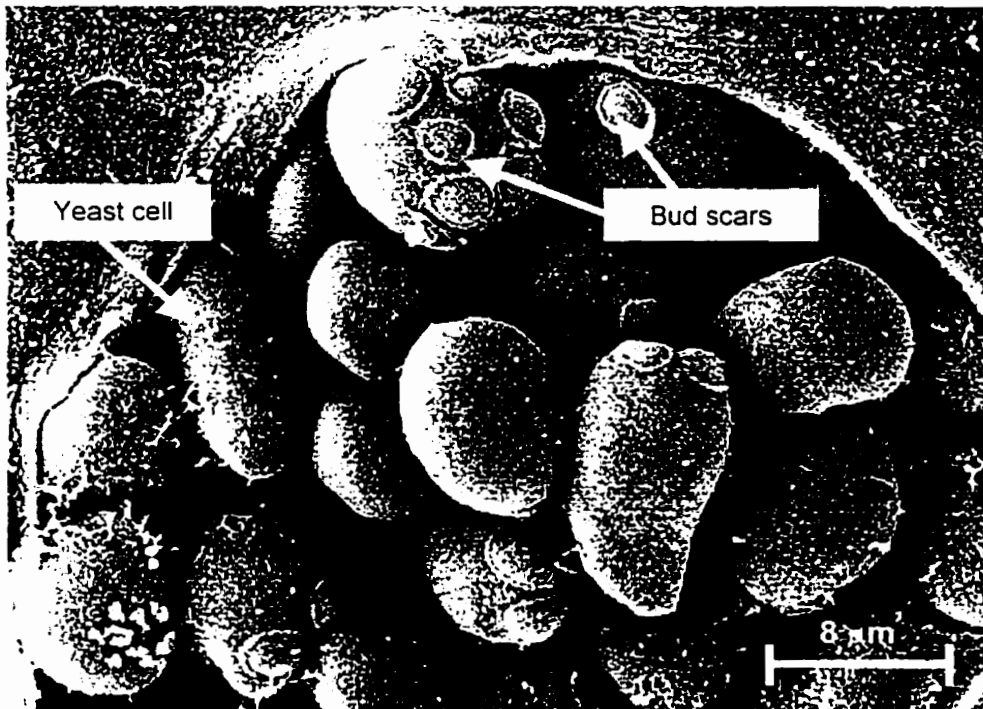


Figure 6.14. Pod of lager yeast entrapped in kappa-carrageenan gel bead after two days of batch fermentation, showing bud scars on individual yeast cells.

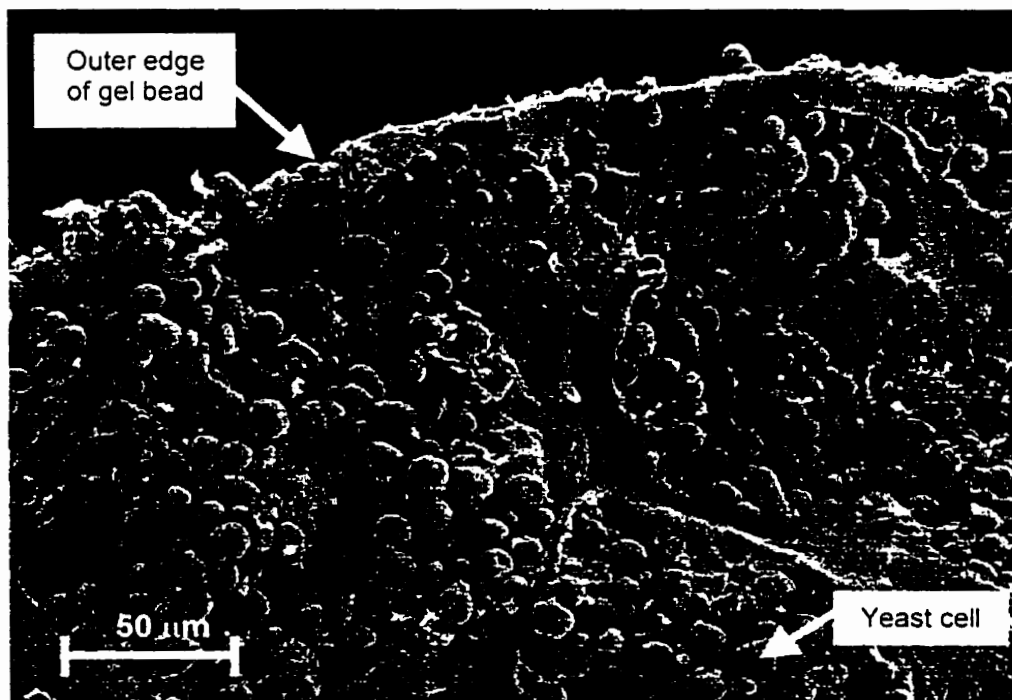


Figure 6.15. Outer edge of kappa-carrageenan gel bead showing lager yeast cells after two months of continuous fermentation.



Figure 6.16. Lager yeast cells at outer region of kappa-carrageenan gel bead after two months of continuous fermentation.

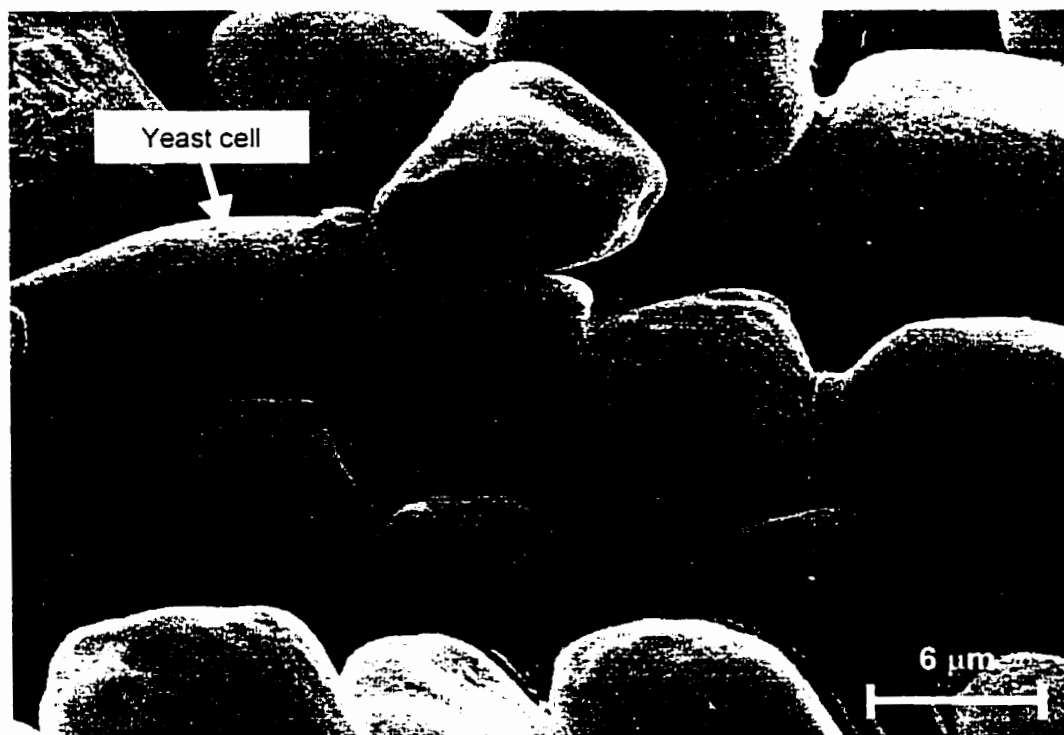


Figure 6.17. Lager yeast cells at the center of a kappa-carrageenan bead after two months continuous fermentation.

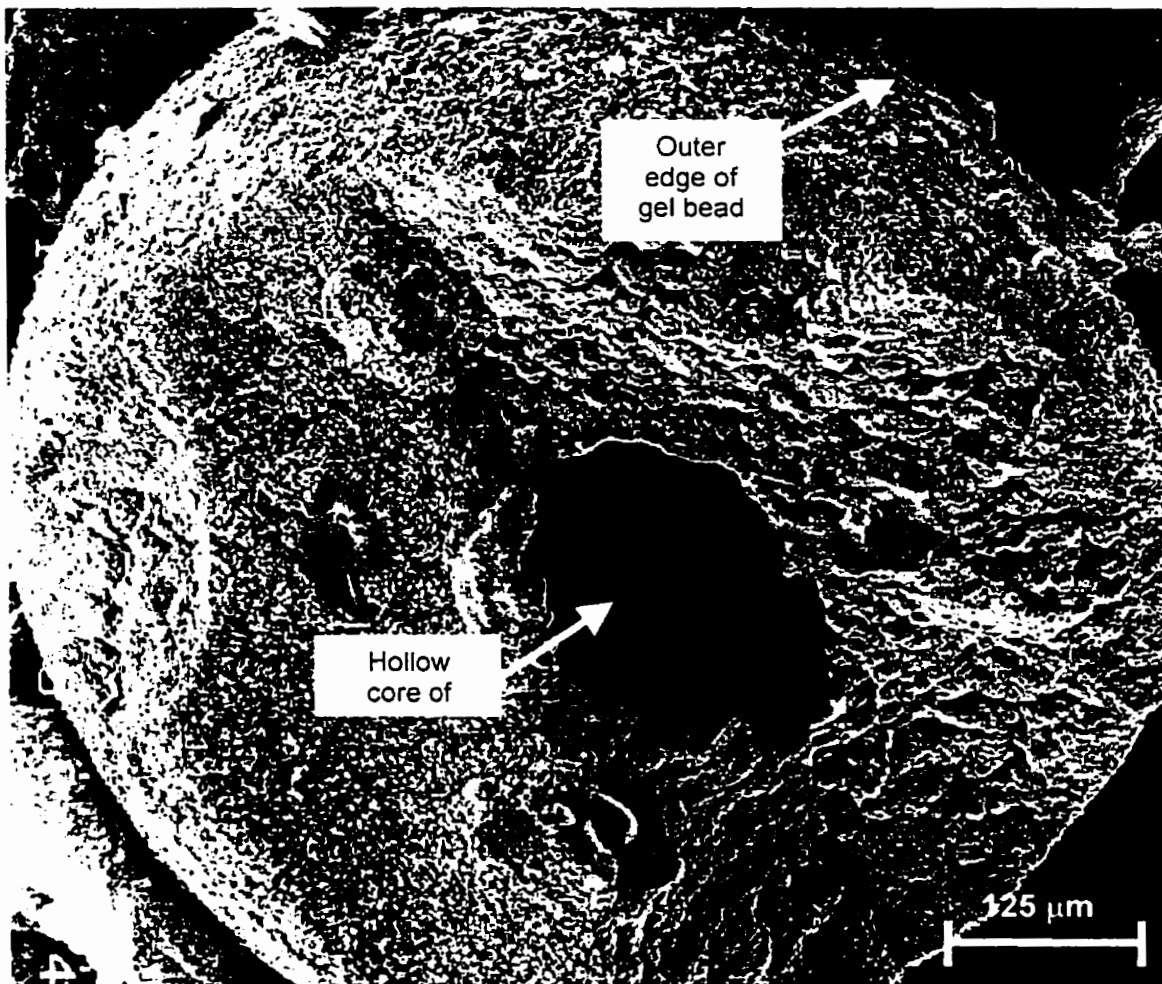


Figure 6.18. Entire kappa-carrageenan gel bead after six months continuous fermentation, many fractured beads had hollow centers.

Over the entire six month beer fermentation experiment, the gas lift bioreactor was tested a minimum of once a week for contamination. No bacterial contaminants were detected at any time during the experiment. In the last two months of the trial, a contaminating yeast was detected in concentrations which fluctuated between 1 and 5 cfu/mL. This yeast was capable of growth on PYN medium at 37°C, but did not grow aerobically or anaerobically on DUBA medium (selective for bacteria), did not ferment dextrins, and showed no growth on CuSO₄ medium (selective for wild yeast).

After five months, the average percentage of respiratory deficient yeast cells was 7%, which is higher than what is normally found using this strain during industrial batch fermentations (2% average). Other researchers have reported similar findings (Norton

and D'Amore, 1995). Respiratory deficient yeast result from a mutation which causes yeast to be incapable of respiring glucose to carbon dioxide and water. These yeast have mitochondria with permanently impaired activity and arise usually because of a mutation of mitochondrial DNA (Hardwick, 1995).

Artifacts from SEM sample preparation can cause confusion. Technologies such as nuclear magnetic resonance (NMR) spectroscopy (Fernandez, 1996) and confocal microscopy (Bancel and Hu, 1996) have been used to examine immobilized cells non-invasively. NMR imaging techniques have allowed researchers to study transport, flow and spatial distribution of cells and biochemicals in biofilms. Researchers (Bancel and Hu, 1996) have also shown that confocal laser scanning microscopy can be used to observe cells immobilized in porous gelatin microcarriers through serial optical sectioning.

Although methylene blue is used as a standard indicator of cell viability in the brewing industry the method has many shortcomings (Mochaba et al., 1998). It measures whether a yeast population is viable or non-viable based on the ability of viable cells to oxidize the dye to its colourless form. Non-viable cells lack the ability to oxidize the stain and therefore remain blue (O'Connor-Cox et al., 1997). Plate count and slide culture techniques are based on the ability of the cells to grow and produce macrocolonies on agar plates or microcolonies on media covered microscope slides (Technical Committee and Editorial Committee of the ASBC, 1992). Ongoing work of examining the viability of yeast in immobilized matrices over extended periods of time at Labatt now uses, not only methylene blue, but also the aforementioned methods as well as developing the confocal microscopy technique using vital staining. In addition to measuring the viability of the cells, the issue of "vitality" of the immobilized cells must also be addressed in future work. Where viability has been used to describe the ability of cells to grow and reproduce, vitality measures yeast fermentation performance, activity, or the ability of the yeast to recover from stress (Smart et al., 1999).

CHAPTER 7. FLAVOUR PRODUCTION IN A GAS-LIFT CONTINUOUS BEER FERMENTATION SYSTEM

7.1 Experimental Procedure

Using continuous fermentation to produce beer is very different from other applications using immobilized cells because the resulting product is not measured in terms of one component of interest such as ethanol. Rather, it is a balance of numerous chemical compounds which must be balanced to make a quality finished product. The effects of oxygen on yeast flavour metabolites during continuous primary fermentation and during a secondary batch holding period were examined. The effect of residence time on flavour metabolites was also examined at two levels. Lastly, a commercial enzyme preparation of alpha-acetolactate decarboxylase was added to the continuous fermentation wort supply and liquid phase total diacetyl concentration was monitored.

7.1.1 Effect of Relative Amounts of Air in the Bioreactor Fluidizing Gas on Yeast Metabolites during Primary Continuous Fermentation

The amount of air and hence oxygen in the bioreactor fluidizing gas was varied while residence time, temperature and all other controllable process variables were held constant. The total volumetric flow rate of gas was held constant at 472 mL/min at STP, temperature was 15°C, and kappa-carrageenan gel beads containing immobilized LCC 3021 yeast were used throughout the trial with an initial cell loading of 1×10^8 cells/mL of gel. Four different volumetric flow rates of air were imposed on the system throughout the trial (Table 7.1), and the average bioreactor residence time, R_t , was 1.18 days.

Table 7.1. Air volumetric flow rates supplied to the bioreactor through the sparger during continuous fermentation. The total volumetric flow rate supplied to the bioreactor was 472 mL/min at STP, with carbon dioxide making up the remainder of the gas.

Air Volumetric Flow Rate (mL/min)	Percent Air in the Fluidizing Gas (% v/v)	Start (Day)	Finish (Day)	Total Time (Days)
94	19.9	10	26	17
354	75.0	27	40	14
34	7.2	41	58	18
0	0	59	66	8

The following analyses were performed repeatedly throughout the experiment: free amino nitrogen (FAN), total fermentable carbohydrate (as glucose), ethanol, total diacetyl, beer volatiles (selected esters and alcohols), and liquid phase yeast cell concentration and viability. The bioreactor was also tested for contamination a minimum of once a week.

The dissolved oxygen concentration in the bulk liquid phase of the bioreactor was measured when the continuous fermentation was assumed to be at pseudo-steady state for each volumetric flow rate of air (minimum of three reactor turn-over times).

7.1.2 Post Fermentation Batch Holding Period: Effects of Oxygen Exposure on Yeast Metabolites

Even when the amount of oxygen in the bioreactor fluidizing gas was relatively low (34 mL/min at STP), the concentrations of acetaldehyde and total diacetyl found during the experiment conducted in section 7.1.2, were unacceptable high for the North American lager beer market. Therefore a novel approach was taken, where liquid taken from the continuous primary bioreactor was held in batch for 48 hours at a slightly elevated temperature of 21°C to reduce the concentration of these two compounds. As well, the results from the previous section 7.1.2 indicated the significant effect that the amount of air in the fluidizing gas had on the flavour compounds measured. Therefore the effect on yeast flavour metabolites of aerobic versus anaerobic conditions downstream of the primary fermentation, where the secondary batch hold occurred, was examined.

Continuous primary fermentation was performed in a 50 L gas lift bioreactor using a highly flocculent variant of the LCC3021 yeast strain for this trial because the sample volume requirement for the study was too large relative to the volume of the 8 L bioreactor. Operating conditions were 1180 mL/min CO₂ and 189 mL/min air at STP in the fluidizing gas, an average bioreactor residence time, R_t , of 1.0 day, a temperature of 15 °C, and high-gravity 17.5°P lager brewer's wort.

A total of 4 samples were taken (100 mL crimp vials), with two handled under anaerobic conditions and the other two were exposed to the aerobic environment.

The anaerobic sampling procedure was as follows: two 100 mL crimp vials and six 25 mL crimp vials were autoclaved and then placed in an anaerobic box (Labmaster 100, mbraun, USA) with argon as the purging gas. The 100 mL vials were allowed to equilibrate for 45 minutes and then they were sealed using aluminum caps and Teflon[®] septa. A 50 mL syringe, fitted with a 3 inch, 16 gauge needle, sanitized using a 70% (v/v) ethanol solution, was used to withdraw sample from the bioreactor by puncturing the septum of the membrane of the sample valve and the sample was injected into the 100 mL pre-purged anaerobic vials. It was necessary to provide a vent to the crimp vial, through an additional sterile syringe needle, to allow release of the pressure within the vial during filling. The aerobic samples were exposed to the atmosphere as they were drained from the bioreactor by fully opening the membrane sample valve into the 100 mL unsealed sample vials, without using a syringe and needle.

The sample liquid was allowed to rest at room temperature for 2 hours in order to allow the yeast to settle out of solution, leaving a cell concentration in the bulk liquid of approximately 10^6 cells/mL. Once settled, the liquid from each 100 mL vial was decanted into three 25 mL vials. The anaerobic samples were handled in an anaerobic box in order to minimize oxygen pickup while the aerobic samples were processed under the laminar flow hood. Each of the samples in the 100 mL vials were split into 3 smaller 25 mL vials, so that sample analyses could be performed without altering the course of the fermentation due to sample removal. Once the aerobic samples were transferred to the smaller vials they were incubated, uncapped at 21°C. The anaerobic samples were transferred to the three smaller vials and sealed using an aluminum cap and Teflon[®] septa. In order to avoid pressure buildup due to carbon dioxide evolution within the vials, while preventing exposure of the samples to the aerobic external environment, the septa were punctured with a needle. The end of the needle exposed to the external environment was submerged in ethanol (less than 1 cm of pressure head), preventing any back-flow of air into the sample. Samples were collected for analysis at 2, 24, and 48 hours. A sample was also taken directly from the bioreactor and analyzed immediately in order to assess the state of the fermentation within the bioreactor at the time of the protocol. The samples were analyzed for total fermentable carbohydrate (as glucose), ethanol, total diacetyl, and beer volatiles (selected esters and alcohols).

7.1.3 Effect of Liquid Residence Time on Yeast Metabolites during Continuous Primary Beer Fermentation

In order to examine the effect of liquid residence time on yeast metabolic activity, an experiment was performed in which a step change in wort volumetric flow rate to the bioreactor was imposed during continuous primary beer fermentation using LCC3021 yeast cells immobilized in kappa-carrageenan gel beads. The bioreactor temperature was held constant at 17°C throughout the trial. The gas volumetric flow rate supplied to the bioreactor was also constant at 472 mL/min at STP. The gas was a mixture of air (11 mL/min at STP) and carbon dioxide (461 mL/min at STP). The initial concentration of yeast cells in the kappa-carrageenan gel was 2.6×10^7 cells/mL of gel bead and the bioreactor contained 40% (v/v) of beads.

The following analyses were performed repeatedly throughout the trial: carbohydrates, free amino nitrogen (FAN), total fermentable carbohydrate (as glucose), ethanol, total diacetyl, beer volatiles (selected esters and alcohols), and liquid phase yeast cell concentration and viability. The bioreactor was also tested for contamination, a minimum of once a week.

7.1.4 Using a Commercial Preparation of Alpha-Acetolactate Decarboxylase to Reduce Total Diacetyl during Continuous Primary Beer Fermentation

High diacetyl concentrations are considered by most North American brewers to be an undesirable flavour defect in their beer. In the continuous primary fermentations performed to date, total diacetyl concentrations have consistently been above the threshold levels for traditional batch fermentations (70 – 150 µg/L) in a North American lager. During batch fermentation, diacetyl is reduced during the later stages of fermentation, when oxygen is no longer present and additional sugars are not being introduced. In the continuous fermentation system a constant low level of oxygen is supplied to the bioreactor through a sparger, and fresh wort is continuously supplied to the bioreactor. Therefore, a novel strategy using a commercial enzyme preparation was explored to control diacetyl concentration in the continuous bioreactor.

In a wort fermentation diacetyl is formed when alpha-acetolactate, an intermediate in the synthesis of valine, is oxidatively decarboxylated outside the yeast

cell. The yeast cell then reabsorbs diacetyl and converts it into the less flavour-active acetoin. This oxidative decarboxylation of alpha-acetolactate to diacetyl is rate-limiting in batch wort fermentations. During the continuous fermentations, total diacetyl exited the bioreactor at unacceptably high concentrations (300-400 $\mu\text{g/L}$). The commercial enzyme alpha-acetolactate decarboxylase (ALDC), from Novo-Nordisk A/S can convert alpha-acetolactate directly into acetoin, thus avoiding the unwanted diacetyl intermediate (Figure 7.1) (Jepsen, 1993).

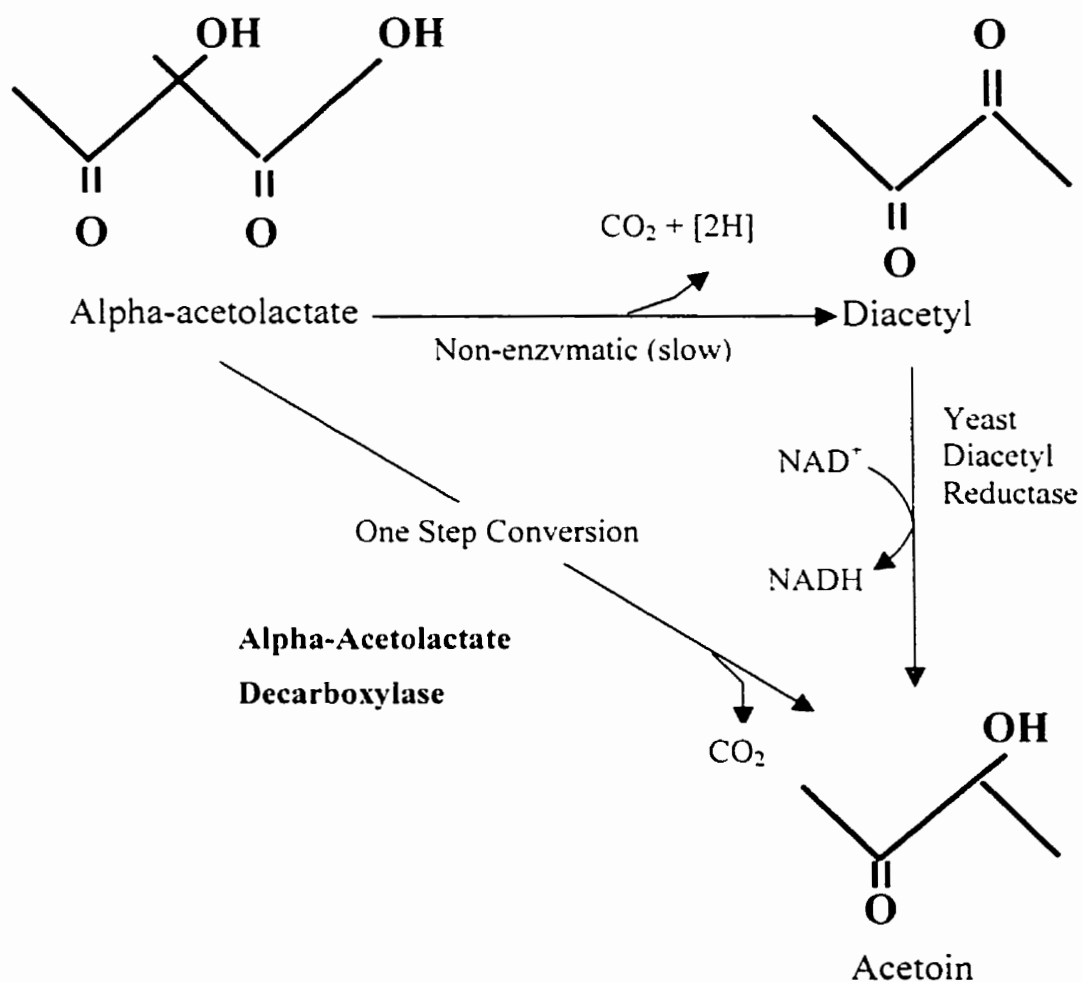


Figure 7.1 The action of alpha-acetolactate decarboxylase (ALDC).

Alpha-acetolactate decarboxylase was added to the wort fed into the bioreactor in order to examine its net effect on total diacetyl concentration. Other strategies for reducing diacetyl, including a batch warm hold period of 48 hours post-fermentation and immobilized secondary fermentation systems, technology from Alpha-Laval (Anon, 1997), were also explored. Both of these other strategies have shown success in reducing diacetyl levels post fermentation, but neither addresses the level of diacetyl at the source (i.e. at the bioreactor outlet). By using ALDC in the wort to reduce the diacetyl concentration coming out of the bioreactor, the post-fermentation treatment periods could be minimized or eliminated.

ALDC activity is optimal at pH 6.0 in lager wort at 10°C. At pH 5.0, typical of industrial worts, ALDC activity is maximized at a temperature of 35°C (Anon, 1994). Thus under typical beer fermentation conditions of reduced temperature and pH, ALDC activity is less than optimal.

Health Canada in 1997 amended Canada's Food and Drug Regulations (SOR/97-81) to allow the use of ALDC in alcoholic beverages, which has opened the door for its use in Canadian breweries. *Bacillus subtilis*, carrying the gene coding for ALDC (E.C. 4.1.1.5) from *Bacillus brevis*, produces the enzyme ALDC. Because ALDC is an enzyme that is produced by a genetically modified organism (GMO), there are public perception issues that would need to be addressed before using such an enzyme in a commercial product.

Lager yeast, LCC3021, was used for these experiments. High gravity, 17.5°P, lager brewer's wort was supplied by the Labatt London brewery. Ethanol, total fermentable carbohydrate (as glucose), total diacetyl, and liquid phase cell concentration were monitored. Yeast cells were immobilized in kappa-carrageenan gel beads as described in the Chapter 4. The bioreactor was allowed three turnover times, before it was assumed to have reached pseudo-steady state. As mentioned earlier, the diacetyl method used in this work is referred to as "total diacetyl" because the method measures the amount of diacetyl and its precursor, alpha-acetolactate. Thus an observed reduction in total diacetyl during this experiment would be due to the combined effect of the enzyme converting alpha-acetolactate directly into acetoin and the subsequent lowered concentration of its derivative, diacetyl.

Alpha-acetolactate decarboxylase (ALDC) was supplied as a generous gift for laboratory purposes from Novo Nordisk A/S, Denmark as Maturex[®] L. The activity of the enzyme was 1500 ADU/g, where ADU is the amount of enzyme which under standard conditions, by decarboxylation of alpha-acetolactate, produces 1 μ mole of acetoin per minute as described in Novo Nordisk Method AF27 (Anon. 1994).

Continuous Fermentation Conditions: Continuous fermentations were performed in the 8 L gas lift draft tube bioreactor pitched at 40% (v/v) with kappa-carrageenan gel beads containing immobilized lager yeast cells. The bioreactor was sparged with a mixture of carbon dioxide (438 mL/min at STP) and air (34 mL/min at STP). Fermentation temperature was controlled at 15°C throughout the trials and the bioreactor residence time, R_t , was 1.5 days. Total diacetyl concentration was monitored under these conditions and an average pseudo-steady state control diacetyl concentration was reached. ALDC was then added to the wort at a concentration of 72 μ g/L (108 ADU/L) and total diacetyl concentration in the bioreactor was monitored for a response.

Experiment 1: Wort was collected from the brewhouse into a 20 L stainless steel vessel, and heated in an autoclave for 45 minutes at 100°C. The wort was held at 2°C in a controlled temperature water bath while feeding the bioreactor. Once a pseudo-steady state total diacetyl concentration had been reached within the bioreactor, 72 μ g/L (108 ADU/L) of ALDC was added to the wort inside the 20 L vessel. The initial biomass loading in the kappa-carrageenan gel beads was 3×10^7 cells/mL of gel.

Experiment 2: In order to minimize the risk of contamination, the system was closed loop at the outlet and other upgrades were also made to the system as described in Chapter 4. As with Experiment 1, wort was collected from the brewhouse into a 20 L stainless steel vessel, and autoclaved for 45 minutes at 100°C. While feeding the bioreactor, the wort was held at 2°C in a controlled temperature water bath. The initial biomass loading in the kappa-carrageenan gel beads was 3×10^7 cells/mL of gel. Once a pseudo-steady state total diacetyl concentration had been reached within the bioreactor, 72 μ g/L (108 ADU/L) of ALDC was added to the wort inside the 20 L vessel.

Experiment 3: Unoxygenated 17.5°P brewery wort (14 hL) was collected into a large wort storage vessel (T-1) in the Pilot Plant. It was then flash pasteurized and stored with carbon dioxide sparging in order to maintain a constant dissolved oxygen

concentration of <0.10 mg/L, as described in Chapter 5. The wort was fed into the bioreactor from this tank until a pseudo-steady state total diacetyl concentration was reached. ALDC (72 $\mu\text{g/L}$) was then aseptically added to the wort for the remainder of the trial. The addition of ALDC was accomplished by measuring the amount of wort remaining in the storage vessel and calculating the amount of ALDC needed to bring the concentration of enzyme up to the target concentration of 72 $\mu\text{g/L}$ (108 ADU/L). The appropriate amount of enzyme was then dissolved in 10 L of sterile wort. This solution was transferred to a 20 L stainless steel pressure vessel, which was connected via sterile tubing to the sample port on the wort holding vessel (T-1). The ALDC solution was then pushed using sterile carbon dioxide pressure into the wort holding vessel. In order to ensure that the ALDC solution was adequately mixed with the wort in the holding vessel, the flow rate of carbon dioxide sparged into the tank was increased to 4720 mL/min at STP for 1 hour and then returned to its normal flow rate. The storage tank then held enough ALDC dosed wort to complete the trial. The initial biomass loading in the kappa-carrageenan gel beads was 10^8 cells/mL of gel.

7.2 Results and Discussion

7.2.1 Effect of Relative Amounts of Air in the Bioreactor Fluidizing Gas on Yeast Metabolites during Primary Continuous Fermentation

In Figures 7.2 - 7.11 liquid phase yeast viability and cell concentration, free amino nitrogen (FAN), total fermentable carbohydrate (as glucose), ethanol, total diacetyl, acetaldehyde, ethyl acetate, 1-propanol, isobutanol, isoamyl acetate, isoamyl alcohol, ethyl hexanoate, and ethyl octanoate concentrations are plotted versus continuous fermentation time. All bioreactor operating conditions were held constant throughout the protocol except the percentage of air in the bioreactor sparging gas, which is marked directly on the figures. In Table 7.2 the averages for each analyte at pseudo-steady state (after a minimum of three reactor turnover times) are summarized.

Table 7.2. Summary table of effect of air volumetric flow rate to the bioreactor through the sparger on liquid phase yeast and key yeast metabolite concentrations in the bioreactor at a residence time, R_t , of 1.18 days, averages at pseudo-steady state.

Average* Analyte Concentration	Air Volumetric Flow Rate (mL/min)		
	94	354	34
Cell Conc (cells/mL)	3.87E+08	2.98E+08	4.73E+08
Total Ferm. Glucose (g/100 mL)	1.36	1.25	2.07
FAN (mg/L)	196.9	171.7	162.8
Ethanol (g/100 mL)	6.14	5.46	5.74
Total diacetyl (ug/L)	346	1417	389
Acetaldehyde (mg/L)	75.62	329.48	28.63
Ethyl Acetate (mg/L)	22.38	21.13	18.01
1-Propanol (mg/L)	44.74	50.89	53.04
Isobutanol (mg/L)	8.73	16.09	8.05
Isoamyl Acetate (mg/L)	0.38	0.21	0.30
Isoamyl Alcohol (mg/L)	58.62	61.64	59.16
Ethyl Hexanoate (mg/L)	0.060	0.030	0.053
Ethyl Octanoate (mg/L)	0.031	0.013	0.025

*average of final four days of each operating condition

Figures 7.2 and 7.3 show that the liquid phase yeast population did not reach zero during this experiment. The flavour compounds that were studied in this work were produced by a combination of free and immobilized yeast cells and the relative contributions from each source were not determined. There was more than one source of freely suspended yeast cells in this work: biomass growth and cells that were released from the gel beads into the bulk liquid medium. Research has shown with compound models of cell release and growth, that when cells are being released from biofilms, even if the bioreactor is operated high dilution rates, there will still be a population of cells in the output liquid (Karamanev, 1991).

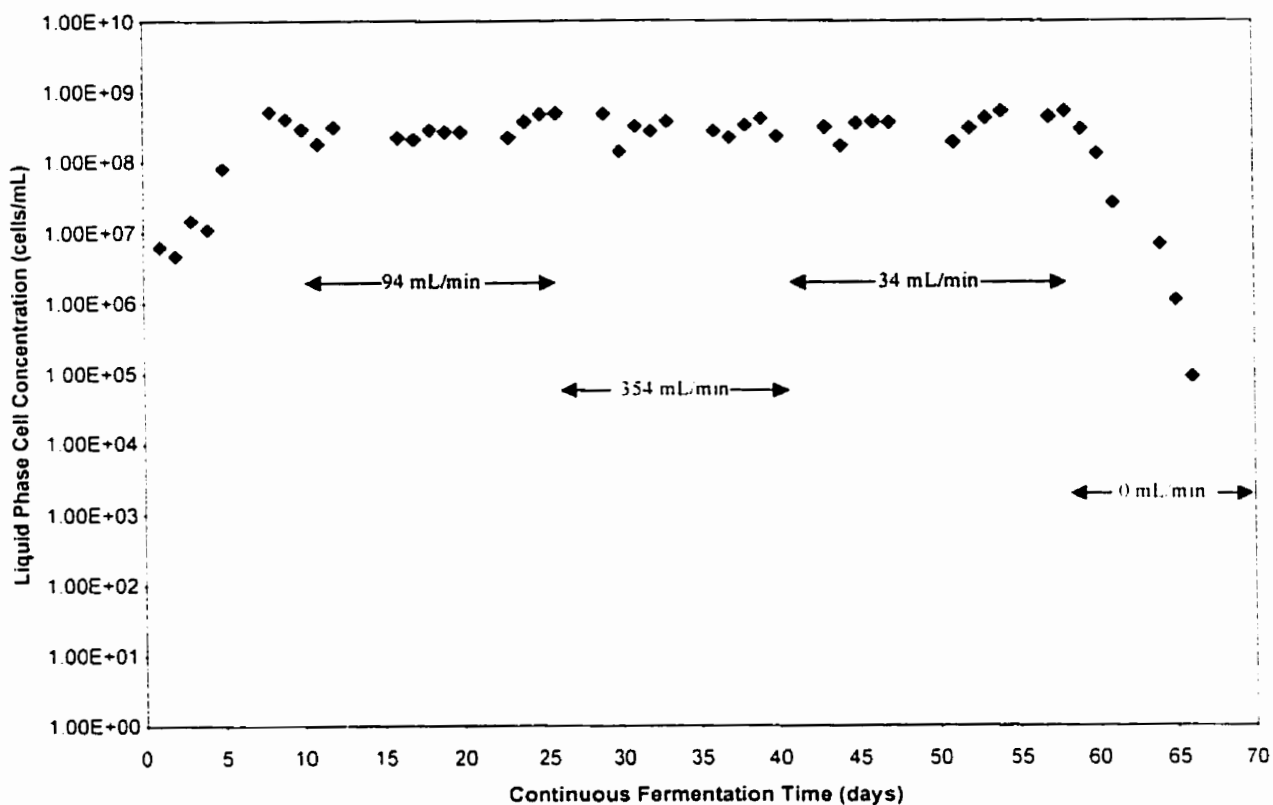


Figure 7.2. Liquid phase yeast cell concentration versus relative continuous fermentation time. The volumetric flow rate of air at STP supplied to the bioreactor through the sparger is indicated on the graph. The remainder of the gas was carbon dioxide and the total volumetric gas flow rate was constant at 472 mL/min at STP throughout the experiment.

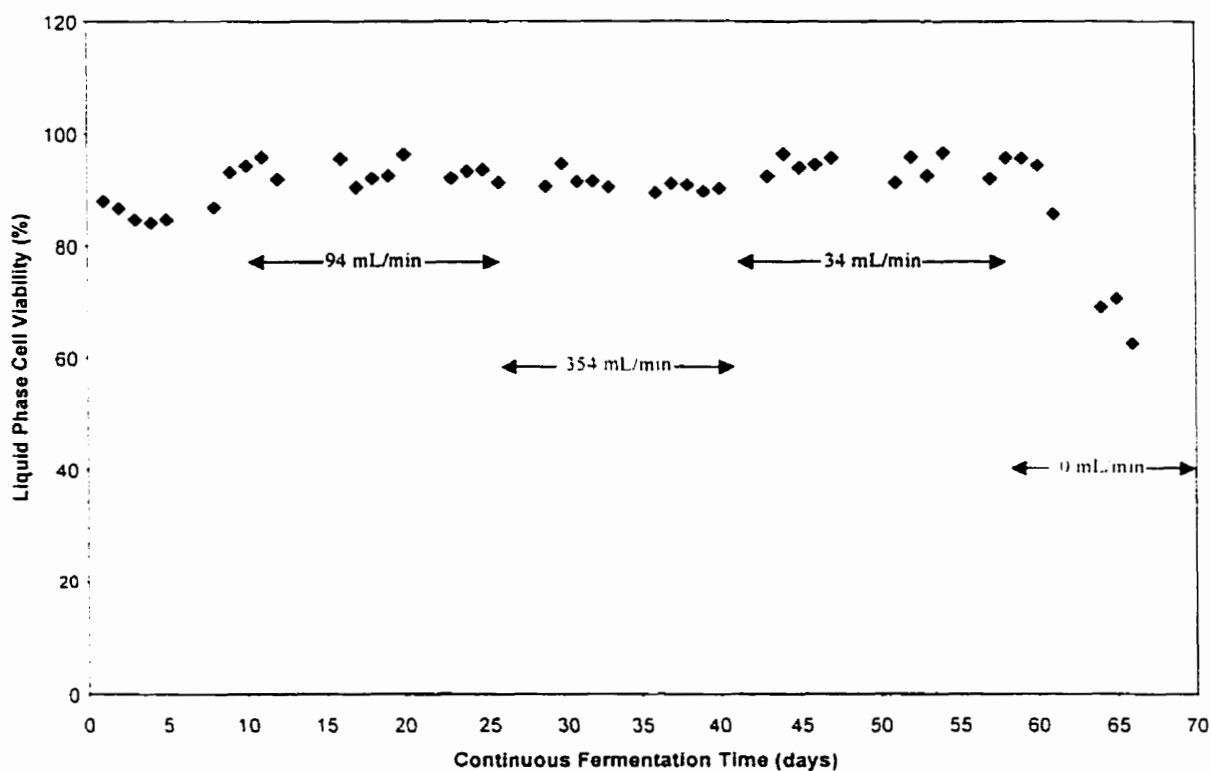


Figure 7.3. Liquid phase yeast viability versus relative continuous fermentation time. The volumetric flow rate of air at STP supplied to the bioreactor through the sparger is indicated on the graph. The remainder of the gas was carbon dioxide and the total volumetric gas flow rate was constant at 472 mL/min at STP throughout the experiment.

In Figure 7.4 the liquid phase concentration of free amino nitrogen (FAN) was tracked. It was interesting to note that the minimum FAN concentrations occurred at 34 mL/min at STP of air. This did not coincide with maximum ethanol concentration or minimum total fermentable carbohydrate (as glucose) concentrations.

The ethanol concentration within the bioreactor liquid phase decreased, while total fermentable carbohydrate (as glucose) increased when the volumetric flow rate of air in the sparge gas was increased from 94 to 354 mL/min, as seen in Figure 7.5. This may indicate that more cell respiration, as opposed to fermentation, was occurring due to the increase in oxygen availability. When the volumetric flow rate was again reduced from 354 mL/min down to 34 mL/min at STP, the ethanol concentration again increased, however it did not reach the concentration seen when the flow rate was at 94 mL/min at

STP. It is difficult to compare in precise terms the concentrations of ethanol at 34 mL/min with those at 94 mL/min at STP, because there have been other factors influencing the system, resulting from cell aging, effects of the continuous exposure to relatively high amount of oxygen for the time at 354 mL/min at STP, and changes in the immobilized cell population. In Figure 2.4, White and Portno (1978) noted changes in yeast flavour metabolite concentrations with continuous fermentation time in their tower fermenter.

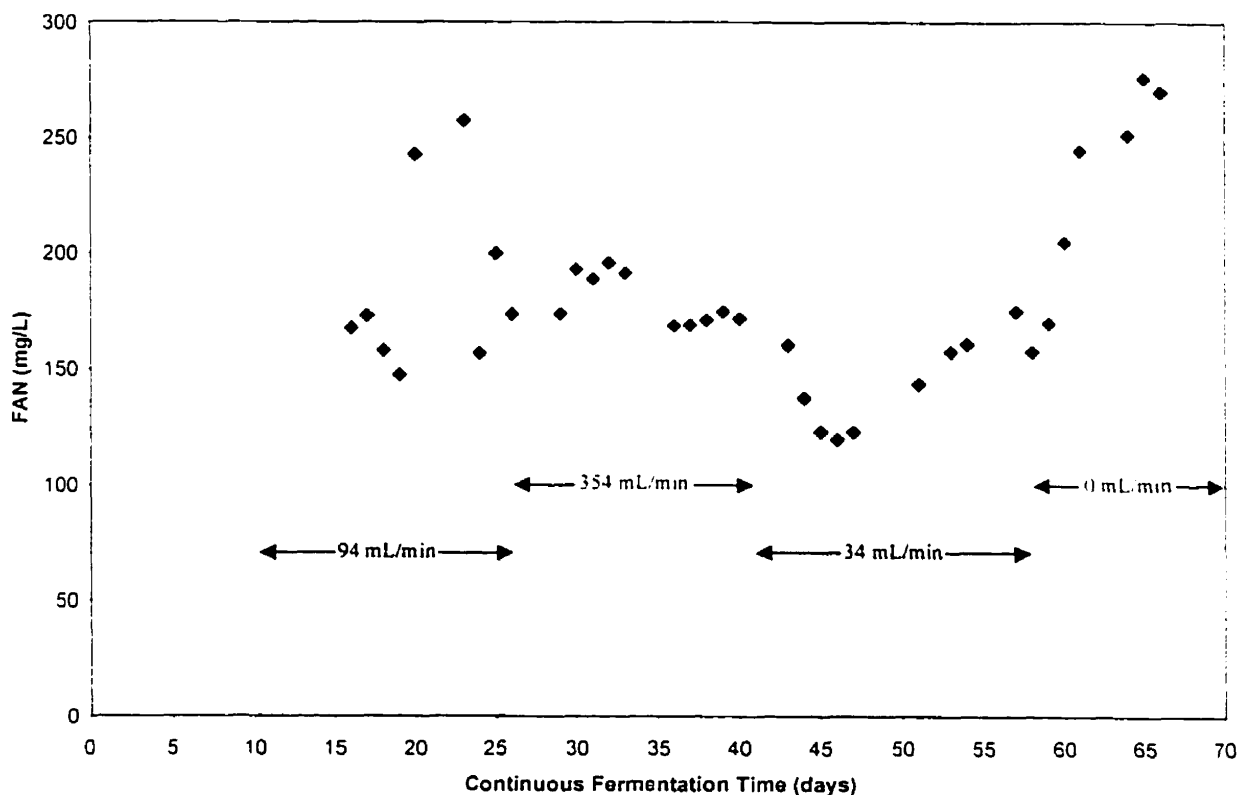


Figure 7.4. Free amino nitrogen concentration remaining in wort versus relative continuous fermentation time. The volumetric flow rate of air at STP through the sparger is indicated on the graph. The remainder of the gas was carbon dioxide and the total volumetric gas flow rate was constant at 472 mL/min at STP throughout the experiment.

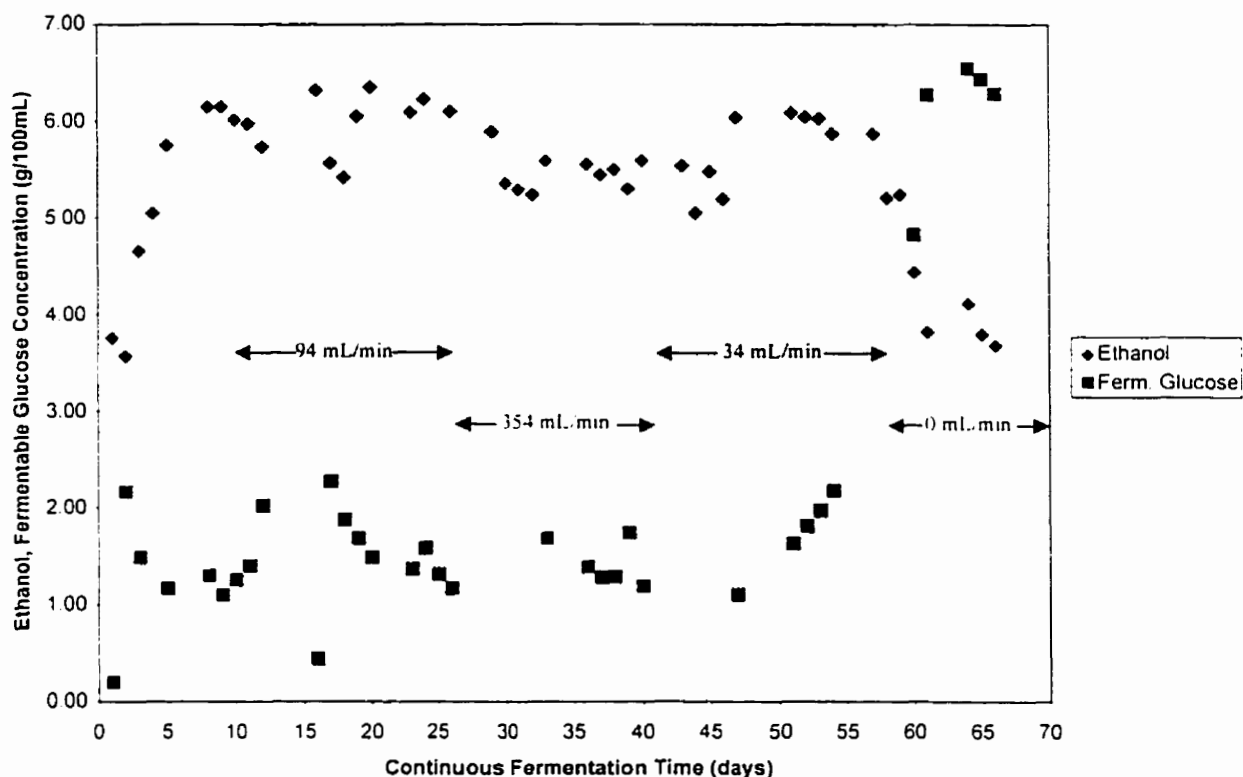


Figure 7.5. Liquid phase ethanol and total fermentable carbohydrate (as glucose) concentration versus relative continuous fermentation time. The volumetric flow rate of air at STP supplied to the bioreactor through the sparger is indicated on the graph. The remainder of the gas was carbon dioxide and the total volumetric gas flow rate was constant at 472 mL/min at STP throughout the experiment.

In Figure 7.6, the pronounced effect of oxygen on the production of total diacetyl is seen. Since diacetyl is generally considered an undesirable flavour compound in beer, one of the main reasons to optimize the amount of oxygen in the bioreactor is to control levels of this flavour compound. After the 354 mL/min air phase, the flow rate was dropped to 34 mL/min at STP and total diacetyl decreased. During batch fermentation, it is known that increased oxygen leads to an increase in the formation of alpha-acetolactate, the precursor of diacetyl (Kunze, 1996).

In Figure 7.7 a clear relationship between the amount of air in the sparge gas and acetaldehyde concentration, arose. As the percent of air in the sparge gas increased, the amount of acetaldehyde also increased. Acetaldehyde imparts a green-apple character to beer, and is normally present in commercial beer at levels of less than 20 mg/L.

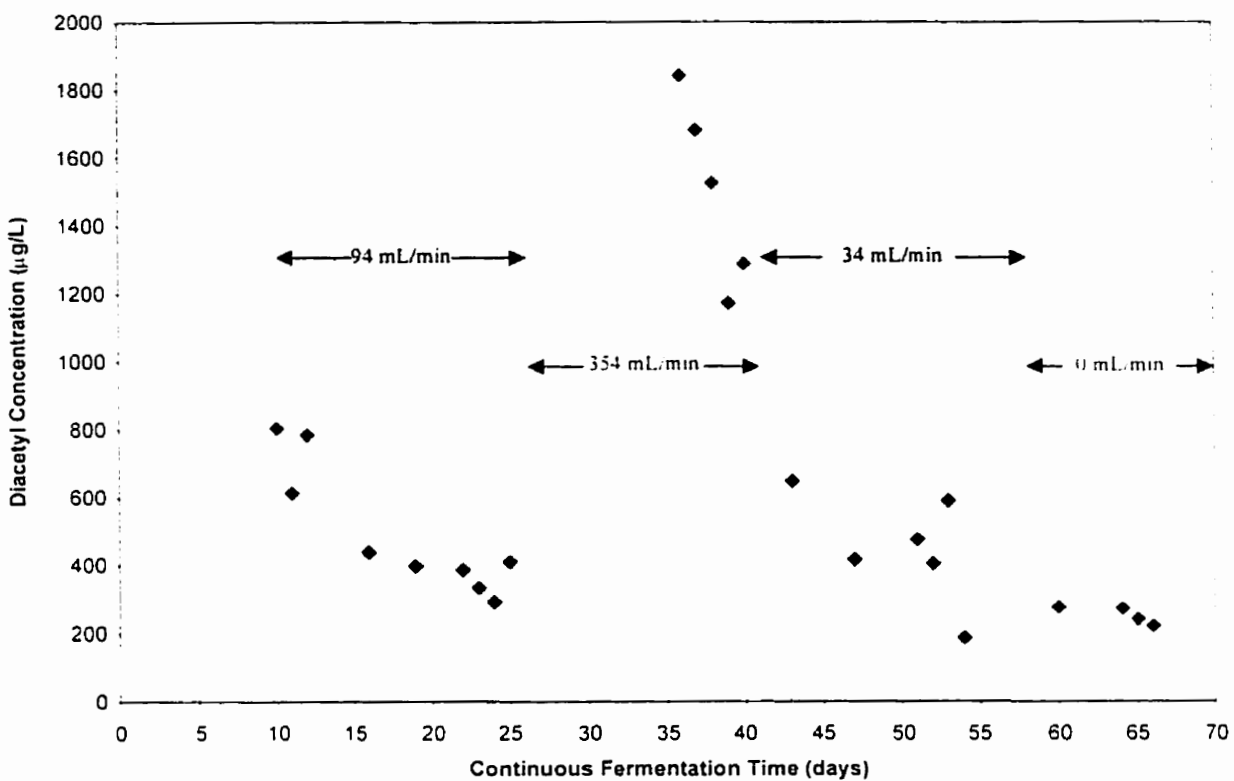


Figure 7.6. Liquid phase total diacetyl concentration versus relative continuous fermentation time. The volumetric flow rate of air at STP supplied to the bioreactor through the sparger is indicated on the graph. The remainder of the gas was carbon dioxide and the total volumetric gas flow rate was constant at 472 mL/min at STP throughout the experiment

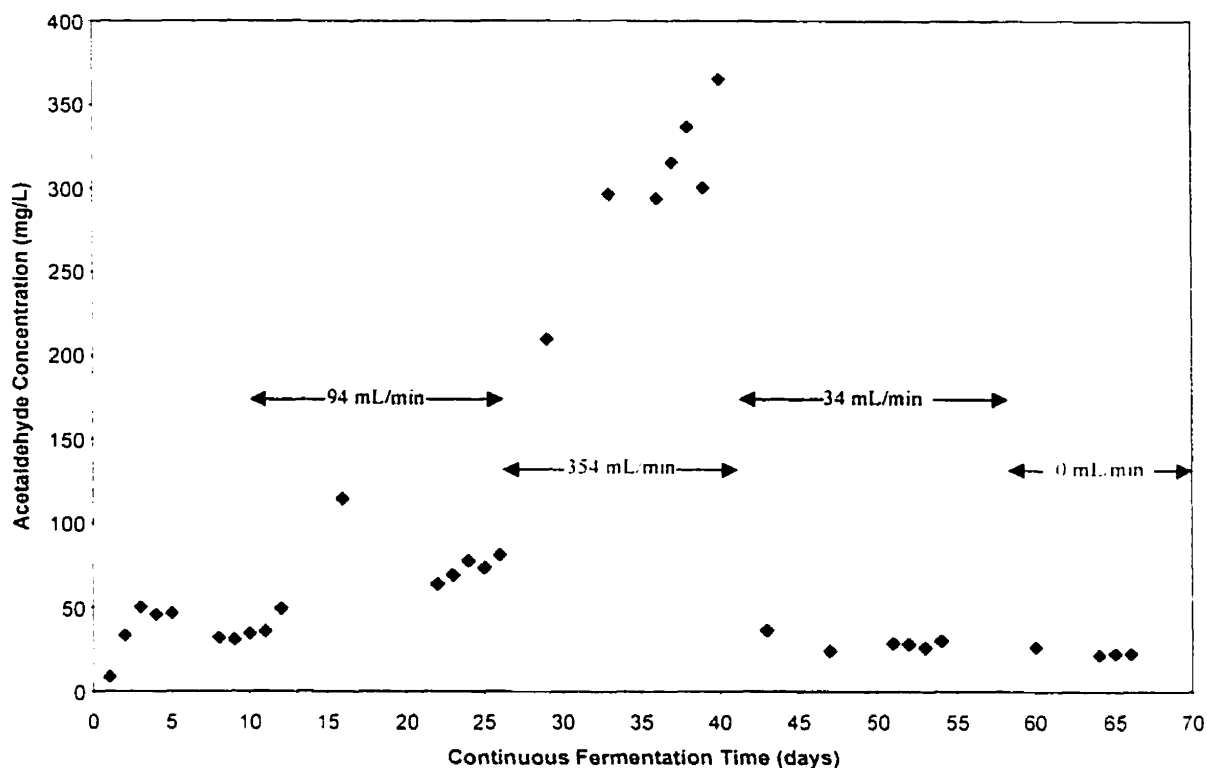


Figure 7.7. Liquid phase acetaldehyde concentration versus relative continuous fermentation time. The volumetric flow rate of air at STP supplied to the bioreactor through the sparger is indicated on the graph. The remainder of the gas was carbon dioxide and the total volumetric gas flow rate was constant at 472 mL/min at STP throughout the experiment.

In Table 7.2 and Figures 7.8 - 7.9 the pseudo-steady state concentrations of ethyl acetate, isoamyl acetate, ethyl hexanoate, and ethyl octanoate are given versus continuous fermentation time. For all the esters measured, the step change in aeration rate from 94 to 354 mL/min at STP resulted in a decrease in concentration. When the aeration rate was decreased from 354 mL/min down to 34 mL/min at STP, the concentration of isoamyl acetate, ethyl hexanoate, and ethyl octanoate increased. However they did not increase to the values seen at the 94 mL/min aeration rate. The pattern of response of these compounds closely matched one another, with ethyl hexanoate and ethyl octanoate showing more relative fluctuations than isoamyl acetate. The concentration of ethyl acetate actually further decreased when the volumetric flow rate of air was reduced to 34

mL/min at STP. For all the esters measured in this study, the concentration showed an increase when the air was completely eliminated from the fluidizing gas. The concentration of each ester rose and then tapered off, as the liquid phase cell concentration decreased rapidly in the bioreactor.

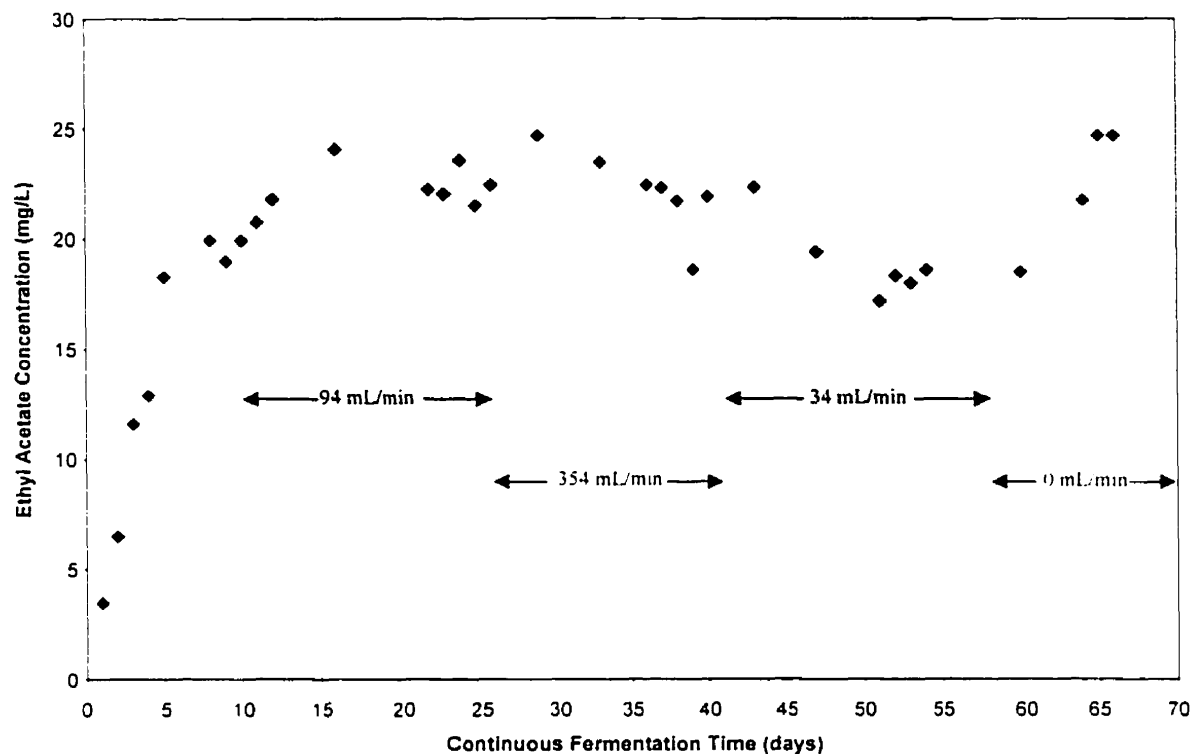


Figure 7.8. Ethyl acetate concentration versus relative continuous fermentation time. The volumetric flow rate of air at STP supplied to the bioreactor through the sparger is indicated on the graph. The remainder of the gas was carbon dioxide and the total volumetric gas flow rate was constant at 472 mL/min at STP throughout the experiment.

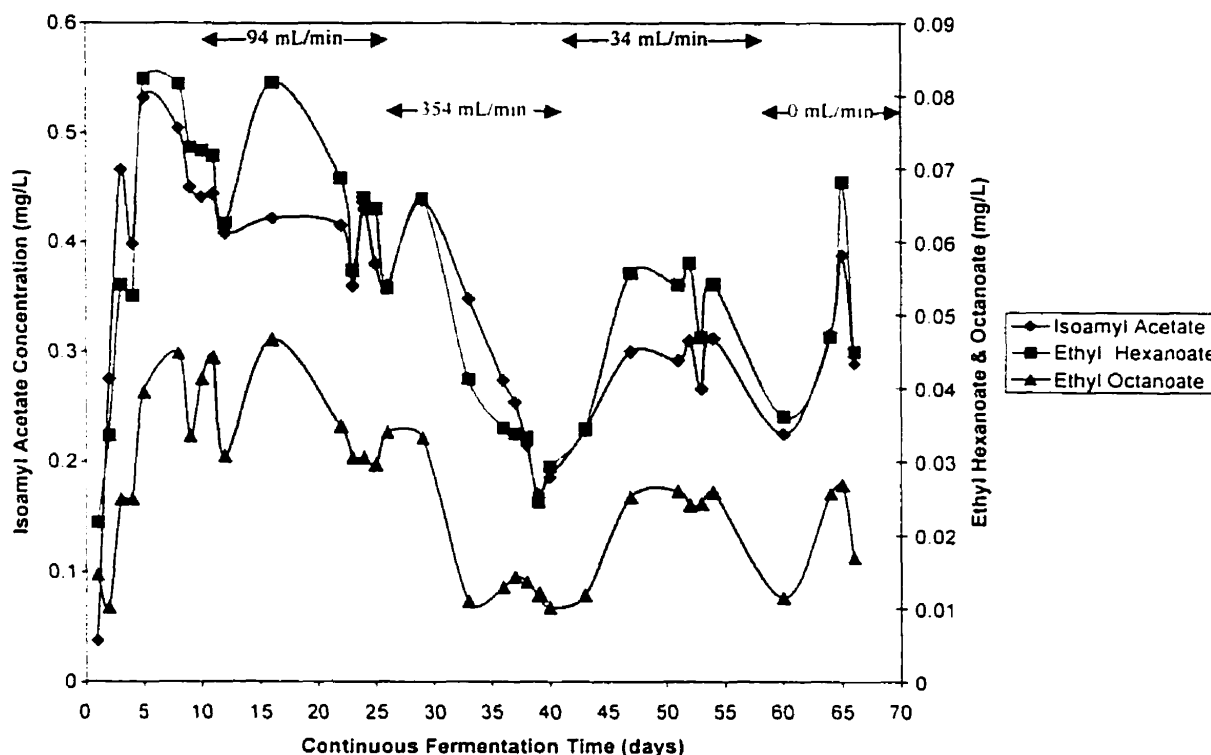


Figure 7.9. Liquid phase isoamyl acetate, ethyl hexanoate and ethyl octanoate concentration versus relative continuous fermentation time. The volumetric flow rate of air at STP supplied to the bioreactor through the sparger is indicated on the graph. The remainder of the gas was carbon dioxide and the total volumetric gas flow rate was constant at 472 mL/min at STP throughout the experiment.

The higher alcohols isoamyl alcohol, isobutanol, and 1-propanol versus continuous fermentation time are given in Figures 7.10 and 7.11. For the alcohols measured, the concentration increased as a result of the step change increase in aeration from 94 to 354 mL/min at STP. Isobutanol showed the largest relative fluctuations when aeration rate was changed. The 1-propanol concentrations were well below the flavour threshold values of 600 – 800 mg/L, however, throughout the continuous fermentation experiment, the concentration was well above that found in typical commercial batch-produced beers, where concentrations are usually below 16 mg/L. This was not the case for isoamyl alcohol or isobutanol, which were within normal ranges. The compound 1-propanol is thought to arise from the reduction of the acid propionate (Gee and Ramirez, 1994). Others (Hough et al., 1982; Yamauchi et al., 1995) have also related the formation of 1-propanol to the metabolism of the amino acids α -aminobutyric acid and threonine.

with the corresponding oxo-acid and aldehyde being α -oxobutyric acid and propionaldehyde, respectively.

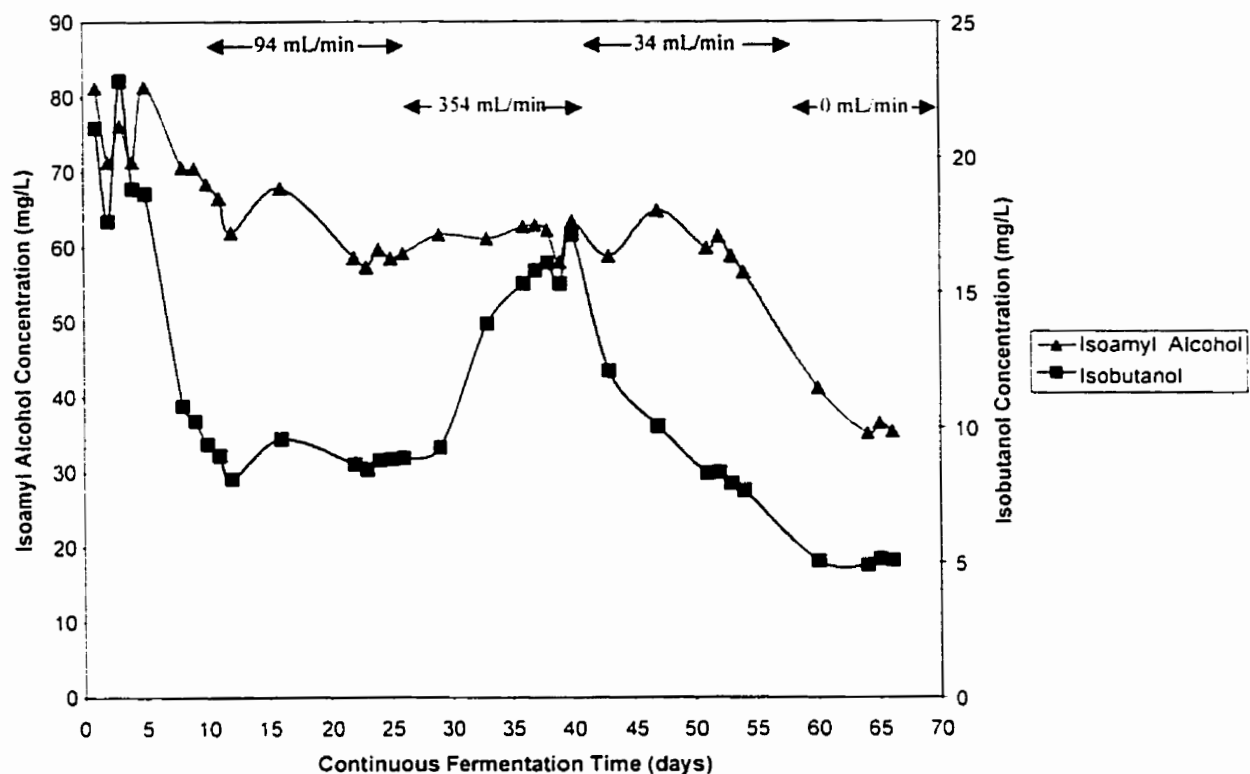


Figure 7.10. Liquid phase isoamyl alcohol and isobutanol concentration versus relative continuous fermentation time. The volumetric flow rate of air at STP supplied to the bioreactor through the sparger is indicated on the graph. The remainder of the gas was carbon dioxide and the total volumetric gas flow rate was constant at 472 mL/min at STP throughout the experiment.

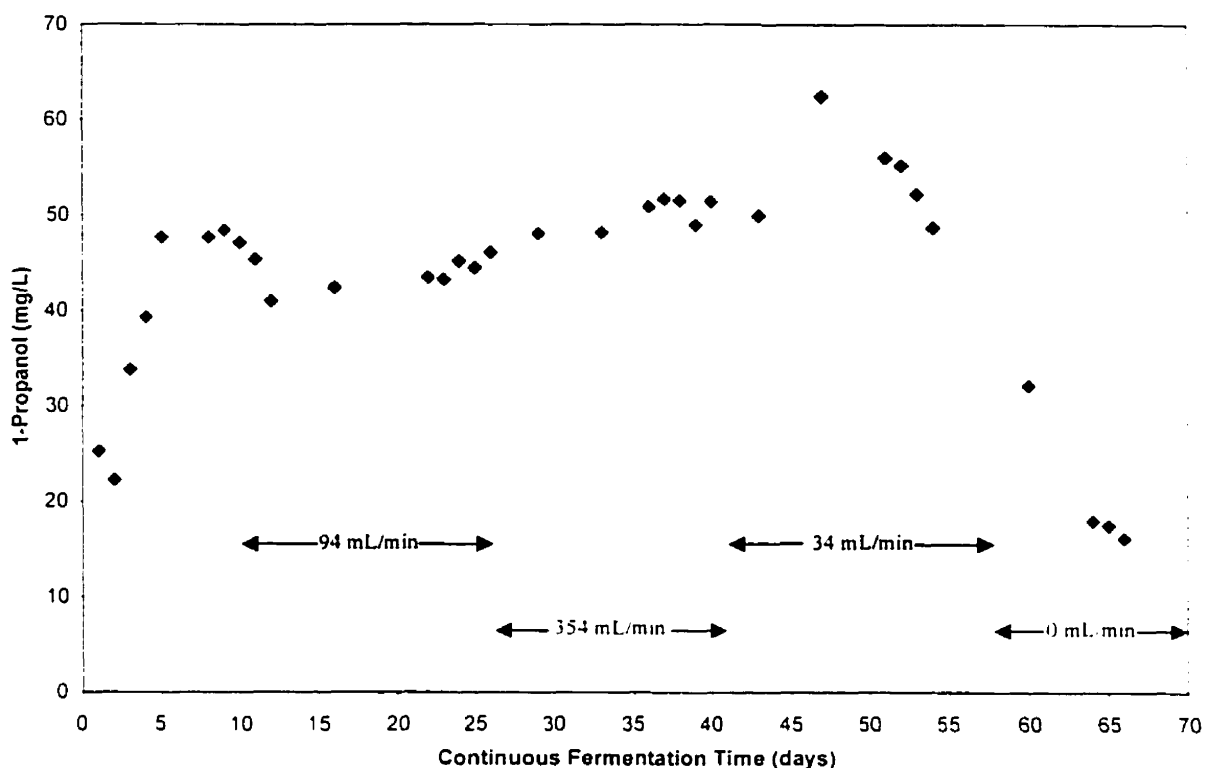


Figure 7.11. Liquid phase 1-propanol concentration versus relative continuous fermentation time. The volumetric flow rate air at STP supplied to the bioreactor through the sparger is indicated on the graph. The remainder of the gas was carbon dioxide and the total volumetric gas flow rate was constant at 472 mL/min at STP throughout the experiment.

Because excess diacetyl, acetaldehyde and fusel alcohols are undesirable in beer, oxygen control to limit their production is important. As discussed in the literature review, when the supply of oxygen to the yeast cells is increased, there is enhanced anabolic formation of amino acid precursors and thus an overflow of higher alcohols, oxo-acids, and diacetyl. The concentration of esters is known to decrease with an increase in oxygen availability because ester formation is catalysed by acetyl transferase. Acetyl transferase is inhibited by unsaturated fatty acids and ergosterol, which in turn will increase in the presence of oxygen (Norton and D'Amore, 1994).

For the bioreactor conditions used in this experiment, the pseudo-steady-state (after a minimum of three reactor turnover times) dissolved oxygen concentrations measured in the liquid phase of the bioreactor were close to zero (less than .03 mg/L).

This experiment did not allow for a direct comparison of the data from the 94 mL/min and 34 mL/min of air at STP in the fluidization gas, because they were separated by the highest air flow rate (354 mL/min). This is because the physiological state of the yeast resulting from the exposure to previous bioreactor conditions, the immobilization matrix and continuous fermentation time may also have caused other changes in flavour production.

No contamination was detected in the bioreactor at any point during this experiment.

In order to balance the requirement of yeast for some oxygen to maintain yeast viability and the need to minimize oxygen to obtain a beer with a desirable flavour profile, other strategies could be explored such as the addition of nutrients such as zinc, magnesium, or providing other exogenous compounds required by the yeast cell to maintain viability. Such additions would allow for a further decrease in the oxygen requirement of the yeast. Another possibility would be to operate at very low oxygen concentrations most of the time, with periodic pulses of oxygen supplied to the yeast on a regular basis to maintain cell viability

7.2.2 Post Fermentation Batch Holding Period: Effects of Oxygen Exposure on Yeast Metabolites

Because total diacetyl was not within normal ranges for a commercial beer at the end of primary fermentation, several approaches were taken to reduce the concentration of this compound to acceptable levels. One such approach was to use a warm holding period immediately following continuous primary fermentation.

In Figures 7.12 – 7.21 liquid phase total fermentable carbohydrate (as glucose), ethanol, total diacetyl, acetaldehyde, ethyl acetate, 1-propanol, isobutanol, isoamyl acetate, isoamyl alcohol, and ethyl hexanoate concentrations are plotted versus post fermentation holding time. Samples collected from the continuous primary fermenter at pseudo-steady state were held under aerobic or anaerobic conditions, as indicated in the legend of each figure.

In Figure 7.12 the concentration of total fermentable carbohydrate (as glucose) declined quickly in the first two hours and then declined at a slower rate during the remainder of the holding period in both the aerobic and anaerobic samples. Possible reasons for this observation were that during the first two hours, more yeast were present prior to decantation, and the concentration of sugars was higher at the start of the holding period. There was not a significant difference in fermentable glucose uptake between the aerobic and anaerobic samples, although some differences were noted initially.

The concentration of ethanol in Figure 7.13 rose quickly at the beginning of the hold period and then the anaerobic and aerobic samples increased in ethanol concentration over time, in an almost parallel fashion. The initial increase in ethanol for the anaerobic sample coincided with the period where the most sugar uptake occurred. At the end of the hold period, ethanol concentration was higher in the anaerobically treated samples.

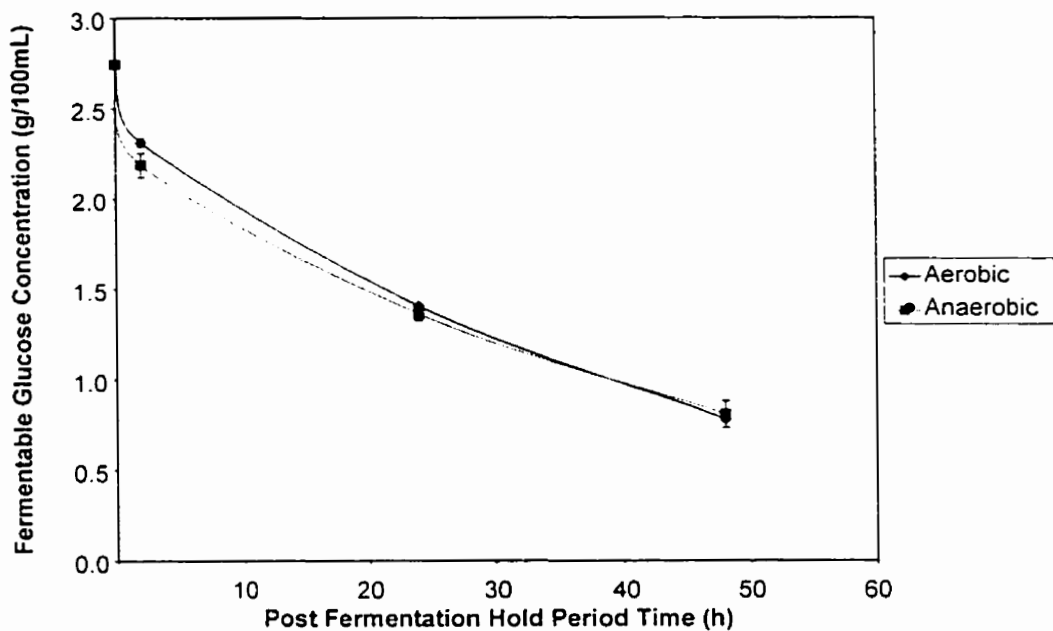


Figure 7.12 Mean fermentable glucose concentration versus post fermentation hold time for aerobic and anaerobic treated samples after continuous primary fermentation in a gas lift bioreactor. Error bars represent the upper and lower limits of the experimental data (n = 2).

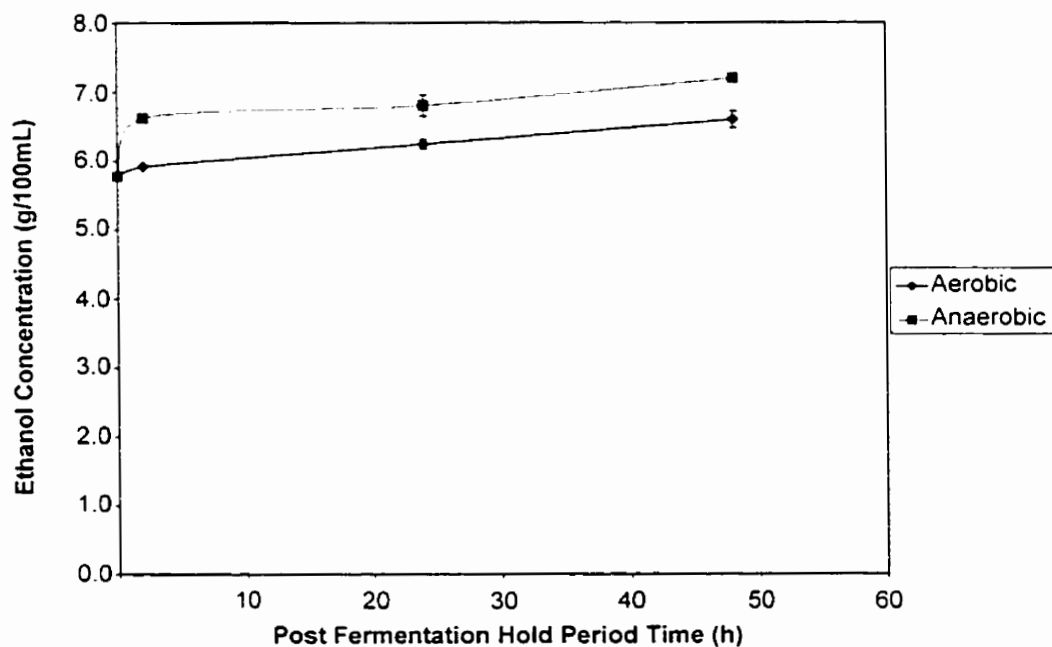


Figure 7.13. Mean ethanol concentration versus post fermentation hold time for aerobic and anaerobic treated samples after continuous primary fermentation in a gas lift bioreactor. Error bars represent the upper and lower limits of the experimental data (n = 2).

In Figure 7.14 the aerobic samples showed an early increase in acetaldehyde upon exposure to aerobic conditions outside the bioreactor. The combination of aerobic conditions, with sugar consumption and ethanol production, could account for this result. By the end of the 48-hour holding period, the concentration of acetaldehyde had dropped from 17 mg/L to 9 mg/L in the anaerobic sample, which brings the liquid concentration to within specifications for a quality North American lager (less than 10 mg/L).

The concentration of total diacetyl versus holding time is given in Figure 7.15. The results show that the elimination of oxygen from the system during this holding period provides more favourable conditions for diacetyl reduction. The shape of the total diacetyl curve may be related to free amino nitrogen depletion and the subsequent intracellular production of valine, of which diacetyl is a byproduct (Nakatani et al., 1984a; Nakatani et al., 1984b). Total diacetyl concentration at the end of the primary continuous fermentation was 326 $\mu\text{g/L}$ and at the end of the anaerobic hold period it was at a concentration of 33 $\mu\text{g/L}$, which is well below the taste threshold in commercial beers.

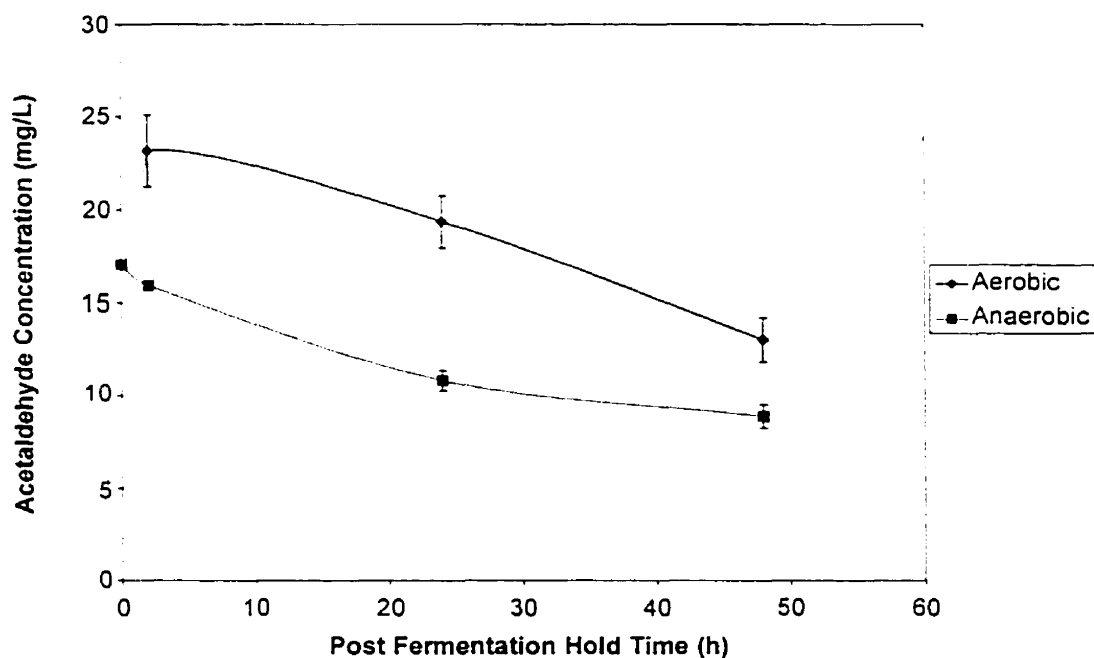


Figure 7.14. Mean acetaldehyde concentration versus post fermentation hold time for aerobic and anaerobic treated samples after continuous primary fermentation in a gas lift bioreactor. Error bars represent the upper and lower limits of the experimental data ($n = 2$).

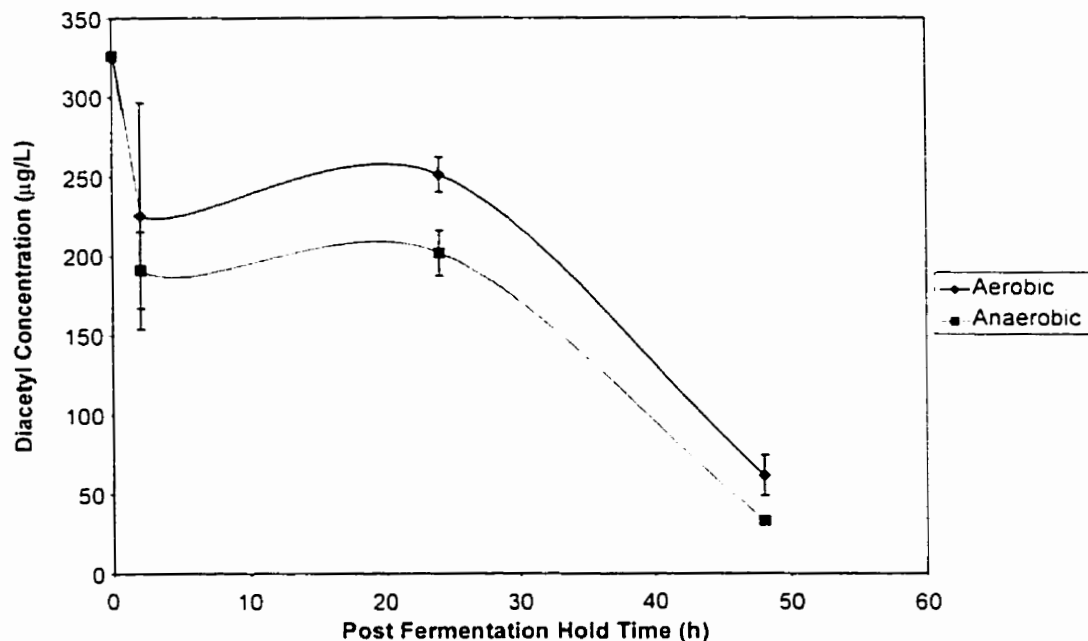


Figure 7.15. Mean total diacetyl concentration versus post fermentation hold time for aerobic and anaerobic treated samples after continuous primary fermentation in a gas lift bioreactor. Error bars represent the upper and lower limits of the experimental data ($n = 2$).

In Figures 7.16 - 7.18 the esters ethyl acetate, isoamyl acetate, and ethyl hexanoate concentrations are plotted versus post fermentation holding time. The same pattern for aerobic and anaerobic samples was observed for all esters. The concentration of esters did not diverge between the anaerobic and aerobic samples until later in the holding period, where the concentration of esters in the aerobic samples declined and the concentration in the anaerobic samples increased. Because the concentration of esters in the continuous fermentations is somewhat low compared with ester concentrations found in commercial beer, it is desirable to select conditions, which favour ester production.

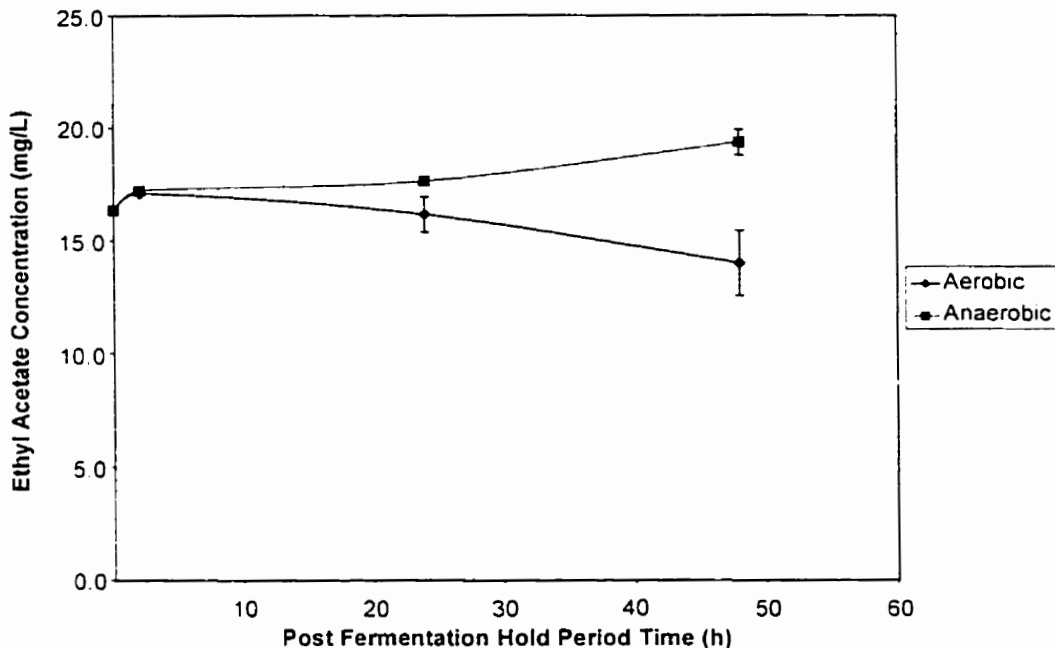


Figure 7.16. Mean ethyl acetate concentration versus post fermentation hold time for aerobic and anaerobic treated samples after continuous primary fermentation in a gas lift bioreactor. Error bars represent the upper and lower limits of the experimental data ($n = 2$).

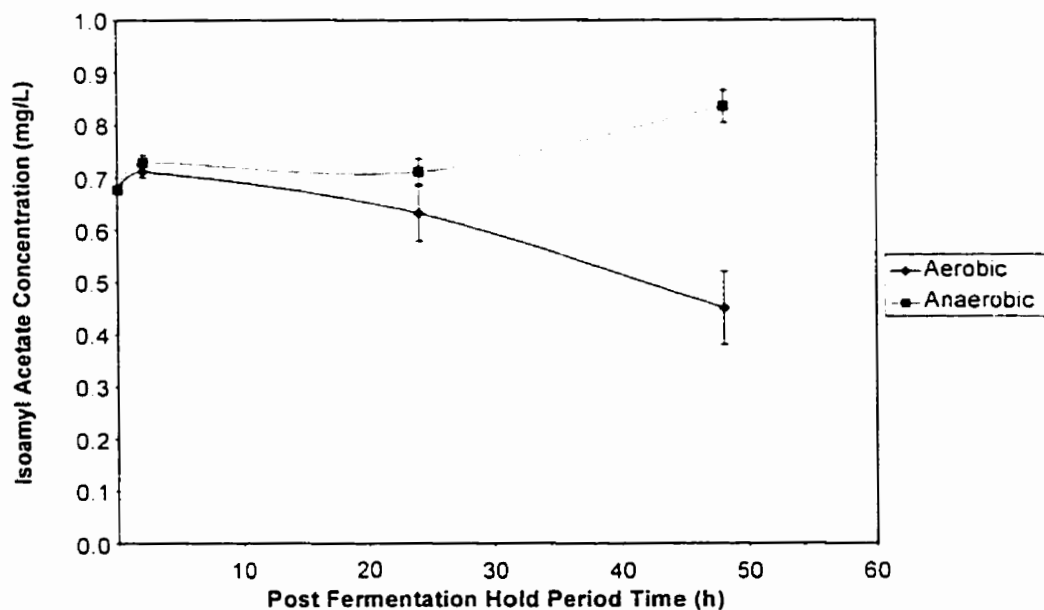


Figure 7.17. Mean isoamyl acetate concentration versus post fermentation hold time for aerobic and anaerobic treated samples after continuous primary fermentation in a gas lift bioreactor. Error bars represent the upper and lower limits of the experimental data ($n = 2$).

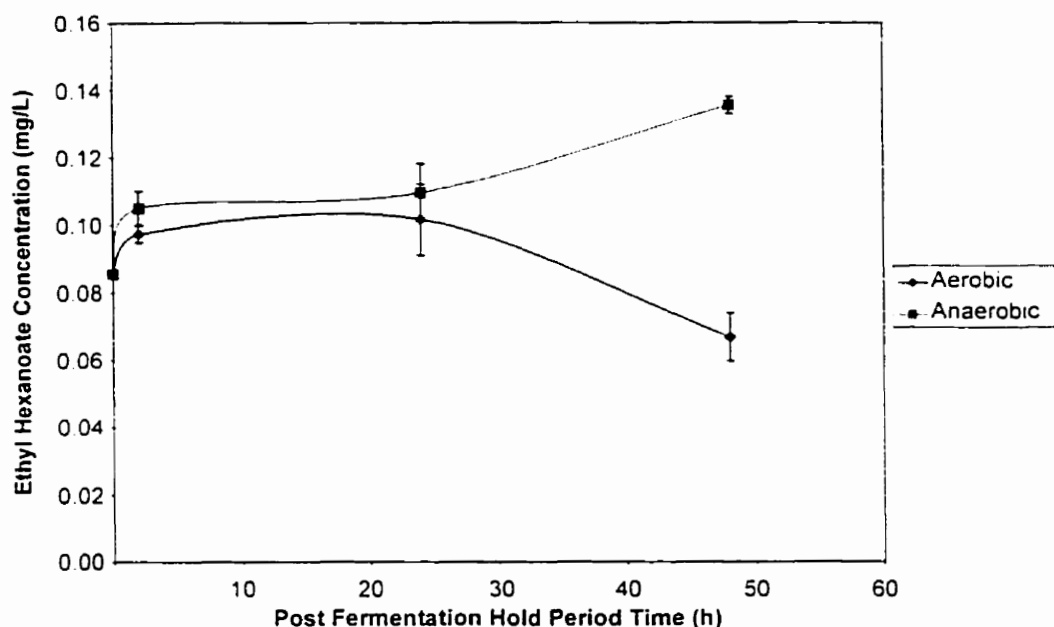


Figure 7.18. Mean ethyl hexanoate concentration versus post fermentation hold time for aerobic and anaerobic treated samples after continuous primary fermentation in a gas lift bioreactor. Error bars represent the upper and lower limits of the experimental data (n = 2).

Figures 7.19 - 7.21 show isoamyl alcohol, 1-propanol, and isobutanol concentration versus post fermentation holding time. At the end of the 48 hour holding period, no significant differences in these alcohols were observed between the aerobic and anaerobic treatments. However, the 24-hour samples showed a higher concentration in all cases for the aerobic treatments.

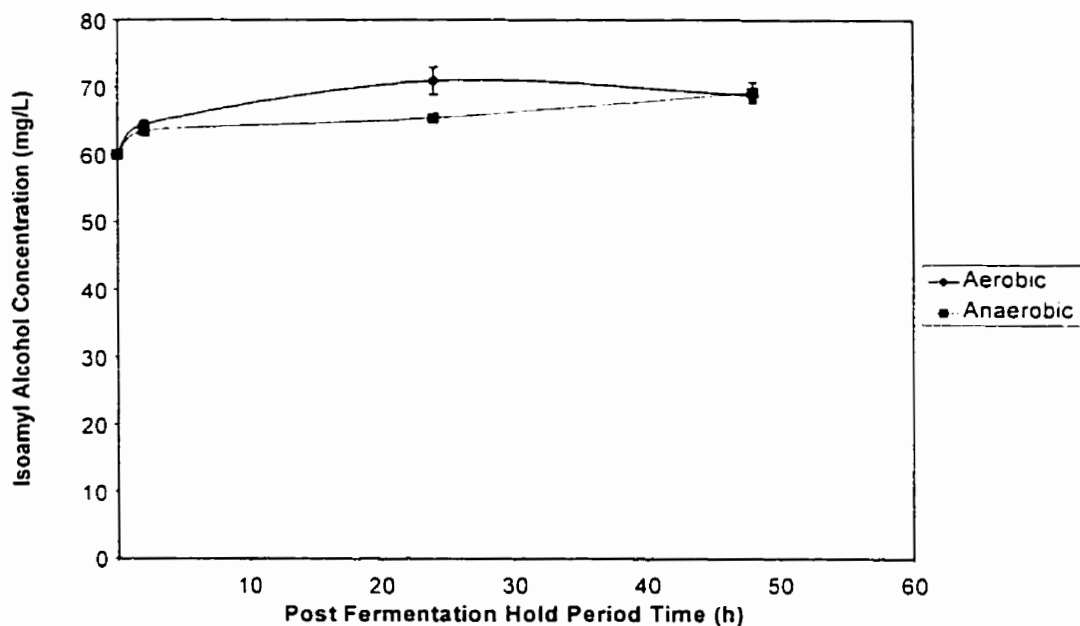


Figure 7.19. Mean isoamyl alcohol concentration versus post fermentation hold time for aerobic and anaerobic treated samples after continuous primary fermentation in a gas lift bioreactor. Error bars represent the upper and lower limits of the experimental data ($n = 2$).

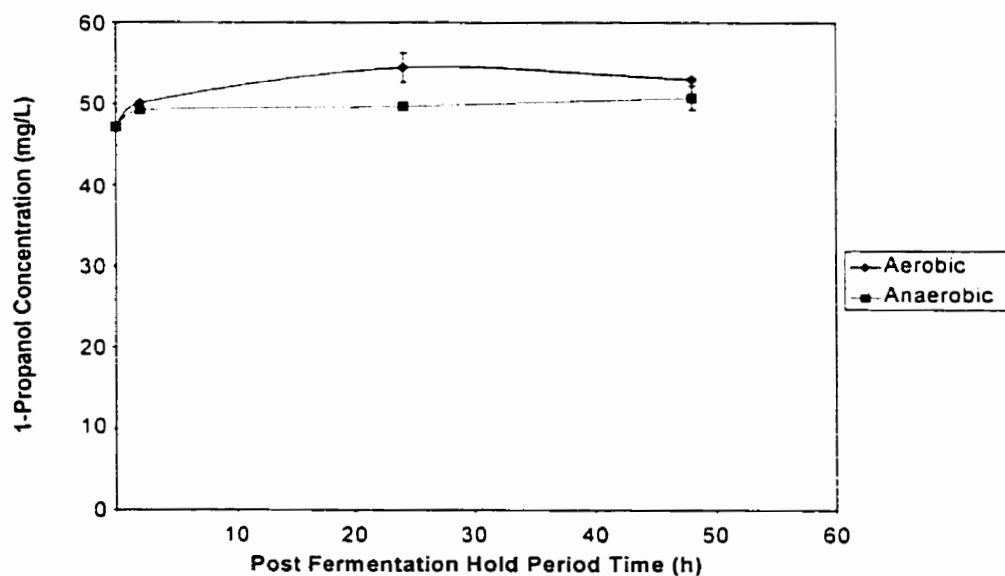


Figure 7.20. Mean 1-propanol concentration versus post fermentation hold time for aerobic and anaerobic treated samples after continuous primary fermentation in a gas lift bioreactor. Error bars represent the upper and lower limits of the experimental data ($n = 2$).

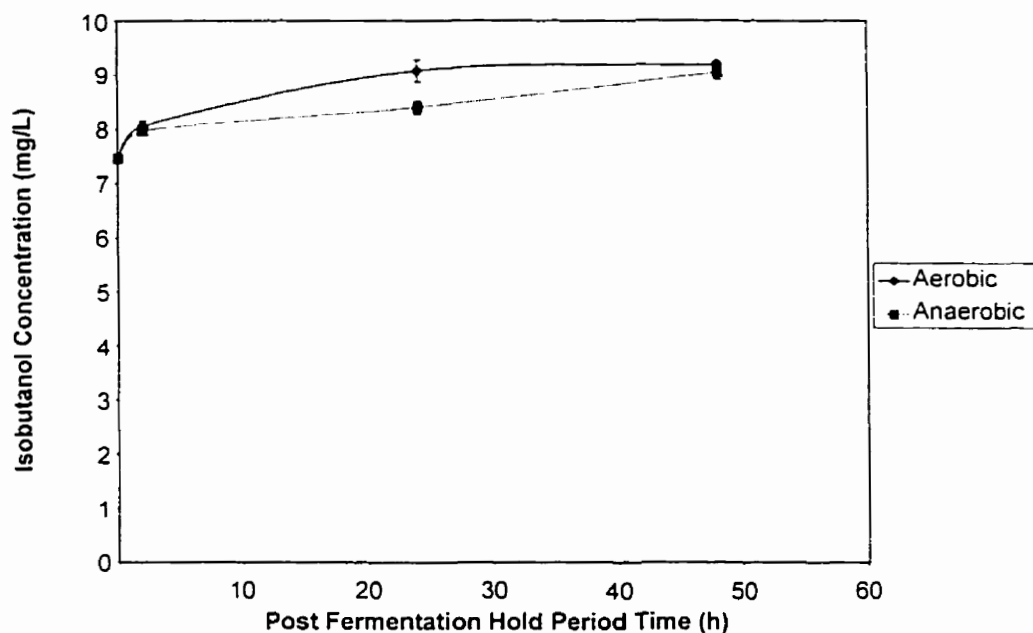


Figure 7.21. Mean isobutanol concentration versus post fermentation hold time for aerobic and anaerobic treated samples after continuous primary fermentation in a gas lift bioreactor. Error bars represent the upper and lower limits of the experimental data ($n = 2$).

In Figure 7.22, a radar graph is given to allow comparison of a number of the flavour compounds after the 48 hour aerobic and anaerobic holding period with a profile from a commercial beer. Radar graphs are commonly used in the brewing industry to allow one to examine and compare a variety of different beer characteristics together on one graph (Sharpe, 1988). From this figure, it can be seen that the anaerobically-held continuously fermented beer is the closest match to a typical market beer. From Appendix 6, it can be seen that the anaerobic liquid was within normal ranges for a market beer, except in the case of 1-propanol, which was significantly higher than batch-fermented beers. This higher than normal 1-propanol was observed in all continuously fermented products from this work.

The formation of 1-propanol occurred during the continuous primary fermentation stage and it did not decrease significantly during the holding period, whether the conditions were aerobic or anaerobic. Kunze (1996) states that the following factors will

increase higher alcohols such as 1-propanol during batch fermentation: mixing, intensive aeration of the wort, and repeated addition of fresh wort to existing yeast.

Ultimately the ideal scenario will be to eliminate the secondary holding period entirely by optimizing the conditions in the primary continuous bioreactor. However, further gains can be made using the holding period, by optimizing the holding temperature (diacetyl removal by yeast is very temperature dependent), the amount of fermentable sugars remaining in the liquid at the beginning of the holding period, optimizing the concentration of yeast present, the hydrodynamic characteristics of the holding vessel (diacetyl removal could be improved by improving the contact between the yeast and the beer), and taking further measures to eliminate oxygen from this stage.

Volumetric beer productivity calculations are given in Appendix 3. The process described in this section, with a continuous bioreactor operating with a 24 hour residence time followed by a 48 hour batch hold, is 1.8 times more productive than a current industrial batch process. A relatively fast industrial batch process with a 7.5 day cycle time has a volumetric beer productivity of $0.093 \text{ m}^3 \text{ beer produced} / (\text{m}^3 \text{ vessel volume} \times \text{day})$, whereas the continuous process described here has a productivity of $0.165 \text{ m}^3 \text{ beer produced} / (\text{m}^3 \text{ vessel volume} \times \text{day})$. If further research allowed the batch holding period to be shorted to 24 hours, beer productivity would become 2.3 times more productive than the industrial batch standard. If the ideal scenario of a 24 hour continuous process with no batch holding were achieved, beer volumetric productivity would become 7.5 times that of the batch standard. In addition to the increased volumetric productivity, the additional benefits realized by moving from a batch to a continuous process, such as shorter time to market, decrease in brewhouse size, and less frequent yeast propagation, must be balanced with a careful analysis of relative operating costs.

Other researchers (Kronlöf and Virkajärvi, 1996; Nakanishi et al., 1993; Yamauchi et al., 1995) have focused on developing multi-staged continuous fermentations in which the first stage of continuous fermentation (aerobic) results in only a partial consumption of the fermentable sugars present in the wort. While this strategy has shown some success in terms of flavour production, these systems are complex. As well, the first aerobic stage of such systems creates an environment, which is more susceptible to microbial contamination (i.e. high sugar concentration, temperature, and

oxygen, with low concentrations of ethanol). In the gas-lift bioreactor system presented in this work, the bioreactor has a low fermentable sugar concentration, low pH, high ethanol concentration, and low concentrations of oxygen, making the environment inhospitable for potential contaminants.

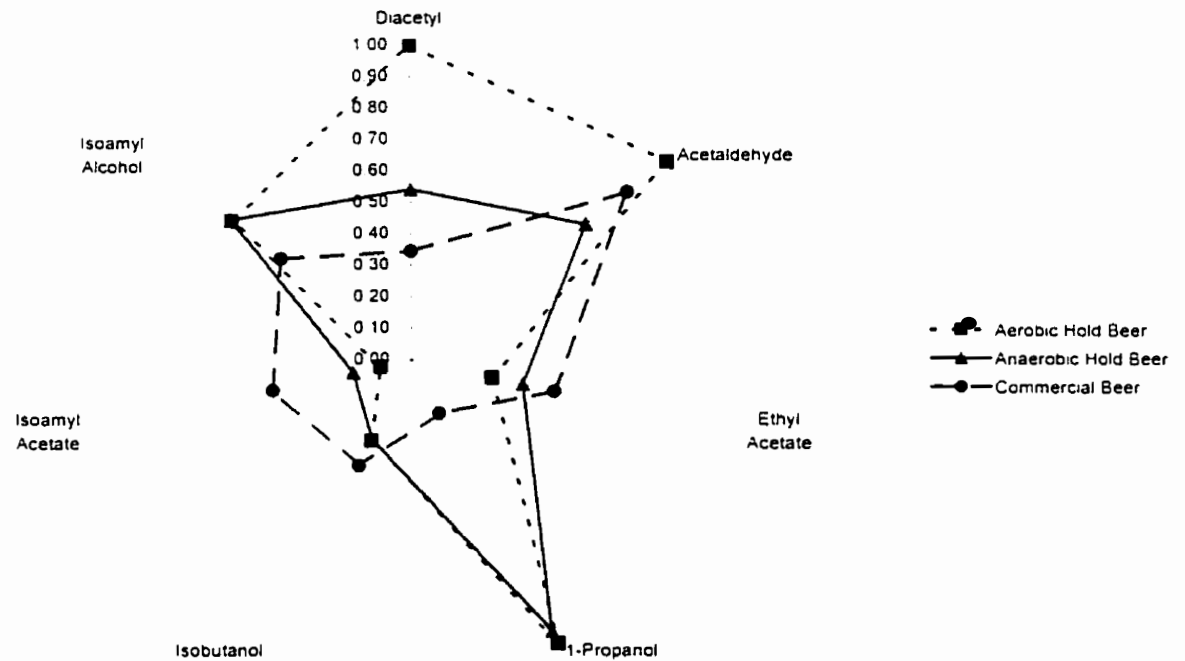


Figure 7.22. Radar graph of normalized concentration data obtained after 48 hours of aerobic or anaerobic holding, following continuous primary fermentation in a gas lift bioreactor. The normalized data is based on the averages of duplicate samples and the commercial beer data was taken as the midpoint of the data listed in Appendix 6.

7.2.3 Effect of Liquid Residence Time on Key Yeast Metabolites during Continuous Primary Beer Fermentation

Figures 7.23 - 7.28 show the analytical results obtained from the bioreactor liquid phase. In Table 7.3, the average concentrations and flow rates of the measured analytes at pseudo-steady state (after a minimum of three bioreactor turnover times) are listed at the two liquid residence times used during this experiment. While liquid phase yeast viability did not change significantly when the flow rate of wort to the bioreactor was increased, the concentration of yeast cells did change as seen in Figure 7.23.

Table 7.3. (a) Summary table of effect of bioreactor residence time on liquid phase yeast and key yeast metabolite concentrations, averages at pseudo-steady state; (b) Summary table of the effect of bioreactor residence time on liquid phase yeast and key yeast metabolite flow rates at the bioreactor outlet, averages at pseudo-steady state.

(a) Average Analyte Concentration	Bioreactor Residence Time	
	1.8 days	0.9 days
Cell Conc (cells/mL)	2.38E+08	1.32E+08
Tot. Ferm. Glucose (g/100 mL)	0.29	6.09
FAN (mg/L)	106.3	246.4
Ethanol (g/100 mL)	5.16	4.80
Total Diacetyl (ug/L)	292	460
Acetaldehyde (mg/L)	19.47	37.07
Ethyl Acetate (mg/L)	41.00	38.29
1-Propanol (mg/L)	44.95	13.53
Isobutanol (mg/L)	22.78	9.13
Isoamyl Acetate (mg/L)	0.90	1.28
Isoamyl Alcohol (mg/L)	76.67	51.39

(b) Average Analyte Flow Rate	Bioreactor Residence Time	
	1.8 days	0.9 days
Cell Flow Rate(cells/min)	7.38E+08	8.22E+08
Tot. Ferm. Glucose (g/min)	8.93E-03	3.72E-01
FAN (g/min)	3.65E-04	1.50E-03
Ethanol (g/min)	1.60E-01	2.93E-01
Total Diacetyl (g/min)	9.06E-07	2.81E-06
Acetaldehyde (g/min)	6.04E-05	2.26E-04
Ethyl Acetate (g/min)	1.27E-04	2.34E-04
1-Propanol (g/min)	1.39E-04	8.25E-05
Isobutanol (g/min)	7.06E-05	5.57E-05
Isoamyl Acetate (g/min)	2.80E-06	7.30E-06
Isoamyl Alcohol (g/min)	2.38E-04	3.13E-04

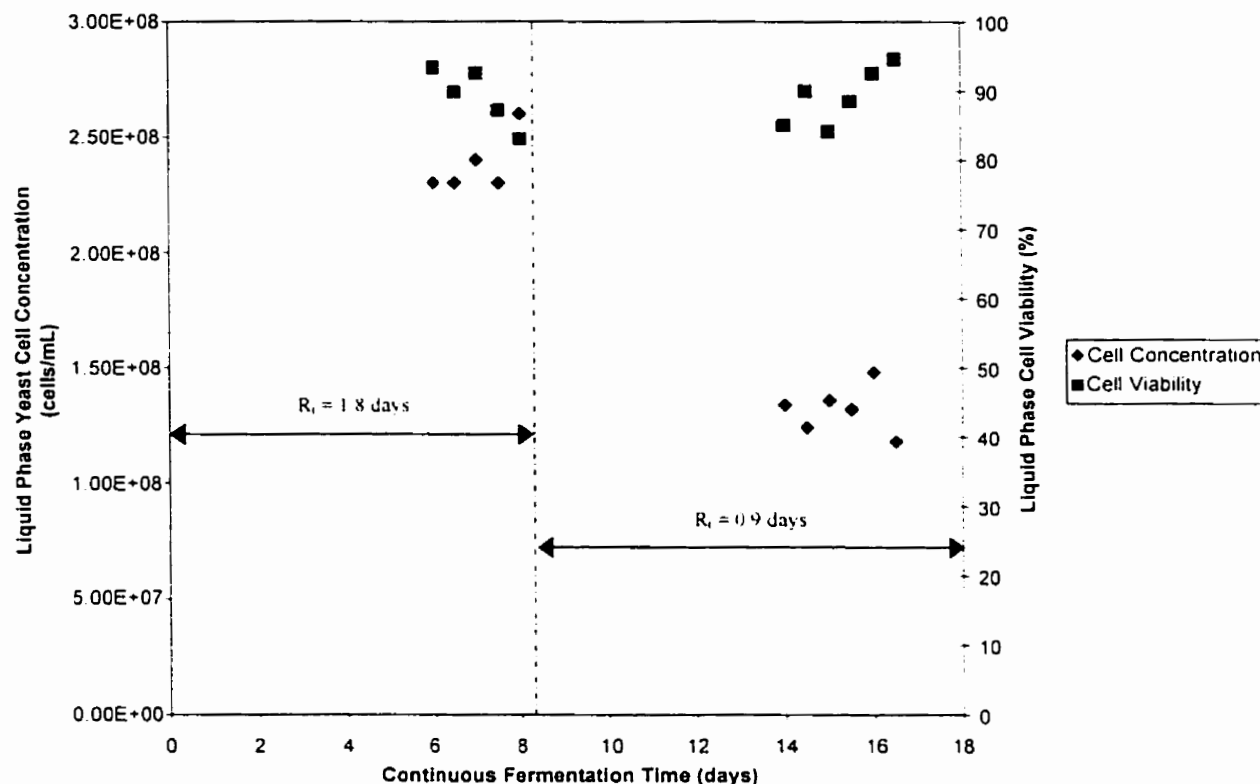


Figure 7.23. Liquid phase yeast cell concentration versus relative continuous fermentation time, effect of liquid residence time in bioreactor. R_L is bioreactor liquid residence time in days.

In Figures 7.24 and 7.25, the concentrations of the wort substrates free amino nitrogen (FAN) and total fermentable carbohydrate (as glucose) both increased when the liquid residence time decreased from 1.8 to 0.9 days. From the mass balances in Table 7.4, the consumption rate of total fermentable carbohydrate (as glucose) increased while free amino nitrogen consumption rate decreased, with decreasing bioreactor residence time. The yield factor, $Y_{P/S}$, of the fermentation product ethanol from fermentable glucose substrate, increased from 0.3 to 0.5 with the reduction in liquid residence time. Because the system was sparged with air and carbon dioxide, there were probably minor losses of ethanol in the gas phase, which would have an impact on the yield factor, $Y_{P/S}$, by affecting the balance on ethanol. Research conducted in collaboration with Budac and Margaritis (1999) has qualitatively demonstrated, using a gas chromatograph-mass spectroscopy technique (GC-MS), that beer flavour volatiles including ethanol.

acetaldehyde, ethyl acetate, and isoamyl acetate are detected in the gas-lift bioreactor headspace during continuous fermentation.

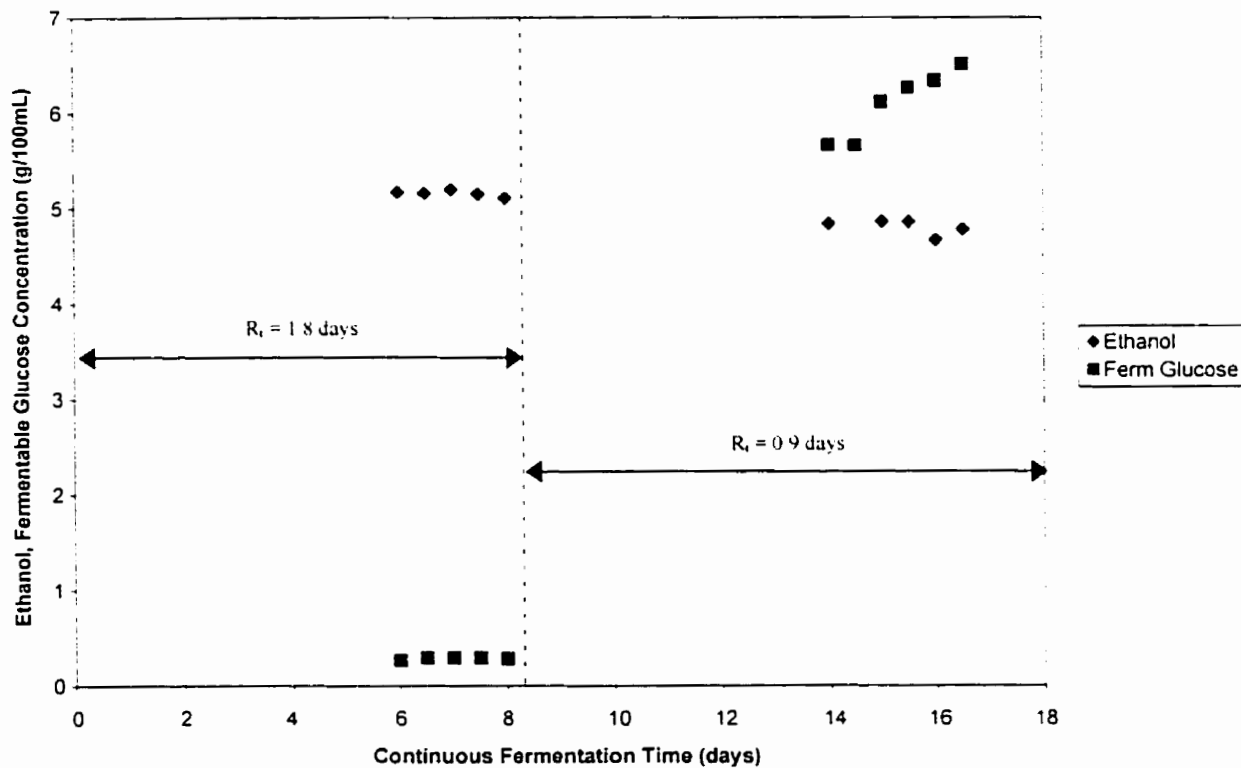


Figure 7.24. Liquid phase ethanol and fermentable glucose concentration versus relative continuous fermentation time. effect of liquid residence time in bioreactor. R_t is bioreactor liquid residence time in days.

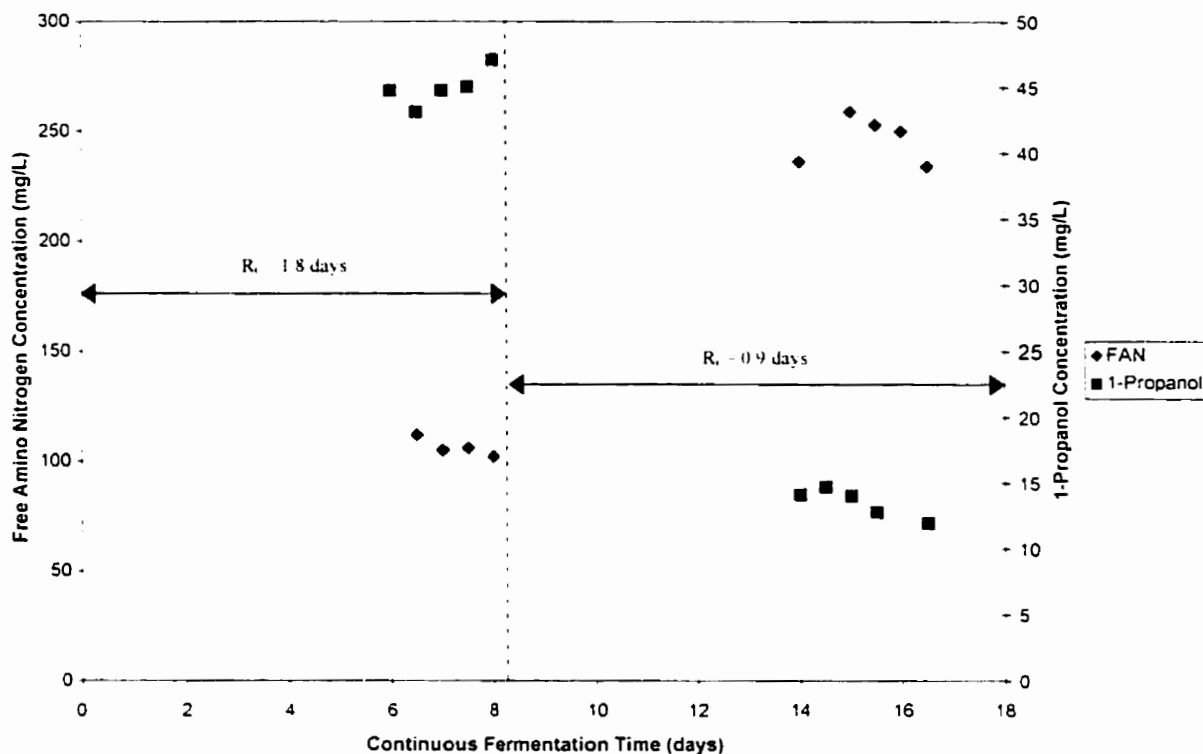


Figure 7.25. Liquid phase free amino nitrogen and 1-propanol concentration versus relative continuous fermentation time, effect of liquid residence time in bioreactor. R_t is bioreactor liquid residence time in days.

Table 7.4. Mass balances on free amino nitrogen and total fermentable carbohydrate (as glucose) based on average data in Table 7.3, effect of residence time.

Residence Time	1.8 days		0.9 days	
	Free Amino Nitrogen (g/min)		Total Ferm. Glucose (g/min)	
Inlet*	8.84E-04	1.74E-03	4.71E-01	9.26E-01
Outlet	3.65E-04	1.50E-03	8.93E-03	3.72E-01
Consumption (ΔS)	5.18E-04	2.35E-04	4.62E-01	5.54E-01
Yield Factor ($Y_{P/S}$)			0.3	0.5

*Inlet concentrations from Appendix 1

The liquid phase concentration of the fermentation product ethanol decreased with the step change in liquid residence time. However, the system as a whole was producing more ethanol on a mass flow rate basis at the faster liquid residence time. Because the

objective of this work was not only to produce ethanol in isolation, but rather a beer with a balance of many components. maximizing ethanol productivity must be balanced with other factors. At the end of a commercial primary beer fermentation, the majority of fermentable glucose substrate must be consumed.

In Figure 7.26, the response of acetaldehyde and total diacetyl concentration, to the step change in wort flow rate is given. Both analytes increased in concentration and in their rate of production when the liquid residence time was decreased. During batch beer fermentations, acetaldehyde is excreted by yeast during the first few days of fermentation (Kunze, 1996).

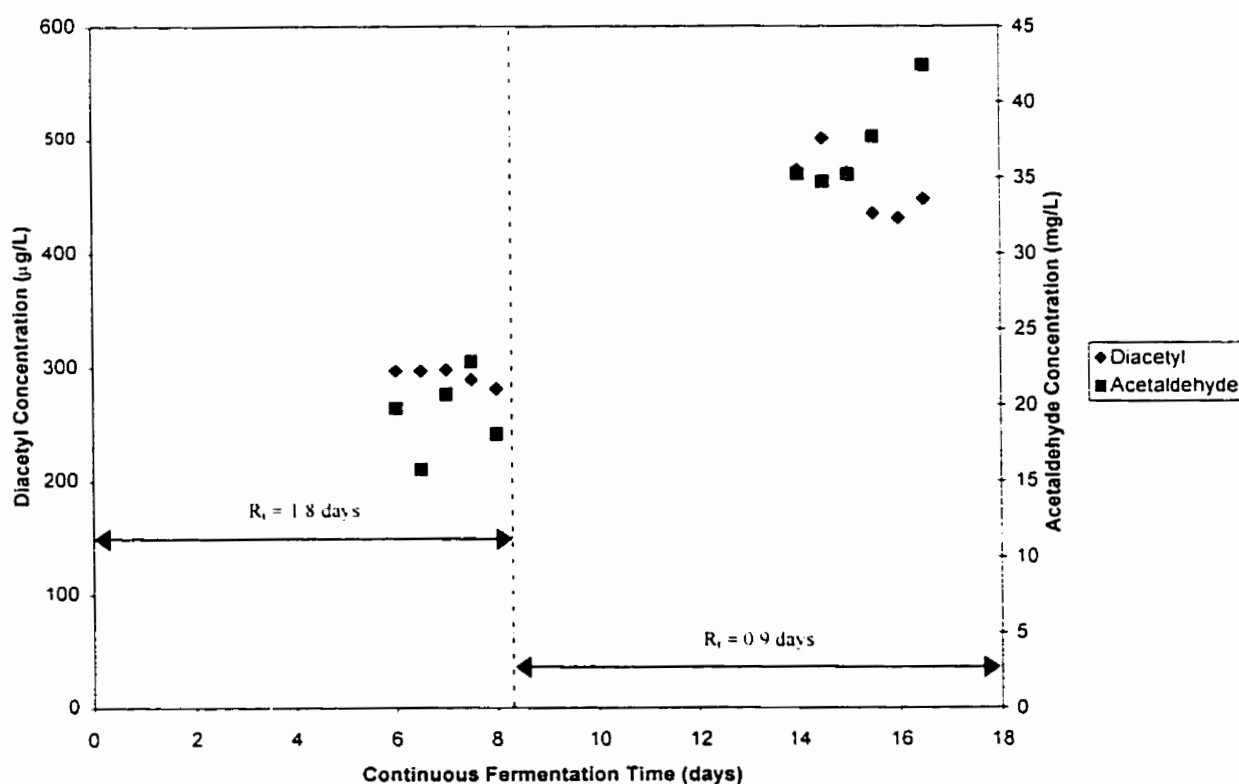


Figure 7.26. Liquid phase total diacetyl and acetaldehyde concentration versus relative continuous fermentation time, effect of liquid residence time in bioreactor. R_t is bioreactor liquid residence time in days.

Figures 7.25 and 7.27 show the effect of decreasing bioreactor residence time on the liquid phase concentrations of the higher alcohols 1-propanol, isobutanol and isoamyl

alcohol. All three higher alcohols decreased in concentration when the bioreactor residence time was decreased.

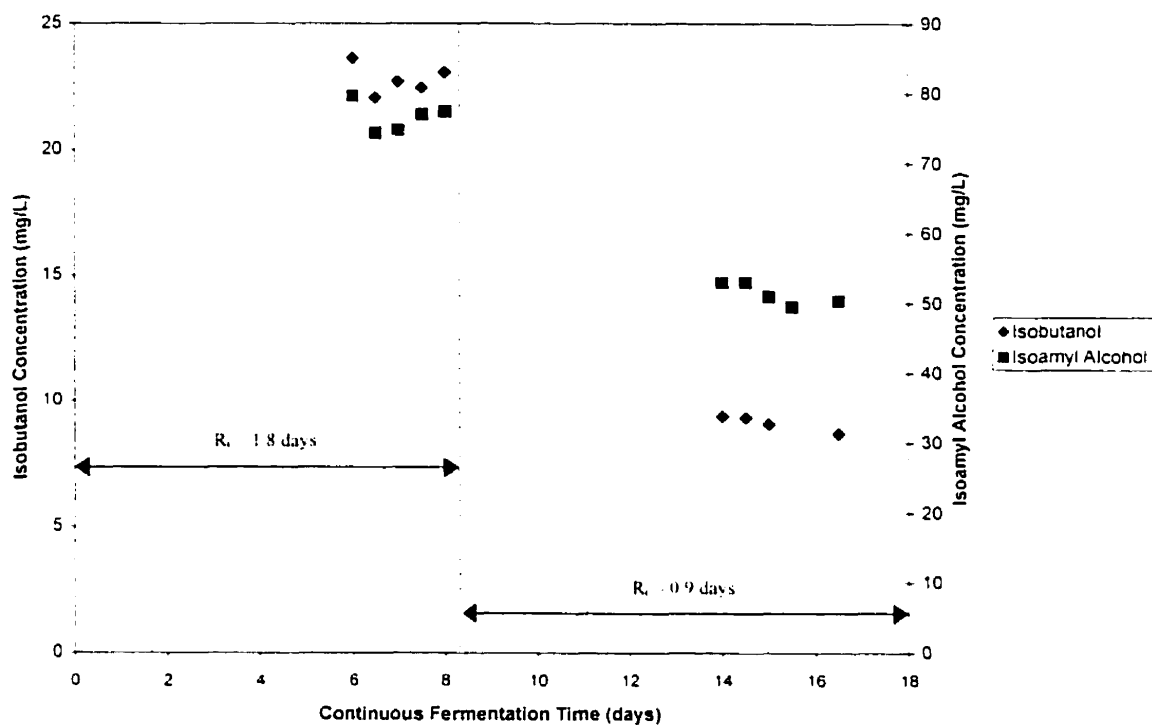


Figure 7.27. Liquid phase isobutanol and isoamyl alcohol concentration versus relative continuous fermentation time, effect of liquid residence time in bioreactor. R_t is bioreactor liquid residence time in days.

Ethyl acetate and isoamyl acetate mass flow rates given in Table 7.3 (b) both increased in response to the decrease in liquid residence time. In Figure 7.28 the liquid phase concentration of ethyl acetate decreased while isoamyl acetate increased. Because this experiment allowed for an increase in liquid phase cell growth without increasing the oxygen supply to the system, the conditions in the bioreactor promoted ester production. Hough et al. (1982) state that increased growth and decreased oxygen conditions encourage ester formation.

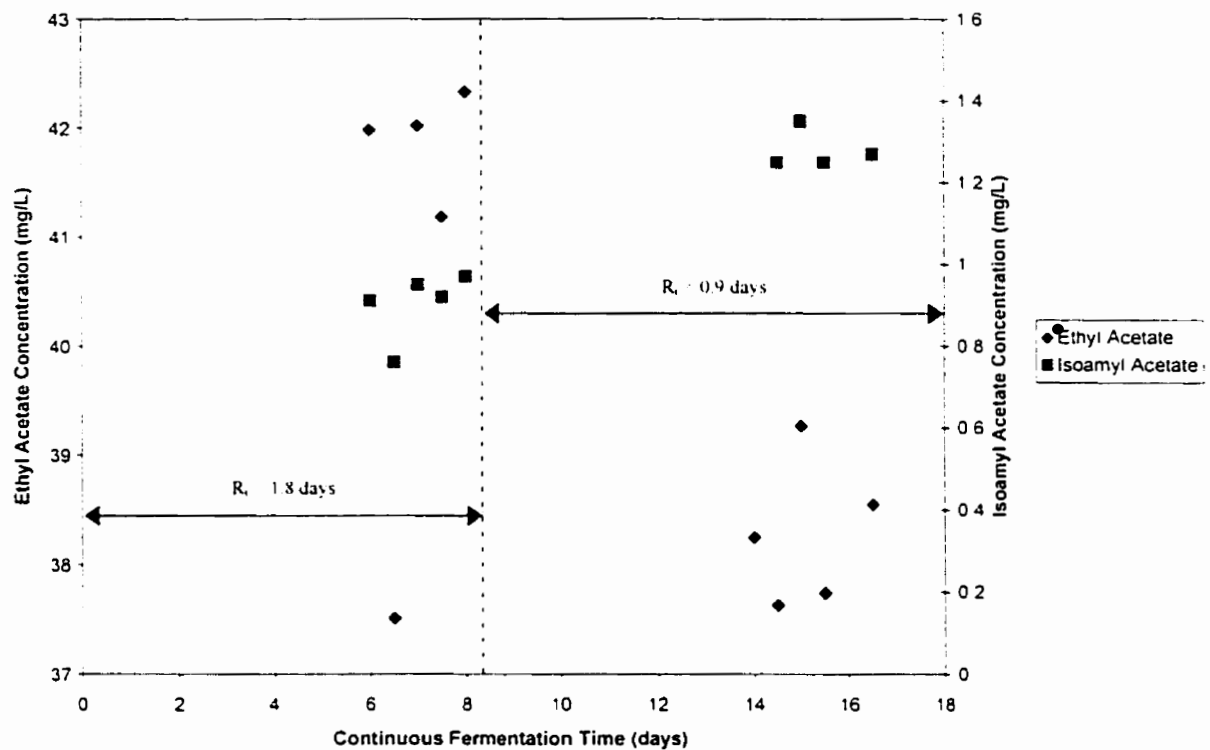


Figure 7.28. Liquid phase ethyl acetate and isoamyl acetate concentration versus relative continuous fermentation time, effect of liquid residence time in bioreactor. R_L is bioreactor liquid residence time in days.

7.2.4 Using a Commercial Preparation of Alpha-Acetylactate Decarboxylase to Reduce Total Diacetyl during Continuous Primary Beer Fermentation

Experiment 1: The bioreactor was contaminated with aerobically growing Gram positive cocci before the trial could be completed. It was determined that the bioreactor itself was contaminated, since microbiological testing of the wort supply showed no contamination. This pointed to the need for bioreactor upgrades with improved safeguards against contamination. However, before the system was shut down, a decrease in total diacetyl concentration was observed when ALDC was added to the wort supply. Unfortunately it was not possible to draw any conclusions from this data due to the confusing effects of bioreactor contamination.

Experiment 2: As a result of numerous bioreactor upgrades, the system operated without contamination throughout the duration of Experiment 2. The data for this experiment is given in Figures 7.29 – 7.31. In Table 7.5 the average pseudo-steady state concentrations of total diacetyl before and after ALDC addition to the wort are summarized. Total diacetyl concentration dropped by 47% with the addition of ALDC to the wort, which makes the use of this enzyme promising for the future (averages taken after three bioreactor turnover times). As seen in Figures 7.30 and 7.31, total fermentable carbohydrate (as glucose) and cell concentration drifted slightly during this trial, which may have been caused by slight differences in the wort, supplied to the bioreactor before and after the addition of ALDC.

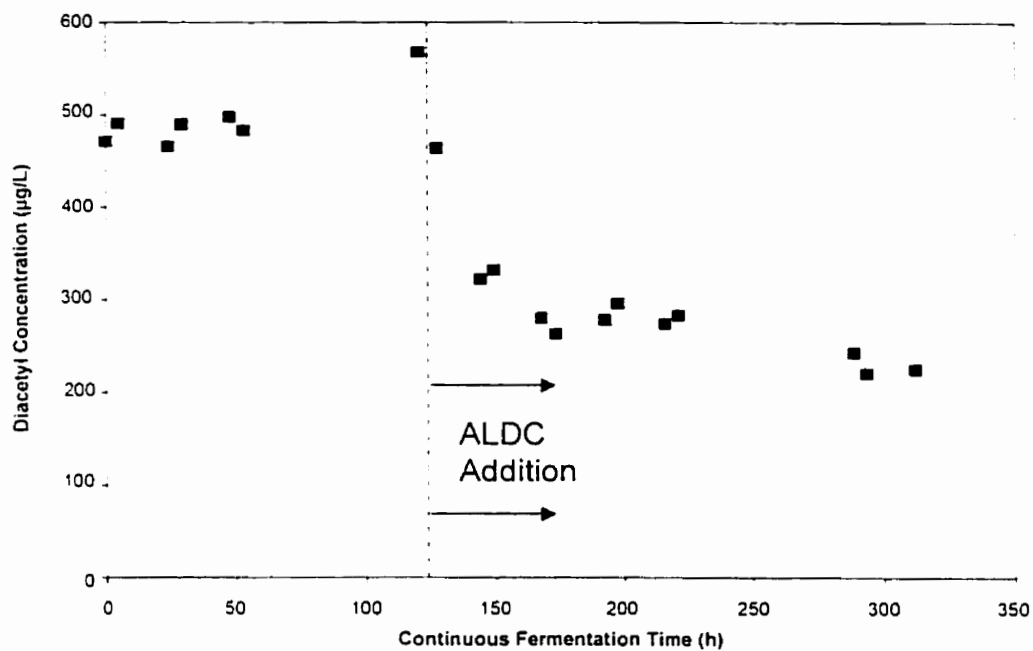


Figure 7.29. Liquid phase total diacetyl concentration versus continuous fermentation time, effect of ALDC addition to the wort fermentation medium, Experiment 2.

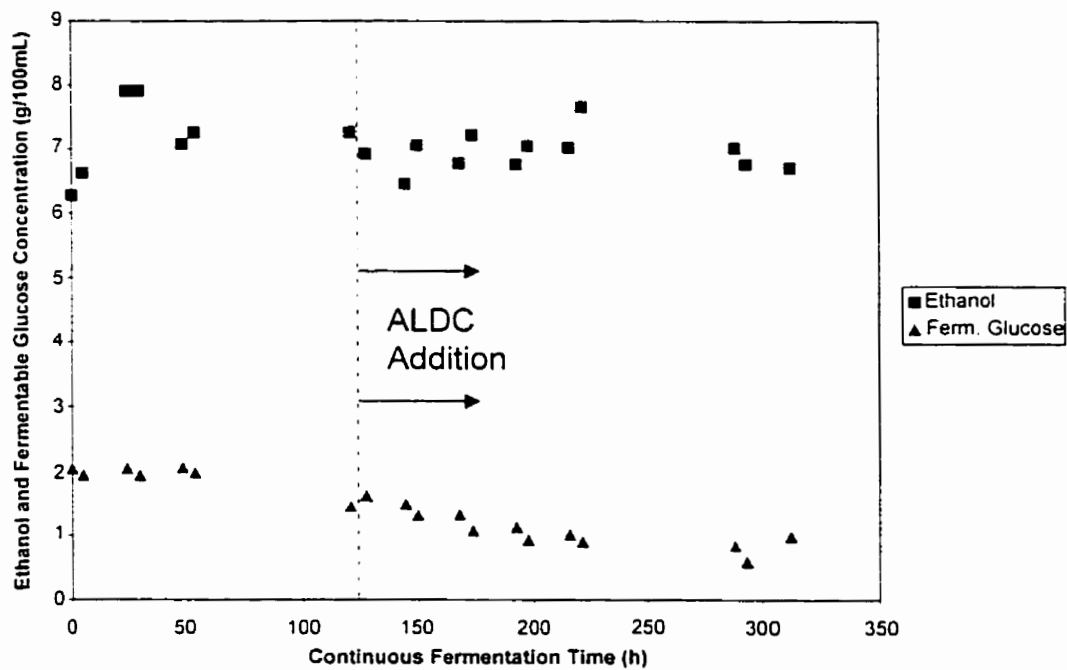


Figure 7.30. Liquid phase fermentable carbohydrate (as glucose) and ethanol concentration versus continuous fermentation time, effect of ALDC addition to the wort fermentation medium, Experiment 2.

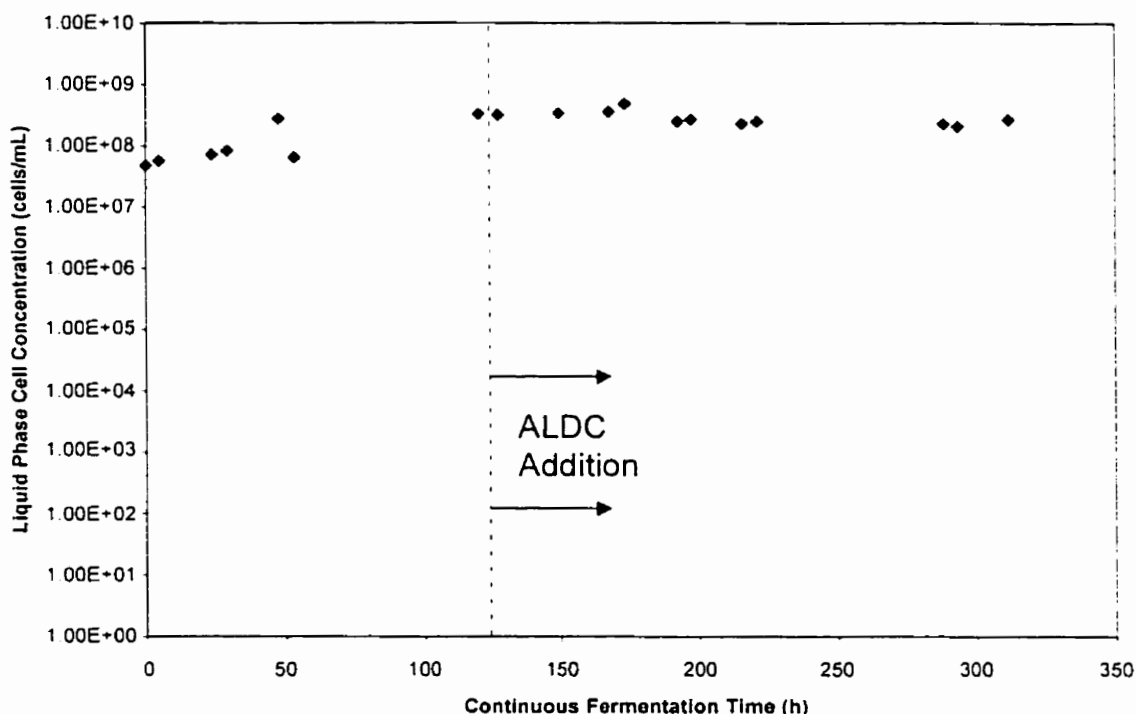


Figure 7.31. Liquid phase cell concentration versus continuous fermentation time, effect of ALDC addition to the wort fermentation medium, Experiment 2.

In order to eliminate the potential confounding effect of wort variability, during Experiment 3 a large quantity of wort from the brewhouse (14 hL) was collected and ALDC was added directly to the wort remaining in this holding vessel, once a pseudo-steady state baseline was reached. This further eliminated any potential wort inconsistencies that could have affected fermentation performance in Experiment 2. This wort storage vessel was also equipped with carbon dioxide sparging, so that dissolved oxygen levels in the wort supply were kept at a consistently low level.

Experiment 3: Figures 7.32 – 7.34 illustrate the effect of ALDC addition to the wort supply, on total diacetyl, total fermentable carbohydrate (as glucose), ethanol, and the freely suspended cell concentration during continuous beer fermentation. Table 7.6 also gives the average pseudo-steady state total diacetyl concentration before and after the addition of ALDC to the wort supply (averages taken after three bioreactor turnover times). No contamination was detected at any point during this experiment. The concentration of total diacetyl was reduced by 45% upon addition of ALDC. No significant differences in ethanol, total fermentable carbohydrate (as glucose) or the

freely suspended cell concentration were observed, which agrees with the batch findings of Aschengreen and Jepsen (1992).

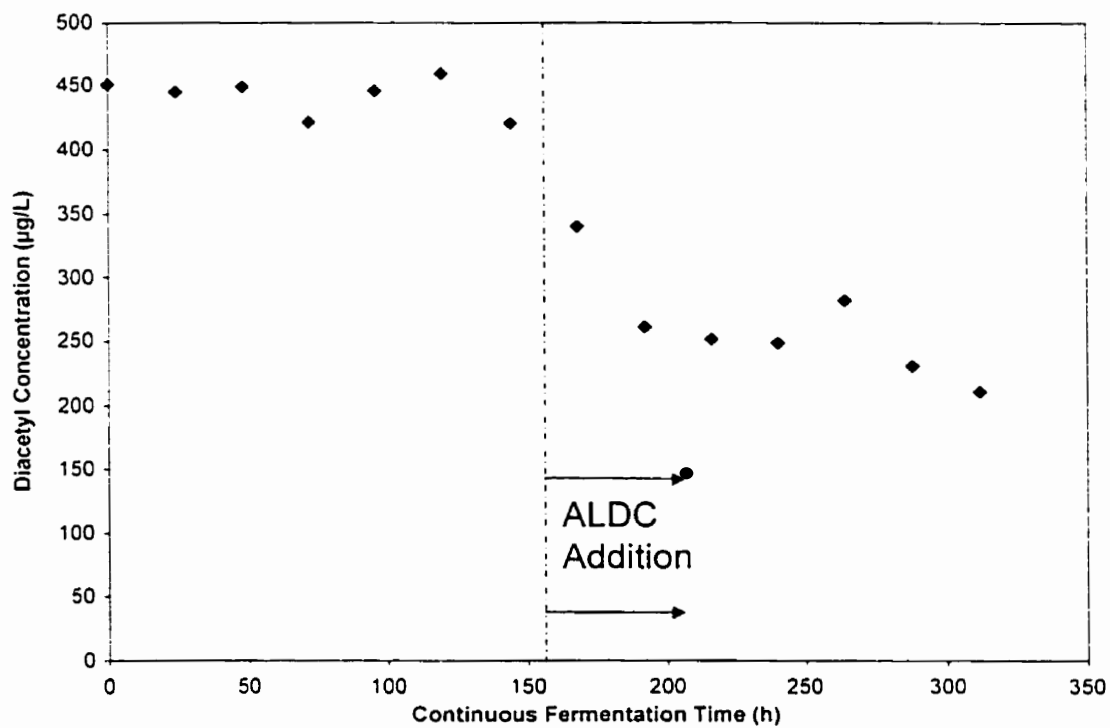


Figure 7.32. Liquid phase total diacetyl concentration versus continuous fermentation time, effect of ALDC addition to the wort fermentation medium, Experiment 3.

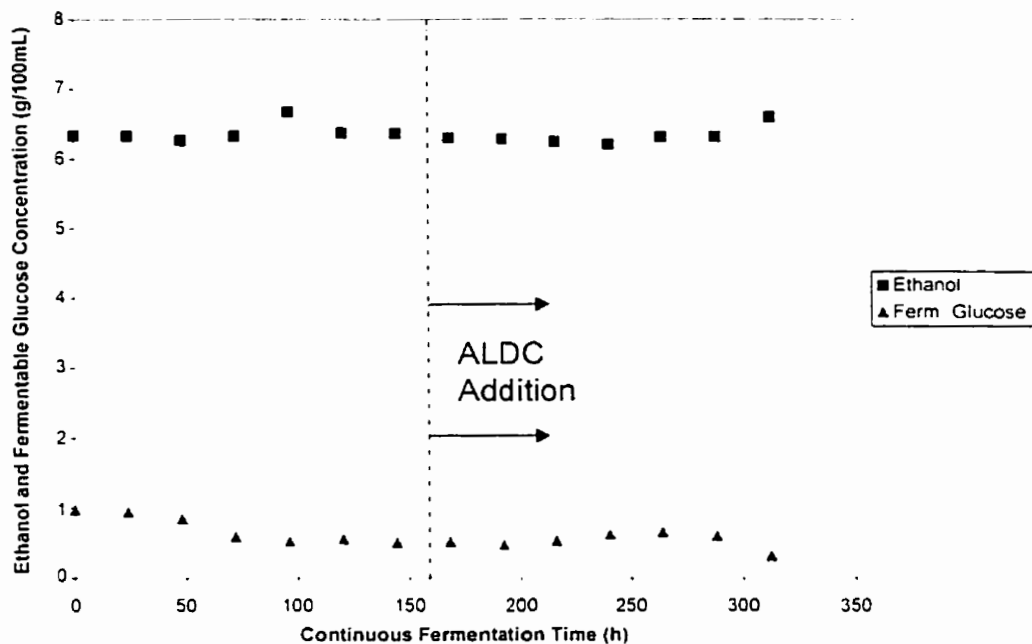


Figure 7.33. Liquid phase ethanol and total fermentable sugar (as glucose) concentration versus continuous fermentation time, effect of ALDC addition to the wort fermentation medium. Experiment 3.

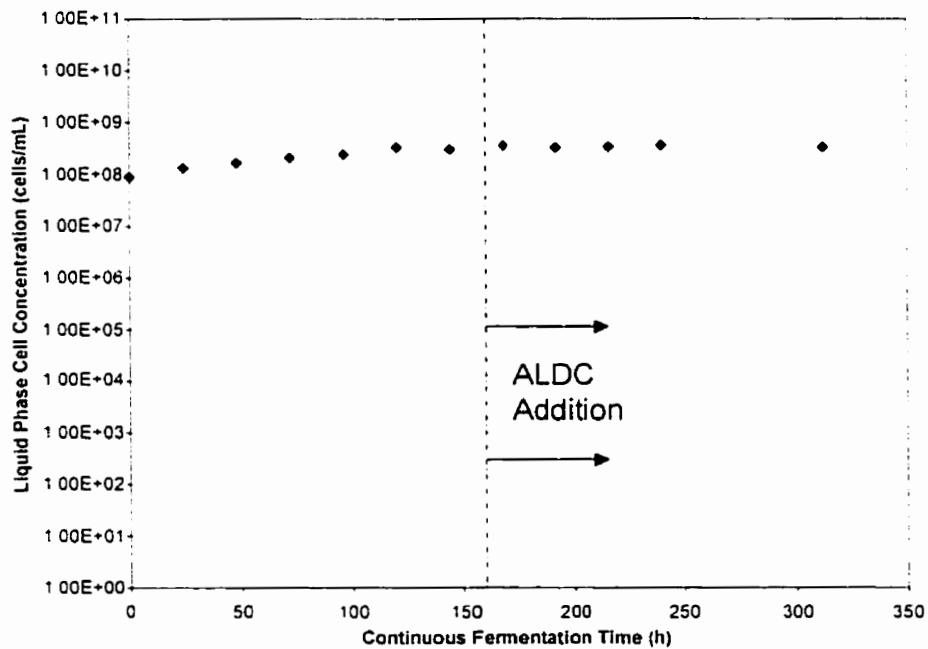


Figure 7.34. Liquid phase cell concentration versus continuous fermentation time, effect of ALDC addition to the wort fermentation medium. Experiment 3.

The results of Experiments 2 and 3 indicate that ALDC did have a significant effect on total diacetyl concentration during continuous fermentation in gas lift bioreactors giving an average reduction in total diacetyl concentration of 46%. This has the potential to decrease, or eliminate secondary processing for diacetyl reduction in continuous gas-lift systems. A relatively high dosage of ALDC was used for these initial experiments, and it would be necessary to optimize the amount, method and timing of ALDC dosing, in wort if this enzyme was to be adopted for the process. Further savings could be realized if an enzyme becomes available with higher activity levels under brewery fermentation conditions or if the enzyme itself was immobilized, thus allowing for its reuse (Dulieu et al., 1996). Another consideration will be public acceptance of enzyme additives that have been produced using genetically modified organisms.

At the supplier's recommended dosage of 2 kg/1000 hL, and, with cost of the commercial enzyme preparation at \$131.05/kg, \$0.26 / hL would be added to the material costs of fermentation. As used in the experiments performed, the enzyme dosage was 72 $\mu\text{g/L}$ (108 ADU/L) or 7.2 kg/1000 hL ALDC, giving an added material cost of \$0.94/hL. The economics of using ALDC for diacetyl reduction during gas lift continuous fermentations will depend on the optimum enzyme dosage under bioreactor conditions and the amount of time saved by its use.

Table 7.5. Summary of average pseudo-steady state effect of ALDC addition to wort fermentation medium on total diacetyl concentration during continuous beer fermentation in a gas lift bioreactor.

Experiment	Average Total Diacetyl Concentration ($\mu\text{g/L}$)		Percent Diacetyl Reduction
	(ALDC absent)	(ALDC, 60 $\mu\text{L/L}$)	
Experiment II	495	260	47
Experiment III	445	245	45

*averages based on pseudo-steady state values after three reactor turnover times

CHAPTER 8. CONCLUSIONS

The experimental results described in this work indicate that continuous fermentation, using immobilized yeast and the associated free cells in a gas-lift draft tube bioreactor system, is a viable alternative to batch fermentation for beer production based on the following criteria:

- flavour match accomplished
- higher bioreactor volumetric productivity
- minimal complexity
- long term continuous operation demonstrated
- control of air (oxygen) in the fluidizing gas for flavour control
- addition of enzyme α -acetolactate decarboxylase for diacetyl control an option
- no bacterial contamination
- financial benefits.

There are still many areas, which need to be studied further, but the technology is ready to be tested at a larger scale. Gas-lift bioreactors are already used at an industrial scale for wastewater treatment, which makes the prospects of scaling up the continuous beer fermentation system technically feasible. The Grolsch brewery in the Netherlands has been reported to use a 230 m³ gas lift bioreactor for treatment of their wastewater (Driessen et al., 1997). One of the biggest barriers to commercial scale continuous fermentation in the brewing industry may be the acceptance by the brewers of a new process, in an industry that is deeply tied to tradition.

Data collected on secondary yeast metabolites produced during continuous beer fermentations conducted in this work highlighted the importance of controlling oxygen in the fluidizing gas for beer flavour formation. The findings showed that under the given operating conditions, increased air in the bioreactor fluidizing gas caused an increase in acetaldehyde, diacetyl, and higher alcohols (isoamyl alcohol and isobutanol), while the concentrations of esters (isoamyl acetate, ethyl hexanoate, ethyl octanoate) and ethanol were reduced. These data suggest that there is the potential for controlling beer flavour through the composition of the bioreactor fluidizing gas, allowing for the production of unique products.

With the exception of when air was eliminated from the fluidizing gas, a freely suspended cell concentration of greater than 10^8 cells/mL was maintained in the bioreactor liquid phase. The system thus has more than one population of yeast cells coexisting in the bioreactor, the immobilized yeast and the liquid phase suspended yeast. Because of the large quantities of viable yeast growing in the bioreactor liquid phase, the possibility exists of using a continuous bioreactor as a yeast propagator.

When a secondary 48-hour batch-holding period was added following continuous primary fermentation, a flavour profile within the range of market beers was obtained. The temperature of this holding period was 21°C and the importance of minimizing the exposure of the liquid to oxygen during the holding period for flavour formation was demonstrated experimentally. The addition of a holding period adds two days to the process as well as additional complexity, however it is still significantly faster than commercial batch fermentations, which take between seven and fourteen days.

Ultimately, the ideal scenario would be to entirely eliminate the secondary holding period by optimizing the conditions in the primary continuous bioreactor. However, further reductions in the secondary holding time can be achieved in the short term by optimizing the holding temperature (diacetyl removal by yeast is very temperature dependent), the amount of fermentable sugars remaining in the liquid at the beginning of the holding period, the concentration of yeast present, the hydrodynamic characteristics of the holding vessel (diacetyl removal could be improved by improving the contact between the yeast and the beer), and by taking further measures to eliminate oxygen from this stage.

Other researchers (Kronlof and Virkajarvi, 1996; Nakanishi et al., 1993; Yamauchi et al., 1995) have focused on developing multi-stage continuous fermentations in which the first stage of continuous fermentation (aerobic) results in only a partial consumption of the fermentable sugars present in the wort. While this strategy has shown some success in terms of flavour production, these systems are complex. As well, the first aerobic stage of such systems creates an environment, which is more susceptible to microbial contamination (i.e. high sugar concentration, temperature, and oxygen, with low concentrations of ethanol). In the gas-lift bioreactor presented in this work, the bioreactor has a low steady state fermentable sugar concentration, low pH, high ethanol

concentration, and low concentrations of oxygen, making the environment inhospitable for potential contaminants. In a less-developed brewery, minimizing complexity and developing a robust, contamination-resistant process is an important success factor.

The addition of a commercial preparation of alpha-acetolactate decarboxylase (ALDC) to the wort supplying the continuous fermentation showed an average diacetyl reduction of 46%. However, because ALDC is an enzyme that is produced by a genetically modified organism (GMO), there are public perception issues that would need to be addressed before using such an enzyme in a commercial product. In addition the commercially available enzymes for diacetyl control do not have optimal activity under fermentation conditions.

Over six months of continuous fermentation using kappa-carrageenan gel immobilization, freely suspended cells in the liquid phase retained viabilities greater than 90%, while immobilized cell viability decreased to less than 60%. Scanning electron micrographs revealed that cells located near the periphery of the gel bead had multiple bud scars and a regular morphology, while those near the bead core had an irregular shape and fewer bud scars, suggesting impaired growth. The micrographs also suggested that the yeast located near the bead core were showing signs of aging. As discussed in section 5, kappa-carrageenan gel has many characteristics that make it a desirable yeast immobilization matrix. However, there is currently no industrial method available for bead manufacture and, because the yeast are entrapped in the matrix as part of the bead-making process, bead-handling in a commercial plant increases complexity and cost. Other immobilization methods such as self-aggregation or flocculation should be explored in the future. This would eliminate the complexity of bead handling in a plant environment, and, if the yeast flocs were disrupted on a regular basis, one could ensure that aged cells are regularly removed from the bioreactor.

Continuous fermentation using a gas-lift bioreactor could potentially replace batch technology currently used in commercial breweries. In the past, flavour formation in continuous fermentations and complexity were major stumbling blocks, but by integrating the operational advantages of a gas-lift bioreactor with the biochemical principles associated with flavour formation discussed in this work, success is more probable.

CHAPTER 9. RECOMMENDATIONS

Unlike batch beer fermentation, which has existed for thousands of years and is classified as a "mature technology", continuous beer fermentation has only received attention from researchers in recent decades. Continuous beer fermentation, a relatively new technology, thus has the capacity to make large gains in improvement through further research. Some recommendations for future research are listed below:

- Alternative immobilization methods, in addition to entrapment within kappa-carrageenan gel beads, such as self-aggregation or flocculation should be explored in the future. It would be desirable to eliminate the complexity of bead handling in a plant environment, and, if the yeast flocs were disrupted on a regular basis, one could ensure that aged cells are regularly removed from the bioreactor.
- Experimental work should continue toward eliminating the secondary holding period by optimizing the conditions in the primary continuous gas lift bioreactor.
- Reductions in the secondary holding time may be achieved in the short term by optimizing the holding temperature, the amount of sugars remaining in the liquid at the beginning of the holding period, the concentration of yeast present, the hydrodynamic characteristics of the holding vessel, and by taking further measures to eliminate oxygen from this stage.
- More research needs to be conducted to improve the activity of the enzyme α -acetolactate decarboxylase in beer medium, or to find other suitable enzymes for diacetyl control.
- New models need to be developed, where the contribution of both the immobilized and freely suspended yeast to beer flavour can be quantitatively assessed during continuous fermentation. In order to complete mass balances on oxygen, carbon dioxide and volatile flavour compounds such as acetaldehyde, esters, and alcohols, gas phase analyses also need to be performed. The model should also be based on fundamental knowledge of the yeast biochemical pathways that generate the flavour compounds in beer. The flavour model of Gee and Ramirez (1994) developed for freely suspended yeast in batch fermentations could be used as a starting point for this work.

- Another approach would be the utilization of multivariate statistical methods which create response surfaces, for studying the interaction of bioreactor operating conditions such as dilution rate, temperature and oxygen to achieve reductions in fermentation time and to further control beer flavour.
- It is recommended that the gas lift draft tube bioreactor system for continuous beer production be tested at a larger scale.

BIBLIOGRAPHY

- Abbott, B.J. 1978. Immobilized cells. In: *Annual Reports on Fermentation Processes*. Ed. Perlman, D., New York: Academic Press, 2: 91.
- Anon. 1994. Maturex[®] L. *Novo Nordisk publication*. B 560c-GB.
- Anon. 1996. Table Curve 2D. *User's Manual*. Jandel Scientific.
- Anon. 1997. Alfa Laval Brewery Systems. *Brewers' Guardian* 126: 26.
- Anon. 1998. Digox 5 Operating Manual. *Dr. Theidig publication*.
- Aquilla, T. 1997. The biochemistry of yeast: debunking the myth of yeast respiration and putting oxygen in its proper place. *Brewing Techniques* 50.
- Aschengreen, N.H., Jepsen, S. 1992. Use of acetolactate decarboxylase in brewing fermentations. *Proceedings of the 22nd Convention of the Institute of Brewing (Australia and New Zealand Section)*, Melbourne 80.
- Atkinson, B. 1986. Immobilised cells, their application and potential. In: *Process engineering aspects of immobilized cell systems*. Ed. Webb, C., Black, G.M. Atkinson, B. Manchester: Institution of Chemical Engineers 3.
- Audet, P., Paquin, C., Lacroix, C. 1988. Immobilized growing lactic acid bacteria with kappa-carrageenan – locust bean gel. *Applied Microbiology and Biotechnology* 29: 11.
- Austin, G.D., Watson, R.W.J., Nordstrom, P.A., D'Amore, T. 1994. An on-line capacitance biomass monitor and its correlation with viable biomass. *MBA Technical Quarterly* 31: 85.
- Axcell, B.C., O'Connor-Cox, E.S.C. 1996. The concept of yeast vitality - an alternative approach. *Proceedings of Convention of the Institute of Brewing (Asia Pacific Sect.)*. Singapore 24:64.
- Axelsson, A., Sisak, C., Westrin, B.A., Szajani, B. 1994. Diffusion characteristics of a swelling gel and its consequences for bioreactor performance. *The Chemical Engineering Journal* 55: B35.
- Bailey, J.E., Ollis, D.F. 1986. *Biochemical Engineering Fundamentals*. New York: McGraw-Hill, Inc.
- Bancel, S., Hu, W. 1996. Confocal laser scanning microscopy examination of cell distribution in macroporous microcarriers. *Biotechnology Progress* 12: 398.

- Barker, M.G. Smart, K.A. 1996. Morphological changes associated with the cellular aging of a brewing yeast strain. *Journal of the American Society of Brewing Chemists* 54(2): 121.
- Bejar, P., Casas, C., Godia, F., Sola, C. 1992. The influence of physical properties on the operation of a three-phase fluidized-bed fermenter with yeast cells immobilized in calcium alginate. *Applied Biochemistry and Biotechnology* 34: 467.
- Bickerstaff, G.F. 1997. Immobilization of enzymes and cells. In: *Immobilization of Enzymes and Cells*, Ed. Bickerstaff, G. F., New Jersey, U.S.A.: Humana Press, Inc. 1.
- Birnbaum, S., Pendleton, R., Larson, P., Mosbach, K. 1981. Covalent stabilization of alginate gel for the entrapment of living whole cells. *Biotechnology Letters* 3: 393.
- Budac, D., Margartis, A. 1999. *Personal communication*.
- Büyükgüngör, H. 1992. Stability of *Lactobacillus bulgaricus* immobilized in kappa-carrageenan gels. *Journal of Chemical Technology and Biotechnology* 53: 173.
- Chahal, P.S. 1992. *Fluorosensor controlled fed-batch production of Cyclosporin-A from Beauveria nivea*. Ph.D. Thesis. University of Western Ontario.
- Chisti, M.Y. 1989. *Airlift bioreactors*. London: Elsevier Applied Science.
- Chisti, Y., Moo-Young, M. 1993. Improve the performance of airlift reactors. *Chemical Engineering Progress* 6: 38.
- Cho, G.H., Choi, C.Y., Choi, Y.D., Han, M.H. 1982. Ethanol production by immobilised yeast and its carbon dioxide gas effects in a packed bed reactor. *Journal of Chemical Technology and Biotechnology* 32: 959.
- Coutts, M.W. 1956. *Britain Patent No. 872,391*.
- Curin, J., Pardonova, B., Polednikova, M., Sedova, H., Kahler, M. 1987. Beer production with immobilized yeast. *European Brewing Convention Congress*, Madrid 433.
- Dale, C.J., Hough, J.S., Young, T.W. 1986. Fractionation of high and low molecular weight components from wort and beer by adsorption chromatography using the gel Sephadex LH20. *Journal of the Institute of Brewing* 92(5): 457.
- Daoud, I.S., Searle, B.A. 1986. Yeast vitality and fermentation performance. *Monograph - XII European Brewery Convention - Symposium on Brewers' Yeast*, Helsinki 108.

- de Backer, L., Willaert, R.G., Baron, G.V. 1996. Modelling of immobilized bioprocesses. In: *Immobilized Living Cell Systems Modelling and Experimental Methods*, Ed. Willaert, R. G., Baron, G. V., and de Backer, L., Toronto: John Wiley and Sons. 47.
- de Beer, D., Van den Heuvel, J.C., Ottengraaf, S.P.P. 1993. Microelectrode measurements of the activity distribution in nitrifying bacterial aggregates. *Applied Environmental Microbiology* 59: 573.
- Debourg, A., Laurent, M., Goossens, E., Borremans, E., Van De Winkel, L., Masschelein, C.A. 1994. Wort aldehyde reduction potential in free and immobilized yeast systems. *Journal of the American Society of Brewing Chemists* 52: 100.
- Dillenhofer, W., Ronn, D. 1996. Secondary fermentation of beer with immobilized yeast. *Brauwelt International* 14: 344.
- Doran, P.M., Bailey, J.E. 1986a. Effects of hydroxyurea on immobilized and suspended yeast fermentation rates and cell cycle operation. *Biotechnology and Bioengineering* 28: 1814.
- Doran, P.M., Bailey, J.E. 1986b. Effects of immobilization on growth, fermentation properties, and macromolecular composition of *Saccharomyces cerevisiae* attached to gelatin. *Biotechnology and Bioengineering* 28: 73.
- dos Santos, V.A.P.M. Bruijnse, M., Tramper, J., Wijffels, R.H. 1996. The magic-bead concept: an integrated approach to nitrogen removal with co-immobilized micro-organisms. *Applied Microbiology and Biotechnology* 45: 447.
- Driessen, W., Habets, L., Vereijken, T. 1997. Novel anaerobic and aerobic process to meet strict effluent plant design requirements. *Proceedings of the Institute of Brewing (Asia Pacific Section)*, Auckland 148.
- Dulieu, C., Boivin, P., Dautzenberg, H., Poncelet, D. 1996. Immobilized enzyme system to avoid diacetyl formation: a new tool to accelerate beer maturation. *International Workshop on Bioencapsulation*, Potsdam 22.
- Dunbar, J., Campbell, S.L., Banks, D.J., Warren, D.R. 1988. Metabolic aspects of a commercial continuous fermentation system. *Proceedings of the Convention of the Institute of Brewing*, Brisbane 151.
- Estapé, D., Gòdia, F., Solà, C. 1992. Determination of glucose and ethanol effective diffusion coefficients in Ca-alginate gel. *Enzyme and Microbial Technology* 14: 396.
- Evans, H.A.V., Cleary, P. 1985. Direct Measurement of Yeast and Bacterial Viability. *Journal of the Institute of Brewing* 91: 73.

- Fan, L.-S. 1989. *Gas-Liquid-Solid Fluidization Engineering*. Boston: Butterworths.
- Fernandez, E. 1996. Nuclear magnetic resonance spectroscopy and imaging. In: *Immobilized Living Cell Systems: Modelling and Experimental Methods*. Toronto: John Wiley and Sons. Chapter 6.
- García, A.I., García, L.A., Díaz, M. 1994. Prediction of ester production in industrial beer fermentation. *Enzyme and Microbial Technology* 16(1): 66.
- Geankoplis, C.J. 1993. *Transport Processes and Unit Operations*. New Jersey: Prentice Hall P.T.R.
- Gee, D.A., Ramirez, W.F. 1994. A flavour model for beer fermentation. *Journal of the Institute of Brewing* 100: 321.
- Geiger, K.H., Compton, J. 1957. *Canada Patent No. 545,867*.
- Gekas, V.C. 1986. Artificial membranes as carriers for the immobilization of biocatalysts. *Enzyme and Microbial Technology* 8: 450.
- Gift, E.A., Park, H.J., Paradis, G.A., Demain, A.L., Weaver, J.C. 1996. FACS-based isolation of slowly growing cells: double encapsulation of yeast in gel microdrops. *Nature Biotechnology* 14: 884.
- Gikas, P., Livingston, A.G. 1993. Use of ATP to characterize biomass viability in freely suspended and immobilized cell bioreactors. *Biotechnology and Bioengineering* 42: 1337.
- Gikas, P., Livingston, A.G. 1996. Viability of immobilised cells: use of specific ATP levels and oxygen uptake rates. *Progress in Biotechnology 11, Immobilized Cells: Basics and Applications*, Noordwijkerhout 11:264.
- Gilson, C.D., Thomas, A. 1995. Ethanol production by alginate immobilised yeast in a fluidised bed bioreactor. *Journal of Chemical Technology and Biotechnology* 62: 38.
- Gòdia, F., Casa, C., Castellano, B., Solà, C. 1987. Immobilized cells: behavior of carrageenan entrapped yeast during continuous ethanol fermentation. *Applied Microbiology and Biotechnology* 26: 342.
- Gopal, C.V., Hammond, J.R.M. 1993. Application of immobilized yeasts for fermenting beer. *Brewing and Distilling International* 24: 72.
- Hannoun, B.J.M., Stephanopoulos, G. 1986. Diffusion coefficients of glucose and ethanol in cell-free and cell-occupied calcium alginate membranes. *Biotechnology and Bioengineering* 28: 829.
- Hardwick, W.A. 1995. *Handbook of Brewing*. New York: Marcel Dekker, Inc.

- Hayat, M.A. 1972. *Basic Electron Microscopy Techniques*. Toronto: van Nostrand Reinhold Co. 96.
- Heijnen, J.J., van Loosdrecht, M.C.M., Mulder, R., Weltevrede, R., Mulder, A. 1993. Development and scale-up of an aerobic biofilm air-lift suspension reactor. *Water Science and Technology* 27: 253.
- Higbie, R. 1935. The role of absorption of a pure gas into a still liquid during short periods of exposure. *Transactions of the American Institute of Chemical Engineers* 31: 365.
- Hines, A.L., Maddox, R.N. 1985. *Mass Transfer Fundamentals and Applications*. U.S.A.: Prentice-Hall, Inc.
- Hinfray, C., Jouenne, T., Junter, G. 1994. Ethanol production from glucose by free and agar-entrapped batch cultures of *Saccharomyces cerevisiae* at different oxygenation levels. *Biotechnology Letters* 16: 1107.
- Hoekstra, S.F. 1975. Wort composition, a review of known and unknown facts. *Proceedings of the European Brewery Convention*, Nice 465.
- Hooijmans, C.M., Ras, C., Luyben, K.Ch.A.M. 1990. Determination of oxygen profiles in biocatalyst particles by means of a combined polarographic oxygen microsensor. *Enzyme and Microbial Technology* 12: 178.
- Hough, J.S., Briggs, D.E., Stevens, R., Young, T.W. 1982. Metabolism of wort by yeast. In: *Malting and Brewing Science Volume 2 Hopped Wort and Beer*, Ed. Hough, J. S., Briggs, D. E., Stevens, R., and Young, T. W., London, U.K.: Chapman and Hall. 566.
- Hüsken, L.E., Tramper, J., Wijffels, R. 1996. Growth and eruption of gel-entrapped microcolonies. In: *Progress in Biotechnology 11, Immobilized Cells: Basics and Applications* Ed. Wijffels, R.H., Buitelaar, R.M., Bucke, C., Tramper, J., Amsterdam: Elsevier Science 336.
- Hutter, K.J. 1996. Flow-cytometric analyses for assessment of fermentative ability of various yeasts. *Brauwelt International* 1: 52.
- Hwang, S.-J., Fan, L.-S. 1986. Some design consideration of a draft tube gas-liquid-solid spouted bed. *The Chemical Engineering Journal* 33: 49.
- Imai, T. 1996. Recent advances in the determination of yeast vitality. *Proceedings of the Congress of the Institute of Brewing (Asia Pacific Section)*, Singapore 24: 60.
- Inloes, D.S., Taylor, D.P., Cohen, S.N., Michaels, A.S., Robertson, C.R. 1983. Ethanol production by *Saccharomyces cerevisiae* immobilized in hollow-fiber membrane bioreactors. *Applied and Environmental Microbiology* 46: 264.

- Inoue, T. 1987. Possibilities opened by "new biotechnology" and application of immobilized yeast to beer brewing. *Reports of the Research Laboratory of Kirin Brewery Co., Ltd.* 7.
- Inoue, T. 1992. A review of diacetyl control technology. *Proceedings of the 22nd Convention of the Institute of Brewing (Australia and New Zealand Section)*, Melbourne 76.
- Jepsen, S. 1993. Using ALDC to speed up fermentation. *Brewers' Guardian*. 55.
- Jones, M., Pierce, J.S. 1964. Absorption of amino acids from wort by yeasts. *Journal of the Institute of Brewing* 70: 307.
- Jones, R.P., Greenfield, P.F. 1984. A review of yeast ionic nutrition – Part I: growth and fermentation requirements. *Process Biochemistry* 19(2): 48.
- Jones, R.P., Pamment, N., Greenfield, P.F. 1981. Alcohol fermentation by yeast – the effect of environmental and other variables. *Process Biochemistry* 16(3): 42.
- Kara, B.V., David, I., Searle, B.A. 1987. Assessment of yeast quality. *Proceedings of the Congress of the European Brewery Convention*, Madrid, 21: 409.
- Karamanev, D.G. 1991. Model of the biofilm structure of *Thiobacillus ferrooxidans*. *Journal of Biotechnology* 10: 51.
- Karel, S.F., Libicki, S.B., Robertson, C.R. 1985. The immobilization of whole cells: engineering principles. *Chemical Engineering Science* 40: 1321.
- Kasten, F.H. 1993. Introduction to fluorescent probes: properties, history and applications. In: *Fluorescent and Luminescent Probes for Biological Activity*, Ed. Mason, W. T. London, U.K.: Academic Press Limited 12.
- Klopper, W.J. 1974. Wort composition, a survey. *European Brewery Convention Monograph 1. Wort Symposium*, Zeist 8.
- Korgel, B.A., Rotem, A., Monbouquette, H.G. 1992. Effective diffusivity of galactose in calcium alginate gels containing immobilized *Zymomonas mobilis*. *Biotechnology Progress* 8: 111.
- Kreger-Van Rij, N. 1984. *The Yeasts: A Taxonomic Study*. Amsterdam: Elsevier Science Publishers B.V.
- Kronlöf, J., Virkajärvi, I. 1996. Main fermentation with immobilized yeast - pilot scale. *Proceedings of the European Brewery Convention Brewing Science Group*, Berlin 94.
- Kunze, W. 1996. *Technology Brewing and Malting*. Berlin: VLB.

- Kuriyama, H., Ishibashi, H., Umeda, I.M.T., Kobayashi, H. 1993. Control of yeast flocculation activity in continuous ethanol fermentation. *Journal of Chemical Engineering Japan* 26(4): 429.
- Kurosawa, H., Matsamura, M., Tanaka, H. 1989. Oxygen diffusivity in gel beads containing viable cells. *Biotechnology and Bioengineering* 34: 926.
- Kurosawa, H., Tanaka, H. 1990. Advances in immobilized cell culture: development of a co-immobilized mixed culture system of aerobic and anaerobic micro-organisms. *Process Biochemistry International* 25: 189.
- Kurtzman, C.P., Fell, J.W. 1998. *The Yeasts, A Taxonomic Study, Fourth Edition*. Amsterdam: Elsevier 361.
- Kyung, K.H., Gerhardt, P. 1984. Continuous production of ethanol by yeast "immobilized" in a membrane-contained fermentor. *Biotechnology and Bioengineering* 26: 252.
- Lee, S.S., Robinson, F.M., Wang, H.Y. 1981. Rapid determination of yeast viability. *Biotechnology and Bioengineering Symposium No. 11*, Gatlingburg, USA 641.
- Lentini, A. 1993. A review of the various methods available for monitoring the physiological status of yeast: yeast viability and vitality. *Ferment* 6: 321.
- Lentini, A., Takis, S., Hawthorne, D.B., Kavanagh, T.E. 1994. The influence of trub on fermentation and flavour development. *Proceedings of the 23rd Convention of the Institute of Brewing (Asia Pacific Section)*, Sydney 89.
- Leudeking, R. 1967. Fermentation process kinetics. In: *Biochemical and Biological Engineering*, Ed. Blakebrough, N., London: Academic Press, Inc. 203.
- Leudeking, R., Piret, E.L. 1959. A kinetic study of the lactic acid fermentation. *Journal of Biochemical and Microbiological Technology and Engineering* 1: 393.
- Lewandowski, Z., Altobelli, A., Fukushima, E. 1993. NMR and microelectrode studies of hydrodynamics and kinetics in biofilms. *Biotechnology Progress* 9: 40.
- Lewandowski, Z., Stoodley, P., Altobelli, S. 1995. Experimental and conceptual studies on mass transport in biofilms. *Water Science Technology* 31: 153.
- Lewis, M., Young, T. 1995. *Brewing*. London: Chapman and Hall.
- Li, J., Humphrey, A.E. 1991. Use of fluorometry for monitoring and control of a bioreactor. *Biotechnology and Bioengineering* 37: 1043.
- Lim, H.-S., Han, B.-K., Kim, J.-H., Peshwa, M.V, Hu, W.-S. 1992. Spatial distribution of mammalian cells grown on macroporous microcarriers with improved attachment kinetics. *Biotechnology Progress* 8: 486.

- Linko, M., Virkajarvi, I., Pohjala, N. 1996. Effect of flocculation characteristics on immobilized yeast performance. *European Brewery Convention Brewing Science Group*, Berlin 102.
- Lloyd, D., Moran, C.A., Suller, M.T.E., Dinsdale, M.G. 1996. Flow cytometric monitoring of rhodamine 123 and a cyanine dye uptake by yeast during cider fermentation. *Journal of Institute of Brewing* 102: 251.
- Lundberg, P., Kuchel, P.W. 1997. Diffusion of solutes in agarose and alginate gels: ^1H and ^{23}Na PFGSE and ^{23}Na TQF NMR studies. *Magnetic Resonance in Medicine* 37: 44.
- Margaritis, A., te Bokkel, D.W., El Kashab, M. 1987. Repeated batch fermentation of ethanol using immobilized cells of *Saccharomyces cerevisiae* in a fluidized bioreactor system. In: *Biological Research on Industrial Yeasts*, Ed. Stewart, G.G., Russell, I., Klein, R.D., Hiebsch, R.R., Boca Raton: CRC Press 121.
- Margaritis, A., Wallace, J.B. 1982. The use of immobilized cells of *Zymomonas mobilis* in a novel fluidized bioreactor to produce ethanol. *Biotechnology and Bioengineering Symposium* 147.
- Margaritis, A., Wilke, C.R. 1978a. The rotorfermentor. Part I: description of the apparatus, power requirements, and mass transfer characteristics. *Biotechnology and Bioengineering* 20: 709.
- Margaritis, A., Wilke, C.R. 1978b. The rotorfermentor. Part II: application to ethanol fermentation. *Biotechnology and Bioengineering* 20: 727.
- Marrs, W.M. 1998. The stability of carrageenans to processing. In: *Gums and Stabilizers for the Food Industry 9*, Cambridge: Royal Society of Chemistry, 218: 3-45.
- Martens, F.B., Egberts, G.T.C., Kempers, J., Robles de Medina, M.H.L., Welton, H.G. 1986. *European Brewery Convention Monograph XII, Symposium on Brewing Yeast*, Helsinki 339.
- Masschelein, C.A. 1990. Yeast metabolism and beer flavour. Proceedings of the Third Aviemore Conference on Malting, Brewing and Distilling 103.
- Masschelein, C.A., Carlier, A., Ramos-Jeunehomme, C., Abe, I. 1985. The effect of immobilization on yeast physiology and beer quality in continuous and discontinuous systems. *Proceedings of the 20th European Brewery Convention Congress*, Helsinki 339.
- Masschelein, C.A., Ramos-Jeunehomme, C. 1985. The potential of alginate immobilized yeast in brewery fermentations. *Institute of Brewing Central and Southern African Section Proceedings of the 1st Scientific and Technical Convention*, Johannesburg 392.

- Masschelein, C.A., Vandenbussche, J. 1999. Current outlook and future perspectives for immobilized yeast technology in the brewing industry. *Brewers' Guardian* 28(4): 35.
- Masters, B.R., Thaer, A.A. 1994. Real-time scanning slit confocal microscopy of the *in vivo* human cornea. *Applied Optics* 33: 695.
- Meilgaard, M. 1982. Prediction of flavor differences between beers from their chemical composition. *Brygmesteren* 5.
- Mensour, N., Margaritis, A., Briens, C.L., Pilkington, H., Russell, I. 1996. Application of immobilized yeast cells in the brewing industry. In: *Progress in Biotechnology 11, Immobilized Cells: Basics and Applications* Ed. Wijffels, R.H., Buitelaar, R.M., Bucke, C., Tramper, J., Amsterdam: Elsevier Science 661.
- Mensour, N., Margaritis, A., Briens, C.L., Pilkington, H., Russell, I. 1997. New Developments in the Brewing Industry Using Immobilized Yeast Cell Bioreactor Systems. *Journal of the Institute of Brewing* 103: 363.
- Merchant, F.J.A. 1986. *Diffusivity Characteristics of Glucose in Alginate Immobilization Matrices*. Ph.D. Thesis. University of Western Ontario.
- Merchant, F.J.A., Margaritis, A., Wallace, J.B. 1987. A novel technique for measuring solute diffusivities in entrapment matrices used in immobilization. *Biotechnology and Bioengineering* 30: 936.
- Mochaba, F.M. 1997. A novel and practical yeast vitality method based on magnesium ion release. *Journal of the Institute of Brewing* 103: 99.
- Mochaba, F., O'Connor-Cox, E.S.C., Axcell, B.C. 1998. Practical procedures to measure yeast viability and vitality prior to pitching. *Journal of the American Society of Brewing Chemists* 56(1): 1.
- Muhr, A.H., Blanshard, J.M.V. 1982. Diffusion in gels. *Polymer* 23: 1012.
- Mulder, M.H.V., Smolders, C.A. 1986. Continuous ethanol production controlled by membrane processes. *Process Biochemistry* 21: 35.
- Nakanishi, K., Murayama, H., Nagara, A., Mitsui, S. 1993. Beer brewing using an immobilized yeast bioreactor system. *Bioprocess Technology* 16: 275.
- Nakanishi, K., Onaka, T., Inoue, T. 1986. A new immobilized yeast reactor system for rapid production of beer. *Reports of the Research Laboratory of Kirin Brewing Company* 13.
- Nakatani, K., Takahashi, T., Nagami, K., Kumada, J. 1984a. Kinetic study of vicinal diketones in brewing (I) formation of total vicinal diketones. *MBAA Technical Quarterly* 21(2): 73.

- Nakatani, K., Takahashi, T., Nagami, K., Kumada, J. 1984b. Kinetic study of vicinal diketones in brewing (II) theoretical aspect for the formation of total vicinal diketones. *MBAA Technical Quarterly* 21(4): 175.
- Nakatani, K., Fukui, N., Nagami, K., Nishigaki, M. 1991. Kinetic analysis of ester formation during beer fermentation. *Journal of the American Society of Brewing Chemists* 49(4): 152.
- Narziß, L., Miedaner, H., Graf, P., Eichhorn, P., Lustig, S. 1993. Technological approach to improve flavour stability. *MBAA Technical Quarterly* 30: 48.
- Nava Saucedo, J.E., Roisin, C., Barbotin, J.-N. 1996. Complexity and heterogeneity of microenvironments in immobilized systems. *Progress in Biotechnology 11, Immobilized Cells: Basics and Applications*, Noordwijkerhout 39.
- Nedovic, A.N., Vunjak-Novakovic, G., Leskosek-Cukalovic, I., Cutkovic, M. 1996. A study on considerably accelerated fermentation of beer using an airlift bioreactor with calcium alginate entrapped yeast cells. *Fifth World Congress of Chemical Engineering* 2: 474.
- Neufeld, R. J., Poncelet, D.J., Norton, S.D. 1996. *Application for Canadian Patent No. 2133789*.
- Norton, S., D'Amore, T. 1994. Physiological effects of yeast cell immobilization: applications for brewing. *Enzyme and Microbial Technology* 16: 365.
- Norton, S., Watson, K., D'Amore, T. 1995. Ethanol tolerance of immobilized brewer's yeast cells. *Applied Microbiology and Biotechnology* 43: 18.
- O'Connor-Cox, E., Mochaba, F.M., Lodolo, E.J., Majara, M., Axcell, B. 1997. Methylene blue staining: use at your own risk. *MBAA Technical Quarterly* 34(1): 306.
- O'Reilly, A.M., Scott, J.A. 1995. Defined coimmobilization of mixed microorganism cultures. *Enzyme and Microbial Technology* 17: 636.
- Okazaki, M., Hamada, T., Fujji, H., Mizobe, A., Matsuzawa, S. 1995. Development of poly(vinyl alcohol) hydrogel for waste water cleaning. I. Study of poly(vinyl alcohol) gel as a carrier for immobilizing organisms. *Journal of Applied Polymer Science* 58: 2235.
- Oldshue, J.Y., Herbst, N.R. 1992. *A Guide to Fluid Mixing*. New York: Lightnin.
- Opekarova, M., Sigler, K. 1982. Acidification power: indicator of metabolic activity and autolytic changes in *Saccharomyces cerevisiae* (yeast). *Folia Microbiologica* 27: 395.

- Oyaas, J., Storro, I., Svendsen, H., Levine, D.W. 1995. The effective diffusion coefficient and the distribution constant for small molecules in calcium-alginate gel beads. *Biotechnology and Bioengineering* 47: 492.
- Paiva, T.C.B., Sato, S., Visconti, A.E.S., Castro, L.A.B. 1996. Continuous alcoholic fermentation process in a tower reactor with recycling of flocculating yeast. *Applied Biochemistry and Biotechnology* 57-58(0): 55.
- Pajunen, E., Makinen, V., Gisler, R. 1987. *Secondary fermentation with immobilized yeast. European Brewery Convention Congress*, Madrid 441.
- Parascandola, P., de Alteriis, E. 1996. Pattern of growth and respiratory activity of *Saccharomyces cerevisiae* (baker's yeast) cells growing entrapped in an insolubilized gelatin gel. *Biotechnology and Applied Biochemistry* 23: 7.
- Perry, R.H., Green, D.W. 1984. *Perry's Chemical Engineers' Handbook*. New York: McGraw-Hill Book Company.
- Pilkington, P.H., Margaritis, A., Mensour, N.A. 1998a. Mass transfer characteristics of immobilized cells used in fermentation processes. *Critical Reviews in Biotechnology* 18(2 & 3): 237.
- Pilkington, P.H., Margaritis, A., Mensour, N.A., Russell, I. 1998b. Fundamentals of immobilized yeast cells for continuous beer fermentation: a review. *Journal of the Institute of Brewing* 104: 19.
- Pilkington, H., Margaritis, A., Mensour, N., Sobczak, J., Hancock, I., Russell, I. 1999. Kappa-carrageenan gel immobilization of lager brewing yeast. *Journal of the Institute of Brewing* 105(6): 398.
- Polson, A. 1950. Some aspects of diffusion in solution and a definition of a colloidal particle. *Journal of Physical and Colloidal Chemistry* 54: 649.
- Power, D.A., McCuen, P.J. 1988. *Manual of BBL[®] Products and Laboratory Procedures, Sixth Edition*. Maryland: Becton Dickinson Microbiology Systems 249.
- Priest, F.G., Campbell, I. 1996. *Brewing Microbiology 2nd Ed.*, UK: Chapman and Hall.
- Rees, D.A. 1972. Polysaccharide gels: a molecular view. *Chemistry and Industry* 19: 630.
- Roca, E., Camesselle, C., Nunez, M. 1995. Continuous ethanolic fermentation by *Saccharomyces cerevisiae* immobilised in Ca-alginate beads hardened with Al³⁺. *Biotechnology Letters* 9: 815.
- Roukas, T. 1994. Continuous ethanol production from carob pod extract by immobilized *Saccharomyces cerevisiae* in a packed-bed reactor. *Journal of Chemical Technology and Biotechnology* 59: 387.

- Russell, I., Stewart, G.G. 1992. Contribution of yeast and immobilization technology to flavour development in fermented beverages. *Food Technology* 148.
- Ryder, D.S. 1985. The growth process of brewing yeast and the biotechnological challenge. *MBAA Technical Quarterly* 22: 124.
- Ryu, D.D., Kim, Y.J., Kim, J.H. 1984. Effect of air supplement on the performance of continuous ethanol fermentation system. *Biotechnology and Bioengineering* 26: 12.
- Salmon, P.M., Robertson, C.R. 1987. Mass transfer limitations in gel beads containing growing immobilized cells. *Journal of Theoretical Biology* 125: 325.
- Schumpe, A., Quicker, G., Deckwer, W.-D. 1982. Gas solubilities in microbial culture media. *Advances in Biochemical Engineering* 24: 1.
- Shindo, S., Sahara, H., Koshino, S. 1994. Suppression of alpha-acetolactate formation in brewing with immobilized yeast. *Journal of the Institute of Brewing* 100: 69.
- Smart, K.A. 1995. The importance of the brewing yeast cell wall. *Brewers' Guardian* 124(4): 44.
- Smart, K.A. 1999. Ageing in brewing yeast. *Brewers' Guardian* 19.
- Smart, K.A., Chambers, K.M., Lambert, I., Jenkins, C. 1999. Use of methylene violet procedures to determine yeast viability and vitality. *Journal of the American Society of Brewing Chemists* 57(1):18.
- Sharpe, F.R. 1988. Assessment and control of beer flavour. *Journal of the Institute of Brewing* 95: 301.
- Stewart, G.G. 1977. Fermentation – yesterday, today and tomorrow. *MBAA Technical Quarterly* 14: 1.
- Stewart, G.G., Russell, I. 1986. The relevance of the flocculation properties of yeast in today's brewing industry. *European Brewery Convention Symposium on Brewers' Yeast*, Helsinki 53.
- Stewart, G.G., Lyness, A., Younis, O. 1999. The control of ester synthesis during wort fermentation. *MBAA Technical Quarterly* 36(1): 61.
- Takahashi, S. and Kimura, Y. 1996. Effect of main fermentation parameters on stale flavour. *Brauwelt International* 14 (3): 253.
- Taylor, D.G. 1989. Influence of brewhouse practice on wort composition. *Brewer's Guardian* 118(2): 30.
- Technical Committee and Editorial Committee of the American Society of Brewing Chemists (ASBC). 1992. *Methods of Analysis*. 8th Edition. Minnesota: ASBC.

- Uttamlal, M., Walt, D.R. 1995. A fiber-optic carbon dioxide sensor for fermentation monitoring. *Biotechnology* 13: 597.
- Venâncio, A., Teixeira, J.A. 1997. Characterization of sugar diffusion coefficients in alginate membranes. *Biotechnology Techniques* 11: 183.
- Vilachá, C., Uhlig, K. 1985. The measurement of low levels of oxygen in bottled beer. *Brauwelt International* 70.
- Virkajärvi, I., Kronlöf, J. 1998. Long-term stability of immobilized yeast columns in primary fermentation. *Journal of the American Society of Brewing Chemists* 56(2): 70.
- Vives, C., Casas, C., Gòdia, F., Solà, C. 1993. Determination of the intrinsic fermentation kinetics of *Saccharomyces cerevisiae* cells immobilized in calcium alginate beads and observation on their growth. *Applied Microbiology and Biotechnology* 38: 467.
- Wada, M., Kato, J., Chibata, I. 1979. A new immobilization of microbial cells. *European Journal of Applied Microbiology and Biotechnology* 8: 241.
- Wang, H.Y., Lee, S.S., Takach, Y., Cawthon, L. 1982. Maximizing microbial cell loading in immobilized-cell systems. *Biotechnology and Bioengineering Symp. No. 12* 139.
- Westrin, B.A., Axelsson, A. 1991. Diffusion in gels containing immobilized cells: a critical review. *Biotechnology and Bioengineering* 38: 439.
- Wheatcroft, R., Lim, Y.M., Hawthorne, D.B., Clarke, B.J., Kavanagh, T.E. 1988. An assessment of the use of specific oxygen uptake measurements to predict the fermentation performance of brewing yeasts. *The Institute of Brewing (Australia and New Zealand Section) Proceedings of the Twentieth Convention*, Brisbane 193.
- White, F.H., Portno, A.D. 1978. Continuous fermentation by immobilized brewers yeast. *Journal of the Institute of Brewing* 84: 228.
- Wijffels, R.H., de Gooijer, C.D., Schepers, A.W., Tramper, J. 1996. Immobilized-cell growth: diffusion limitation in expanding micro-colonies. In: *Progress in Biotechnology 11, Immobilized Cells: Basics and Applications* Ed. Wijffels, R.H., Buitelaar, R.M., Bucke, C., Tramper, J., Amsterdam: Elsevier Science 249.
- Wijffels, R.H., Englund, G., Hunik, J.H., Leenen, J.T.M., Bakketun, A. et al. 1995. Effects of diffusion limitation on immobilized nitrifying microorganisms at low temperatures. *Biotechnology and Bioengineering* 45: 1.

- Wijffels, R.H. 1994. *Nitrification by immobilized cells*. Ph.D. Thesis. Wageningen Agricultural University.
- Willaert, R.G., de Backer, L., Baron, G.V. 1996. Mass transfer in immobilized cell systems. In *Immobilized Living Cell Systems Modelling and Experiments*, Ed. Willaert, R. G., Baron, G. V., and de Backer, L. Toronto: John Wiley and Sons. 21.
- Yamauchi, Y., Okamoto, T., Murayama, H., Nagara, A., Kashihara, T., Nakamishi, K. 1994. Beer brewing using an immobilized yeast bioreactor design of an immobilized yeast bioreactor for rapid beer brewing system. *Journal of Fermentation and Bioengineering* 78: 443.
- Yamauchi, Y., Okamoto, T., Murayama, H., Nagara, A., Kashihara, T. et al. 1995. Rapid fermentation of beer using an immobilized yeast multistage bioreactor system: balance control of extract and amino acid uptake. *Applied Biochemistry and Biotechnology* 53: 245.

APPENDIX 1

Tabulation of experimental results for Tables and Figures in main text.

Mixing time data for section 5.1.3.

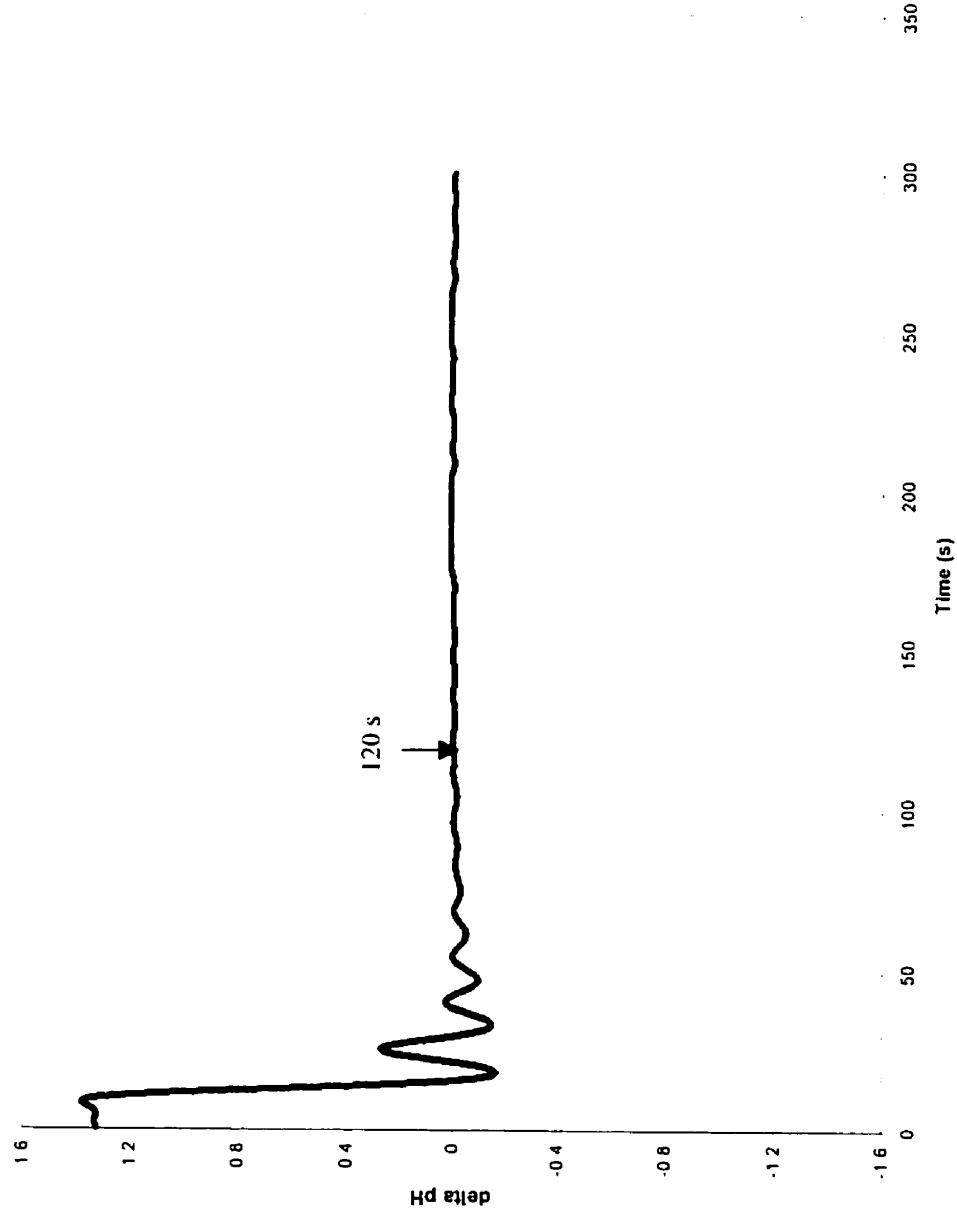


Figure A1.1. Bioreactor pH versus time, where time, $t = 0$ was taken at the time of acid injection. The data was smoothed using the Savitzky-Golay method. The volumetric flow rate of gas was 283 mL/min at STP.

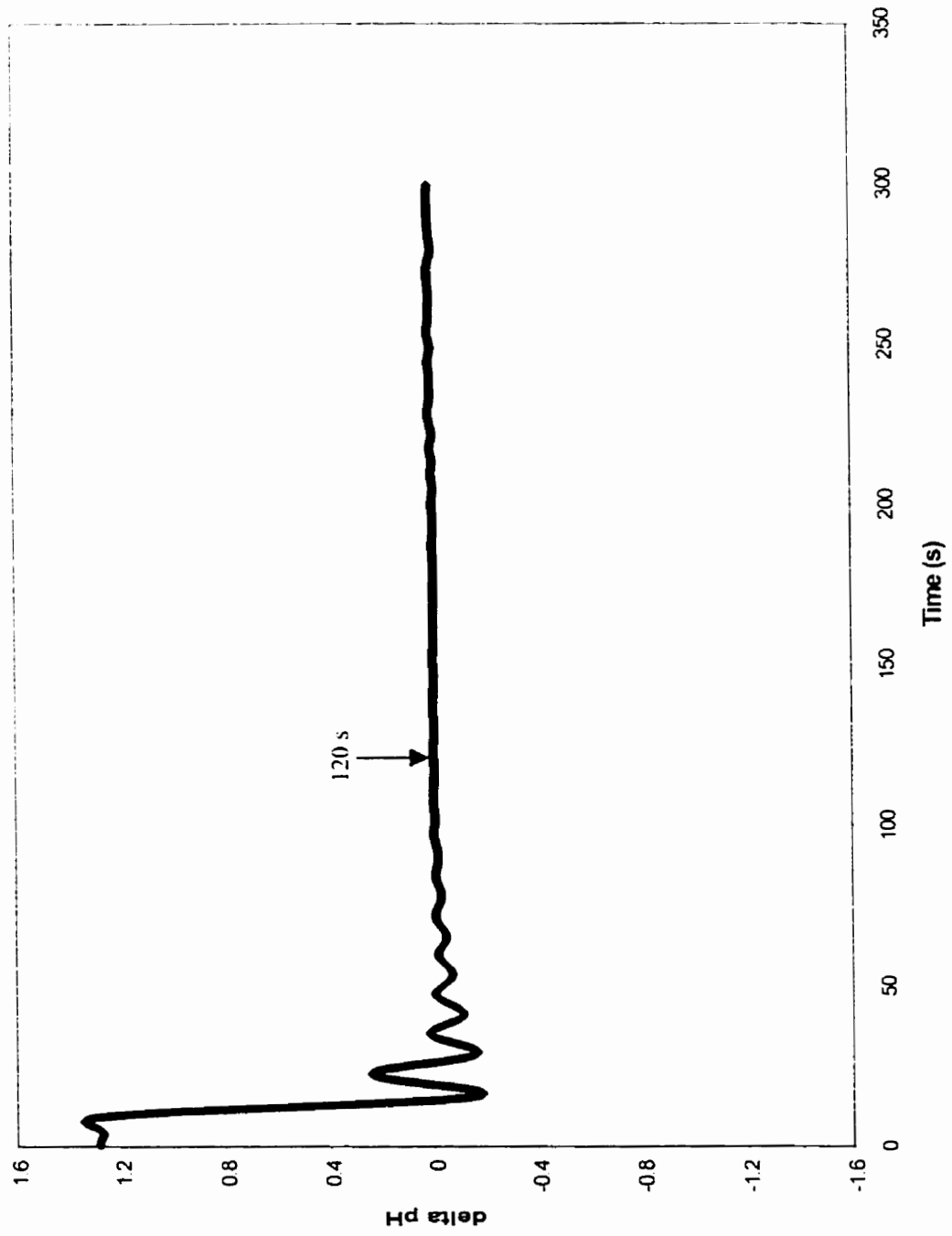


Figure A1.2. Bioreactor pH versus time, where time, $t = 0$ was taken at the time of acid injection. The data was smoothed using the Savitzky-Golay method. The volumetric flow rate of gas was 472 ml./min at STP.

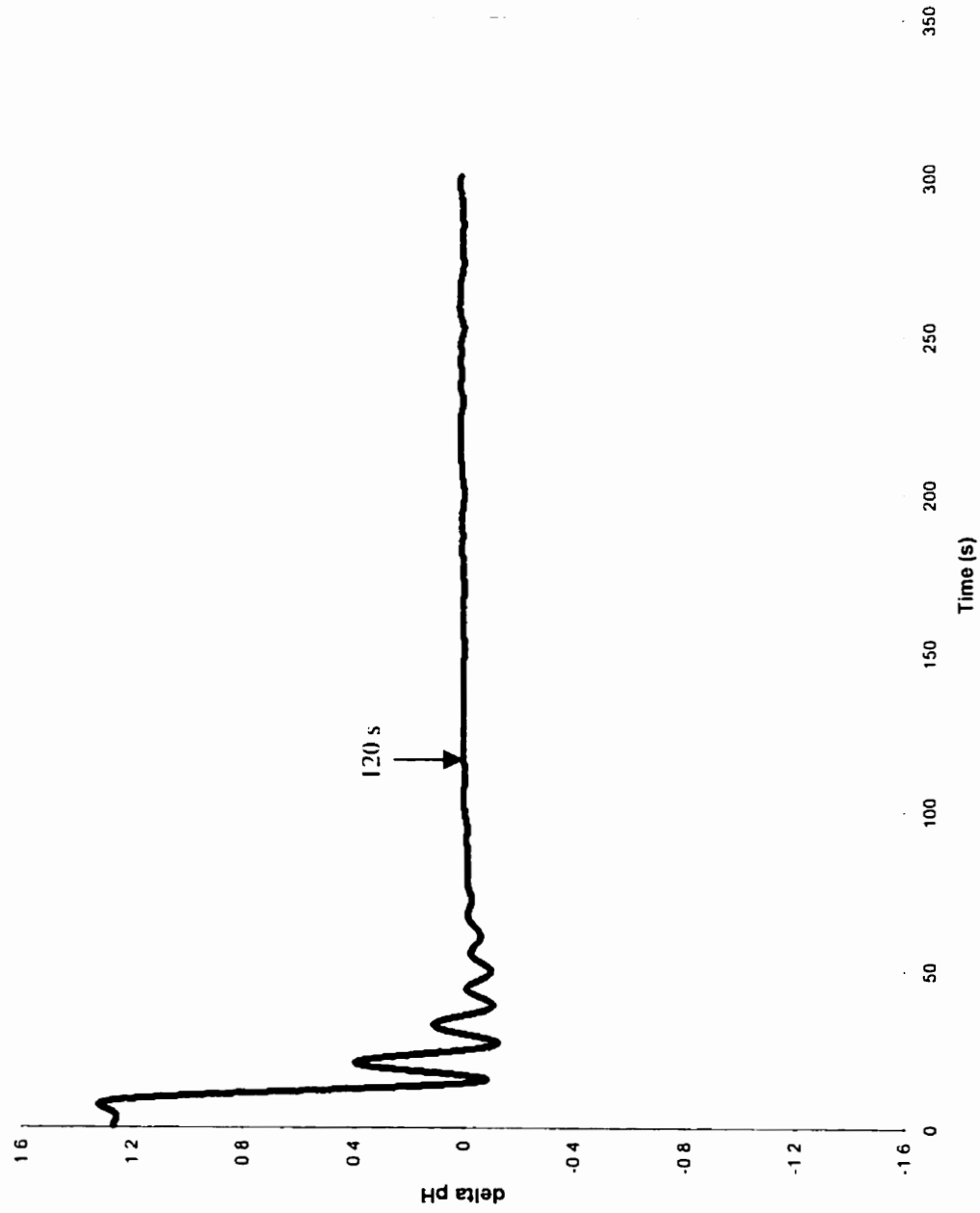


Figure A1.3. Bioreactor pH versus time, where time, $t = 0$ was taken at the time of acid injection. The data was smoothed using the Savitzky-Golay method. The volumetric flow rate of gas was 472 mL/min at STP

Experimental data used to obtain a particle size distribution for kappa-carrageenan gel beads, given in Figure 5.8.

Table A1.1. Particle size data for kappa-carrageenan gel beads.

Grid Size (mm)	Mass of Beads (g)					Average	Average % (w/w)	SE of Average % (w/w)
	Sample 1	Sample 2	Sample 3	Sample 4	Sample 5			
0.5-1	102.93	104.23	89.88	91.03	94.23	96.46	19.86	0.005
1-1.18	83.54	171.68	86.74	104.47	99.19	109.12	22.47	0.024
1.18-1.4	145.78	117.79	101.38	114.67	137.87	123.50	25.43	0.02
1.4-1.7	108.83	122.08	162.69	104.77	87.74	117.22	24.14	0.026
1.7-2.0	56.47	47.45	31.84	32.69	27.95	39.28	8.09	0.0091
Total	497.55	563.23	472.53	447.63	446.98	485.58	100.00	

Table A1.2. Cumulative particle size data calculated from Table A1.1 and used for Figure 5.8.

Grid Size (mm)	% (w/w) Undersize	Cumulative % Undersize
0.5	0.00	0.00
1	19.86	19.86
1.18	22.47	42.34
1.4	25.43	67.77
1.7	24.14	91.91
2	8.09	100.00

Table Curve 2D was used to determine a function of best-fit for the data of particle size versus cumulative % undersize in Table A1.2. The function is given in Equation A.1.

$$D_{pi} = 0.5 a (1 + \operatorname{erf}((X - b) / (2^{0.5} c))) \quad \text{A.1}$$

where $a = 1.0034107$, $b = 1.2537128$, $c = 0/31376046$

and $r^2 = 0.9993636$

See Appendix 2 for statistical definitions.

Table A1.3. Fitted data using equation A.1, for calculation of Sauter mean diameter and arithmetic mean diameter for kappa-carrageenan gel beads.

Particle Diameter D_{pi} , (mm)	Cumulative Undersize X_i , (w/w)	Delta Undersize $dif(X_i)$	Normalized Delta Undersize $n[dif(X_i)]$	X_i / D_{pi}	$X_i * D_{pi}$
0.5	0.008176	0.008176	0.008220	0.016440	0.004110
0.51	0.008917	0.000740	0.000744	0.001459	0.000380
0.52	0.009715	0.000798	0.000803	0.001544	0.000417
0.53	0.010575	0.000860	0.000865	0.001632	0.000458
0.54	0.011501	0.000926	0.000931	0.001723	0.000503
0.55	0.012496	0.000995	0.001001	0.001819	0.000550
0.56	0.013565	0.001069	0.001075	0.001919	0.000602
0.57	0.014712	0.001147	0.001153	0.002023	0.000657
0.58	0.015942	0.001230	0.001236	0.002131	0.000717
0.59	0.017259	0.001317	0.001324	0.002244	0.000781
0.6	0.018667	0.001409	0.001416	0.002360	0.000850
0.61	0.020173	0.001505	0.001513	0.002481	0.000923
0.62	0.021780	0.001607	0.001616	0.002606	0.001002
0.63	0.023493	0.001714	0.001723	0.002735	0.001085
0.64	0.025319	0.001826	0.001836	0.002868	0.001175
0.65	0.027262	0.001943	0.001954	0.003006	0.001270
0.66	0.029329	0.002066	0.002077	0.003147	0.001371
0.67	0.031523	0.002195	0.002206	0.003293	0.001478
0.68	0.033852	0.002329	0.002341	0.003443	0.001592
0.69	0.036320	0.002468	0.002482	0.003596	0.001712
0.7	0.038934	0.002614	0.002628	0.003754	0.001839
0.71	0.041699	0.002765	0.002780	0.003915	0.001974
0.72	0.044621	0.002922	0.002938	0.004080	0.002115
0.73	0.047706	0.003085	0.003101	0.004248	0.002264
0.74	0.050960	0.003253	0.003271	0.004420	0.002420
0.75	0.054387	0.003428	0.003446	0.004595	0.002584
0.76	0.057995	0.003608	0.003627	0.004772	0.002756
0.77	0.061788	0.003793	0.003813	0.004952	0.002936
0.78	0.065772	0.003984	0.004005	0.005135	0.003124
0.79	0.069952	0.004180	0.004203	0.005320	0.003320
0.8	0.074334	0.004382	0.004405	0.005507	0.003524
0.81	0.078923	0.004589	0.004613	0.005695	0.003737
0.82	0.083724	0.004800	0.004826	0.005885	0.003957
0.83	0.088740	0.005016	0.005043	0.006076	0.004186
0.84	0.093977	0.005237	0.005265	0.006268	0.004423
0.85	0.099439	0.005462	0.005491	0.006460	0.004667
0.86	0.105129	0.005690	0.005721	0.006652	0.004920
0.87	0.111052	0.005923	0.005954	0.006844	0.005180
0.88	0.117210	0.006158	0.006191	0.007035	0.005448
0.89	0.123606	0.006396	0.006430	0.007225	0.005723
0.9	0.130243	0.006637	0.006672	0.007414	0.006005
0.91	0.137123	0.006880	0.006916	0.007601	0.006294
0.92	0.144247	0.007124	0.007162	0.007785	0.006589
0.93	0.151617	0.007370	0.007409	0.007967	0.006891
0.94	0.159233	0.007616	0.007657	0.008146	0.007197
0.95	0.167096	0.007863	0.007905	0.008321	0.007509

Particle Diameter D_{pi} , (mm)	Cumulative Undersize X_i , (w/w)	Delta Undersize $dif(X_i)$	Normalized Delta Undersize $n[dif(X_i)]$	X_i / D_{pi}	$X_i * D_{pi}$
0.96	0.175205	0.008109	0.008152	0.008492	0.007826
0.97	0.183560	0.008355	0.008399	0.008659	0.008147
0.98	0.192159	0.008599	0.008645	0.008821	0.008472
0.99	0.201000	0.008841	0.008888	0.008978	0.008800
1	0.210081	0.009081	0.009130	0.009130	0.009130
1.01	0.219400	0.009318	0.009368	0.009275	0.009462
1.02	0.228951	0.009552	0.009603	0.009415	0.009795
1.03	0.238733	0.009781	0.009834	0.009547	0.010129
1.04	0.248739	0.010006	0.010060	0.009673	0.010462
1.05	0.258965	0.010226	0.010280	0.009791	0.010794
1.06	0.269404	0.010440	0.010495	0.009901	0.011125
1.07	0.280051	0.010647	0.010704	0.010004	0.011453
1.08	0.290899	0.010848	0.010905	0.010098	0.011778
1.09	0.301939	0.011041	0.011100	0.010183	0.012099
1.1	0.313165	0.011226	0.011286	0.010260	0.012414
1.11	0.324567	0.011402	0.011463	0.010327	0.012724
1.12	0.336137	0.011570	0.011632	0.010386	0.013028
1.13	0.347866	0.011728	0.011791	0.010434	0.013324
1.14	0.359742	0.011877	0.011940	0.010474	0.013612
1.15	0.371757	0.012015	0.012079	0.010503	0.013890
1.16	0.383898	0.012142	0.012207	0.010523	0.014160
1.17	0.396156	0.012258	0.012323	0.010533	0.014418
1.18	0.408519	0.012363	0.012429	0.010533	0.014666
1.19	0.420974	0.012455	0.012522	0.010523	0.014901
1.2	0.433511	0.012536	0.012603	0.010503	0.015124
1.21	0.446115	0.012605	0.012672	0.010473	0.015333
1.22	0.458776	0.012661	0.012729	0.010433	0.015529
1.23	0.471481	0.012704	0.012772	0.010384	0.015710
1.24	0.484216	0.012735	0.012803	0.010325	0.015876
1.25	0.496969	0.012753	0.012821	0.010257	0.016026
1.26	0.509726	0.012758	0.012826	0.010179	0.016160
1.27	0.522476	0.012749	0.012818	0.010093	0.016278
1.28	0.535204	0.012728	0.012796	0.009997	0.016379
1.29	0.547898	0.012694	0.012762	0.009893	0.016463
1.3	0.560546	0.012648	0.012715	0.009781	0.016530
1.31	0.573135	0.012588	0.012656	0.009661	0.016579
1.32	0.585651	0.012517	0.012583	0.009533	0.016610
1.33	0.598084	0.012433	0.012499	0.009398	0.016624
1.34	0.610421	0.012337	0.012403	0.009256	0.016619
1.35	0.622650	0.012229	0.012294	0.009107	0.016597
1.36	0.634760	0.012110	0.012175	0.008952	0.016558
1.37	0.646740	0.011980	0.012044	0.008791	0.016500
1.38	0.658579	0.011839	0.011903	0.008625	0.016425
1.39	0.670267	0.011688	0.011751	0.008454	0.016334
1.4	0.681795	0.011528	0.011589	0.008278	0.016225
1.41	0.693153	0.011358	0.011418	0.008098	0.016100
1.42	0.704332	0.011179	0.011239	0.007914	0.015959
1.43	0.715323	0.010992	0.011050	0.007727	0.015802
1.44	0.726120	0.010797	0.010854	0.007538	0.015630

Particle Diameter D_{pi} , (mm)	Cumulative Undersize X_i , (w/w)	Delta Undersize $dif(X_i)$	Normalized Delta Undersize $n[dif(X_i)]$	X_i / D_{pi}	$X_i * D_{pi}$
1.45	0.736714	0.010594	0.010651	0.007345	0.015444
1.46	0.747099	0.010385	0.010441	0.007151	0.015243
1.47	0.757269	0.010170	0.010224	0.006955	0.015029
1.48	0.767218	0.009949	0.010002	0.006758	0.014803
1.49	0.776940	0.009723	0.009775	0.006560	0.014564
1.5	0.786433	0.009492	0.009543	0.006362	0.014314
1.51	0.795690	0.009258	0.009307	0.006164	0.014054
1.52	0.804710	0.009020	0.009068	0.005966	0.013783
1.53	0.813489	0.008779	0.008826	0.005769	0.013504
1.54	0.822025	0.008536	0.008582	0.005573	0.013216
1.55	0.830317	0.008292	0.008336	0.005378	0.012920
1.56	0.838362	0.008046	0.008089	0.005185	0.012618
1.57	0.846162	0.007799	0.007841	0.004994	0.012310
1.58	0.853714	0.007553	0.007593	0.004806	0.011997
1.59	0.861021	0.007306	0.007345	0.004620	0.011679
1.6	0.868082	0.007061	0.007099	0.004437	0.011358
1.61	0.874899	0.006817	0.006853	0.004257	0.011034
1.62	0.881474	0.006575	0.006610	0.004080	0.010708
1.63	0.887809	0.006335	0.006369	0.003907	0.010381
1.64	0.893906	0.006097	0.006130	0.003738	0.010053
1.65	0.899768	0.005863	0.005894	0.003572	0.009725
1.66	0.905400	0.005631	0.005661	0.003410	0.009398
1.67	0.910803	0.005404	0.005432	0.003253	0.009072
1.68	0.915983	0.005180	0.005208	0.003100	0.008749
1.69	0.920943	0.004960	0.004987	0.002951	0.008428
1.7	0.925689	0.004745	0.004771	0.002806	0.008110
1.71	0.930224	0.004535	0.004559	0.002666	0.007796
1.72	0.934554	0.004330	0.004353	0.002531	0.007487
1.73	0.938683	0.004129	0.004151	0.002400	0.007182
1.74	0.942617	0.003934	0.003955	0.002273	0.006882
1.75	0.946362	0.003745	0.003765	0.002151	0.006588
1.76	0.949923	0.003561	0.003580	0.002034	0.006300
1.77	0.953305	0.003382	0.003400	0.001921	0.006019
1.78	0.956515	0.003209	0.003227	0.001813	0.005743
1.79	0.959557	0.003042	0.003059	0.001709	0.005475
1.8	0.962438	0.002881	0.002896	0.001609	0.005214
1.81	0.965164	0.002726	0.002740	0.001514	0.004960
1.82	0.967740	0.002576	0.002590	0.001423	0.004713
1.83	0.970171	0.002432	0.002445	0.001336	0.004474
1.84	0.972465	0.002294	0.002306	0.001253	0.004243
1.85	0.974626	0.002161	0.002173	0.001174	0.004019
1.86	0.976660	0.002034	0.002045	0.001099	0.003803
1.87	0.978573	0.001913	0.001923	0.001028	0.003596
1.88	0.980369	0.001796	0.001806	0.000961	0.003395
1.89	0.982055	0.001686	0.001695	0.000897	0.003203
1.9	0.983635	0.001580	0.001589	0.000836	0.003019
1.91	0.985115	0.001480	0.001488	0.000779	0.002842
1.92	0.986499	0.001384	0.001392	0.000725	0.002672
1.93	0.987793	0.001294	0.001301	0.000674	0.002510

Particle Diameter D_{pi} , (mm)	Cumulative Undersize X_i , (w/w)	Delta Undersize $dif(X_i)$	Normalized Delta Undersize $n[dif(X_i)]$	X_i / D_{pi}	$X_i * D_{pi}$
1.94	0.989001	0.001208	0.001214	0.000626	0.002356
1.95	0.990128	0.001127	0.001133	0.000581	0.002209
1.96	0.991178	0.001050	0.001055	0.000538	0.002068
1.97	0.992155	0.000977	0.000982	0.000499	0.001935
1.98	0.993063	0.000908	0.000913	0.000461	0.001808
1.99	0.993907	0.000844	0.000848	0.000426	0.001688
2	0.994690	0.000783	0.000787	0.000394	0.001574
Total		0.994690	1.000000	0.856078	1.252066

Experimental data used for Tables 6.1 – 6.2 and Figures 6.4 – 6.6.

Table A1.4. Carbohydrate and ethanol batch fermentation data for repeated batch fermentations, R1.

R1		Concentration (kg / m ³)			
Time (h)	Maltose	Maltotriose	Glucose	Fructose	Ethanol
0	n/a	n/a	n/a	2.9	0.0
12	54.5	15.4	9.0	2.4	0.8
24	55.7	15.7	2.9	1.7	5.7
36	35.9	11.6	0.0	0.0	16.1
48	15.8	6.3	0.0	0.0	31.2
60	1.3	2.5	0.0	0.0	52.2
72	n/a	2.3	0.0	0.0	50.1
96	0.0	2.5	0.0	0.0	41.5

R1		Concentration (kg / m ³)			
Time (h)	Maltose	Maltotriose	Glucose	Fructose	Ethanol
0	59.6	17.3	13.0	n/a	0.0
12	58.6	16.1	10.2	2.2	2.7
24	53.1	15.3	1.5	0.1	8.5
36	33.9	11.3	0.0	0.0	27.0
48	14.0	5.6	0.0	0.0	35.0
60	0.0	2.8	0.0	0.0	48.3
72	0.0	2.5	0.0	0.0	
96	0.0	2.3	0.0	0.0	

R1 Average		Concentration (kg / m ³)			
Time (h)	Maltose	Maltotriose	Glucose	Fructose	Ethanol
0	60.0	17.4	13.0	3.0	0.0
12	56.6	15.8	9.6	2.3	1.8
24	54.4	15.5	2.2	0.9	7.1
36	34.9	11.4	0.0	0.0	21.6
48	14.9	6.0	0.0	0.0	33.1
60	0.7	2.6	0.0	0.0	50.3
72	0.0	2.4	0.0	0.0	50.1
96	0.0	2.4	0.0	0.0	41.5

Table A1.5. Carbohydrate and ethanol batch fermentation data for repeated batch fermentations. R2.

R2		Concentration (kg / m ³)			
Time (h)	Maltose	Maltotriose	Glucose	Fructose	Ethanol
0	55.2	15.9	9.9	2.3	0.0
12	49.8	14.9	0.0	0.0	19.4
24	7.8	4.2	0.0	0.0	35.6
36	1.3	3.5	0.0	0.0	33.7
48	0.0	3.0	0.0	0.0	
60	0.0	3.1	0.0	0.0	51.1
72	0.0	2.6	0.0	0.0	57.8
96	0.0	2.9	0.0	0.0	45.3

R2		Concentration (kg / m ³)			
Time (h)	Maltose	Maltotriose	Glucose	Fructose	Ethanol
0	53.4	15.4	9.5	1.6	1.6
12	48.7	14.9	0.0	0.0	25.9
24	7.3	4.7	0.0	0.0	35.0
36	1.0	3.4	0.0	0.0	26.1
48	0.0	3.1	0.0	0.0	
60	0.0	2.9	0.0	0.0	49.8
72	0.0	3.1	0.0	0.0	40.5
96	0.0	3.1	0.0	0.0	37.7

R2 Average		Concentration (kg / m ³)			
Time (h)	Maltose	Maltotriose	Glucose	Fructose	Ethanol
0	54.3	15.7	9.7	2.0	11.0
12	49.3	14.9	0.0	0.0	22.7
24	7.6	4.4	0.0	0.0	35.3
36	1.2	3.5	0.0	0.0	
48	0.0	3.1	0.0	0.0	49.3
60	0.0	3.0	0.0	0.0	50.5
72	0.0	2.9	0.0	0.0	49.2
96	0.0	3.0	0.0	0.0	41.5

Table A1.6. Carbohydrate and ethanol batch fermentation data for repeated batch fermentations, R3.

R3*	Concentration (kg / m ³)					
	Time (h)	Maltose	Maltotriose	Glucose	Fructose	Ethanol
	0	52.0	16.0	8.9	2.8	14.0
	12	37.3	12.5	0.0	0.0	42.3
	24	1.0	3.0	0.0	0.0	53.5
	36	0.0	3.2	0.0	0.0	54.3
	48	0.0	3.2	0.0	0.0	
	60	0.0	3.0	0.0	0.0	56.0
	72	0.0	2.9	0.0	0.0	58.8
	96	0.0	2.8	0.0	0.0	57.2

*not replicated

Table A1.7. Carbohydrate and ethanol batch fermentation data for repeated batch fermentations, freely suspended cell control.

Ctrl (R1)					
Concentration (kg / m ³)					
Time (h)	Maltose	Maltotriose	Glucose	Fructose	Ethanol
0	87.29	26.10	22.53	5.34	0.00
12	99.04	28.60	10.56	5.42	4.85
24	72.82	21.50	0.00	0.00	14.74
36	34.01	10.40	0.00	0.00	33.25
48	12.61	6.00	0.00	0.00	48.09
60	1.73	4.30	0.00	0.00	101.36
72	1.81	4.20	0.00	0.00	86.67
96	0.00	4.50	0.00	0.00	92.90

Ctrl (R2)					
Concentration (kg / m ³)					
Time (h)	Maltose	Maltotriose	Glucose	Fructose	Ethanol
0	95.6	28.1	18.8	2.9	0.00
12	93.60	26.86	8.96	3.31	4.27
24	79.66	23.51	0.00	0.00	11.41
36	40.50	12.35	0.00	0.00	18.50
48	4.40	4.98	0.00	0.00	41.33
60	0.00	4.56	0.00	0.00	52.07
72	0.00	3.92	0.00	0.00	58.29
96	0.00	3.88	0.00	0.00	62.72

Ctrl (R3)					
Concentration (kg / m ³)					
Time (h)	Maltose	Maltotriose	Glucose	Fructose	Ethanol
0	85.92	25.50	16.39	2.90	0.00
12	84.05	23.80	9.01	3.17	13.03
24	70.76	21.70	0.00	0.00	28.30
36	42.02	12.50	0.00	0.00	41.59
48	7.63	5.20	0.00	0.00	51.15
60	2.13	4.20	0.00	0.00	53.74
72	0.00	4.50	0.00	0.00	53.05
96	0.00	3.20	0.00	0.00	64.37

Ctrl Average					
Concentration (kg / m ³)					
Time (h)	Maltose	Maltotriose	Glucose	Fructose	Ethanol
0	89.60	26.57	19.24	3.71	0.00
12	92.23	26.42	9.51	3.97	7.38
24	74.42	22.24	0.00	0.00	18.15
36	38.84	11.75	0.00	0.00	31.11
48	8.22	5.39	0.00	0.00	46.86
60	1.28	4.35	0.00	0.00	69.06
72	0.60	4.21	0.00	0.00	66.00
96	0.00	3.86	0.00	0.00	73.33

Experimental data used for Figures 6.7 – 6.12.

Table A1.8. Cell Concentration data for repeated batch fermentations. R1.

R1		Immobilized Cells		Liquid Phase Cells	
Time (h)	Concentration (cells/mL of gel)	Viability (%)	Concentration (cell/mL of liquid)	Viability (%)	
0	2.62E+07	44	0.00E+00	n/a	
12	3.64E+07		0.00E+00	n/a	
24	1.70E+08	86	7.15E+06	99	
36	2.54E+08	82	2.54E+07	99	
48	2.30E+08	92	5.47E+07	98	
60			6.45E+07	98	
72	3.17E+08	95			
96	3.50E+08	93	7.75E+07	97	

R1		Immobilized Cells		Liquid Phase Cells	
Time (h)	Concentration (cells/mL of gel)	Viability (%)	Concentration (cell/mL of liquid)	Viability (%)	
0	2.40E+07	79	0.00E+00	n/a	
12	4.40E+07	86	8.50E+05	100	
24	9.20E+07	93	5.50E+06	100	
36	3.03E+08	95	4.23E+07	99	
48	2.83E+08	95	2.87E+07	98	
60	3.42E+08	94	3.56E+07	99	
72	3.97E+08	89	4.73E+07	98	
96	2.45E+08	93	4.63E+07	97	

R1 average		Immobilized Cells		Liquid Phase Cells	
Time (h)	Concentration (cells/mL of gel)	Viability (%)	Concentration (cell/mL of liquid)	Viability (%)	
0	2.51E+07	62	0.00E+00	n/a	
12	4.02E+07	86	4.25E+05	100	
24	1.31E+08	90	6.33E+06	100	
36	2.79E+08	89	3.39E+07	99	
48	2.57E+08	94	4.17E+07	98	
60		94	5.01E+07	99	
72	3.57E+08	92		98	
96	2.98E+08	93	6.19E+07	97	

R1 Average		Immobilized Cells		Liquid Phase Cells	
Time (h)	Concentration (cells/mL of gel)	Error Bars	Concentration (cells/mL of liquid)	Error Bars	
0	2.51E+07	1.10E+06	0.00E+00	0.00E+00	
12	4.02E+07	3.80E+06	4.25E+05	4.25E+05	
24	1.31E+08	3.90E+07	6.33E+06	8.25E+05	
36	2.79E+08	2.45E+07	3.39E+07	8.45E+06	
48	2.57E+08	2.65E+07	4.17E+07	1.30E+07	
60			5.01E+07	1.45E+07	

72	3.57E+08	4.00E+07		
96	2.98E+08	5.25E+07	6.19E+07	1.56E+07

R1 Average	Immobilized Cells		Liquid Phase Cells	
Time (h)	Concentration (cells/mL total bioreactor volume)	Error Bars	Concentration (cells/mL total bioreactor volume)	Error Bars
0	1.00E+07	4.40E+05	0.00E+00	0.00E+00
12	1.61E+07	1.52E+06	2.55E+05	2.55E+05
24	5.24E+07	1.56E+07	3.80E+06	4.95E+05
36	1.11E+08	9.80E+06	2.03E+07	5.07E+06
48	1.03E+08	1.06E+07	2.50E+07	7.80E+06
60			3.00E+07	8.67E+06
72				
96	1.19E+08	2.10E+07	3.71E+07	9.36E+06

R1 Average	Immobilized + Liquid Phase Cells	
Time (h)	Concentration (cells/mL total bioreactor volume)	Error Bars
0	1.00E+07	4.40E+05
12	1.63E+07	1.78E+06
24	5.62E+07	1.61E+07
36	1.32E+08	1.49E+07
48	1.28E+08	1.84E+07
60		
72		
96	1.56E+08	3.04E+07

Table A1.9. Cell Concentration data for repeated batch fermentations, R2.

R2	Immobilized Cells		Liquid Phase Cells	
Time (h)	Concentration (cells/mL of gel)	Viability (%)	Concentration (cell/mL of liquid)	Viability (%)
0	4.08E+08	94	2.04E+06	95
12	2.46E+08	96	1.25E+07	98
24	7.93E+08	96	5.36E+07	97
36	5.80E+08	93	7.23E+07	95
48	6.62E+08	94	7.53E+07	95
60	8.89E+08	95	9.10E+07	95
72	7.96E+08	93	8.45E+07	94
96	6.40E+08	94	9.15E+07	95

R2	Immobilized Cells		Liquid Phase Cells	
Time (h)	Concentration (cells/mL of gel)	Viability (%)	Concentration (cell/mL of liquid)	Viability (%)
0	2.91E+08	89	2.47E+06	98
12	2.44E+08	95	1.63E+07	98
24	5.09E+08	96	6.70E+07	97
36	5.17E+08	92	8.15E+07	94
48	7.59E+08	94	9.40E+07	95
60	6.03E+08	95	1.03E+08	96
72	6.77E+08	93	9.40E+07	95
96	6.41E+08	93	1.12E+08	95

R2 Average	Immobilized Cells		Liquid Phase Cells	
Time (h)	Concentration (cells/mL of gel)	Viability (%)	Concentration (cell/mL of liquid)	Viability (%)
0	3.50E+08	92	2.26E+06	97
12	2.45E+08	96	1.44E+07	98
24	6.51E+08	96	6.03E+07	97
36	5.49E+08	93	7.69E+07	95
48	7.11E+08	94	8.47E+07	95
60	7.46E+08	95	9.70E+07	96
72	7.37E+08	93	8.93E+07	95
96	6.41E+08	94	1.02E+08	95

R2 Average	Immobilized Cells		Liquid Phase Cells	
Time (h)	Concentration (cells/mL of gel)	Error Bars	Concentration (cells/mL of liquid)	Error Bars
0	3.50E+08	5.85E+07	2.26E+06	2.15E+05
12	2.45E+08	1.00E+06	1.44E+07	1.90E+06
24	6.51E+08	1.42E+08	6.03E+07	6.70E+06
36	5.49E+08	3.15E+07	7.69E+07	4.60E+06
48	7.11E+08	4.85E+07	8.47E+07	9.35E+06
60	7.46E+08	1.43E+08	9.70E+07	6.00E+06
72	7.37E+08	5.95E+07	8.93E+07	4.75E+06
96	6.41E+08	5.00E+05	1.02E+08	1.03E+07

R2 Average		Immobilized Cells		Liquid Phase Cells	
Time (h)	Concentration (cells/mL total bioreactor volume)	Error Bars	Concentration (cells/mL total bioreactor volume)	Error Bars	
0	1.40E+08	2.34E+07	1.35E+06	1.29E+05	
12	9.80E+07	4.00E+05	8.64E+06	1.14E+06	
24	2.60E+08	5.68E+07	3.62E+07	4.02E+06	
36	2.19E+08	1.26E+07	4.61E+07	2.76E+06	
48	2.84E+08	1.94E+07	5.08E+07	5.61E+06	
60			5.82E+07	3.60E+06	
72	2.95E+08	2.38E+07			
96	2.56E+08	2.00E+05	6.11E+07	6.15E+06	
R2 Total		Immobilized + Liquid Phase Cells			
Time (h)	Concentration (cells/mL total bioreactor volume)	Error Bars			
0	1.41E+08	2.35E+07			
12	1.07E+08	1.54E+06			
24	2.97E+08	6.08E+07			
36	2.66E+08	1.54E+07			
48	3.35E+08	2.50E+07			
60					
72					
96	3.17E+08	6.35E+06			

Table A1.10. Cell Concentration data for repeated batch fermentations. R3.

R3				
Time (h)	Immobilized Cells		Liquid Phase Cells	
	Concentration (cells/mL of gel)	Viability (%)	Concentration (cell/mL of liquid)	Viability (%)
0	7.16E+08	93	1.58E+07	94
12	7.04E+08	97	2.95E+07	96
24	9.79E+08	92	7.30E+07	95
36	7.94E+08	87	7.25E+07	94
48	5.74E+08	82	1.17E+08	87
60	1.07E+09	87	1.10E+08	94
72	8.46E+08	87	1.18E+08	90
96	7.02E+08	85	9.90E+07	87

R3*				
Time (h)	Immobilized Cells		Liquid Phase Cells	
	Concentration (cells/mL of gel)	Viability (%)	Concentration (cell/mL of liquid)	Viability (%)
0	6.96E+08	88	1.97E+07	96
12	6.09E+08	96	2.90E+07	94
24	8.23E+08	91	6.45E+07	97
36	6.90E+08	87	7.40E+07	89
48	5.37E+08	83	1.03E+08	94
60	9.72E+08	86	1.10E+08	94
72	8.38E+08	86	1.31E+08	90
96	6.22E+08	85	1.44E+08	89

R3 average				
Time (h)	Immobilized Cells		Liquid Phase Cells	
	Concentration (cells/mL of gel)	Viability (%)	Concentration (cell/mL of liquid)	Viability (%)
0	7.06E+08	90.5	1.78E+07	95
12	6.57E+08	96.5	2.93E+07	95
24	9.01E+08	91.5	6.88E+07	96
36			7.33E+07	92
48			1.10E+08	91
60	1.02E+09	86.5	1.10E+08	94
72	8.42E+08	86.5	1.25E+08	90
96	6.62E+08	85	1.22E+08	88

R3 Average				
Time (h)	Immobilized Cells		Liquid Phase Cells	
	Concentration (cells/mL of gel)	Error Bars	Concentration (cells/mL of liquid)	Error Bars
0	7.06E+08	1.00E+07	1.78E+07	1.95E+06
12	6.57E+08	4.75E+07	2.93E+07	2.50E+05
24	9.01E+08	7.80E+07	6.88E+07	4.25E+06
36			7.33E+07	7.50E+05
48			1.10E+08	7.00E+06
60	1.02E+09	5.00E+07	1.10E+08	0.00E+00
72	8.42E+08	4.00E+06	1.25E+08	6.50E+06
96	6.62E+08	4.00E+07	1.22E+08	2.25E+07

R3 Average		Immobilized Cells		Liquid Phase Cells	
Time (h)	Concentration (cells/mL total bioreactor volume)	Error Bars	Concentration (cells/mL total bioreactor volume)	Error Bars	
0	2.82E+08	4.00E+06	1.07E+07	1.17E+06	
12	2.63E+08	1.90E+07	1.76E+07	1.50E+05	
24	3.60E+08	3.12E+07	4.13E+07	2.55E+06	
36			4.40E+07	4.50E+05	
48			6.60E+07	4.20E+06	
60	4.09E+08	2.00E+07	6.60E+07	0.00E+00	
72	3.37E+08	1.60E+06			
96	2.65E+08	1.60E+07	7.29E+07	1.35E+07	
R3 Total		Immobilized + Liquid Phase Cells			
Time (h)	Concentration (cells/mL total bioreactor volume)	Error Bars			
0	2.93E+08	5.17E+06			
12	2.80E+08	1.92E+07			
24	4.02E+08	3.38E+07			
36					
48					
60	4.75E+08	2.00E+07			
72					
96	3.38E+08	2.95E+07			

*replicate data was collected from same experimental unit (fermentation)

Table A1.11. Cell Concentration data for repeated batch fermentations, freely suspended cell controls.

Ctrl (R1)		
Time (h)	Liquid Phase Cells	
	Concentration (cell/mL of liquid)	Viability (%)
0	1.90E+07	99
12	5.34E+07	99
24		
36	2.30E+08	99
48	2.48E+08	99
60		
72	2.97E+08	98
96	2.46E+08	93

Ctrl (R2)		
Time (h)	Liquid Phase Cells	
	Concentration (cell/mL of liquid)	Viability (%)
0	2.14E+07	100
12	6.09E+07	98
24	2.01E+08	99
36	2.53E+08	99
48	3.16E+08	98
60	3.23E+08	98
72	3.03E+08	96
96	3.20E+08	95

Ctrl (R3)		
Time (h)	Liquid Phase Cells	
	Concentration (cell/mL of liquid)	Viability (%)
0	2.18E+07	100
12	7.61E+07	100
24	2.16E+08	100
36	2.63E+08	100
48	2.54E+08	98
60	3.26E+08	99
72		
96	3.34E+08	96

Ctrl Average		
Time (h)	Liquid Phase Cells	
	Concentration (cell/mL of liquid)	Viability (%)
0	2.07E+07	100
12	6.35E+07	99
24	2.09E+08	100
36	2.49E+08	99
48	2.73E+08	98
60	3.25E+08	99
72	3.00E+08	97
96	3.00E+08	95

<u>Ctrl Average</u>	<u>Liquid Phase Cells</u>
<u>Time</u>	<u>Concentration</u>
<u>(h)</u>	<u>(cells/mL of liquid)</u>
0	2.07E+07
12	6.35E+07
24	2.09E+08
36	2.49E+08
48	2.73E+08
60	3.25E+08
72	3.00E+08
96	3.00E+08

Experimental data used for Table 7.2 and Figures 7.2 – 7.11.

Table A1.12 (a). Experimental data examining the effect of the amount of air in the fluidizing gas on fermentation parameters.

Continuous	Wort		Air Volumetric	Liquid Phase Yeast	Tot. Ferm.	Free Amino			
Ferm. Time	Flow Rate	Temp	Flow Rate	Concentration	Viability	Glucose	Nitrogen	Ethanol	Diacetyl
(days)	(mL/min)	(°C)	(mL/min)	(cells/mL)	(% viab.)	(g/100 mL)	(mg/L)	(g/100 mL)	(µg/L)
1	0	14.7	0	6.25E+06	88	0.20		3.76	
2	3	14.9	44	4.65E+06	86.7	2.16		3.57	
3	3	15.5	91	1.48E+07	84.7	1.48		4.66	
4	3.5	13.7	91	1.10E+07	84.1			5.05	
5	3.5	16	94	8.10E+07	84.6	1.17		5.75	
8	4	14.4	94	5.15E+08	86.9	1.30		6.15	
9	4	15.1	94	4.00E+08	93.1	1.10		6.15	
10	4.5	15.4	94	2.90E+08	94.2	1.25		6.01	803
11	4.5	14.3	94	1.80E+08	95.8	1.40		5.97	613
12	5	14.4	94	3.08E+08	91.9	2.02		5.73	784
16	4.7	14.5	94	2.20E+08	95.5	0.44	167.7	6.32	439
17	5	15.5	94	2.08E+08	90.4	2.27	172.9	5.57	
18	4.7	15.1	94	2.83E+08	92	1.87	158.1	5.42	
19	4.7	14.9	94	2.65E+08	92.5	1.68	147.5	6.05	399
20	4.7	14.9	94	2.63E+08	96.3	1.49	242.8	6.35	387
23	4.7	14.9	94	2.20E+08	92	1.37	257.5	6.09	334
24	4.7	14.8	94	3.70E+08	93.3	1.58	156.8	6.23	293
25	4.7	14.8	94	4.70E+08	93.5	1.31	199.9		410
26	4.7	15	94	4.88E+08	91.3	1.17	173.5	6.10	
29	4.7	14.9	354	4.78E+08	90.6		173.7	5.89	
30	4.7	14.8	354	1.40E+08	94.6		193.0	5.36	
31	4.7	15.3	354	3.20E+08	91.4		188.7	5.29	
32	4.7	15.6	354	2.70E+08	91.5		195.8	5.24	
33	4.7	15.1	354	3.70E+08	90.4	1.68	191.4	5.58	425
36	4.7	15.2	354	2.70E+08	89.4	1.39	168.8	5.55	1843

37	4.7	15.1	354	2.20E+08	91	1.28	169.1	5.44	1682
38	4.7	15.1	354	3.30E+08	90.8	1.29	171.1	5.50	1526
39	4.7	15.1	354	4.10E+08	89.6	1.74	174.7	5.30	1172
40	4.7	14.5	354	2.30E+08	90.2	1.19	171.8	5.59	1287
43	4.7	14.3	34	3.10E+08	92.4		160.4	5.54	647
44	4.7	14.5	34	1.70E+08	96.4		137.6	5.05	
45	4.7	14.3	34	3.50E+08	93.9		123.2	5.47	
46	4.7	14.7	34	3.70E+08	94.5		119.7	5.19	
47	4.7	14.8	34	3.60E+08	95.7	1.10	123.0	6.04	417
51	4.7	14	34	1.90E+08	91.3	1.63	143.8	6.08	476
52	4.7	15	34	3.00E+08	95.8	1.81		6.04	405
53	4.7	15.2	34	4.20E+08	92.5	1.97	157.6	6.03	590
54	4.7	14.9	34	5.20E+08	96.6	2.17	160.9	5.87	187
57	4.7	15.3	34	4.30E+08	92		175.0	5.87	
58	4.7	14.9	34	5.20E+08	95.7		157.7	5.20	
59	4.7	16.3	0	2.90E+08	95.6		169.9	5.24	
60	4.7	16.1	0	1.30E+08	94.3	4.83	205.0	4.44	276
61	4.7		0	2.60E+07	85.7	6.27	244.6	3.82	
64	4.7	15.5	0	6.80E+06	69.1	6.55	251.4	4.11	272
65	4.7	14.9	0	1.10E+06	70.6	6.43	276.0	3.80	241
66	4.7	15.3	0	9.00E+04	62.5	6.29	270.1	3.68	221

Table A1.12 (b). Experimental data examining the effect of the amount of air in the sparge gas on fermentation parameters.

Continuous Ferm. Time (days)	Wort Flow Rate (mL/min)	Temp. (°C)	Air Volumetric Flow Rate (mL/min)	Acet- aldehyde (mg/L)	Ethyl Acetate (mg/L)	1-Prop- anol (mg/L)	Iso- butanol (mg/L)	Isoamyl Acetate (mg/L)	Isoamyl Alcohol (mg/L)	Ethyl Hex- anoate (mg/L)	Ethyl Oct- anoate (mg/L)
1	0	14.7	0	8.77	3.46	25.28	21.10	0.04	81.27	0.022	0.015
2	3	14.9	44	33.49	6.48	22.23	17.62	0.28	71.33	0.034	0.010
3	3	15.5	91	50.32	11.58	33.86	22.84	0.47	76.20	0.054	0.025
4	3.5	13.7	91	45.94	12.88	39.31	18.83	0.40	71.41	0.053	0.025
5	3.5	16	94	46.50	18.27	47.68	18.64	0.53	81.39	0.082	0.040
8	4	14.4	94	32.06	19.92	47.67	10.80	0.50	70.65	0.082	0.045
9	4	15.1	94	30.93	18.96	48.43	10.24	0.45	70.54	0.073	0.034
10	4.5	15.4	94	34.59	19.92	47.11	9.37	0.44	68.42	0.073	0.041
11	4.5	14.3	94	35.97	20.75	45.33	8.97	0.44	66.52	0.072	0.044
12	5	14.4	94	49.69	21.80	40.98	8.10	0.41	61.88	0.063	0.031
16	4.7	14.5	94	114.54	24.04	42.41	9.57	0.42	67.81	0.082	0.047
20	4.7	14.9	94	64.13	22.24	43.46	8.64	0.42	58.56	0.069	0.035
23	4.7	14.9	94	69.30	22.03	43.24	8.46	0.36	57.28	0.056	0.031
24	4.7	14.8	94	77.93	23.55	45.18	8.79	0.43	59.65	0.066	0.031
25	4.7	14.8	94	73.73	21.50	44.45	8.82	0.38	58.44	0.065	0.030
26	4.7	15	94	81.53	22.43	46.07	8.85	0.36	59.09	0.054	0.034
29	4.7	14.9	354	209.81	24.68	48.08	9.26	0.44	61.62	0.066	0.033
33	4.7	15.1	354	296.50	23.46	48.18	13.83	0.35	61.10	0.041	0.011
36	4.7	15.2	354	293.71	22.42	50.89	15.32	0.27	62.70	0.035	0.013
37	4.7	15.1	354	315.36	22.30	51.67	15.81	0.25	62.93	0.034	0.014
38	4.7	15.1	354	336.77	21.72	51.49	16.09	0.22	62.22	0.033	0.014
39	4.7	15.1	354	300.31	18.59	48.98	15.31	0.17	57.93	0.025	0.012
40	4.7	14.5	354	365.47	21.91	51.42	17.14	0.19	63.48	0.029	0.010
43	4.7	14.3	34	36.75	22.33	49.93	12.09	0.23	58.79	0.035	0.012
47	4.7	14.8	34	24.43	19.39	62.44	10.05	0.30	64.83	0.056	0.025
51	4.7	14	34	28.99	17.17	56.01	8.30	0.29	59.84	0.054	0.026
52	4.7	15	34	28.52	18.32	55.22	8.34	0.31	61.41	0.057	0.024
53	4.7	15.2	34	26.50	17.97	52.22	7.92	0.27	58.79	0.047	0.024
54	4.7	14.9	34	30.52	18.57	48.70	7.66	0.31	56.62	0.054	0.026
60	4.7	16.1	34	26.56	18.48	32.17	5.05	0.23	41.21	0.036	0.012
64	4.7	15.5	0	21.91	21.73	17.99	4.89	0.32	35.22	0.047	0.026

Continuous Ferm. Time (days)	Wort Flow Rate (mL/min)	Temp. (°C)	Air Volumetric Flow Rate (mL/min)	Acet- aldehyde (mg/L)	Ethyl Acetate (mg/L)	1-Prop- anol (mg/L)	Iso- butanol (mg/L)	Isoamyl Acetate (mg/L)	Isoamyl Alcohol (mg/L)	Ethyl Hex- anoate (mg/L)	Ethyl Oct- anoate (mg/L)
65	4.7	14.9	0	22.71	24.68	17.51	5.13	0.39	36.56	0.068	0.027
66	4.7	15.3	0	22.73	24.68	16.17	5.07	0.29	35.45	0.045	0.017

Table A1.12 (c). Experimental data examining the effect of the amount of air in the sparge gas on fermentation parameters.

Continuous Ferm. Time (days)	Wort Flow Rate (mL/min)	Temp (°C)	Air Volumetric Flow Rate (mL/min)	Malto- triose	Maltose	Glucose (g/100 mL)	Fructose	Tot. Ferm. Glucose
1	0	14.7	0	1.43	4.72	0.35	0.30	0.20
2	3	14.9	44	0.74	2.04	0	0	2.16
3	3	15.5	91	0.24		0	0	1.48
4	3.5	13.7	91					
5	3.5	16	94	0.54	0.53	0	0	1.17
8	4	14.4	94	0.54	0.66	0	0	1.30
9	4	15.1	94	0.49	0.53	0	0	1.10
10	4.5	15.4	94	0.51	0.65	0	0	1.25
11	4.5	14.3	94	0.56	0.74	0	0	1.40
12	5	14.4	94	0.68	1.20	0	0	2.02
16	4.7	14.5	94	0.40		0	0	0.44
17	5	15.5	94	0.72	1.40	0	0	2.27
18	4.7	15.1	94	0.69	1.06	0	0	1.87
19	4.7	14.9	94	0.64	0.92	0	0	1.68
20	4.7	14.9	94	0.61	0.77	0	0	1.49
23	4.7	14.9	94	0.53	0.74	0	0	1.37
24	4.7	14.8	94	0.59	0.88	0	0	1.58
25	4.7	14.8	94	0.54	0.68	0	0	1.31
26	4.7	15	94	0.50	0.58	0	0	1.17
29	4.7	14.9	354					
30	4.7	14.8	354					
31	4.7	15.3	354					
32	4.7	15.6	354					
33	4.7	15.1	354	0.64	0.92	0	0	1.68
36	4.7	15.2	354	0.58	0.71	0	0	1.39
37	4.7	15.1	354	0.55	0.64	0	0	1.28
38	4.7	15.1	354	0.56	0.63	0	0	1.29
39	4.7	15.1	354	0.62	1.00	0	0	1.74

Continuous Ferm. Time (days)	Wort Flow Rate (mL/min)	Temp (°C)	Air Volumetric Flow Rate (mL/min)	Malto- triose	Maltose	Glucose (g/100 mL)	Fructose	Tot. Ferm. Glucose
40	4.7	14.5	354	0.52	0.58	0	0	1.19
43	4.7	14.3	34					
44	4.7	14.5	34					
45	4.7	14.3	34					
46	4.7	14.7	34					
47	4.7	14.8	34	0.46	0.56	0	0	1.10
51	4.7	14	34	0.64	0.88	0	0	1.63
52	4.7	15	34	0.69	0.99	0	0	1.81
53	4.7	15.2	34	0.73	1.11	0	0	1.97
54	4.7	14.9	34	0.76	1.26	0	0	2.17
57	4.7	15.3	34					
58	4.7	14.9	34					
59	4.7	16.3	0					
60	4.7	16.1	0	1.12	3.41	0	0	4.83
61	4.7		0	1.41	4.47	0	0	6.27
64	4.7	15.5	0	1.49	4.66	0	0	6.55
65	4.7	14.9	0	1.45	4.58	0	0	6.43
66	4.7	15.3	0	1.37	4.53	0	0	6.29

Experimental data used for Figures 7.12 – 7.22.

Table A1.13 (a). Data used to examine the effect of oxygen on fermentation parameters during a post fermentation hold period.

Aerobic I				Ethyl			Isoamyl	Isoamyl	Ethyl
Hold time	Ethanol	Acetaldehyde	Diacetyl	Acetate	1-Propanol	Isobutanol	Acetate	Alcohol	Hexanoate
(h)	(g/100 mL)	(mg/L)	(μ g/L)	(mg/L)					
	5.78	17.04	326.0	16.34	47.18	7.46	0.68	60.03	0.086
2	5.94	21.24	153.90	17.19	50.10	8.15	0.72	64.95	0.10
24	6.31	17.96	261.93	15.38	52.65	8.87	0.58	68.87	0.09
48	6.47	11.80	74.45	12.55	52.79	9.14	0.38	68.05	0.06
Aerobic II				Ethyl			Isoamyl	Isoamyl	Ethyl
Hold time	Ethanol	Acetaldehyde	Diacetyl	Acetate	1-Propanol	Isobutanol	Acetate	Alcohol	Hexanoate
(h)	(g/100 mL)	(mg/L)	(μ g/L)	(mg/L)					
	5.78	17.04	326.0	16.34	47.18	7.46	0.68	60.03	0.086
2	5.90	25.12	296.60	17.01	50.10	7.97	0.70	63.96	0.09
24	6.18	20.74	239.98	16.94	56.26	9.29	0.68	72.97	0.11
48	6.71	14.19	49.21	15.46	53.19	9.23	0.52	69.57	0.07
Anaerobic I				Ethyl			Isoamyl	Isoamyl	Ethyl
Hold time	Ethanol	Acetaldehyde	Diacetyl	Acetate	1-Propanol	Isobutanol	Acetate	Alcohol	Hexanoate
(h)	(g/100 mL)	(mg/L)	(μ g/L)	(mg/L)					
	5.78	17.04	326.0	16.34	47.18	7.46	0.68	60.03	0.086
2	6.61	16.16	215.33	17.08	48.79	7.90	0.71	62.76	0.10
24	6.65	11.35	187.33	17.50	49.24	8.28	0.69	64.71	0.10
48	7.17	8.24	34.59	18.81	49.27	8.91	0.81	67.64	0.13
Anaerobic II				Ethyl			Isoamyl	Isoamyl	Ethyl
Hold time	Ethanol	Acetaldehyde	Diacetyl	Acetate	1-Propanol	Isobutanol	Acetate	Alcohol	Hexanoate
(h)	(g/100 mL)	(mg/L)	(μ g/L)	(mg/L)					
	5.78	17.04	326.0	16.34	47.18	7.46	0.68	60.03	0.086
2	6.63	15.68	166.99	17.36	49.58	8.05	0.74	64.18	0.11
24	6.96	10.25	216.04	17.77	50.14	8.51	0.74	66.10	0.12
48	7.22	9.52	32.26	19.95	52.22	9.18	0.87	70.75	0.14

Table A1.13 (b). Data used to examine the effect of oxygen on fermentation parameters during a post fermentation hold period.

Aerobic I		Maltotriose	Glucose (g/100 mL)	Fructose	Glucose	Total Ferm. Glucose
Hold time (h)						
	0.69	1.88	0.00	0.00	2.75	
2	0.63	1.56	0.00	0.00	2.33	
24	0.51	0.79	0.00	0.00	1.40	
48	0.34	0.38	0.00	0.00	0.78	

Aerobic II		Maltotriose	Glucose (g/100 mL)	Fructose	Glucose	Total Ferm. Glucose
Hold time (h)						
	0.69	1.88	0.00	0.00	2.75	
2	0.65	1.50	0.00	0.00	2.29	
24	0.51	0.81	0.00	0.00	1.42	
48	0.38	0.34	0.00	0.00	0.78	

Anaerobic I		Maltotriose	Glucose (g/100 mL)	Fructose	Glucose	Total Ferm. Glucose
Hold time (h)						
	0.69	1.88	0.00	0.00	2.75	
2	0.63	1.47	0.00	0.00	2.25	
24	0.49	0.81	0.00	0.00	1.40	
48	0.34	0.34	0.00	0.00	0.73	

Anaerobic II		Maltotriose	Glucose (g/100 mL)	Fructose	Glucose	Total Ferm. Glucose
Hold time (h)						
	0.69	1.88	0.00	0.00	2.75	
2	0.62	1.36	0.00	0.00	2.12	
24	0.49	0.74	0.00	0.00	1.32	
48	0.40	0.41	0.00	0.00	0.88	

Table A1.14. Data used to create the Figure 7.22. The data for the aerobic and anaerobic held beer was averaged from the results obtained at 48 hours from Table A1.13, undiluted results. The commercial beer data was averaged from the ranges specified in Appendix 4 on finished product. The data were normalized to the largest concentration for each analyte for graphical purposes.

	Diacetyl (µg/L)	Acetaldehyde	Ethyl Acetate	1-Propanol	Iso- butanol	Isoamyl Acetate	Isoamyl Alcohol
							(mg/L)
Aerobic Hold Beer	61.00	13.00	14.01	52.99	9.19	0.45	68.81
Anaerobic Hold Beer	33.00	8.88	19.38	50.74	9.04	0.84	69.20
Commercial Beer	21.00	11.00	25.00	10.00	12.00	2.00	50.00

Normalized Data

	Diacetyl	Acetaldehyde	Acetate Ethyl	1-Propanol	Iso- butanol	Isoamyl Acetate	Isoamyl Alcohol
Aerobic Hold Beer	1.00	1.00	0.25	1.00	0.29	0.10	0.70
Anaerobic Hold Beer	0.54	0.68	0.34	0.96	0.28	0.18	0.70
Commercial Beer	0.34	0.85	0.44	0.19	0.37	0.43	0.51

Experimental data used for Figures 7.23 – 7.28.

Table A1.15 (a). Experimental data used to examine the effect of bioreactor liquid residence time on continuous fermentation parameters.

Continuous Ferm. Time (days)	Wort Flow Rate (mL/min)	Temp. (°C)	Air Vol. Flow Rate (mL/min)	Liquid Phase Yeast Concentration (cells/mL)	Yeast Viability (% viab)	Malto- triose	Maltose	Glucose	Fructose	Total Ferm. Glucose	Ethanol	Free Amino Nitrogen (mg/L)	Diacetyl (µg/L)
6	3.1	18.3	11	2.30E+08	93.3	0.24	0	0	0	0.27	5.17		297
6.5	3.1	17.5	11	2.30E+08	89.8	0.27	0	0	0	0.30	5.16	112	297
7	3.1	16	11	2.40E+08	92.5	0.27	0	0	0	0.30	5.2	105	298
7.5	3.1	17	11	2.30E+08	87.2	0.26	0	0	0	0.29	5.15	106	289
8	3.1	18	11	2.60E+08	83	0.26	0	0	0	0.29	5.11	102	281
14	6.1	17.7	11	1.34E+08	85	1.29	4.02	0	0	5.66	4.84	236	473
14.5	6.1	16.7	11	1.24E+08	90	1.27	3.97	0.07	0	5.66			501
15	6.1	17	11	1.36E+08	84.1	1.36	4.30	0.09	0	6.12	4.86	259	471
15.5	6.1	17	11	1.32E+08	88.5	1.40	4.39	0.10	0	6.27	4.86	253	435
16	6.1	16.9	11	1.48E+08	92.5	1.40	4.45	0.11	0	6.34	4.67	250	431
16.5	6.1	17.3	11	1.18E+08	94.6	1.43	4.57	0.11	0	6.51	4.78	234	448

Table A1.15 (b). Experimental data used to examine the effect of bioreactor liquid residence time on continuous fermentation parameters.

Relative Ferm. Time (days)	Wort Flow Rate (mL/min)	Temp (°C)	Air Volumetric Flow Rate (mL / min)	Acet- aldehyde	Ethyl Acetate	1-Prop- anol	Iso- butanol (mg/L)	Isoamyl Acetate	Isoamyl Alcohol
6	3.1	18.3	11	19.83	41.98	44.73	23.62	0.91	79.66
6.5	3.1	17.5	11	15.79	37.51	43.13	22.07	0.76	74.38
7	3.1	16	11	20.74	42.02	44.76	22.7	0.95	74.84
7.5	3.1	17	11	22.87	41.18	45.04	22.45	0.92	77.04
8	3.1	18	11	18.11	42.33	47.08	23.06	0.97	77.44
14	6.1	17.7	11	35.25	38.25	14.11	9.39		52.98
14.5	6.1	16.7	11	34.72	37.63	14.71	9.34	1.25	53.07
15	6.1	17	11	35.21	39.27	14.02	9.08	1.35	50.97
15.5	6.1	17	11	37.71	37.74	12.82		1.25	49.53
16	6.1	16.9	11						
16.5	6.1	17.3	11	42.45	38.55	11.98	8.71	1.27	50.38

Experimental data used for Figures 7.29 – 7.34.

Table A1.16. Experimental data used to examine the effect of ALDC on diacetyl concentration during continuous fermentation, Experiment 2.

Continuous Ferm. Time (h)	Malto- triose	Maltose	Glucose	Fructose	Total Ferm. Glucose	Ethanol	Diacetyl ($\mu\text{g/L}$)	Liquid Phase Yeast Concentration (cells/mL)
(g/100 mL)								
0	0.56	1.34	0	0	2.04	6.28	471	4.80E+07
5	0.55	1.26	0	0	1.94	6.63	491	5.70E+07
24	0.61	1.29	0	0	2.04	7.91	466	7.20E+07
29	0.61	1.20	0	0	1.94	7.91	490	8.40E+07
48	0.61	1.31	0	0	2.06	7.08	498	2.80E+08
53	0.60	1.24	0	0	1.97	7.26	483	6.50E+07
120	0.49	0.86	0	0	1.45	7.26	568	3.30E+08
127	0.55	0.95	0	0	1.61	6.93	464	3.20E+08
144	0.54	0.84	0	0	1.49	6.46	322	
150	0.52	0.70	0	0	1.31	7.06	332	3.40E+08
168	0.51	0.72	0	0	1.33	6.78	280	3.60E+08
174	0.45	0.55	0	0	1.07	7.22	263	4.90E+08
193	0.46	0.59	0	0	1.13	6.76	278	2.50E+08
198	0.44	0.42	0	0	0.93	7.05	296	2.70E+08
216	0.43	0.52	0	0	1.02	7.02	274	2.30E+08
221	0.41	0.43	0	0	0.90	7.66	283	2.50E+08
288	0.40	0.39	0	0	0.85	7.02	243	2.30E+08
293	0.32	0.23	0	0	0.59	6.77	221	2.10E+08
312	0.42	0.49	0	0	0.98	6.71	225	2.70E+08

ALDC added at 72 $\mu\text{g/L}$ (108 ADU/L) to wort at time = 121 h

Table A1.17. Experimental data used to examine the effect of ALDC on diacetyl concentration during continuous fermentation, Experiment 3.

Continuous Ferm. Time (h)	Malto- Triose	Maltose	Glucose	Fructose	Total Ferm. Glucose	Ethanol	Diacetyl ($\mu\text{g/L}$)	Liquid Phase Yeast Concentration (cells/mL)
			(g/100 mL)					
0	0.46	0.45	0	0	0.98	6.34	451	8.78E+07
24	0.47	0.41	0	0	0.95	6.33	446	1.31E+08
48	0.43	0.36	0	0	0.85	6.26	450	1.64E+08
72	0.32	0.23	0	0	0.59	6.33	422	2.05E+08
96	0.33	0.16	0	0	0.53	6.67	447	2.40E+08
120	0.34	0.18	0	0	0.56	6.37	460	3.24E+08
144	0.32	0.15	0	0	0.51	6.36	421	2.98E+08
168	0.31	0.16	0	0	0.52	6.30	340	3.50E+08
192	0.30	0.13	0	0	0.47	6.28	261	3.23E+08
216	0.32	0.18	0	0	0.54	6.24	252	3.35E+08
240	0.34	0.23	0	0	0.63	6.20	249	3.55E+08
264	0.35	0.25	0	0	0.65	6.30	282	
288	0.33	0.23	0	0	0.61	6.31	231	
312	0.29	0	0	0	0.32	6.60	211	3.28E+08

ALDC added at 72 $\mu\text{g/L}$ (108 ADU/L) to wort at time = 160 h

APPENDIX 2

Concentration of some components in Brewer's wort.

Table A2.1. Fermentable carbohydrates, specific gravity, and free amino nitrogen concentration in samples of the brewer's wort used for continuous fermentations throughout this work.

	Malto- triose	Maltose	Glucose (g/100 mL)	Fructose	Tot. Ferm. Carb.	Specific Gravity (°P)	Free Amino Nitrogen (mg/L)
Wort 1	2.82	9.40	1.76	0.28	15.06	17.71	291
Wort 2	2.95	8.74	1.72	0.43	14.62	17.46	272
Wort 3	2.93	9.82	2.08	0.48	16.14	17.27	284
Wort 4	2.68	9.29	1.73	0.33	14.81	17.28	289
Wort 5	2.71	9.75	1.73	0.31	15.30	17.31	288
Mean	2.82	9.40	1.80	0.37	15.18	17.41	285
Error Bars	0.055	0.193	0.069	0.038	0.37	0.083	3.4

APPENDIX 3

Bioreactor volumetric beer productivity calculations

Table A3.1. Bioreactor volumetric beer productivity numbers for Section 7.2.2.

Process Name	Vol. Beer Prod. per unit Time, Q_B (m^3/day)	Tot Vessel Installed Vol., V_T (m^3)	Beer Productivity, P_B (m^3 beer prod./ m^3 of vessel vol./day)
Industrial Batch ¹	1.0	10.714	0.093
This Work ²	1.0	6.071	0.165
The Near Future ³	1.0	4.643	0.215
Ultimate Goal ⁴	1.0	1.429	0.700

¹ Modern industrial standard: vertical cylindro-conical batch fermentation with a 7.5 day cycle time

² This work: continuous gas lift draft tube bioreactor operating at a 24 hour residence time, with batch holding vessels filled for 24 hours, followed by a 48 hour batch holding time

³ The near future: continuous gas lift draft tube bioreactor operating at a 24 hour residence time, with batch holding vessels filled for 24 hours, followed by a 24 hour batch holding time, achieved by further optimization of process

⁴ Ultimate goal: continuous gas lift draft tube bioreactor(s) operating at a 24 hour total residence time, no batch holding

Assumptions:

- 24 hour filling time from continuous bioreactor into batch holding vessel
- 70% tank utilization

Where:

$$P_B = Q_B / V_T$$

$$V_T = V_W / 0.70$$

V_W = total bioreactor working volume for process

This Work:

Basis: 1 m^3 of beer per day, assuming 24 hour residence time in gas lift bioreactor

1 m^3 gas lift bioreactor

3 x 1 m^3 batch holding vessels (fill 24 hours, then hold 48 hours)

0.25 m^3 buffer vessel for cleaning (6 hours of holding, 0.25 m^3)

$$V_W = 4.25 \text{ m}^3$$

$$V_T = 4.25 / 0.70 = 6.071 \text{ m}^3$$

APPENDIX 4

Statistical analyses of data.

Statistic analyses of data

Mean (\bar{y})

$$\bar{y} = \sum y / n$$

Standard Deviation (s)

- a measure of the intrinsic variability of the individual observations in a sample

$$s = \sqrt{((\sum (y - \bar{y})^2) / (n - 1))}$$

Standard Error of the Mean (SE)

- used to express the level of uncertainty in the mean

$$SE = s / \sqrt{n}$$

Coefficient of Determination (r^2)

- where SSE is sum of squares due to error. SSM is sum of squares about the mean and y_{hat} is the predicted y value

$$r^2 = 1 - (SSE / SSM)$$

$$SSE = \sum w (y - y_{\text{hat}})^2$$

$$SSM = \sum w (y - \bar{y})^2$$

Arithmetic Mean Diameter (D_{am})

- where X_i is the fraction, and D_{pi} is sphere diameter

$$D_{\text{pam}} = \sum X_i D_{pi}$$

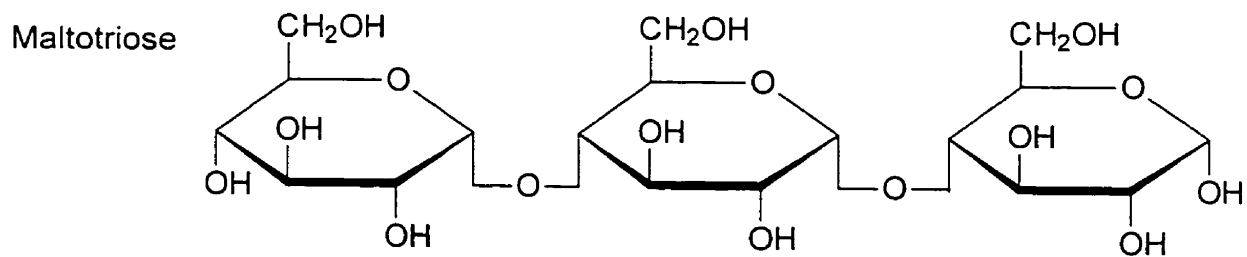
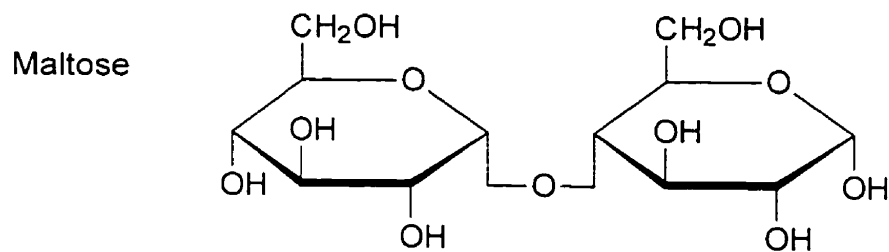
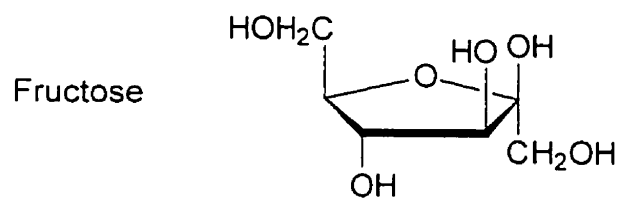
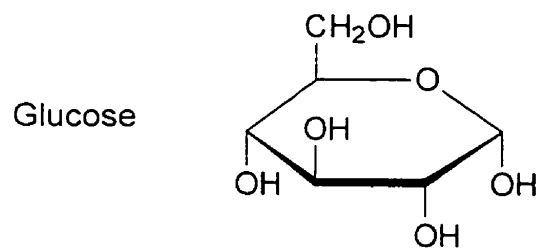
Sauter Mean Diameter (D_{psm})

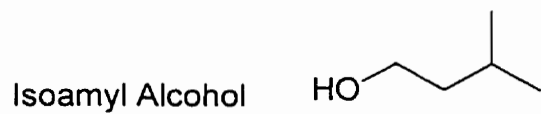
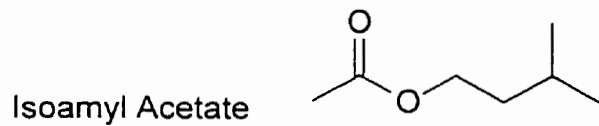
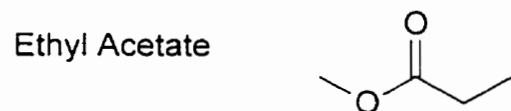
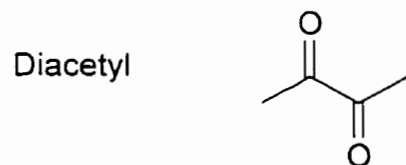
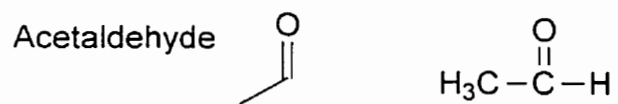
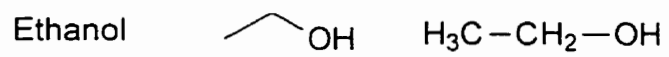
$$D_{\text{psm}} = 1 / (\sum (X_i / D_{pi}))$$

APPENDIX 5

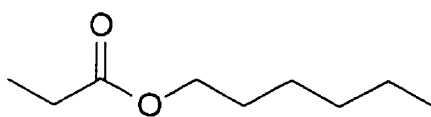
Structural formulae of key yeast substrates and metabolic products.

Chemical formulae of key yeast substrates and products

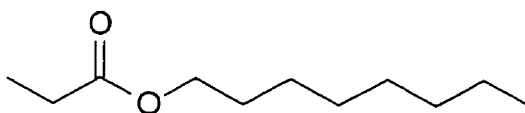




Ethyl Hexanoate



Ethyl Octanoate



APPENDIX 6

Typical concentrations and threshold values for flavour compounds in market beers.

Table A6.1. Flavour thresholds, typical concentration and flavour contributions of some components reported in market beer (adapted from Meilgaard, 1982).

Beer Flavour Compound	Flavour Threshold* (mg / L)	Typical Concentration in Beer (mg / L)	Flavour in Beer
Diacetyl	0.07 to 0.15	0.01 to 0.4	buttery, butterscotch
Acetaldehyde	25	2 to 20	green leaves, appleskin, fruity
Ethyl Acetate	30, 21	8 to 42	solvent-like, fruity, sweet
1-Propanol	600, 800	3 to 16	alcoholic
Isobutanol	100, 160, 200	5 to 20	alcoholic
Isoamyl Acetate	1.2, 0.6	0.6 to 4	banana, estery, solvent-like, apple
Isoamyl Alcohol	70	30 to 70	alcoholic, vinous, banana, sweet
Ethyl Hexanoate	0.21, 0.17	0.1 to 0.5	apple, fruity, aniseed, sweet
Ethyl Octanoate	0.9, 0.37	0.1 to 1.5	apple, sweet, fruity

APPENDIX 7

Copyright releases from previous publications

Journal of the Institute of Brewing

Editor:
C M Brown

Phone: 0131 539 9031
Fax: 0131 539 9031
Email: C.M.Brown@iaw.ac.uk

Please reply to:
Professor C M Brown
ICBD
Heriot-Watt University
Riccarton
Edinburgh EH14 4AS
UK

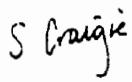
Ms Heather Pilkington
Labatt Brewing Company Limited
Technology Development
197 Richmond Street
London
Ontario
N6A 4M3

2 February 2000

Dear Ms Pilkington

I am writing to agree to your request to include versions of your papers "Kappa-carrageenan gel immobilisation of lager brewing yeast" and "Fundamentals of immobilised yeast cells for continuous beer fermentation: a review" in your PhD thesis.

Yours sincerely


H C M Brown

January 26, 2000

RECEIVED

CRC Press LLC
2000 Corporate Blvd., N.W.
Boca Raton, FL
33431 USA

FEB 01 2000

Dear Sir or Madam,

Currently, I am in the process of finishing up my Ph.D. thesis at the University of Western Ontario, London, Canada and I would like permission to include a version of the following article, which appeared in Critical Reviews in Biotechnology in 1998, in my thesis:

P.H. Pilkington, A. Margaritis, N.A. Mensour (1998) "Mass Transfer characteristics of Immobilized Cells Used in Fermentation Processes". Critical Reviews in Biotechnology, Vol. 18 (2 & 3), pp. 237-255.


I would appreciate your reply to this request in writing at your earliest convenience.

Sincerely,



Heather Pilkington

cc: Dr. Graham Stewart
Dr. Inge Russell

 CRC PRESS, LLC 1440 Corporate Blvd. S.W. Boca Raton, FL 33431	PERMISSION TO REPRINT IS GRANTED BY CRC PRESS, LLC CREDIT LINE REQUIRED: Reprinted with permission from (full book or journal reference). Copyright CRC Press, Boca Raton, Florida
	Date: <u>2/14/00</u> Permission Requester: <u>[Signature]</u>

Permissions is granted, at no charge, subject to the terms below:
 * Permission is granted for one-time use of the specified material only in the edition designated in your request and does not extend to future editions of your Work.
 * Permission applies to printed form only and does not extend to electronic media, customized, derivative or ancillary Works. Permissions for such must be separately requested.
 * Material to be used has appeared in our publication without credit or acknowledgment to another source. Permission must be obtained for materials in our Work that is modified to another source.